Summer 1990

A Mathematical Model of the Dynamics of an Optically Pumped Codoped Solid State Laser System

Thomas G. Wangler
Old Dominion University

A MATHEMATICAL MODEL OF THE DYNAMICS OF AN OPTICALLY PUMPED CODOPED SOLID STATE LASER SYSTEM

by

Thomas G. Wangler

B.S., December 1985, Old Dominion University

A Dissertation Submitted to the Faculty of Old Dominion University
in Partial Fulfilment of the Requirements for the Degree of

DOCTOR OF PHILOSOPHY
in
COMPUTATIONAL AND APPLIED MATHEMATICS

August 1990

Approved by:

John J. Swetits (Director)

ABSTRACT

A Mathematical Model of the Dynamics of an Optically Pumped Codoped Solid State Laser System

Thomas Gerard Wangler

Old Dominion University, 1990
Director: Dr. John J. Swetits

This is a study of a mathematical model for the dynamics of an optically pumped codoped solid state laser system. The model comprises five first order, nonlinear, coupled, ordinary differential equations which describe the temporal evolution of the dopant electron populations in the laser crystal as well as the photon density in the laser cavity. The analysis of the model is conducted in three parts.

First, a detailed explanation of the modeling process is given and the full set of rate equations is obtained. The model is then simplified and certain qualitative properties of the solution are obtained.

In the second part the equilibrium solutions are obtained and a local stability analysis is performed. The system of rate equations is solved numerically and the effects, on the solution, of varying physical parameters is discussed.

Finally, the third part addresses the oscillatory behavior of the system by "tracking" the eigenvalues of the linearized system. A comparison is made between the frequency of oscillations in the linear and nonlinear system. Pertinent

physical processes—back transfer, Q-switching, and up-conversion— are then examined.

The laser system consists of thulium and holmium ions in a YAG crystal operated in a Fabrey-Perot cavity. All computer programs were written in FORTRAN and currently run on either an IBM-PC or a DEC VAX 11/750.

to my lovely wife Vicky and the

three most precious children in the world

Ben, Michael and Esther Joy

ACKNOWLEDGEMENTS

As I consider the multitude of people who have helped me in one way or another during my studies at Old Dominion University, it becomes immediately apparent to me that I owe a debt of gratitude to a lot of people. Were it not for these peoples' altruism and self-abnegations this work would not have been accomplished.

I would like to start by thanking Dr. Phil Wohl who, while teaching me calculus many years ago, encouraged me to pursue a degree in mathematics and expressed his confidence in me—kind words never die. I am indebted to Dr. John Heinbockel who is largely responsible for diagnosing and curing me of the dreadful disease of "symbolitis". I especially thank Dr. Mark Dorrepaal who willingly gave of his time on numerous occasions— sometimes to help with mathematics and other times to simply be a friend.

I would like to thank my dissertation committee, Dr. John Swetits, Dr. Mark Dorrepaal, Dr. John Heinbockel, Dr. Stan Weinstein and Dr. Marty Buoncristiani for their advice and constructive criticism throughout my research work. A special thanks goes to Dr. Swetits— my thesis advisor— and Dr. Buoncristiani: Dr. Swetits for his generosity, forbearance, and sagacious guidance and Dr. Buoncristiani who—busy as he was—always seemed to find time to help me out with the physics.

The support for this research was provided by a fellowship (NGT-50346) under the NASA Graduate Researchers Program. I would like to express my

appreciation to Dr. Clay Bair, Dr. Phil Brockman and Dr. Bob Hess in the Laser Technology and Applications Branch at NASA Langley for their concern for my work and the many helpful discussions we had.

I would also like to express my gratitude to the math department secretaries, Gayle Tarkelson and Barbara Jeffrey, for being so accommodating and flexible as we shared computers and printers in the preparation of my dissertation. A sincere thank you is in order for Barbara for steering me through a labyrinth of administrative paperwork and whose expertise at LaTeX most certainly saved me countless hours of frustration.

I would like to thank Dr. John Tweed— chairman of the mathematics department— for the financial support I received during my tenure as a teaching assistant and for his helpfullness at strategic points along the way.

Finally, I would like to thank my wife, Vicky, for the loving support she gave me at every stage of my educational pursuits. Her confidence in my abilities and unwaivering commitment to the children and me have been a constant source of encouragement. Solomon said, (Proverbs 12:4) "A wife of noble character is her husband's crown ..." — she has proven to be a crown of jewels to me.

TABLE OF CONTENTS

List of Figures vi

1 Introduction 1

2 Construction of the Model of the Laser Dynamics 9

2.1 The Physical Processes Considered in the Model 9

2.2 The Photon Equation 24

2.3 The Threshold Condition 29

2.4 The Dopant Population Rate Equations 30

2.5 Normalization and Initial Conditions 41

3 Qualitative Properties of the Solution 45

3.1 The Modified Equations 45

4 Stability Analysis 69

4.1 The Equilibrium Solutions 69

4.2 Local Stability Analysis 74

4.3 Bifurcation Points 82

5 Numerical Solutions, Oscillations, and Q-Switching 88

5.1 Numerical Solutions 88

5.2 Oscillatory Behaviour of the Solutions 96

5.3 Q-Switching 107

5.4 Error Analysis 121

6 Upgrading the Model **124**

6.1 Back Transfer & An Alternate Averaging Technique 124

6.2 Up-Conversion 133

6.3 Q-Switching Revisited 145

Bibliography **152**

Appendices

A Computer Program: Findroot 154

B Computer Program: Oldthho 162

C Computer Program: Newthho 172

Autobiographical Statement **183**

LIST OF FIGURES

Figure		Page
2.1	Energy levels of Cr, Tm and Ho in YAG	10
2.2	The overlap between the normalized emission spectrum of Tm and absorption spectrum of Ho in YAG	11
2.3	Emission spectrum of holmium in YAG	12
2.4	A diagram of the radiative processes (a) spontaneous emission, (b) stimulated absorption and (c) stimulated emission	14
2.5	Decay curves for thulium level $^3H_4$	17
2.6	The lifetime of the $^3H_4$ level of thulium (830 nm emission) as a function of the concentration of thulium ions	18
2.7	Decay curves and lifetimes of the 1.8 μm emission at $T = 300K$	19
2.8	Spectroscopic evidence of the back transfer of energy from Ho to Tm in YAG where Ho is pumped in both cases	21
2.9	Spectroscopic evidence of up-conversion in the Tm-Ho:YAG system. (a) Holmium pumped in YAG:Ho(2%) and (b) Thulium pumped in YAG:Tm(6%),Ho(1%)	23
2.10	A Fabrey-Perot cavity of length ℓ_c with the x-axis superimposed over the crystal and pointing in the positive direction	25
2.11	Idealized model of the Tm-Ho:YAG laser representing all processes accounted for in the mathematical model with the exception of spontaneous emission	31
4.1	P coordinate of equilibrium point 2 as a function of W_p	84

4.2 P coordinate of equilibrium point 2 as a function of τ_c 85

4.3 Numerical solution of photon density with $\tau_c = 4.8 \times 10^{-5}$ 86

4.4 Numerical solution of photon density with $\tau_c = 4.9 \times 10^{-5}$ 87

5.1 Numerical solution of the upper thulium energy level, $x(t)$ 91

5.2 Numerical solution of the lower thulium energy level, $y(t)$ 92

5.3 Numerical solution of the upper lasing level, $z(t)$ 93

5.4 Numerical solution of the photon density, $P(t)$ 94

5.5 Numerical solution of the photon density when the pumping term is taken to be of the form $W_p(t) = \alpha t e^{-\alpha^2 t^2}$ 97

5.6 Upper lasing level of holmium and the photon density with a constant pumping term 98

5.7 Photon density plotted on a stretched time scale 104

5.8 One of the discriminants (DISC1) associated with the time dependent characteristic equation of the linearized system showing oscillations beginning at the onset of lasing 105

5.9 DISC1 as a function of τ_c 108

5.10 Normalized upper lasing level when Q-switching at 350 μs 111

5.11 Normalized photon density when Q-switching at 350 μs 112

5.12 Upper lasing level of holmium and photon density plotted together when Q-switching at 350 μs 113

5.13 Upper lasing level of holmium and photon density plotted together over the interval of Q-switching and showing the shape of the output pulse.....114

5.14 All four variables when Q-switching at 170 μs.....115

5.15 All four variables plotted over the interval of Q- switching.....116

5.16 All four variables when Q-switching and holding x and y fixed subsequent to Q-switching.....118

5.17 Normalized upper lasing level of holmium and the photon density when Q-switching and holding x and y fixed subsequent to switching.....119

6.1 Photon density with back transfer turned off and the length of the crystal equal to the length of the optical cavity.....127

6.2 Photon density with back transfer turned on and the length of the crystal equal to the length of the optical cavity.....128

6.3 Photon density with back transfer once again turned off and the length of the crystal not equal to the length of the optical cavity.....129

6.4 Photon density with back transfer turned on and the length of the crystal not equal to the length of the optical cavity.....130

6.5 Photon density plotted on a stretched time scale.....131

6.6 The energy output of the Tm-Ho:YAG laser as displayed on the screen of an oscilloscope in the laboratory.....132

6.7 Deviation as a function of time.....136

6.8 A graph of the element of the Jacobian matrix of maximal absolute value.....137

6.9 Numerical solution of the photon density with the up-conversion level included in the model 138

6.10 Numerical solution of the photon density with the up-conversion level excluded from the model 139

6.11 The difference between the numerical solution to the system including up-conversion and the numerical solution to the system excluding up-conversion 141

6.12 The difference between the numerical solution to the photon density in the system including up-conversion and the numerical solution to the photon density in the system excluding up-conversion 142

6.13 Upper lasing level and photon density plotted together with up-conversion level included in the model 143

6.14 Phase portrait of upper lasing level and photon density 144

6.15 Upper lasing level when Q-switching at 180 μs and up-conversion level included in the model 146

6.16 Photon density when Q-switching at 180 μs and up-conversion level included in the model 147

6.17 Upper lasing level when Q-switching is delayed until 250 μs and up-conversion is included in the model 148

6.18 Photon density when Q-switching is delayed until 250 μs and up-conversion is included in the model 149

6.19 Upper lasing level when Q-switching at 250 μs and the up-conversion parameter has been decreased 150

6.20 Photon density when Q-switching at 250 μs and the up-conversion parameter has been decreased 151

Chapter 1

Introduction

In 1916 Albert Einstein conceived the idea of stimulated emission of radiation. Prior to that time physicists believed that a photon could interact with an atom in only two ways: it could be absorbed thereby raising the atom to a higher energy level or it could be spontaneously emitted as the atom dropped to a lower energy level. Einstein advanced a third possibility — that a photon with energy corresponding to that of an energy level transition could stimulate an atom in the upper level to drop to the lower level, in the process stimulating the emission of another photon with the same energy as the first.

The first one to utilize the concept of stimulated emission was Charles H. Townes, one of the inventors of the *maser*—an acronym coined by Townes to stand for *m*icrowave *a*mplification by *s*timulated *e*mission of *r*adiation. Townes, collaborating with colleague Herbert Zeiger and graduate student James P. Gordon, had a working maser by 1953 [14]. At about the same time, A.M.Prokhorov

and N.G.Basov achieved similar results in the Soviet Union and later shared the Nobel Prize with Townes.

It wasn't long before physicists and others began looking beyond the microwave region to shorter wavelengths. Townes and Arthur L. Schawlow made pivotal contributions in this area and published their results in a notable paper (Schawlow and Townes,1958) which pointed out important differences between requirements in the microwave and visible regions.

Meanwhile, a Columbia graduate student—Gordon Gould—was working on his own analysis of the requirements for stimulated emission to occur at visible wavelengths. Gould recorded his findings in a set of notebooks dated 1957 but did not publish his results. Consequently, Gould did not receive recognition for laying down the theoretical groundwork for the *laser*; however, he is the one who coined the term —which is an acronym for *l*ight *a*mplification by *s*timulated *e*mission of *r*adiation.

The Schawlow-Townes paper of 1958 proved to be a catalyst for the scientific community, stimulating many new efforts to build lasers. Most researchers—including Schawlow and Gould—thought the best materials for building lasers were gases. However, a physicist at Hughes Research Laboratories— Theodore H. Maiman—preferred synthetic ruby crystals instead. In spite of some theorists insistence that ruby would not work, Maiman persevered. In 1960 he vindicated himself and ushered in a new era by demonstating the world's first laser: a rod of synthetic ruby with reflecting coatings on the ends and surrounded by a helical

flashlamp.

Maiman's demonstration of the ruby laser paved the way for a proliferation of solid-state lasers. Before years end, a second type of solid-state laser was reported by P. P. Sorokin and M.J. Stevenson: trivalent uranium ions doped in calcium fluoride. Then in 1961, L.F. Johnson & K. Nassan demonstrated the first solid-state neodymium laser, in which the neodymium ion was a dopant in calcium tungstate ($CaWO_4$). Three years later the optimal host for most commercial applications—yttrium aluminum garnet (YAG)—was demonstrated as a laser material by Geusic, et.al. [14]. Subsequently, Nd:YAG became the standard solid-state laser material, displacing ruby in many applications.For the remainder of the 60's and throughout the 70's, research and development of solid-state lasers lagged while attention was directed to other types of laser systems.

Around 1980 there was a renewal of interest in solid-state lasers, due in large part to the development and availability of new host materials. At about this time (the early 1980's) NASA began investigating tunable solid-state lasers as promising candidates for the Earth Observing System (Eos). One facet of Eos is active remote sensing of the earth's atmosphere using the *lidar* (*li*ght *d*etection *a*nd *r*anging) and *dial* (*di*fferential *a*bsorption and *l*idar) techniques. These techniques measure the distribution of various chemical components of the earth's atmosphere; for instance, H_2O, CO, CO_2, and CH_4. Two of the more prominent tunable solid-state lasers are alexandrite and titanium-doped

sapphire.

The alexandrite (Cr^{3+} :$BeAl_2O_4$) laser which can operate at wavelengths ranging from 700 to 800 nm is being developed for an autonomous DIAL experiment in which it will make range resolved measurements of atmospheric water vapor, pressure, and temperature [1].

A newer laser—Titanium-doped Sapphire (Ti^{3+} :Al_2O_3)—is tunable from 660 nm to about 986 nm, a range which encompasses the 940 nm spectral lines of water. Ti:Sapphire was discovered in 1982 by P.F. Moulton who later (1985) reported on its performance capabilities and spectroscopic measurements [17]. Also in 1985, the temperature dependence of lifetimes in Ti:Sapphire was studied by C.E. Byvik and A.M. Buoncrisiani [11]. In 1986, P. Brockman et. al. [7] performed pulsed injection control (also known as injection seeding) on the Ti:Sapphire laser. From 1986–1988, L.F. Roberts, J.J. Swetits, and A.M. Buoncristiani conducted research on the Ti:Sapphire laser by employing a mathematical model which accurately accounted for the dynamical processes taking place in the active medium [10]. In order to ascertain the suitability of using the Ti:Sapphire laser as a possible replacement for the alexandrite laser many aspects of the laser had to be studied; for example, injection seeding, quantum efficiency, and stability. The Ti:Sapphire laser was found to be a viable tunable laser capable of satisfying the stringent requirements imposed by atmospheric scientists for remote sensing. Recently, F. Allario reported [1] that titanium-doped sapphire technology has been proposed by the NASA Langley team for

the LASA (*L*idar *A*tmospheric *S*ounder and *A*ltimeter) facility and as a payload attached to the manned space station (project "TALOS").

During the past several years, research on the optical properties of materials associated with the development of a solid-state laser in the 2 micron region has been conducted. In particular, one likely candidate is the sensitized holmium laser. The sensitized holmium laser operates in the near infra-red region and can be used as a source for both LIDAR and DIAL. In addition, it may be used aboard an aircraft to make Doppler lidar measurements of windshear, since it operates in the eye-safe region.

In a solid-state laser, a dopant ion substitutes directly into the host lattice. When the lanthanide rare earth ion holmium (Ho) is used as a dopant in the host crystal yttrium aluminum garnet ($Y_3\ Al_5\ O_{12}$), the holmium ion substitutes into the yttrium sites. This induces a weak coupling to the host lattice which results in narrower absorption and emission features than those commonly observed in transition metals. Although the holmium laser has high gain and good energy storage properties, ionic interactions among the holmium ions limit the concentration of holmium possible in any host; therefore to increase the optical energy absorbed, a sensitizing ion is included. In the present laser system, the lanthanide rare earth ion thulium (Tm) is used as a sensitizer for holmium.

In order to develop a 2 μm eye-safe laser, based on holmium emission sensitized by thulium, it is essential to understand the inter-ionic energy transfer processes at work within the host material. This is a study of a mathematical

model of an end-pumped holmium laser sensitized by thulium ions, doped in YAG. This laser will be referred to as a Tm-Ho:YAG laser or just Tm-Ho for short.

The model was developed for the Tm-Ho laser, but with slight modifications it may be used for other sensitizer and activator ions. The model comprises two sets of rate equations; one set for thulium and one set for holmium. These two sets, along with the equation for the photon flux, describe the temporal behaviour of the laser system. The purpose of this study is to establish qualitative properties of the solutions using analytic techniques, investigate the local stability of the solutions, examine the effects of Q-switching, study the oscillatory behaviour of the solutions, and finally to subject the model to a numerical treatment and compare the results with experimental data obtained in the laboratory.

In Chapter 2, a mathematical model is derived which describes the temporal evolution of the electron populations in the active medium as well as the photon flux throughout the optical cavity. The optical cavity is taken to be a Fabry-Perot cavity and the laser is assumed to be end pumped. The model is composed of five first order, nonlinear ordinary differential equations.

In Chapter 3, a simplified version of the model is obtained by excluding certain processes. This effectively reduces the system from five nonlinear o.d.e.'s down to four. The following qualitative properties of the solutions are then established: nonnegativity, boundedness, and integrability.

A local stability analysis is conducted in Chapter 4 to determine the stability properties of the equilibrium solutions (also known as steady state solutions, constant solutions, equilibrium points, fixed points, or critical points). The affect on the equilibrium solutions, of varying appropriate physical parameters is examined numerically.

In Chapter 5, a numerical solution to the system is obtained. In the case where the pumping term is constant, i.e.$W_p(t) \equiv W_p$, a comparison is made between the computed solution and the asymptotic solution predicted by the stability analysis. The oscillatory nature of the system is then examined in some detail and a process known as Q-switching is incorporated into the mathematical model.

Chapter 6 is an investigation of back transfer and up-conversion. A study of the qualitative and quantitative influence of these two processes on the solution is performed and a comparison with experimental results is made. Q- switching and up-conversion are then examined concomitantly. Also, an alternate spatial averaging technique for the photon density is discussed.

All computer programs are written in FORTRAN and run on either a DEC VAX 11/750 or an IBM PC. Three computer programs are included in the appendices. Appendix A contains the program that locates the equilibrium points and determines their stability properties. Appendix B contains the program that solves the simplified system of o.d.e.^{s} numerically. It can also track the roots of the characteristic equation associated with the linearized system and

implement Q-switching. Appendix C contains the program that solves the system with back transfer turned on and the holmium up-conversion level included. The modified coefficients—as discussed in Chapter 6—are incorporated into the rate equation for the photon density and various pumping schemes are available.

Chapter 2

Construction of the Model of the Laser Dynamics

2.1 The Physical Processes Considered in the Model

The energy level diagram for the Tm^{3+} ion and the Ho^{3+} ion in YAG is shown in Figure 2.1. The spectrum for thulium emission and holmium absorption is given in Figure 2.2 and the emission spectrum for holmium is given in Figure 2.3. The model comprises thulium ions in energy levels $^3H_4$,$^3F_4$, and $^3H_6$; holmium ions in energy levels $^5I_5$,$^5I_7$, and $^5I_8$; and the photon density in the optical cavity.

Processes considered in the laser system will be divided into two main categories; namely, those processes which are inter-ionic— involving the transfer

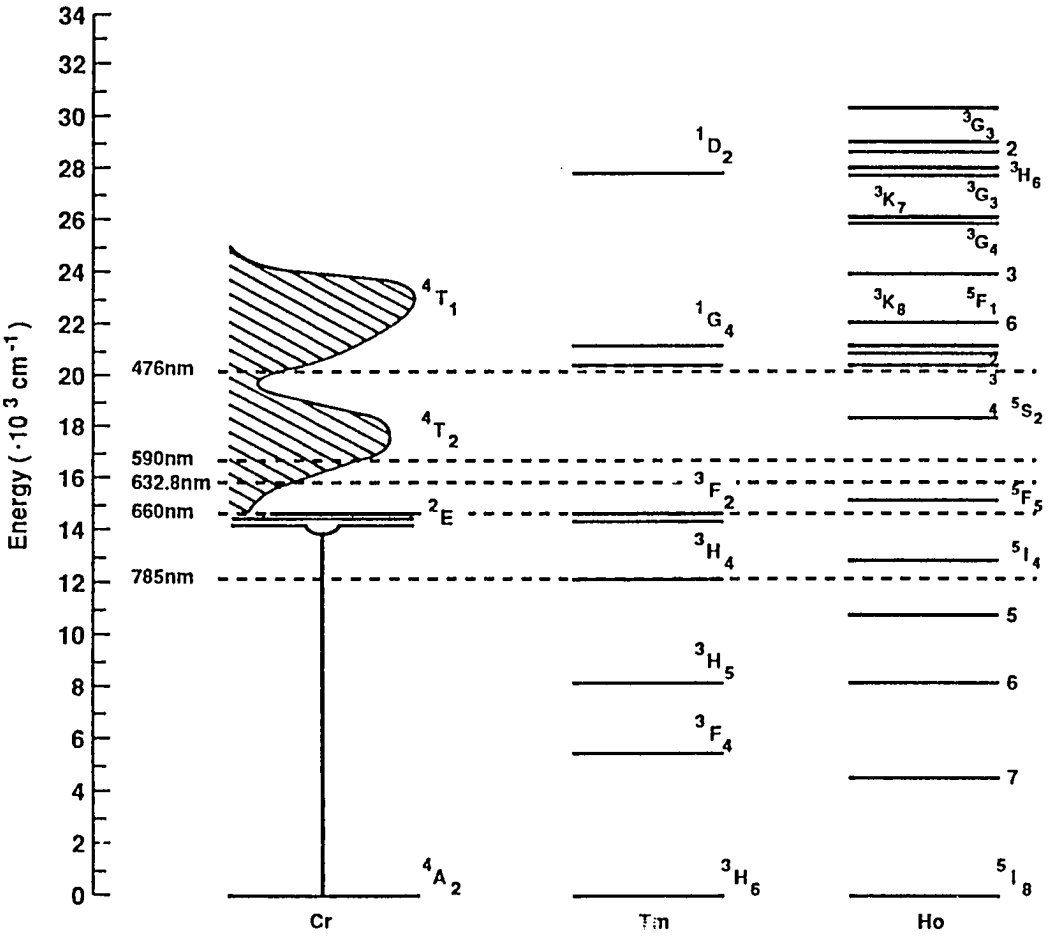

Figure 2.1 Energy levels of Cr, Tm, and Ho in YAG.

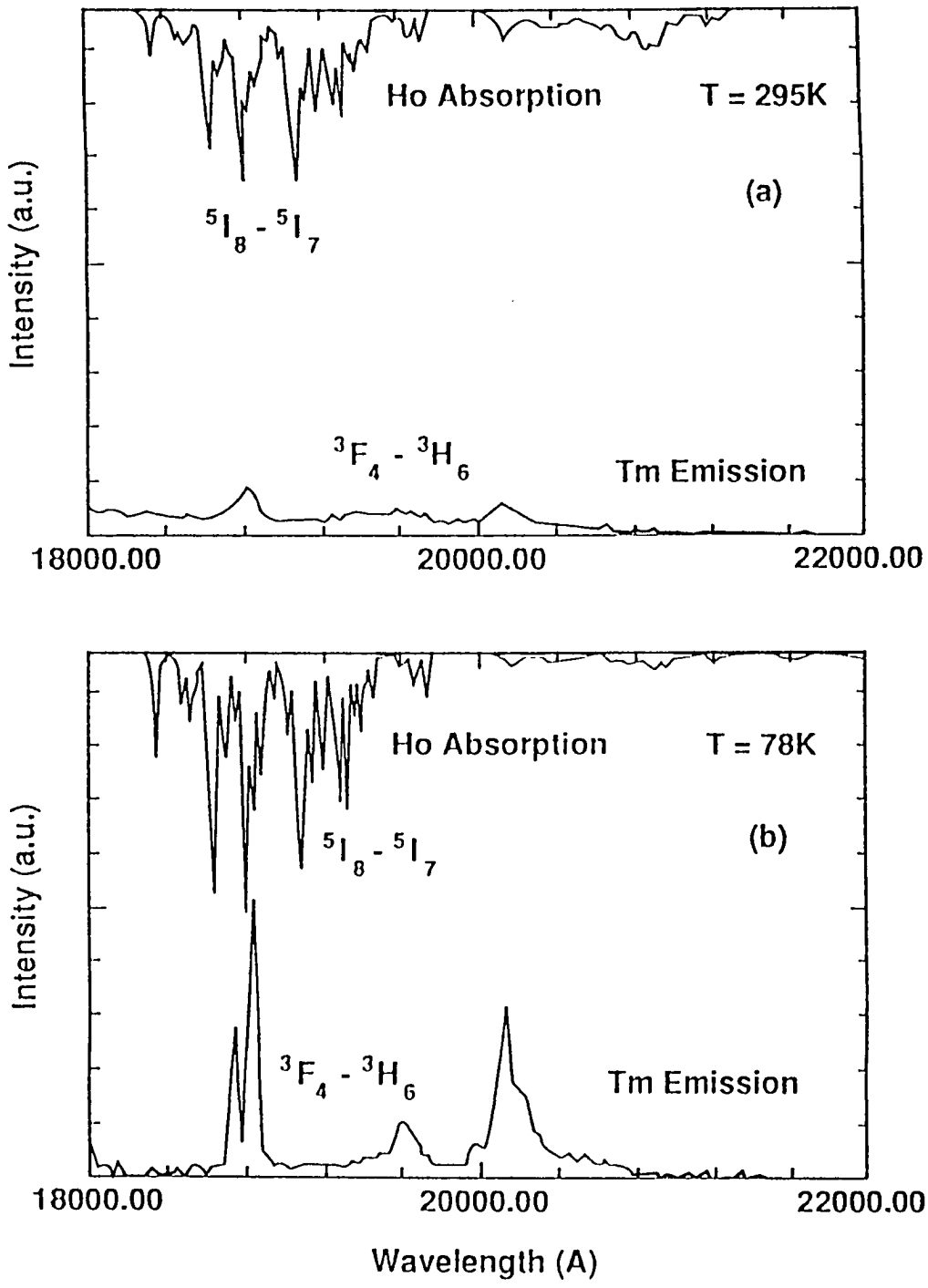

Figure 2.2 The overlap between the normalized emission spectrum of Tm and absorption spectrum of Ho in YAG.

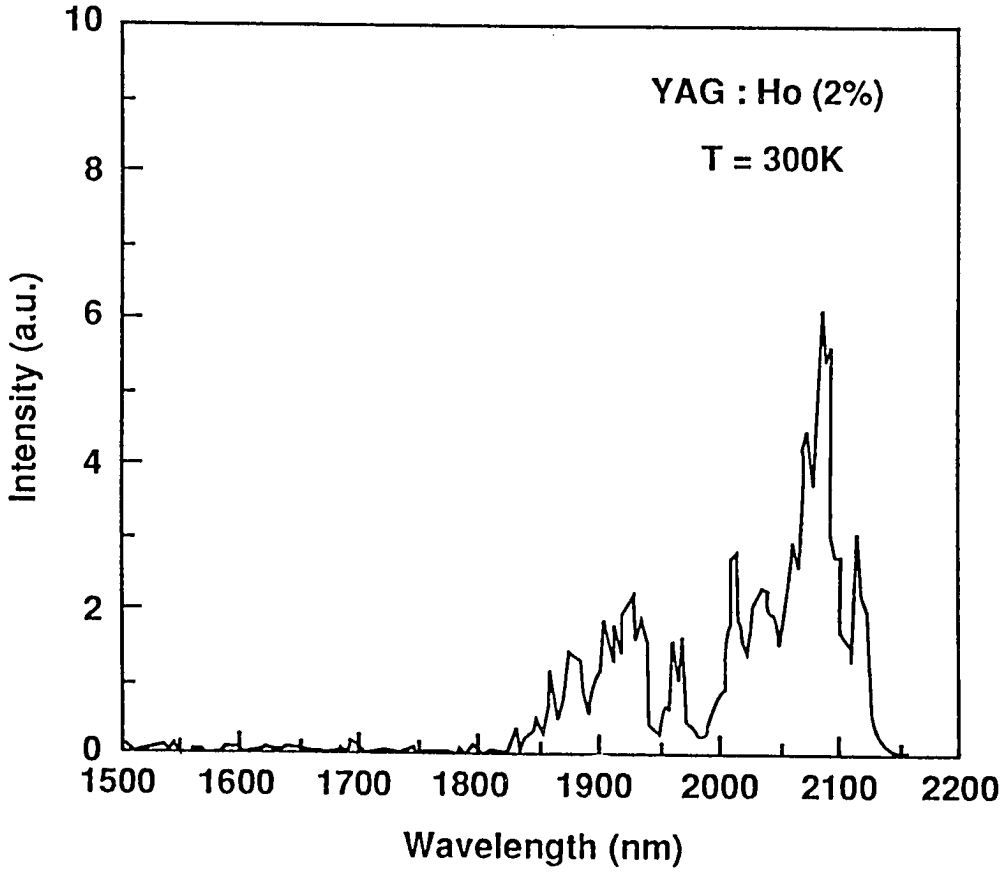

Figure 2.3 Emission spectrum of holmium in YAG.

of an excitation from one ion to another—and those which are not. Inter-ionic processes include: cross relaxation, back transfer, and up conversion. Processes which are not inter-ionic include: spontaneous emission, absorption, and stimulated emission. The latter processes will be considered first.

Spontaneous emission is represented in Figure 2.4 (a). It is characterized by the emission of a photon with energy $h\nu$ when the ion decays from energy level 1 to energy level 0. Here, h is Planck's constant and ν is the frequency of the radiated wave. The probability of spontaneous emission is given in [21] and is denoted A_{10}. A_{10} is also referred to as the Einstein coefficient and represents the rate at which this process occurs. In the laser model, the spontaneous emission lifetime of a holmium ion in the $^5I_7$ energy level (which is the upper lasing level) is denoted τ_1' . This gives the relation $\tau_1' = A_{10}^{-1}$.

Stimulated absorption is represented in Figure 2.4 (b). The rate at which stimulated absorption occurs, W_{01}, can be written [21]

$$W_{01}(t;\lambda) = \sigma_{01}(\lambda)F(t;\lambda) \tag{2.1.1}$$

where λ is the wavelength, $\sigma_{01}(\lambda)$ is called the absorption cross section and represents the probability of an atom absorbing energy from a passing photon, and $F(t;\lambda)$ is the photon flux of the incident wave at time t .

Stimulated emission is represented in Figure 2.4 (c). The rate at which stimulated emission occurs, W_{10}, can be written [21]

$$W_{10}(t;\lambda) = \sigma_{10}(\lambda)F(t;\lambda) \tag{2.1.2}$$

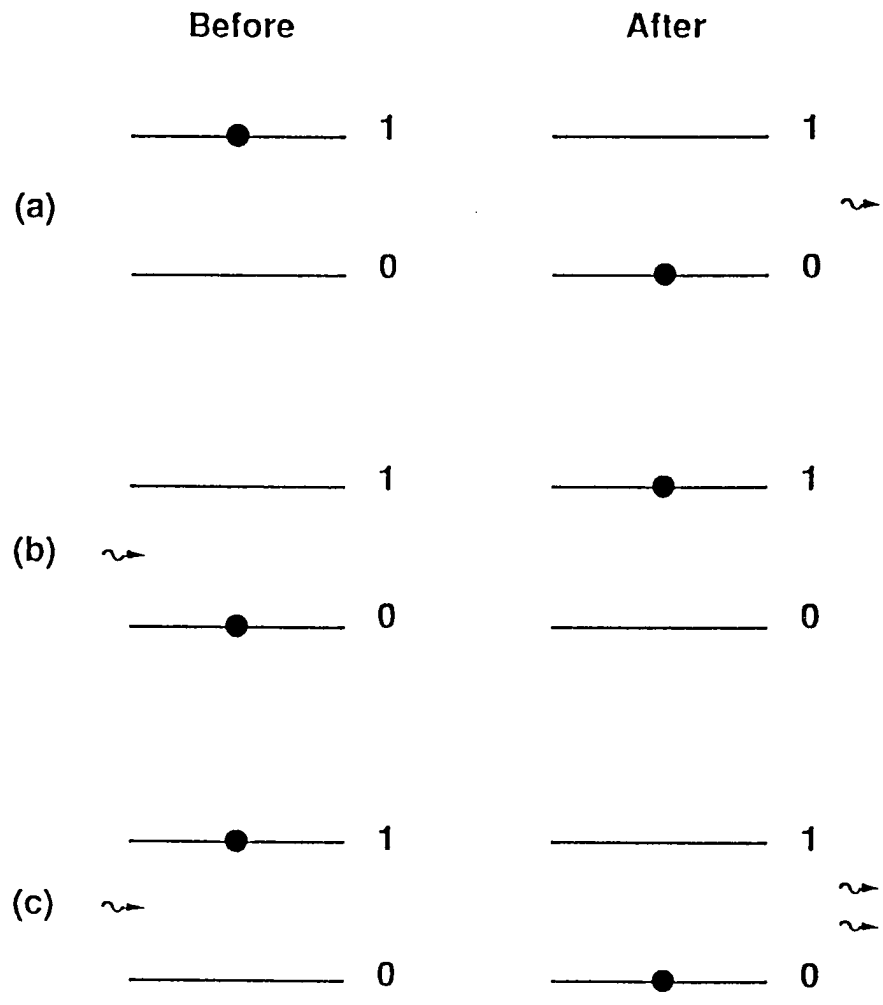

Figure 2.4 A diagram of the radiative processes (a)spontaneous emission,(b)stimulated absorption, and (c)stimulated emission

where $\sigma_{10}(\lambda)$ is the emission cross section and represents the probability of an atom being stimulated, by a passing photon, to emit its energy . Einstein showed that, for a two level system, the probability of stimulated emission is equal to the probability of stimulated absorption. Hence, from now on let $\sigma_{01}(\lambda) = \sigma_{10}(\lambda) = \sigma(\lambda)$, where $\sigma(\lambda)$ will be referred to as the "transition cross section". Also, the number of electrons (per unit volume) in a given level will be referred to as the "population" of that level.

The following inter-ionic processes increase the efficiency of the Tm-Ho laser but at the cost of introducing more nonlinearities into the model. These nonlinearities make both the analysis and the laser dynamics significantly different than solid-state laser dynamics studied previously. It should be noted that all of the inter-ionic processes considered here are non-radiative processes.

The first process considered is called cross relaxation and is depicted in Diagram 2.1.

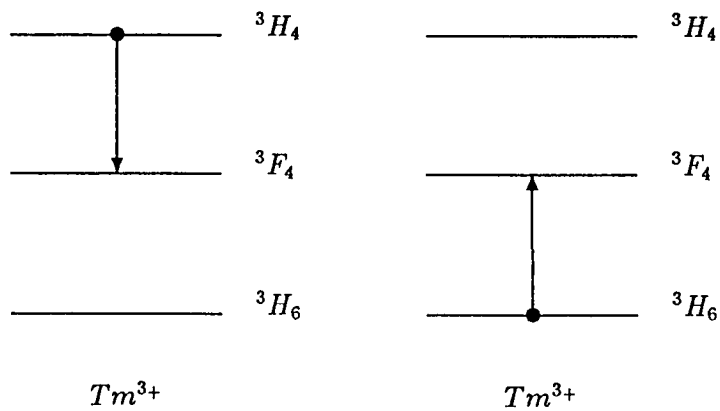

Diagram 2.1

In cross relaxation, a thulium ion in energy level $^3H_4$ loses energy and goes to

energy level $^3F_4$; a "nearby" thulium ion in ground level $^3H_6$ gains this energy thus raising it to energy level $^3F_4$. How "near" two thulium ions must be for this process to occur and the probability of cross relaxation occurring are addressed in [12]. Figure 2.5 gives spectroscopic evidence in support of cross relaxation in thulium. From this it is seen that the upper thulium energy level,$^3H_4$, decays faster at higher concentrations of thulium. Furthermore,D.L. Dexter and J.H. Schulman [12] give an expression for the lifetime of a thulium ion in energy level $^3H_4$ as a function of the thulium concentration; this is given in Figure 2.6 . In the model, the probability of cross relaxation occurring is denoted by C.

The second inter-ionic process considered, forward transfer, is represented in Diagram 2.2.

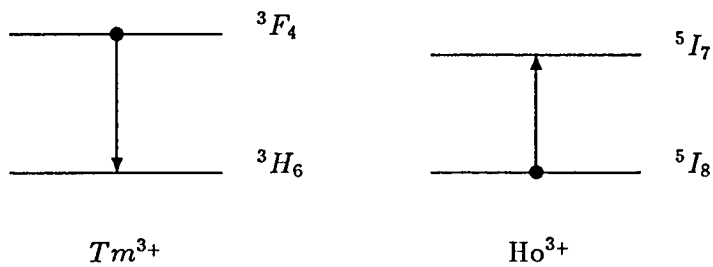

Diagram 2.2

In forward transfer, a thulium ion in energy level $^3F_4$ loses energy and goes to level $^3H_6$; a nearby holmium ion in energy level $^5I_8$ gains this energy and is raised to level $^5I_7$. This results in a forward transfer of energy from thulium to holmium. Figure 2.7 shows decay curves which are indicative of forward transfer. The probability of this process occuring is denoted by C_1 .

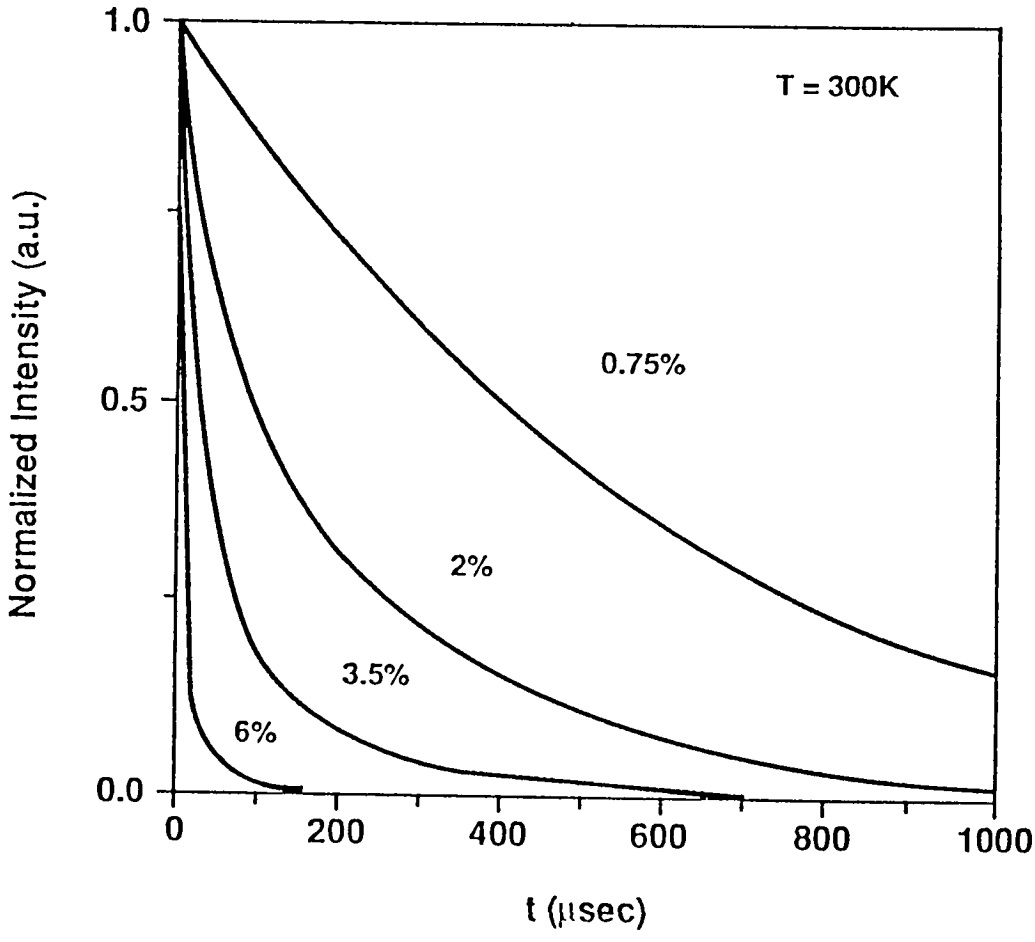

Figure 2.5 Decay curves for thulium level $^3H_4$.

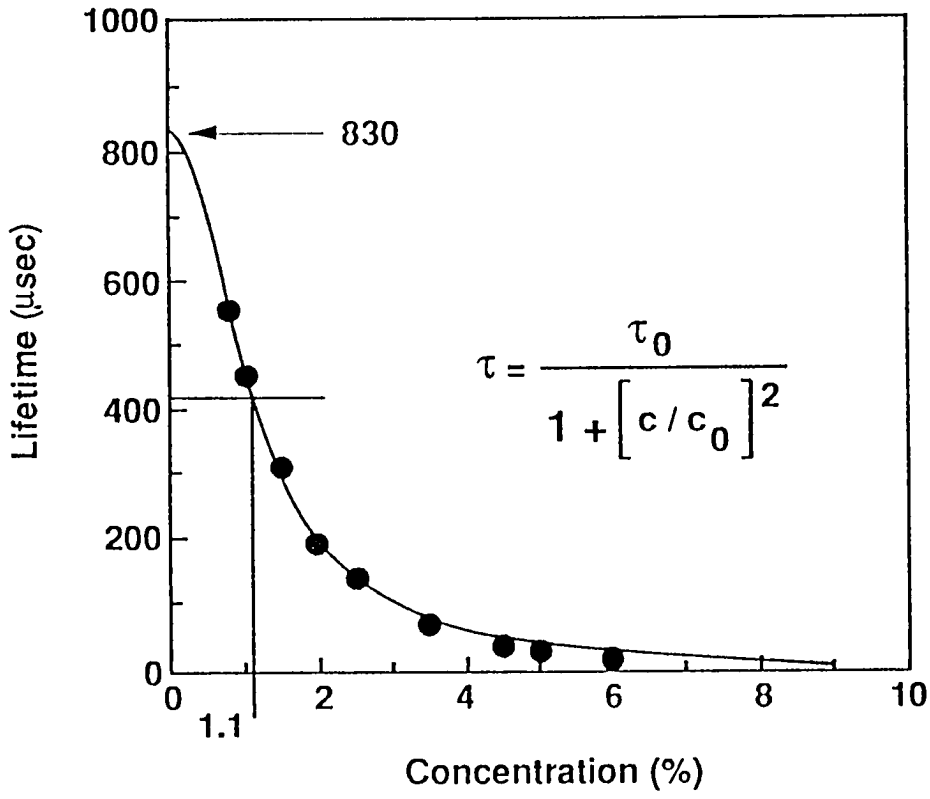

Figure 2.6 The lifetime of the $^3H_4$ level of Tm (830 nm emission) as a function of Tm concentration.

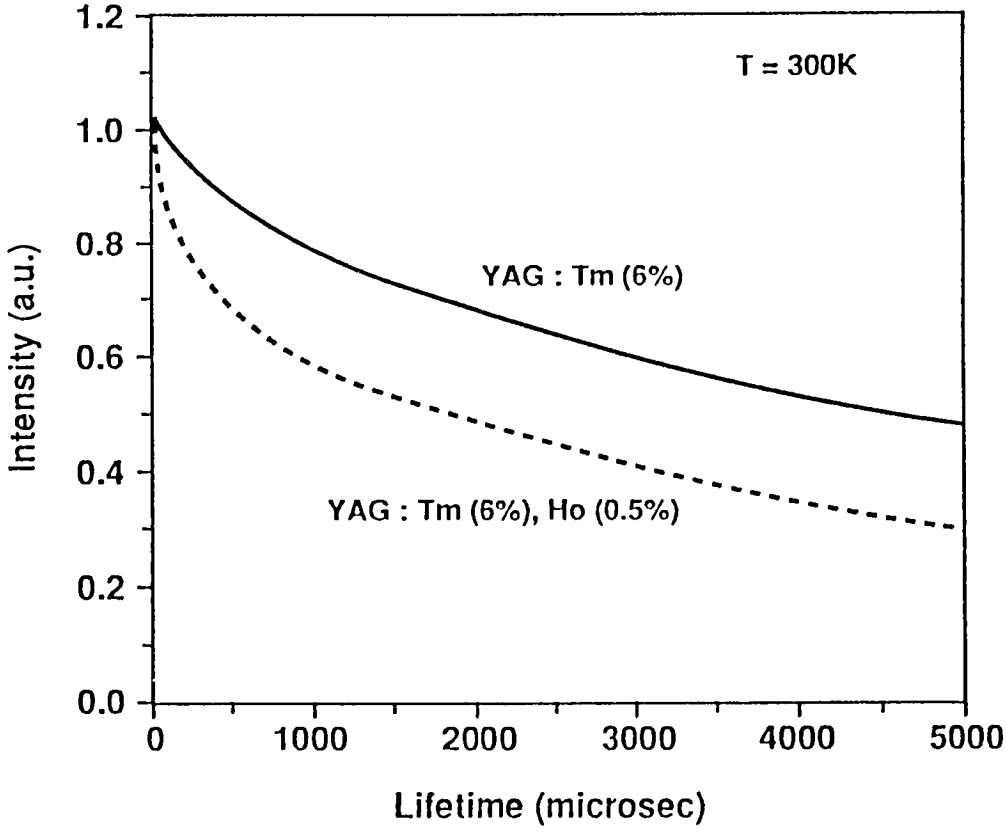

Figure 2.7 Decay curves and lifetimes of the 1.8 micrometer emission at T=300K.

The inverse of this process, back transfer, is depicted in Diagram 2.3 below.

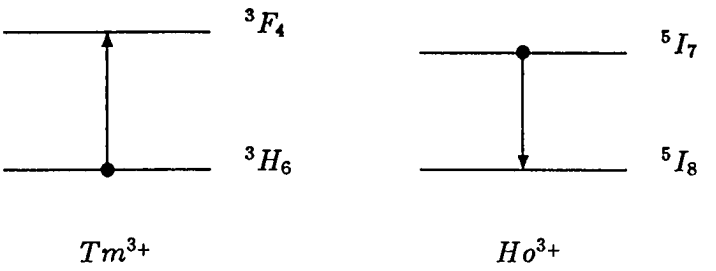

Diagram 2.3

In back transfer, a holmium ion in energy level $^5I_7$ loses energy and goes to energy level $^5I_8$; a nearby thulium ion in energy level $^3H_6$ gains this energy and is raised to energy level $^3F_4$. Spectroscopic evidence, indicative of back transfer, was reported in [2] and is seen in Figure 2.8 . The net result is a transfer of energy from holmium back to thulium. The probability of back transfer occurring is denoted by C_1^* .

The last inter-ionic process considered is up-conversion which is illustrated in Diagram 2.4.

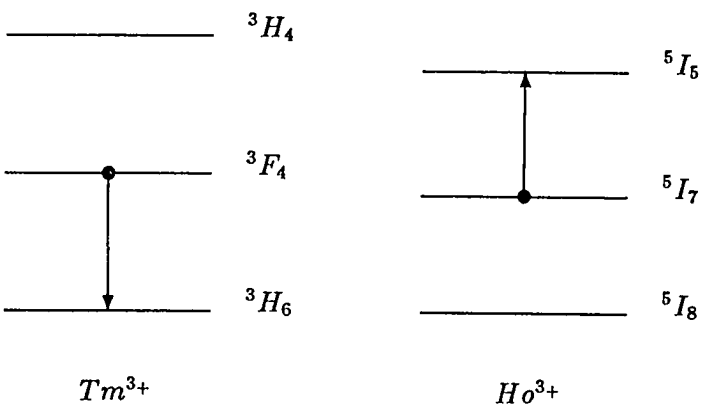

Diagram 2.4

In up-conversion, a thulium ion in energy level $^3F_4$ loses energy thereby going

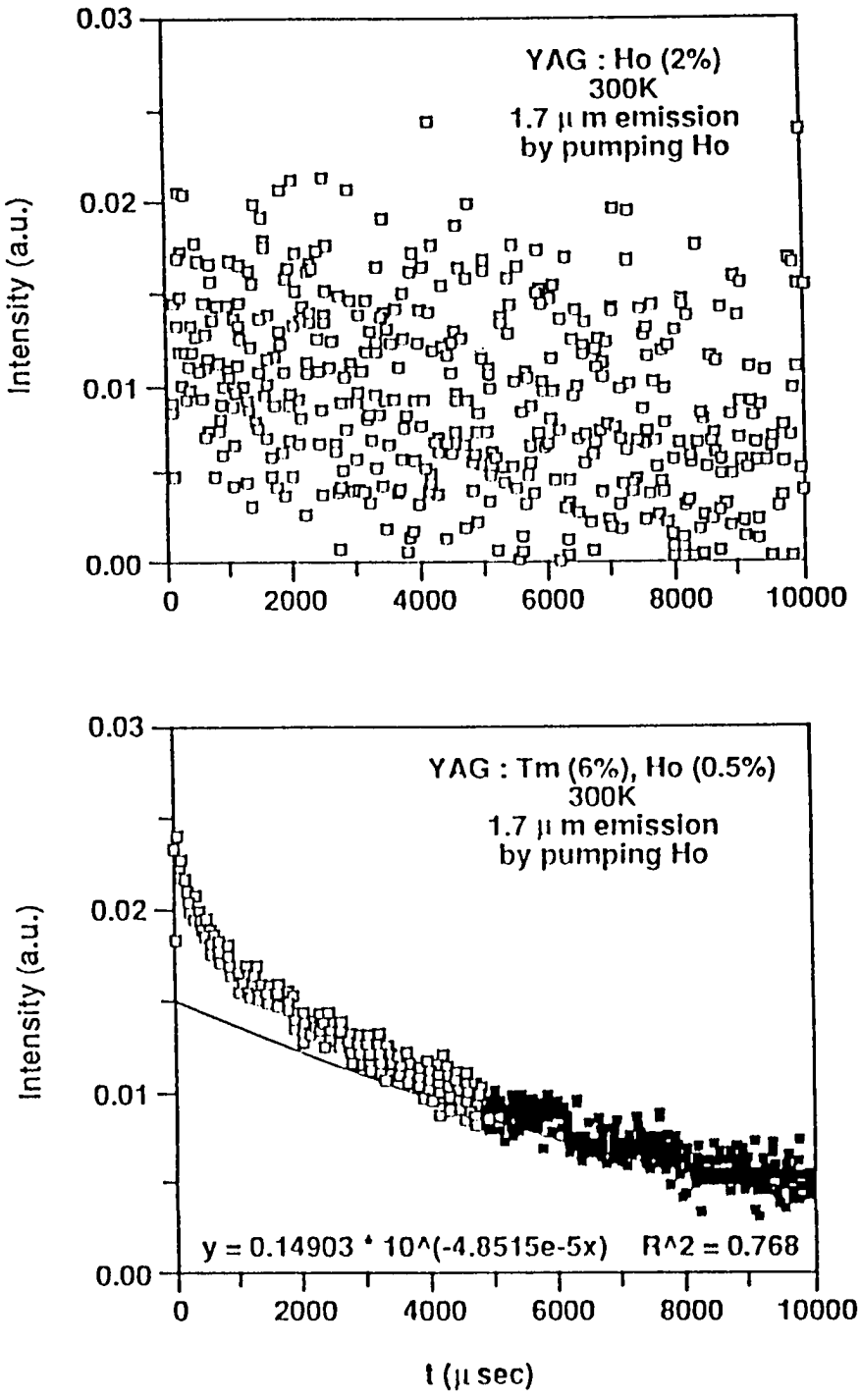

Figure 2.8 Indication of back transfer from Ho to Tm in YAG where holmium is pumped in both cases.

to energy level $^3H_6$; a nearby holmium ion in energy level $^5I_7$ gains this energy and is raised to level $^5I_5$. This results in a transfer of energy from the thulium $^3F_4$ level up to the holmium $^5I_5$ level. The probability of up-conversion taking place is denoted by q_1 . Spectroscopic evidence of up-conversion in the Tm-Ho laser was reported in [2] and is seen in Figure 2.9 .

The inverse process of up-conversion, call it down-conversion, is illustrated in Diagram 2.5.

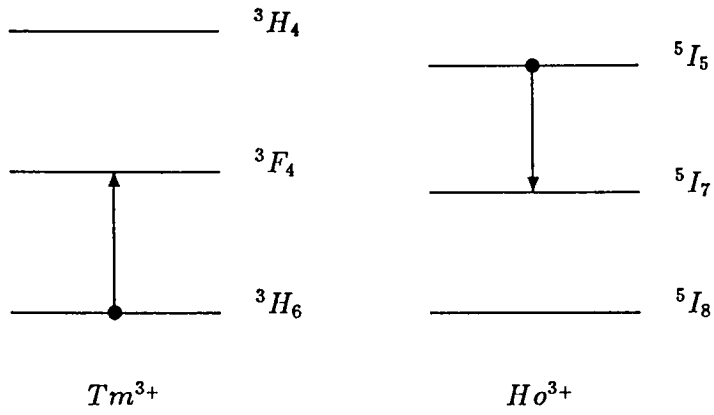

Diagram 2.5

In this process, a holmium ion in energy level $^5I_5$ loses energy and goes to level $^5I_7$; a nearby thulium ion in energy level $^3H_6$ gains this energy and is raised to level $^3F_4$. The result is a transfer of energy from the holmium $^5I_5$ energy level down to the thulium $^3F_4$ energy level. The probability of this process taking place is denoted by q_1' .

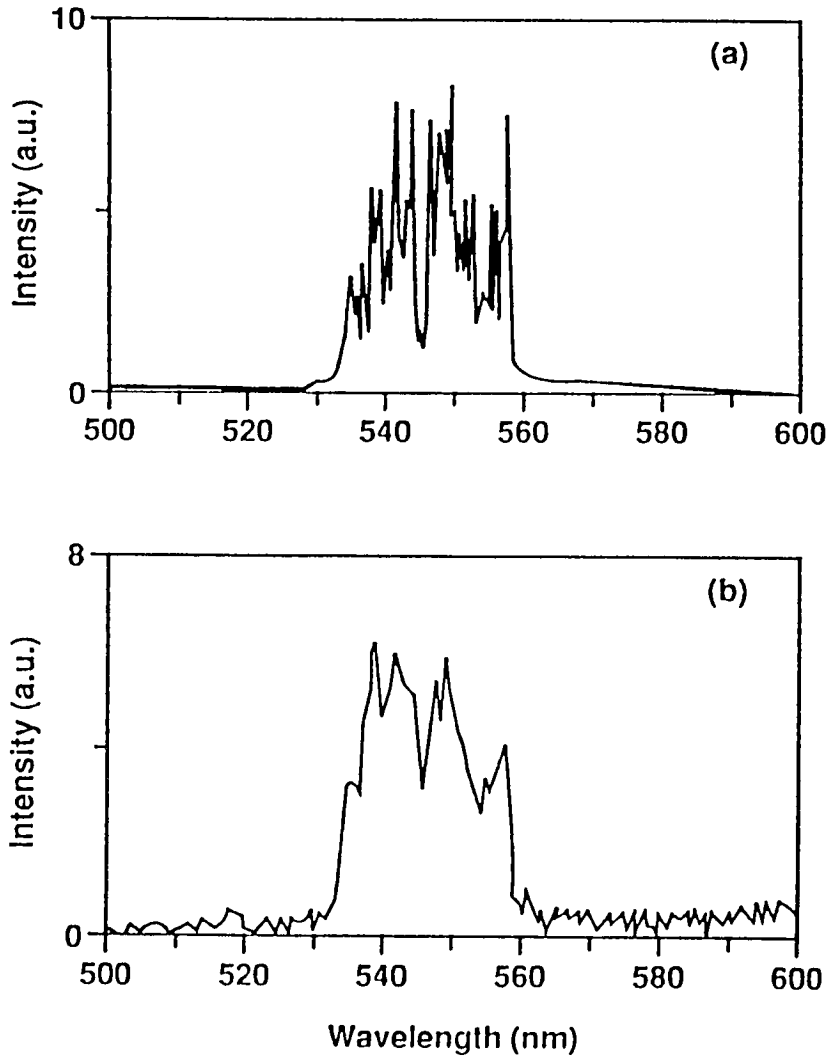

Figure 2.9 Indication of up-conversion in the Tm-Ho system.(a)Holmium pumped in YAG:Ho(2%) (b)Thulium pumped in YAG:Tm(6%),Ho(1%)

2.2 The Photon Equation

In this section we develop the equation which describes the change in the photon flux as it traverses the optical cavity. Throughout this discussion, the crystal is taken to be within a Fabrey-Perot cavity as in Figure 2.10 .

Consider two energy levels, 0 and 1, of a given material. If a plane wave with intensity corresponding to photon flux $F_+(t;\lambda)$ is traveling in the positive x direction in the material, the elemental change of this flux due to both stimulated emission and absorption processes is given by

$$dF_+(t;\lambda) = \sigma(\lambda)F_+(t;\lambda)\left(n_1(t) - n_0(t)\right)dx \tag{2.2.1}$$

where $n_0(t)$ & $n_1(t)$ are the number of atoms in energy level 0 & 1 , respectively and $\sigma(\lambda)$ is the transition cross section at wavelenth λ . This is illustated below in Diagram 2.6.

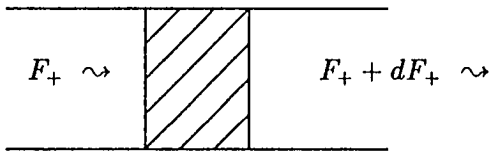

Diagram 2.6

If there are g_1 manifolds associated with energy level 1 and g_0 manifolds associated with energy level 0, then equation (2.2.1) must be replaced by

$$dF_+(t;\lambda) = \sigma(\lambda)F_+(t;\lambda)\left(n_1(t) - \frac{g_1}{g_0}n_0(t)\right)dx \tag{2.2.2}$$

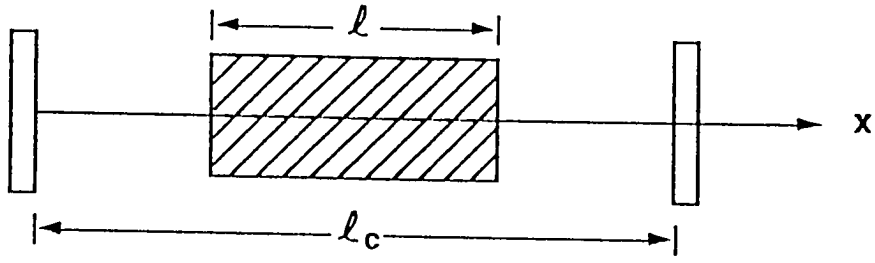

Figure 2.10 A Fabrey-Perot cavity of length ℓ_c with the x axis superimposed over the crystal and pointing in the positive direction

For the instantaneous rate of change in the right traveling photon flux with respect to time, divide through by dt in equation (2.2.2) .This yields

$$\frac{dF_+(t;\lambda)}{dt} = v\sigma(\lambda)F_+(t;\lambda)\left(n_1(t) - \frac{g_1}{g_0}n_0(t)\right) \tag{2.2.3}$$

where we have used $\frac{dx}{dt} = \frac{c}{n} = v$. Here n denotes the index of refraction in the active medium, c denotes the velocity of light in vacuo, v is the velocity of light in the laser crystal and x is the direction parallel to the major axis of the laser crystal as indicated in Figure 2.10.

Similarly, denoting the left traveling photons by $F_-(t;\lambda)$ we obtain

$$\frac{dF_-(t;\lambda)}{dt} = v\sigma(\lambda)F_-(t;\lambda)\left(n_1(t) - \frac{g_1}{g_0}n_0(t)\right) \tag{2.2.4}$$

The rate at which spontaneous emission from level 1 to level 0 occurs is denoted by $\frac{1}{\tau_1'}$. Only those photons emitted in the positive or negative x direction will contribute to the photon flux in the crystal. We denote these by $s_+(t;\lambda)$ & $s_-(t;\lambda)$, respectively. Incorporating these quantities into equations (2.2.3) and (2.2.4) yields

$$\begin{aligned}\frac{dF_+(t;\lambda)}{dt} &= v\sigma(\lambda)F_+(t;\lambda)\left(n_1(t) - \frac{g_1}{g_0}n_0(t)\right) + s_+(t;\lambda)\\ \\ \frac{dF_-(t;\lambda)}{dt} &= v\sigma(\lambda)F_-(t;\lambda)\left(n_1(t) - \frac{g_1}{g_0}n_0(t)\right) + s_-(t;\lambda)\end{aligned} \tag{2.2.5}$$

Now let $F(t;\lambda)$ be the total photon flux in both directions at wavelength λ, so

$$F(t;\lambda) = F_+(t;\lambda) + F_-(t;\lambda). \tag{2.2.6}$$

Also let s be the total number of photons contributing to the photon flux in either direction due to spontaneous emission at wavelength λ, so

$$s(t;\lambda) = s_+(t;\lambda) + s_-(t;\lambda). \tag{2.2.7}$$

Adding the two equations in (2.2.5) and using (2.2.6) and (2.2.7) we obtain

$$\frac{dF(t;\lambda)}{dt} = v\sigma(\lambda)F(t;\lambda)\left(n_1(t) - \frac{g_1}{g_0}n_0(t)\right) + s(t;\lambda). \tag{2.2.8}$$

The rate of spontaneous emission, $\frac{1}{\tau_1'}$, can be written

$$\frac{1}{\tau_1'} = \frac{1}{\tau_{fl}} + \frac{1}{\tau_{nr}}$$

where τ_{fl} is the fluorescent lifetime of the material and $\frac{1}{\tau_{nr}}$ is the transition rate for non-radiative transitions [9]. The spontaneous emission function, $s(t;\lambda)$, can be expressed as a product of two terms [9] as follows

$$s(t;\lambda) = \frac{n_1(t)}{\tau_{fl}}\left(8\pi n^2 c\frac{\sigma(\lambda)}{\lambda^4}\tau_{fl}\right)$$

where the first term is the rate of fluorescent decay from the upper lasing level and the second term is the probability of emission at wavelength λ . Equation (2.2.8) can now be written

$$\frac{1}{v}\frac{dF(t;\lambda)}{dt} = \sigma(\lambda)F(t;\lambda)\left(n_1(t) - \frac{g_1}{g_0}n_0(t)\right) + s_\lambda\frac{n_1(t)}{\tau_{fl}} \tag{2.2.9}$$

where s_λ is given by

$$s_\lambda = 8\pi n^3\frac{\sigma(\lambda)}{\lambda^4}\tau_{fl}.$$

The photon flux, $F(t;\lambda)$, is related to the photon density, $\phi(t;\lambda)$, by the equation

$$\phi(t;\lambda) = \frac{1}{v}F(t;\lambda)$$

Substituting this quantity into equation (2.2.9) we obtain the following rate equation for the photon density

$$\frac{d\phi(t;\lambda)}{dt} = v\sigma(\lambda)\phi(t;\lambda)\left(n_1(t) - \frac{g_1}{g_0}n_0(t)\right) + s_\lambda\frac{n_1(t)}{\tau_{fl}} \qquad (2.2.10)$$

The Tm-Ho laser emits at about 2 μm . Hence, we will take $\lambda = \lambda^*$, where λ^* is a wavelength in the 2 micron region. Further, let $\phi(t)$, σ, and sp_o denote the photon density, transition cross section, and the probability of spontaneous emission, respectively, at wavelength λ^*. Equation (2.2.10) now becomes

$$\frac{d\phi(t)}{dt} = v\sigma\phi(t)\left(n_1(t) - \frac{g_1}{g_0}n_0(t)\right) + sp_o\frac{n_1(t)}{\tau_{fl}}. \qquad (2.2.11)$$

The lifetime of a photon in the cavity will be denoted by τ_c , the length of the optical cavity by ℓ_c , and the reflectivity of the two mirrors by R_1 & R_2 . The cavity lifetime, τ_c, can also be thought of as the decay time for photons in the optical resonator; as such, it represents all the losses in the optical resonator of the laser oscillator. It can be expressed [21] as

$$\tau_c = \frac{2\ell_c/c}{-\ln R_1R_2}.$$

Since τ_c is the lifetime of a photon in the optical resonator, $\frac{1}{\tau_c}$ represents the rate at which photons leave the optical cavity. Therefore, the total number of photons leaving the cavity at time t, due to losses in the optical resonator, is given by

$$\frac{\phi(t)}{\tau_c}.$$

Incorporating this loss term into equation (2.2.11) we obtain the following rate equation for the photon density, which is valid throughout the optical cavity

$$\frac{d\phi(t)}{dt} = v\sigma\phi(t)\left(n_1(t) - \frac{g_1}{g_0}n_0(t)\right) - \frac{\phi(t)}{\tau_c} + sp_o\frac{n_1(t)}{\tau_{fl}}. \tag{2.2.12}$$

2.3 The Threshold Condition

Before oscillations can occur a threshold condition must be achieved. Oscillations will begin when the gain of the active medium compensates for the losses in the laser. Assuming sp_o is negligible close to threshold we take $sp_o \equiv 0$ in equation (2.2.12). We then have

$$\dot{\phi}(t) = \left(v\sigma\left(n_1(t) - \frac{g_1}{g_0}n_0(t)\right) - \frac{1}{\tau_c}\right)\phi(t) \tag{2.3.1}$$

where $\dot{\phi} \equiv \frac{d\phi}{dt}$. The gain in the photon density will exactly compensate for the losses when

$$v\sigma\left(n_1 - \frac{g_1}{g_0}n_0\right) - \frac{1}{\tau_c} = 0. \tag{2.3.2}$$

The values of n_1 & n_0 which satisfy equation (2.3.2) are called equilibrium values and will be denoted by $\bar{n}_1$ & $\bar{n}_0$, respectively. With this notation, equation (2.3.2) becomes

$$\bar{n}_1 - \frac{g_1}{g_0}\bar{n}_0 = \frac{1}{v\sigma\tau_c} \tag{2.3.3}$$

If $n_1(t) - \frac{g_1}{g_0}n_0(t) > 0$, then the laser crystal will act as an amplifier in which case we say there exists a "population inversion" in the material. When $n_1(t)$ & $n_0(t)$ attain their equilibrium values, i.e. satisfy equation (2.3.3), the system is on the

threshold of lasing. Hence, a necessary condition for lasing to occur is that the following inequality be satisfied.

$$n_1(t) - \frac{g_1}{g_0} n_0(t) \; > \; \frac{1}{v\sigma\tau_c}. \tag{2.3.4}$$

When this happens, photons which are spontaneously emitted along the cavity axis will initiate the amplification process. Oscillations are introduced into the system by placing the crystal between two highly reflective mirrors. This causes photons traveling along the main axis of the crystal to bounce back and forth between the two mirrors, thus amplifying the photon density on each pass through the active medium. One of the mirrors is made partially transparent so the laser beam can be extracted from the optical cavity. This capability of amplifying the photon density — when a population inversion exists— is the *sine qua non* of laser systems.

2.4 The Dopant Population Rate Equations

The energy level diagram, Figure 2.1, is the basis for the idealized model, Figure 2.11, of lasing action in Tm-Ho:YAG. For the remainder of the discussion the following correspondence is made as a matter of notational convenience: thulium energy levels $^3H_6$, $^3F_4$, and $^3H_4$ correspond to energy levels 0,1, and 2, respectively and holmium energy levels $^5I_8$, $^5I_7$, and $^5I_5$ correspond to energy levels 0′,1′, and 2′ respectively. The number of thulium ions, per cm^3, in energy level i and at time t will be denoted $N_i(t)$; $i = 0, 1, 2$. Similarly, the number of

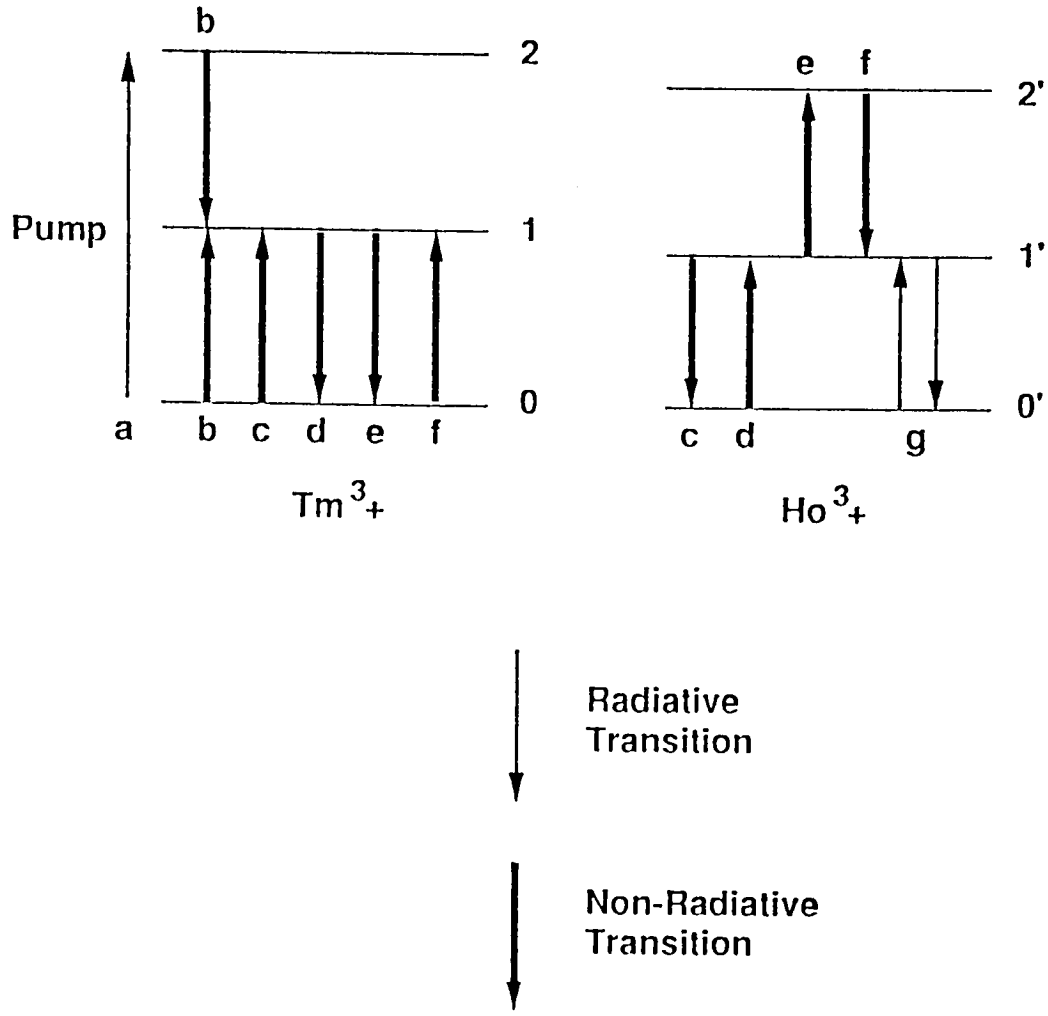

Figure 2.11 Idealized model of the Tm-Ho:YAG laser with the following processes:(a) Stimulated Absorption,(b) Cross Relaxation,(c) Back Transfer,(d) Forward Transfer,(e) Up Conversion,(f) Down Conversion,and (g)Stimulated Emission

holmium ions, per cm^3, in energy level i' and at time t will be denoted $n_i(t)$; $i = 0, 1, 2$.

The electron populations of thulium and holmium are constrained by the relations

$$N_T = N_0(t) + N_1(t) + N_2(t) \tag{2.4.1}$$

and

$$n_T = n_0(t) + n_1(t) + n_2(t) \tag{2.4.2}$$

where N_T is the concentration of thulium ions, per cm^3, and n_T is the concentration of holmium ions, per cm^3.

The crystal is end pumped at a wavelength within the absorption band of thulium. Hence, thulium electrons in the ground state are excited to level 2 at a rate

$$W_p(t)N_0(t)$$

where $W_p(t)$ is called the pumping rate and represents the number of photons, per microsecond (μs), available to excite electrons in energy level 0 to energy level 2. These excited electrons decay to the lower energy levels, due to spontaneous emission, at the rate

$$\frac{N_2(t)}{\tau_2} = \frac{N_2(t)}{\tau_{20}} + \frac{N_2(t)}{\tau_{21}}$$

where $\frac{1}{\tau_{20}}$ & $\frac{1}{\tau_{21}}$ represent the transition rates from energy level 2 to energy levels 0 & 1, respectively. Level 2 is also depopulated due to cross relaxation at

the rate

$$CN_0(t)N_2(t).$$

Therefore, the rate equation for the electron population density of energy level 2 is given by

$$\frac{dN_2(t)}{dt} = W_p(t)N_0(t) - \frac{N_2(t)}{\tau_2} - CN_0(t)N_2(t). \tag{2.4.3}$$

Electrons arrive in level 1 from level 2 at the rate

$$\frac{N_2(t)}{\tau_{21}}$$

and decay to the ground level, due to spontaneous emission, at the rate

$$\frac{N_1(t)}{\tau_1}.$$

Electrons are added to level 1 due to cross relaxation at the rate

$$2CN_0(t)N_2(t).$$

Level 1 is also populated due to back transfer. This is represented by the term

$$C_1^* N_0(t)n_1(t),$$

and depopulated due to forward transfer at the rate

$$C_1 N_1(t)n_0(t).$$

Finally, electrons leave level 1 due to up-conversion at the rate

$$q_1 n_1(t)N_1(t)$$

and arrive in level 1 due to down-conversion at the rate

$$q_1' N_0(t) n_2(t).$$

Hence, the rate equation for the electron population of energy level 1 is given by

$$\frac{dN_1(t)}{dt} = \frac{N_2(t)}{\tau_{21}} - \frac{N_1(t)}{\tau_1} + 2CN_0(t)N_2(t) + C_1^* N_0(t) n_1(t)$$

$$- C_1 N_1(t) n_0(t) + q_1' N_0(t) n_2(t) - q_1 N_1(t) n_1(t). \qquad (2.4.4)$$

Level 0 is depopulated due to excitation at the rate

$$W_p(t) N_0(t).$$

It is populated, due to spontaneous emission of upper level electrons, at the rate

$$\frac{N_2(t)}{\tau_{20}} + \frac{N_1(t)}{\tau_1}.$$

Level 0 loses electrons due to cross relaxation at the rate

$$CN_0(t)N_2(t).$$

Electrons are added to level 0 due to forward transfer at the rate

$$C_1 N_1(t) n_0(t)$$

and are lost due to back transfer at the rate

$$C_1^* N_0(t) n_1(t).$$

Finally, the population of level 0 will be incremented due to up-conversion by the amount

$$q_1 N_1(t) n_1(t)$$

and decremented due to down-conversion by the amount

$$q_1' N_0(t) n_2(t).$$

Therefore, the rate equation for the electron population of energy level 0 is

$$\begin{aligned} \frac{dN_0(t)}{dt} &= -W_p(t)N_0(t) + \frac{N_2(t)}{\tau_{20}} + \frac{N_1(t)}{\tau_1} - CN_0(t)N_2(t) + C_1 N_1(t) n_0(t) \\ &- C_1^* N_0(t) n_1(t) + q_1 N_1(t) n_1(t) - q_1' N_0(t) n_2(t). \end{aligned} \tag{2.4.5}$$

Energy level $2'$ is populated by holmium electrons due to up- conversion at the rate

$$q_1 N_1(t) n_1(t).$$

Electrons decay from level $2'$ due to spontaneous emission at the rate

$$\frac{n_2(t)}{\tau_2'} = \frac{n_2(t)}{\tau_{20}'} + \frac{n_2(t)}{\tau_{21}'}$$

and due to down-conversion at the rate

$$q_1' N_0(t) n_2(t).$$

This gives the following rate equation for the electron population of level $2'$

$$\frac{dn_2(t)}{dt} = q_1 N_1(t) n_1(t) - \frac{n_2(t)}{\tau_2'} - q_1' N_0(t) n_2(t). \tag{2.4.6}$$

Electrons arrive in level $1'$ due to spontaneous emission of electrons in level $2'$ at the rate

$$\frac{n_2(t)}{\tau_{21}'}$$

and leave level $1'$ due to spontaneous emission at the rate

$$\frac{n_1(t)}{\tau_1'}.$$

Level $1'$ is populated due to forward transfer by the quantity

$$C_1 N_1(t) n_0(t)$$

and depopulated due to back transfer by the quantity

$$C_1^* N_0(t) n_1(t).$$

Electrons leave level $1'$ due to up-conversion at the rate

$$q_1 N_1(t) n_1(t)$$

and arrive in level $1'$ due to down-conversion at the rate

$$q_1' N_0(t) n_2(t).$$

Finally, since level $1'$ is the upper lasing level, it will lose electrons due to stimulated emission. This loss is represented by the quantity

$$\sigma v \phi(t) \left(n_1(t) - \frac{g_1}{g_0} n_0(t) \right).$$

Collecting terms yields the following population rate equation for level $1'$

$$\frac{dn_1(t)}{dt} = \frac{n_2(t)}{\tau_{21}'} - \frac{n_1(t)}{\tau_1'} + C_1 N_1(t) n_0(t) - C_1^* N_0(t) n_1(t)$$

$$+ \quad q_1' N_0(t) n_2(t) - q_1 N_1(t) n_1(t) - \sigma v \phi(t) \left(n_1(t) - \frac{g_1}{g_0} n_0(t) \right) \quad (2.4.7)$$

Energy level 0′ increases due to spontaneous emission of upper energy level electrons at the rate

$$\frac{n_2(t)}{\tau_{20}'} + \frac{n_1(t)}{\tau_1'}.$$

It is populated due to back transfer at the rate

$$C_1^* N_0(t) n_1(t),$$

and depopulated due to forward transfer at the rate

$$C_1 N_1(t) n_0(t).$$

Finally, energy level 0′ gains electrons from stimulated emission which is represented by the quantity

$$\sigma v \phi(t) \left(n_1(t) - \frac{g_1}{g_0} n_0(t) \right).$$

Therefore, the rate equation for the electron population of energy level 0′ is given by

$$\frac{dn_0(t)}{dt} = \frac{n_2(t)}{\tau_{20}'} + \frac{n_1(t)}{\tau_1'} + C_1^* N_0(t) n_1(t) - C_1 N_1(t) n_0(t)$$

$$+ \quad \sigma v \phi(t) \left(n_1(t) - \frac{g_1}{g_0} n_0(t) \right). \quad (2.4.8)$$

Collecting equations (2.4.3)–(2.4.8) , we obtain the following set of rate equations for the dopant electron populations.

$$\frac{dN_2(t)}{dt} = W_p(t) N_0(t) - \frac{N_2(t)}{\tau_2} - C N_0(t) N_2(t)$$

$$\frac{dN_1(t)}{dt} = \frac{N_2(t)}{\tau_{21}} - \frac{N_1(t)}{\tau_1} + 2CN_0(t)N_2(t) + C_1^* N_0(t)n_1(t)$$

$$- C_1 N_1(t)n_0(t) + q_1' N_0(t)n_2(t) - q_1 N_1(t)n_1(t)$$

$$\frac{dN_0(t)}{dt} = -W_p(t)N_0(t) + \frac{N_2(t)}{\tau_{20}} + \frac{N_1(t)}{\tau_1} - CN_0(t)N_2(t)$$

$$+ C_1 N_1(t)n_0(t) - C_1^* N_0(t)n_1(t) + q_1 N_1(t)n_1(t) - q_1' N_0(t)n_2(t)$$

$$\frac{dn_2(t)}{dt} = q_1 N_1(t)n_1(t) - \frac{n_2(t)}{\tau_2'} - q_1' N_0(t)n_2(t)$$

$$\frac{dn_1(t)}{dt} = \frac{n_2(t)}{\tau_{21}'} - \frac{n_1(t)}{\tau_1'} + C_1 N_1(t)n_0(t) - C_1^* N_0(t)n_1(t)$$

$$+ q_1' N_0(t)n_2(t) - q_1 N_1(t)n_1(t) - \sigma v\phi(t)\left(n_1(t) - \frac{g_1}{g_0}n_0(t)\right)$$

$$\frac{dn_0(t)}{dt} = \frac{n_2(t)}{\tau_{20}'} + \frac{n_1(t)}{\tau_1'} + C_1^* N_0(t)n_1(t) - C_1 N_1(t)n_0(t)$$

$$+ \sigma v\phi(t)\left(n_1(t) - \frac{g_1}{g_0}n_0(t)\right) \qquad (2.4.9)$$

In the system (2.4.9), the quantities τ_i, τ_i' $i = 1,2$ represent the spontaneous emission lifetime of energy level i, i', respectively. The quantity, $\frac{1}{\tau_{ij}}$, represents

the transition rate (due to spontaneous emission) from level i to level j. Similarly, $\frac{1}{\tau'_{ij}}$ represents the spontaneous emission transition rate from level i' to level j' . These two quantities satisfy the relations

$$\frac{1}{\tau_i} = \sum_{j=0}^{i-1} \frac{1}{\tau_{ij}} \qquad i = 1,2$$

and

$$\frac{1}{\tau'_i} = \sum_{j=0}^{i-1} \frac{1}{\tau'_{ij}} \qquad i = 1,2$$

From constraint (2.4.1) it is clear that the dependent variables, $N_0(t)$, $N_1(t)$, & $N_2(t)$, must satisfy

$$\frac{dN_0(t)}{dt} + \frac{dN_1(t)}{dt} + \frac{dN_2(t)}{dt} = 0$$

and from constraint (2.4.2) the variables, $n_0(t)$, $n_1(t)$ and $n_2(t)$, must satisfy

$$\frac{dn_0(t)}{dt} + \frac{dn_1(t)}{dt} + \frac{dn_2(t)}{dt} = 0.$$

Indeed, using equations (2.4.9), it is easily verified that the above two "rate constraints" are satisfied. The "population constraints" (2.4.1) and (2.4.2) can be rewritten as

$$N_0(t) = N_T - N_1(t) - N_2(t) \tag{2.4.10}$$

and

$$n_0(t) = n_T - n_1(t) - n_2(t) \tag{2.4.11}$$

Constraints (2.4.10) and (2.4.11) can now be used to eliminate $N_0(t)$ & $n_0(t)$ from the rate equations (2.4.9). Substituting the expressions on the right hand

side of constraints (2.4.10) and (2.4.11) into equations (2.4.9) for $N_0(t)$ & $n_0(t)$, respectively , yields

$$\frac{dN_2(t)}{dt} = W_p(t)(N_T - N_1(t) - N_2(t)) - \frac{N_2(t)}{\tau_2} - CN_2(t)(N_T - N_1(t) - N_2(t))$$

$$\frac{dN_1(t)}{dt} = \frac{N_2(t)}{\tau_{21}} - \frac{N_1(t)}{\tau_1} + 2CN_2(t)(N_T - N_1(t) - N_2(t))$$

$$+ C_1^* n_1(t)(N_T - N_1(t) - N_2(t)) - C_1 N_1(t)(n_T - n_1(t) - n_2(t))$$

$$+ q_1' n_2(t)(N_T - N_1(t) - N_2(t)) - q_1 N_1(t) n_1(t)$$

$$\frac{dn_2(t)}{dt} = q_1 N_1(t) n_1(t) - \frac{n_2(t)}{\tau_2'} - q_1' n_2(t)(N_T - N_1(t) - N_2(t))$$

$$\frac{dn_1(t)}{dt} = \frac{n_2(t)}{\tau_{21}'} - \frac{n_1(t)}{\tau_1'} + C_1 N_1(t)(n_T - n_1(t) - n_2(t))$$

$$- C_1^* n_1(t)(N_T - N_1(t) - N_2(t)) + q_1' n_2(t)(N_T - N_1(t) - N_2(t))$$

$$- q_1 N_1(t) n_1(t) - \sigma v \phi(t) \left(n_1(t) - \frac{g_1}{g_0}(n_T - n_1(t) - n_2(t)) \right) \qquad (2.4.12)$$

2.5 Normalization and Initial Conditions

The coupled system (2.4.12) along with the photon density equation (2.2.12) compose the temporal model of the laser system. The dopant electron populations $N_i(t)$ & $n_i(t)$ $i = 1,2$, are normalized by the quantities N_T & n_T, respectively. The photon density, $\phi(t)$, is normalized by the quantity ϕ_{norm} . Hence, let

$$\begin{aligned} x(t) &= \frac{N_2(t)}{N_T} \\ y(t) &= \frac{N_1(t)}{N_T} \\ z(t) &= \frac{n_1(t)}{n_T} \\ w(t) &= \frac{n_2(t)}{n_T} \\ P(t) &= \frac{\phi(t)}{\phi_{norm}} \end{aligned} \tag{2.5.1}$$

be the normalized electron populations, photon density, respectively. Rewriting the rate equations (2.4.12) and the photon density equation (2.2.12) in terms of the normalized variables yields

$$\frac{dx(t)}{dt} = W_p(t)(1-x(t)-y(t)) - \frac{x(t)}{\tau_2} - D_1x(t)(1-x(t)-y(t))$$

$$\frac{dy(t)}{dt} = \frac{x(t)}{\tau_{21}} - \frac{y(t)}{\tau_1} + 2D_1x(t)(1-x(t)-y(t))$$

$$+ D_3z(t)(1-x(t)-y(t)) - D_2y(t)(1-z(t)-w(t))$$

$$+ D_6w(t)(1-x(t)-y(t)) - D_7y(t)z(t)$$

$$\frac{dw(t)}{dt} = D_8y(t)z(t) - \frac{w(t)}{\tau_2'} - D_9w(t)(1-x(t)-y(t))$$

$$\frac{dz(t)}{dt} = \frac{w(t)}{\tau_{21}'} - \frac{z(t)}{\tau_1'} + D_4y(t)(1-z(t)-w(t))$$

$$- D_5z(t)(1-x(t)-y(t)) + D_9w(t)(1-x(t)-y(t))$$

$$- D_8y(t)z(t) - \beta_1[\gamma z(t) + (1-\gamma)(1-w(t))]P(t)$$

$$\frac{dP(t)}{dt} = \left\{\beta_2[\gamma z(t) + (1-\gamma)(1-w(t))] - \frac{1}{\tau_c}\right\}P(t) + \beta_3 z(t) \qquad (2.5.2)$$

where

$$D_1 = CN_T \qquad D_4 = C_1N_T \qquad D_7 = q_1n_T \qquad \beta_1 = \sigma v\phi_{norm}$$

$$D_2 = C_1n_T \qquad D_5 = C_1^*N_T \qquad D_8 = q_1N_T \qquad \beta_2 = \sigma vn_T$$

$$D_3 = C_1^*n_T \qquad D_6 = q_1'n_T \qquad D_9 = q_1'N_T \qquad \beta_3 = \frac{sp_o n_T}{\tau_{fl}\phi_{norm}}$$

$$\gamma = 1 + \frac{g_1}{g_0}$$

The initial conditions for the normalized populations in the active medium are given by

$$\begin{aligned} x(0) &= x_0 \\ y(0) &= y_0 \\ z(0) &= z_0 \\ w(0) &= w_0 \\ P(0) &= P_0. \end{aligned} \tag{2.5.3}$$

If the laser starts from quiescence, then the photons in the cavity as well as the upper level populations are negligible and hence x_0, y_0, z_0, w_0, & P_0 would all

be taken to be zero. The system of rate equations (2.5.2) along with the initial conditions (2.5.3) constitute the initial value problem (I.V.P.) which will be the topic of the subsequent discussion.

Chapter 3

Qualitative Properties of the Solution

3.1 The Modified Equations

In this section the full set of equations, (2.5.2), is modified by excluding two physical processes—up-conversion and back transfer. This yields a simplified system for which certain qualitative properties of the solution are established. Throughout this discussion, the parameters are assumed to satisfy the following (physically realistic) relationships :

$$\tau_{21} > \tau_2 > 0$$

$$\tau_1 > \tau_{20} > 0$$

$$\tau_1' > \tau_c > 0$$

$$\beta_1 , \beta_2 , \beta_3 > 0$$

$$D_1\,,\ D_2\,,\ D_4 \ > \ 0$$

$$1 \ < \ \gamma$$

$$sp_o \ << \ 1$$

Excluding the above mentioned processes yields the following simplified system of rate equations

$$\frac{dx}{dt} = W_p(t)(1-x-y)_+ - \frac{x}{\tau_2} - D_1 x(1-x-y)_+$$

$$\frac{dy}{dt} = \frac{x}{\tau_{21}} - \frac{y}{\tau_1} + 2D_1 x(1-x-y)_+ - D_2 y(1-z)_+$$

$$\frac{dz}{dt} = -\frac{z}{\tau_1'} + D_4 y(1-z)_+ + \beta_1(\gamma(1-z)_+ - 1)P$$

$$\frac{dP}{dt} = \left\{\beta_2[1-\gamma(1-z)_+] - \frac{1}{\tau_c}\right\} P + \beta_3 z \qquad (3.1.1)$$

where

$$(1-x-y)_+ = \left\{ \begin{array}{cc} 1-x-y & if\ 1-x-y \geq 0 \\ 0 & otherwise \end{array} \right\}$$

$$(1-z)_+ = \left\{ \begin{array}{cc} 1-z & if\ 1-z \geq 0 \\ 0 & otherwise \end{array} \right\} \qquad (3.1.2)$$

The following theorem which can be found in [6] is used to establish the first qualitative property of the solution.

Theorem 1 *Let* $\mathbf{f}$ *be a vector function (with n components) defined in a domain* D *of* $(n+1)$*-dimensional Euclidean space. Let the vectors* $\mathbf{f}$, $\partial\mathbf{f}/\partial y_k (k = 1, ..., n)$ *be continuous in* D. *Then given any point* (t_0, η) *in* D *there exists a unique solution* ϕ *of the system*

$$\mathbf{y}' = \mathbf{f}(t, \mathbf{y})$$

satisfying the initial condition $\phi(t_0) = \eta$. *The solution* ϕ *exists on any interval* I *containing* t_0 *for which the points* $(t, \phi(t))$, *with* t *in* I, *lie in* D. *Furthermore, the solution* ϕ *is a continuous function of the "triple"* (t, t_0, η) .

Equations (3.1.1) can be written symbolically as

$$\mathbf{y}' = \mathbf{f}(t, \mathbf{y})$$

where

$$\mathbf{y} = \begin{bmatrix} y_1 \\ y_2 \\ y_3 \\ y_4 \end{bmatrix} = \begin{bmatrix} x \\ y \\ z \\ P \end{bmatrix}$$

and

$$\mathbf{f}(t, \mathbf{y}) = \begin{bmatrix} f_1 \\ f_2 \\ f_3 \\ f_4 \end{bmatrix} = \begin{bmatrix} W_p(t)(1-x-y)_+ - \dfrac{x}{\tau_2} - D_1 x(1-x-y)_+ \\ \dfrac{x}{\tau_{21}} - \dfrac{y}{\tau_1} + 2D_1 x(1-x-y)_+ - D_2 y(1-z)_+ \\ -\dfrac{z}{\tau_1'} + D_4 y(1-z)_+ + \beta_1(\gamma(1-z)_+ - 1)P \\ \left\{\beta_2[1-\gamma(1-z)_+] - \dfrac{1}{\tau_c}\right\} P + \beta_3 z \end{bmatrix}$$

Let $\mathcal{D} = \{(t, \mathbf{y}) : 0 \leq t < \infty \text{ and } 0 \leq y_k < \infty \text{ for } k = 1, \ldots, 4\}$ and $I = [0, +\infty)$ for the remainder of the discussion. It now follows directly from Theorem 1 that there exists a unique, continuous solution of the system (3.1.1) on any subinterval of I containing t_0 for which (i) the pumping term, $W_p(t)$, is continuous and (ii) the solution vector, $\mathbf{y}$, is bounded. The following theorem establishes the nonnegativity of the solution vector, $\mathbf{y}$, as well as the ground states of thulium and holmium.

Theorem 2 (Nonnegativity) *If $W_p(t) > 0$ for $t > 0$ and $x(0) \geq 0$, $y(0) \geq 0$, $z(0) \geq 0$, and $P(0) \geq 0$ then*

(i) If $1 - x(0) - y(0) > 0$ then $1 - x(t) - y(t) > 0$ for all $t > 0$;

(ii) If $1 - x(0) - y(0) < 0$ then there exists a T such that $1 - x(t) - y(t) > 0$ for all $t > T$;

(iii) (a) If $1 - x(0) - y(0) > 0$ then $x(t) > 0$ and $y(t) > 0$ for all $t > 0$

(b) If $1 - x(0) - y(0) \leq 0$ then $x(t) \geq 0$ and $y(t) > 0$ for all $t > 0$;

(iv) If $1 - z(0) > 0$ then $1 - z(t) > 0$ for all $t > 0$;

(v) If $1 - z(0) < 0$ then there exists a T^* such that $1 - z(t) > 0$ for all $t > T^*$;

(vi) $z(t) > 0$ and $P(t) > 0$ for all $t > 0$.

Proof of Theorem 2:

(i) Since $x(0) + y(0) < 1$, then by continuity of $x(t) + y(t)$ we know that $x(t) + y(t) < 1$ for t near zero. Suppose that at $t = T$, $x(T) + y(T) = 1$ and

$x(t) + y(t) < 1$ for $0 \leq t < T$, then at $t = T$

$$\frac{d}{dt}(x+y) = \left(-\frac{1}{\tau_2} + \frac{1}{\tau_{21}}\right)x + \left(-\frac{1}{\tau_1} - D_2(1-z)_+\right)y \qquad (3.1.3)$$

Now since $\frac{1}{\tau_{21}} - \frac{1}{\tau_2} < 0$ and $-\frac{1}{\tau_1} - D_2(1-z)_+ < 0$, then if $x(T) \geq 0$ and $y(T) \geq 0$ and not both are zero, then from (3.1.3), $\frac{d}{dt}(x+y) < 0$ at $t = T$ which contradicts $x(t) + y(t) < 1$ for $t < T$ and therefore $x(t) + y(t) < 1$ for all t. Now since $x(T) + y(T) = 1$, not both x and y are zero at $t = T$, hence it remains to be shown that $x(T) \geq 0$ and $y(T) \geq 0$.

Suppose $y(T) < 0$, then since $y(0) \geq 0$ and y is continuous, there exists a $T_y < T$ such that $y(T_y) = 0$ and $y(t) \geq 0$ for $0 \leq t \leq T_y$. Then at $t = T_y$

$$\frac{dy}{dt} = x\left[\frac{1}{\tau_{21}} + 2D_1(1-x-y)_+\right]$$

The quantity in brackets above is positive so if $x(T_y) > 0$,then $\dot{y}(T_y) > 0$ which means y is increasing at $t = T_y$. But this contradicts $y(t) \geq 0$ for $0 \leq t \leq T_y$, and this contradiction implies $y(t) \geq 0$ for all t. Now suppose $x(T_y) < 0$, then since $x(0) \geq 0$ and x is continuous, there exists a $T_x < T_y$ such that $x(T_x) = 0$ and $x(t) \geq 0$ for $0 \leq t \leq T_x$. Then at $t = T_x$

$$\frac{dx}{dt} = W_p(T_x)(1-x-y)_+ > 0$$

Hence $\dot{x}(T_x) > 0$ which means x is increasing at $t = T_x$ which contradicts $x(t) \geq 0$ for $0 \leq t \leq T_x$. Therefore, $x(T_y) \geq 0$ and $x(t) \geq 0$ for $0 \leq t \leq T_y$. Now suppose $x(T_y) = 0$, then $\dot{y}(T_y) = 0$ and $\dot{x}(T_y) = W_p(T_y) > 0$. Additionally,

$$\begin{aligned}\frac{d^2y}{dt^2} &= \frac{\dot{x}}{\tau_{21}} - \frac{\dot{y}}{\tau_1} + 2D_1x\frac{d}{dt}(1-x-y)_+ + 2D_1\dot{x}(1-x-y)_+ \\ &- D_2y\frac{d}{dt}(1-z)_+ - D_2\dot{y}(1-z)_+\end{aligned}$$

From which we obtain

$$\begin{aligned} \frac{d^2y}{dt^2}(T_y) &= \left(\frac{1}{\tau_{21}} + 2D_1\right)\dot{x}(T_y) \\ &> 0 \end{aligned}$$

So $y(T_y) = 0$, $\dot{y}(T_y) = 0$, and $\ddot{y}(T_y) > 0$. Hence, y is concave up at $t = T_y$ which implies that y is increasing to the right of $t = T_y$ and so

$$y(T) > 0 \tag{3.1.4}$$

Now suppose $x(T) < 0$, then since $x(0) \geq 0$ and x is continuous, we can choose $T_1 < T$ such that $x(T_1) = 0$ and $x(t) \geq 0$ for $0 \leq t \leq T_1$, then at $t = T_1$

$$\begin{aligned} \frac{dx}{dt} &= W_p(T_1)(1 - x - y)_+ \\ &> 0 \end{aligned}$$

so x is increasing at $t = T_1$ which contradicts $x(t) \geq 0$ for $0 \leq t \leq T_1$ hence the above supposition is false which implies $x(T) \geq 0$. This together with (3.1.4) show that at $t = T$

$$\frac{d}{dt}(x + y) < 0$$

From prior comments, this implies that $x(t) + y(t) < 1$ for all t. *Q.E.D.* (i)

(ii) The proof of (i) shows that if $x(0) + y(0) = 1$, then $x(t) + y(t) < 1$ for all $t > 0$. Suppose $x(0) + y(0) > 1$, then for t near zero

$$\begin{aligned} \frac{d}{dt}(x + y) &= \left(-\frac{1}{\tau_2} + \frac{1}{\tau_{21}}\right)x + \left(-\frac{1}{\tau_1} - D_2(1 - z)_+\right)y \\ &< 0 \end{aligned}$$

since for t near zero $-\frac{1}{\tau_2}+\frac{1}{\tau_{21}}<0$, $-\frac{1}{\tau_1}-D_2(1-z)_+<0$, $x(t)\geq 0$, $y(t)\geq 0$, and not both are zero at $t=0$. So $x(t)+y(t)$ is decreasing for t near zero. Now assume there exists a ξ such that $x(t)+y(t)\geq \xi > 1$ for all t, then

$$\begin{aligned}\frac{d}{dt}(x+y) &= \left(-\frac{1}{\tau_2}+\frac{1}{\tau_{21}}\right)x+\left(-\frac{1}{\tau_1}-D_2(1-z)_+\right)y \\ &= \left(-\frac{1}{\tau_2}+\frac{1}{\tau_{21}}+\frac{1}{\tau_1}\right)x-\frac{1}{\tau_1}(x+y)-D_2(1-z)_+y \\ &\leq -\frac{1}{\tau_1}\xi\end{aligned}$$

since $-\frac{1}{\tau_2}+\frac{1}{\tau_{21}}+\frac{1}{\tau_1}<0$, $-D_2(1-z)_+\leq 0$, and an argument similar to that given in (i) can be adduced to show that $x\geq 0$, $y\geq 0$. This inequality holds for all t so upon integrating from 0 to t we obtain

$$x(t)+y(t)-(x(0)+y(0))\leq -\frac{1}{\tau_1}\xi t$$

or equivalently

$$x(t)+y(t)\leq -\frac{1}{\tau_1}\xi t+x(0)+y(0) \qquad (3.1.5)$$

From inequality (3.1.5) and since $\tau_1>0$, it follows that

$$\lim_{t\to\infty}(x(t)+y(t))=-\infty$$

which contradicts $x(t)+y(t)\geq \xi>1$ for all t. Hence, our assumption was false, which implies there exists a T such that $x(T)+y(T)=1$ and $x(t)+y(t)<1$ for t near T. The analysis from (i) now applies to show that $x(t)+y(t)<1$ for all $t>T$ as required. *Q.E.D.* (ii)

(*iii*) (*a*) Let $x(0) + y(0) < 1$,then from (*i*) we know $x(t) + y(t) < 1$ for all t. Also, by hypothesis $x(0) \geq 0$, hence since x is continuous $x(t) \geq 0$ for t near zero. Assume at some point, say $t = T_1$,that $x(T_1) = 0$ and $x(t) \geq 0$ for $0 \leq t \leq T_1$. Then at $t = T_1$,

$$\begin{aligned} \frac{dx}{dt} &= W_p(T_1)(1 - y(T_1))_+ \\ &> 0 \end{aligned}$$

which means x is increasing. This contradicts $x(t) \geq 0$ for $0 \leq t \leq T_1$. Hence the above assumption is false which implies $x(t) > 0$ for all $t > 0$.

Similarly, assume that at some point, say $t = T_2$, $y(T_2) = 0$ and $y(t) \geq 0$ for $0 \leq t \leq T_2$. Then at $t = T_2$ we have

$$\begin{aligned} \frac{dy}{dt} &= \overbrace{\left[\frac{1}{\tau_{21}} + 2D_1(1 - x)_+\right]}^{positive} x \\ &> 0 \end{aligned}$$

since $x > 0$,and $\frac{1}{\tau_{21}} + 2D_1(1 - x)_+ > 0$. This implies that y is increasing at $t = T_2$ which contradicts $y(t) > 0$ for $0 \leq t \leq T_2$ .Hence, the assumption was fallacious which shows $y(t) > 0$ for all $t > 0$. *Q.E.D.* (*a*)

(*iii*) (*b*) Let $x(0) + y(0) \geq 1$,then from (*ii*) we know there exists a T such that $x(t) + y(t) < 1$ for all $t > T$, and $x(T) + y(T) = 1$. Suppose that at $T_1 < T$, $x(T_1) = 0$ and $x(t) \geq 0$ for $0 \leq t \leq T_1$. Then at $t = T_1$

$$\frac{dx}{dt} = 0$$

Also, at $t = T_1$ we have

$$\begin{aligned}\frac{d^2x}{dt^2}(T_1) &= -W_p(T_1)\dot{y}(T_1) \\ &= -W_p(T_1)\left[-\frac{1}{\tau_1}y(T_1) - D_2y(T_1)(1-z)_+\right] \\ &= W_p(T_1)y(T_1)\underbrace{\left[\frac{1}{\tau_1} + D_2(1-z)_+\right]}_{positive} \\ &> 0\end{aligned}$$

Hence, x is concave up at $t = T_1$ and consequently increases to the right of it. From this it follows that $x(t) \geq 0$ for $0 \leq t \leq T$; furthermore, for $t > T$ the analysis from (iii) (a) applies to show $x(t) > 0$ for all $t > T$.

Again, assume that at $T_2 < T$, $y(T_2) = 0$ and $y(t) \geq 0$ for $0 \leq t \leq T_2$,then at $t = T_2$

$$\begin{aligned}\frac{dy}{dt} &= \frac{1}{\tau_{21}}x(T_2) \\ &> 0\end{aligned}$$

So y is increasing at $t = T_2$ which contradicts $y(t) \geq 0$ for $0 \leq t \leq T_2$, hence the assumption was false which shows that $y(t) > 0$ for $0 < t \leq T$. Also, for $t > T$ the analysis from (iii) (a) pertains to show $y(t) > 0$ for $t > T$.Taken together we have, $y(t) > 0$ for all $t > 0$. *Q.E.D.* (iii) (b)

(iv) Let $z(0) < 1$,then since z is continuous we know that for t near zero, $z(t) < 1$. Now suppose that at $t = T^*$,$z(T^*) = 1$ and $z(t) < 1$ for $0 \leq t < T^*$. Then at $t = T^*$

$$\frac{dz}{dt} = -\frac{1}{\tau_1'} - \beta_1 P$$

Since $\tau_1' > 0$ and $\beta_1 > 0$ then if $P(T^*) \geq 0$ then $\dot{z}(T^*) < 0$ in contradiction to $z(t) < 1$ for $0 \leq t \leq T^*$ which would imply $z(t) < 1$ for all $t > 0$. Hence, it suffices to show $P(T^*) \geq 0$. Assume $P(T^*) < 0$, then since $P(0) \geq 0$ and P is continuous we can choose $T_P < T^*$ such that $P(T_P) = 0$ and $P(t) \geq 0$ for $0 \leq t \leq T_P$. Then at $t = T_P$

$$\frac{dP}{dt} = \beta_3 z(T_P) \tag{3.1.6}$$

$(R.T.S.\ z(T_P) > 0)$ Suppose $z(T_P) < 0$, then choose $T_z < T_P$ such that $z(T_z) = 0$ and $z(t) \geq 0$ for $0 \leq t \leq T_z$. Then at $t = T_z$

$$\begin{aligned} \frac{dz}{dt} &= D_4 y + (\gamma - 1)\beta_1 P \\ &> 0 \end{aligned}$$

since $D_4 > 0$, $(\gamma - 1)\beta_1 > 0$, $P(T_z) \geq 0$ (because $T_z < T_P$), and from $(iii)(a)$ & $(iii)(b)$ we see that $y(T_z) > 0$.Hence, z is increasing at $t = T_z$ which is in contradiction to $z(t) \geq 0$ for $0 \leq t \leq T_z$. Therefore, the supposition $(z(T_P) < 0)$ was false which implies that $z(T_P) \geq 0$ and $z(t) \geq 0$ for $0 \leq t \leq T_P$. Now suppose $z(T_P) = 0$, then at $t = T_P$

$$\begin{aligned} \frac{dz}{dt} &= D_4 y(T_P) \\ &> 0 \end{aligned}$$

so z is increasing at $t = T_P$ which contradicts $z(t) \geq 0$ for $0 \leq t \leq T_P$. Therefore, $z(T_P) > 0$ and from equation (3.1.6) this implies that $\dot{P}(T_P) > 0$ so P is increasing at $t = T_P$. But this contradicts $P(t) \geq 0$ for $0 \leq t \leq T_P$. Hence, the

assumption ($P(T^*) < 0$) was fallacious which implies that $P(T^*) \geq 0$. From this it follows that $z(t) < 1$ for all $t > 0$. *Q.E.D.* (iv)

(v) The proof of (iv) shows that if $z(0) = 1$, then $z(t) < 1$ for all $t > 0$. Now suppose $z(0) > 1$, then for t near zero

$$\begin{aligned} \frac{dz}{dt} &= -\frac{1}{\tau_1'} z - \beta_1 P \\ &< 0 \end{aligned}$$

since $\tau_1' > 0$, $\beta_1 > 0$, $P(0) \geq 0$, & $z(0) > 1$. So z is decreasing for t near zero. Now assume there exists a μ such that $z(t) \geq \mu > 1$ for all $t > 0$, then

$$\frac{dz}{dt} = -\frac{1}{\tau_1'} z - \beta_1 P \tag{3.1.7}$$

Now since $P(0) \geq 0$, suppose $P(T_P) = 0$ and $P(t) \geq 0$ for $0 \leq t \leq T_P$, then at $t = T_P$

$$\begin{aligned} \frac{dP}{dt} &= \beta_3 z(T_P) \\ &> 0 \end{aligned}$$

So P is increasing at $t = T_P$ which contradicts $P(t) \geq 0$ for $0 \leq t \leq T_P$ and so $P(t) > 0$ for all $t > 0$. Now from (3.1.7) we have

$$\begin{aligned} \frac{dz}{dt} &< -\frac{z}{\tau_1'} \\ &\leq -\frac{\mu}{\tau_1'} \end{aligned} \tag{3.1.8}$$

Since inequality (3.1.8) is valid for all $t > 0$ we can integrate from 0 to t to obtain

$$z(t) - z(0) < -\frac{\mu}{\tau_1'} t$$

or equivalently

$$z(t) < -\frac{\mu}{\tau_1'} t + z(0) \tag{3.1.9}$$

From equation (3.1.9) we see that

$$\lim_{t \to \infty} z(t) = -\infty$$

which contradicts $z(t) \geq \mu > 1$ for all $t > 0$. Hence, there exists a T^* such that $z(T^*) = 1$ and $z(t) < 1$ for t near T^*. The analysis of part (iv) now applies to show that $z(t) < 1$ for all $t > T^*$. *Q.E.D.* (v)

(vi) The arguments in (iv) show that z is positive on the interval where $z(t) < 1$, therefore if $z(0) \leq 1$ then $z(t) > 0$ for all $t > 0$. Now since $P(0) \geq 0$, suppose that at some point T_3 we have $P(T_3) = 0$ and $P(t) \geq 0$ for $0 \leq t \leq T_3$. Then at $t = T_3$

$$\begin{aligned} \frac{dP}{dt} &= \beta_3 z \\ &> 0 \end{aligned}$$

So P is increasing at $t = T_3$ which contradicts $P(t) \geq 0$ for $0 \leq t \leq T_3$. Therefore, the preceding supposition was false which implies $P(t) > 0$ for all $t > 0$.

To round things out, suppose $z(0) > 1$, then choose T^* such that $z(T^*) = 1$ and $z(t) > 1$ for $0 \leq t < T^*$. Clearly for $0 \leq t \leq T^*$, $z(t) > 0$ and for $t > T^*$ the analysis from (iv) applies to show that $z(t) > 0$ for all $t > 0$. Finally, using the same arguments as above for $P(t)$ we obtain $P(t) > 0$ for all $t > 0$. *Q.E.D.* (vi)

Theorem 2 tells us that the normalized ground levels of thulium and holmium remain nonnegative on I or in other words that the constraints (3.1.2) are self-

enforcing. Consequently, we will drop the "+" subscripts in system (3.1.1) for the remainder of the discussion.

Theorem 3 (Integrability) *Let $W_p(t)$ be positive, continuous, and integrable on I. Then if $x(0) \geq 0$, $y(0) \geq 0$, $z(0) \geq 0$, & $P(0) \geq 0$, then $x(t)$, $y(t)$, $z(t)$, & $P(t)$ are all integrable on I.*

Proof: Fix T such that $x(t) + y(t) < 1$ for all $t > T$, then for $t > T$ we have

$$\begin{aligned} \frac{dx}{dt} &= -\frac{x}{\tau_2} - D_1 x(1-x-y) + W_p(t) - W_p(t)x - W_p(t)y \\ &= \left(-\frac{1}{\tau_2} - W_p(t)\right) x + W_p(t) - D_1 x(1-x-y) - W_p(t)y \\ &\leq -\left(\frac{1}{\tau_2} + W_p(t)\right) x + W_p(t) \end{aligned}$$

since $W_p(t) > 0$, $y > 0$, $(1-x-y) > 0$, and $x \geq 0$. Rearranging we get

$$\frac{dx}{dt} + \left(\frac{1}{\tau_2} + W_p(t)\right) x \leq W_p(t)$$

Now multiply both sides by $E(t) = e^{\int_T^t \left(\frac{1}{\tau_2} + W_p(\varsigma)\right) d\varsigma}$ to obtain

$$E(t)\frac{dx}{dt} + \left(\frac{1}{\tau_2} + W_p(t)\right) E(t)x \leq E(t)W_p(t)$$

which implies

$$\frac{d}{dt}\{E(t)x(t)\} \leq E(t)W_p(t). \tag{3.1.10}$$

Upon integrating inequality (3.1.10) from $T \rightarrow t$ and noting that $E(T) = 1$ we obtain

$$E(t)x(t) - x(T) \leq \int_T^t W_p(u)E(u)du$$

which holds for $t > T$. It now follows that

$$0 \leq x(t) \leq \int_T^t W_p(u)E(u)E^{-1}(t)du \;+\; x(T)E^{-1}(t). \tag{3.1.11}$$

Since

$$E(u)E^{-1}(t) = e^{-\int_u^t \left(\frac{1}{\tau_2} + W_p(\varsigma)\right) d\varsigma}$$

we can express (3.1.11) as

$$0 \leq x(t) \leq \int_T^t W_p(u) e^{-\int_u^t \left(\frac{1}{\tau_2} + W_p(\varsigma)\right) d\varsigma} du \;+\; x(T) e^{-\int_T^t \left(\frac{1}{\tau_2} + W_p(\varsigma)\right) d\varsigma}.$$

Hence, integrating from $T \rightarrow s$ yields

$$0 \leq \int_T^s x(t)dt \;\leq\; \int_T^s \left\{ \int_T^t W_p(u) e^{-\int_u^t \left(\frac{1}{\tau_2} + W_p(\varsigma)\right) d\varsigma} du \right\} dt$$

$$+ \int_T^s x(T) e^{-\int_u^t \left(\frac{1}{\tau_2} + W_p(\varsigma)\right) d\varsigma} dt.$$

Now since W_p is continuous on I the order of integration may be interchanged to obtain the following equivalent expression

$$0 \leq \int_T^s x(t)dt \;\leq\; \int_T^s \left\{ \int_u^s W_p(u) e^{-\int_u^t \left(\frac{1}{\tau_2} + W_p(\varsigma)\right) d\varsigma} dt \right\} du$$

$$+ \;x(T) \int_T^s e^{-\int_T^t \left(\frac{1}{\tau_2} + W_p(\varsigma)\right) d\varsigma} dt \tag{3.1.12}$$

Using the relation

$$e^{-\int_u^t \left(\frac{1}{\tau_2} + W_p(\varsigma)\right) d\varsigma} \;=\; e^{-\int_u^t W_p(\varsigma)d\varsigma} \;.\; e^{-(t-u)/\tau_2}$$

$$\leq \; e^{-(t-u)/\tau_2}$$

it follows from (3.1.12) that

$$\int_T^s x(t)dt \leq \int_T^s W_p(u)\left\{\int_u^s e^{-(t-u)/\tau_2}dt\right\}du + x(T)\left\{\int_T^s e^{-(t-T)/\tau_2}dt\right\}$$

$$= \int_T^s \tau_2 W_p(u)\left\{1-e^{-(s-u)/\tau_2}\right\}du + x(T)\tau_2\left\{1-e^{-(s-T)/\tau_2}\right\}.$$

Since $\tau_2 > 0$ and $W_p(t)$ is integrable on I, it now follows that $x(t)$ is integrable on I.

To show that $y(t)$ is integrable on I consider the following quantity

$$\frac{d}{dt}(x+y) = \left(-\frac{1}{\tau_2}+\frac{1}{\tau_{21}}\right)x - \frac{y}{\tau_1} - D_2y(1-z) + D_1x(1-x-y)$$
$$+ W_p - W_px - W_py$$

Now fix T^* such that $z(t) < 1$ for all $t > T^*$ and let $T_1 = \max\{T, T^*\}$, then for $t > T_1$ we have

$$\frac{d}{dt}(x+y) \leq \left(-\frac{1}{\tau_2}+\frac{1}{\tau_{21}}+\frac{1}{\tau_1}\right)x - \left(\frac{1}{\tau_1}+W_p+D_1x\right)(x+y) + D_1x + W_p$$

Rearranging yields

$$\frac{d}{dt}(x+y) + \left(\frac{1}{\tau_1}+W_p+D_1x\right)(x+y) \leq \left(-\frac{1}{\tau_2}+\frac{1}{\tau_{21}}+\frac{1}{\tau_1}+D_1\right)x + W_p \quad (3.1.13)$$

For convenience, adopt the following notation

$$\kappa = -\frac{1}{\tau_2}+\frac{1}{\tau_{21}}+\frac{1}{\tau_1}+D_1$$

and

$$\Psi(t) = e^{\int_{T_1}^t \left(\frac{1}{\tau_1}+W_p(r)+D_1x(r)\right)dr}.$$

Multiplying both sides of inequality (3.1.13) by $\Psi(t)$ yields

$$\Psi(t)\frac{d}{dt}(x+y)+\Psi(t)\left(\frac{1}{\tau_1}+W_p+D_1x\right)(x+y)\leq(\kappa x+W_p)\Psi(t).$$

Therefore,

$$\frac{d}{dt}\{\Psi(t)(x(t)+y(t))\}\leq(\kappa x(t)+W_p(t))\Psi(t). \tag{3.1.14}$$

Upon integrating (3.1.14) from $T_1 \rightarrow t$ we obtain

$$\Psi(t)(x(t)+y(t))-[x(T_1)+y(T_1)]\leq\int_{T_1}^{t}(\kappa x(u)+W_p(u))\Psi(u)du.$$

From which it follows

$$\begin{aligned}0\leq x(t)+y(t) \;&\leq\; \int_{T_1}^{t}(\kappa x(u)+W_p(u))\Psi(u)\Psi^{-1}(t)du \;+\; [x(T_1)+y(T_1)]\Psi^{-1}(t)\\ &=\; \int_{T_1}^{t}(\kappa x(u)+W_p(u))e^{-\int_u^t\left(\frac{1}{\tau_1}+W_p(r)+D_1x(r)\right)dr}du\\ &+\; [x(T_1)+y(T_1)]e^{-\int_{T_1}^{t}\left(\frac{1}{\tau_1}+W_p(r)+D_1x(r)\right)dr}\end{aligned} \tag{3.1.15}$$

Using

$$e^{-\int_{T_1}^{t}\left(\frac{1}{\tau_1}+W_p(r)+D_1x(r)\right)dr}\leq e^{-(t-T_1)/\tau_1}$$

and

$$e^{-\int_{u}^{t}\left(\frac{1}{\tau_1}+W_p(r)+D_1x(r)\right)dr}\leq e^{-(t-u)/\tau_1}$$

along with relation (3.1.15) we obtain

$$\begin{aligned}0\leq x(t)+y(t) \;&\leq\; \int_{T_1}^{t}(\kappa x(u)+W_p(u))\,e^{-(t-u)/\tau_1}\,du\\ &+\; [x(T_1)+y(T_1)]e^{-(t-T_1)/\tau_1}.\end{aligned} \tag{3.1.16}$$

Now integrate (3.1.16) from $T_1 \rightarrow s$ to get

$$0 \leq \int_{T_1}^{s}(x(t)+y(t))dt \;\leq\; \int_{T_1}^{s}\left\{\int_{T_1}^{t}(\kappa x(u)+W_p(u))e^{-(t-u)/\tau_1}\,du\right\}dt$$

$$+\;\; [x(T_1)+y(T_1)]\int_{T_1}^{s}e^{-(t-T_1)/\tau_1}\,dt\,. \qquad (3.1.17)$$

Again, since x and W_p are continuous we can interchange the order of integration in (3.1.17) to obtain

$$0 \leq \int_{T_1}^{s}(x(t)+y(t))dt \;\leq\; \int_{T_1}^{s}(\kappa x(u)+W_p(u))\left\{\int_{u}^{s}(-\tau_1)e^{-(t-u)/\tau_1}\left(-\frac{dt}{\tau_1}\right)\right\}du$$

$$+\;\; [x(T_1)+y(T_1)](-\tau_1)\int_{T_1}^{s}e^{-(t-T_1)/\tau_1}\left(-\frac{dt}{\tau_1}\right)$$

Integrating the right hand side over t yields

$$0 \leq \int_{T_1}^{s}(x(t)+y(t))dt \;\leq\; \int_{T_1}^{s}\tau_1(\kappa x(u)+W_p(u))\left\{1-e^{-(s-u)/\tau_1}\right\}du$$

$$+\;\; [x(T_1)+y(T_1)](\tau_1)\left\{1-e^{-(s-T_1)/\tau_1}\right\} \quad (3.1.18)$$

Now since both x and W_p are integrable on I and $\tau_1 > 0$, it follows from relation (3.1.18) that $x(t)+y(t)$ is integrable on I. From the nonnegativity of x and y we conclude that $y(t)$ is integrable on I. Finally, to show that $z(t)$ and $P(t)$ are integrable on I it is expedient (and equivalent) to show that the physical variables, $n_1(t)$ and $\phi(t)$, are integrable on I. From the rate equations we have

$$\frac{d}{dt}(n_1+\phi) \;=\; \left(\frac{sp_o}{\tau_1'}-\frac{1}{\tau_1'}\right)n_1 + C_1N_1(n_T-n_1)-\frac{\phi}{\tau_c}$$

$$= \frac{1}{\tau_1'}(sp_o - 1)(n_1 + \phi) + C_1 N_1 n_T - C_1 N_1 n_1 + \left(\frac{1}{\tau_1'} - \frac{sp_o}{\tau_1'} - \frac{1}{\tau_c}\right)\phi$$

$$< \frac{1}{\tau_1'}(sp_o - 1)(n_1 + \phi) + D_2 N_1$$

Let $\rho = \frac{1}{\tau_1'}(sp_o - 1)$, so $\rho < 0$, then

$$\frac{d}{dt}(n_1 + \phi) - \rho(n_1 + \phi) < D_2 N_1 . \tag{3.1.19}$$

Now letting $\Gamma(t) = e^{-\rho(t - T^*)}$ and multiplying (3.1.19) by $\Gamma(t)$ yields

$$\frac{d}{dt}\{\Gamma(t)(n_1 + \phi)\} < D_2 N_1(t)\Gamma(t)$$

Upon integrating from $T^* \rightarrow t$ we obtain

$$\Gamma(t)(n_1(t) + \phi(t)) < \int_{T^*}^{t} D_2 N_1(u)\Gamma(u)du \; + \; [n_1(T^*) + \phi(T^*)].$$

From this inequality and the nonnegativity of n_1 and ϕ we may write

$$0 \leq n_1(t) + \phi(t) \; < \; \int_{T^*}^{t} D_2 N_1(u)\Gamma(u)\Gamma^{-1}(t)du \; + \; [n_1(T^*) + \phi(T^*)]\Gamma^{-1}(t)$$

$$= \int_{T^*}^{t} D_2 N_1(u) e^{\rho(t-u)} du \; + \; [n_1(T^*) + \phi(T^*)] e^{\rho(t - T^*)}$$

Now integrate from $T^* \rightarrow s$ to get

$$0 \leq \int_{T^*}^{s} [n_1(t) + \phi(t)]dt \; < \; \int_{T^*}^{s} \left\{ \int_{T^*}^{t} D_2 N_1(u) e^{\rho(t-u)} du \right\} dt$$

$$+ \; [n_1(T^*) + \phi(T^*)] \left\{ \int_{T^*}^{s} e^{\rho(t - T^*)} dt \right\} \tag{3.1.20}$$

Since N_1 is continuous we may interchange the order of integration in (3.1.20). Doing this and integrating over t yields

$$0 \leq \int_{T^*}^{s} [n_1(t) + \phi(t)]dt \;<\; \int_{T^*}^{s} \frac{D_2 N_1(u)}{\rho} \left[e^{\rho(s-u)} - 1\right] du$$

$$+ \;\frac{[n_1(T^*) + \phi(T^*)]}{\rho} \left[e^{\rho(s-T^*)} - 1\right] \quad (3.1.21)$$

Now since $\rho < 0$ and N_1 is integrable on I , it follows that $n_1(t) + \phi(t)$ is integrable on I. Finally, from the nonnegativity of $n_1(t)$ and $\phi(t)$ we conclude that both $n_1(t)$ and $\phi(t)$ are integrable on I. *Q.E.D.*

Theorem 4 (Boundedness) *If $W_p(t) > 0$ on I then $x(t)$, $y(t)$, $z(t)$, and $P(t)$ are all bounded on I.*

Proof: Previous discussion shows that $x(t)$, $y(t)$, and $z(t)$ are bounded on I . Hence, it suffices to show that $P(t)$ is bounded on I. For expediency, we once again switch from the normalized variables to the physical variables . Clearly, showing that $\phi(t)$ is bounded is equivalent to showing that $P(t)$ is bounded. Rewriting the $\dot{z}$ and $\dot{P}$ equations in (3.1.1) in terms of the physical variables and adding them together yields

$$\frac{d}{dt}(n_1 + \phi) = \left(\frac{sp_o}{\tau_1'} - \frac{1}{\tau_1'}\right) n_1 - \frac{\phi}{\tau_c} + C_1 N_1 (n_T - n_1)$$

or equivalently

$$\frac{d}{dt}(n_1 + \phi) = \left(\frac{sp_o}{\tau_1'} - \frac{1}{\tau_1'} + \frac{1}{\tau_c}\right) n_1 - \frac{1}{\tau_c}(n_1 + \phi) + C_1 N_1 (n_T - n_1)$$

Setting $k = \frac{sp_o}{\tau_1'} - \frac{1}{\tau_1'} + \frac{1}{\tau_c}$ we may rewrite this as

$$\frac{d}{dt}(n_1 + \phi) + \frac{1}{\tau_c}(n_1 + \phi) = kn_1 + C_1N_1(n_T - n_1) \qquad (3.1.22)$$

Now multiplying equation (3.1.22) by the integrating factor e^{t/τ_c} we may express it in the form

$$\frac{d}{dt}\left\{e^{t/\tau_c}(n_1 + \phi)\right\} = \{kn_1 + C_1N_1(n_T - n_1)\}e^{t/\tau_c}.$$

Integrating from $T \rightarrow t$ and rearranging yields

$$e^{t/\tau_c}(n_1(t) + \phi(t)) = \int_T^t \{kn_1 + C_1N_1(n_T - n_1)\}e^{u/\tau_c}\,du \; + \; e^{T/\tau_c}(n_1(T) + \phi(T)).$$

From which it follows

$$0 \leq n_1(t) + \phi(t) \;\; = \;\; \int_T^t \{kn_1 + C_1N_1(n_T - n_1)\}e^{(u-t)/\tau_c}\,du$$

$$+ \;\; e^{(T-t)/\tau_c}(n_1(T) + \phi(T)). \qquad (3.1.23)$$

Now since n_1 and N_1 are bounded for all $t > 0$, $\tau_c > 0$, $u < t$, and $T < t$, the right hand side of equation (3.1.23) is bounded on I. Hence, $n_1 + \phi$ is bounded on I. The nonnegativity of n_1 and ϕ now implies that $\phi(t)$ is bounded on I. *Q.E.D.*

Theorem 4 states that if $W_p(t) > 0$ on I then the solution vector, $\mathbf{y}$, is bounded on I and so the point $(t,\mathbf{y}(t))$ remains in D for all t in I. Hence, if $W_p(t)$ is continuous on I it follows directly from Theorem 1 that there exists a unique, continuous solution to the system (3.1.1) on all of I.

Theorem 5 *Let W_p, x, y, z, and P satisfy the hypotheses of Theorem 2. Furthermore, let $W_p(t) \to 0$ as $t \to \infty$. Then, the solution vector $\mathbf{y} \to \mathbf{0}$ as $t \to \infty$.*

Proof: Showing $\mathbf{y} \to \mathbf{0}$ is the same as showing that each component of $\mathbf{y}$ approaches zero. Hence, consider

$$\frac{dx}{dt} = (W_p(t) - D_1x)(1 - x - y) - \frac{x}{\tau_2}.$$

Now fix T such that $x(t)+y(t) < 1$ for all $t > T$. If $W_p(t) > D_1x(t)$ for all $t > T$, then the nonnegativity of $x(t)$ along with $W_p(t) \to 0$ as $t \to \infty$ implies $x(t) \to 0$ as $t \to \infty$. Now suppose at some point $\hat{T} > T$ we have $D_1x(\hat{T}) = W_p(\hat{T})$ and $0 \leq D_1x(t) < W_p(t)$ for $0 \leq t < \hat{T}$, then at $t = \hat{T}$

$$\frac{d\,D_1x}{dt} = -\frac{D_1x}{\tau_2} < 0$$

so $D_1x(t)$ is decreasing.Also, on any interval where $D_1x(t) > W_p(t)$, $D_1x(t)$ will be decreasing, since then

$$\begin{aligned} \frac{d\,D_1x}{dt} &= \underbrace{D_1(W_p(t) - D_1x)(1 - x - y)}_{negative} - \frac{D_1x}{\tau_2} \\ &< -\frac{D_1x}{\tau_2} \\ &< 0\,. \end{aligned}$$

Therefore, $D_1x(t)$ is decreasing whenever $D_1x(t) \geq W_p(t)$. There are three possibilities which must be considered. Firstly, suppose there exists a $T^* \geq \hat{T}$ such that $D_1x(t) \leq W_p(t)$ for all $t \geq T^*$, then clearly $x(t) \to 0$ as $t \to \infty$. Secondly, suppose that on $[\hat{T}, +\infty)$, $D_1x(t) \leq W_p(t)$ on some intervals and

$D_1x(t) > W_p(t)$ on others; then since $W_p(t) \to 0$ as $t \to \infty$ and $D_1x(t)$ is decreasing whenever $D_1x(t) > W_p(t)$, this implies $x(t) \to 0$ as $t \to \infty$. Thirdly, suppose there exists a point $\tilde{T} \geq \hat{T}$ such that $D_1x(t) > W_p(t)$ for all $t \geq \tilde{T}$; then $D_1x(t)$ is decreasing on $[\tilde{T}, +\infty)$. Furthermore, suppose there exists a ξ such that $D_1x(t) \geq \xi > 0$ for $\tilde{T} \leq t < +\infty$. Then

$$\frac{d\,D_1x}{dt} < -\frac{D_1x}{\tau_2} \leq -\frac{\xi}{\tau_2}.$$

Integrating from $\tilde{T} \to t$ yields

$$D_1x(t) < -\frac{\xi}{\tau_2}(t - \tilde{T}) + D_1x(\tilde{T})$$

from which it follows

$$\lim_{t\to\infty} x(t) = -\infty.$$

This, however, contradicts $x(t) \geq 0$ for all $t > 0$ and hence there exists no such ξ. From this we conclude that $x(t) \to 0$ as $t \to \infty$.

To show $y(t) \to 0$ as $t \to \infty$ consider

$$\frac{dy}{dt} = x\left(\frac{1}{\tau_{21}} + 2D_1(1 - x - y)\right) - D_2y(1 - z) - \frac{y}{\tau_1}. \tag{3.1.24}$$

Now fix T^* such that $z(t) < 1$ for all $t > T^*$, and let T_1=max$\{T, T^*\}$. Then, whenever

$$x\left(\frac{1}{\tau_{21}} + 2D_1(1 - x - y)\right) \geq D_2y(1 - z) \tag{3.1.25}$$

we have that $D_2y(1 - z) \to 0$ since $x \to 0$. This implies either $y \to 0$ or $z \to 1$. Assume $z \to 1$ as $t \to \infty$, then since $0 < z(t) < 1$ for $t > T_1$, $z(t)$ must approach

one from below.Now, from equations (3.1.1) we see that the rate equation for $z(t)$ can be written as

$$\frac{dz}{dt} = \frac{(1-z)}{\tau_1'} - \frac{1}{\tau_1'} + D_4 y(1-z) + \beta_1\gamma(1-z)P - \beta_1 P \, .$$

Collecting all terms involving $(1-z)$ yields

$$\frac{dz}{dt} = -\frac{1}{\tau_1'} - \beta_1 P + \left(D_4 y + \beta_1\gamma P + \frac{1}{\tau_1'} \right)(1-z) \, . \qquad (3.1.26)$$

Since $z \to 1$ as $t \to \infty$ and—from Theorem 4—both y and P are bounded on I, the third term in (3.1.26) can be made arbitrarily small and certainly smaller than $\frac{1}{2\tau_1'}$ simply by taking t large enough, say $t > T'$. Then for all $t > T'$ we have

$$\frac{dz}{dt} < \frac{1}{2\tau_1'} - \frac{1}{\tau_1'} - \beta_1 P < 0$$

so $z(t)$ is decreasing on $[T', +\infty)$ which contradicts $z \to 1$ from below. Therefore, on the intervals where inequality (3.1.25) holds, $y(t) \to 0$. On the remaining intervals we have from equation (3.1.24) that

$$\frac{dy}{dt} < -\frac{y}{\tau_1} < 0$$

which implies $y(t)$ is decreasing. Once again there are three cases to consider which are analogous to those considered for $x(t)$. It is easily verified, using the same types of arguments as before, that in all three cases $y(t) \to 0$ as $t \to \infty$.

Finally, it will be shown that the normalized variables, z & P, approach zero as $t \to \infty$, by showing the corresponding physical variables, n_1 & ϕ, approach

zero as $t \to \infty$. Since, $n_1(t)$ & $\phi(t)$ are both nonnegative, this is equivalent to showing $n_1(t) + \phi(t) \to 0$ as $t \to \infty$. Previously we obtained

$$\frac{d}{dt}(n_1+\phi) = C_1N_1(n_T - n_1) - \left(\frac{1}{\tau_c} + \frac{sp_o}{\tau_1'} - \frac{1}{\tau_1'}\right)\phi - \frac{(1-sp_o)}{\tau_1'}(n_1+\phi). \quad (3.1.27)$$

Since $\phi(t) > 0$ for $t > 0$ and $N_1(t) \to 0$ as $t \to \infty$, then whenever

$$C_1N_1(n_T - n_1) \geq \left(\frac{1}{\tau_c} + \frac{sp_o}{\tau_1'} - \frac{1}{\tau_1'}\right)\phi \quad (3.1.28)$$

then $\phi(t) \to 0$. By considering the rate equation for $n_1(t)$ it is easily shown that this implies $n_1(t) \to 0$ as $t \to \infty$. Hence, on the intervals where inequality (3.1.28) is satisfied $n_1(t)$ & $\phi(t)$ both converge to zero as $t \to \infty$. Now suppose inequality (3.1.28) holds on some intervals and not on others. Then wherever (3.1.28) is not satisfied, we see from equation (3.1.27) that

$$\frac{d}{dt}(n_1+\phi) < -\frac{(1-sp_o)}{\tau_1'}(n_1+\phi) < 0$$

so $(n_1(t) + \phi(t))$ is decreasing. This together with $N_1(t) \to 0$ as $t \to \infty$ implies $n_1(t) + \phi(t) \to 0$. Finally, consider the case where there exists a $\bar{T} > T_1$ such that for all $t > \bar{T}$

$$C_1N_1(n_T - n_1) < \left(\frac{1}{\tau_c} + \frac{sp_o}{\tau_1'} - \frac{1}{\tau_1'}\right)\phi\,.$$

Then from equation (3.1.27) it follows that

$$\frac{d}{dt}(n_1+\phi) < 0$$

so $n_1(t) + \phi(t)$ is decreasing on $[\bar{T}, +\infty)$.Using the same type of argument as before, it can easily be shown that this implies $n_1(t) + \phi(t) \to 0$ as $t \to \infty$. *Q.E.D.*

Chapter 4

Stability Analysis

4.1 The Equilibrium Solutions

In this chapter the equilibrium solutions (also called equilibrium points or critical points) are obtained and a local stability analysis is performed. Before doing this however we make the simplifying assumption that the spontaneous emission term, sp_o, has a negligible affect on the asymptotic behaviour of the system and hence may be dropped. This is reasonable from a physical point of view and —as will be seen in section 5.1—the numerics corroborate this assumption. Furthermore, we will consider the case of continuous wave (CW) pumping. These two considerations are equivalent to taking $\beta_3 \equiv 0$ and $W_p(t) \equiv W_p$ in equations (3.1.1), where W_p is a positive constant. Doing this yields the following system of rate equations :

$$\frac{dx}{dt} = W_p(1-x-y) - \frac{x}{\tau_2} - D_1 x(1-x-y)$$

$$\frac{dy}{dt} = \frac{x}{\tau_{21}} - \frac{y}{\tau_1} + 2D_1 x(1-x-y) - D_2 y(1-z)$$

$$\frac{dz}{dt} = -\frac{z}{\tau_1'} + D_4 y(1-z) + \beta_1[\gamma(1-z)-1]P$$

$$\frac{dP}{dt} = \left\{\beta_2[1-\gamma(1-z)] - \frac{1}{\tau_c}\right\} P \qquad (4.1.1)$$

The equilibrium solutions are obtained by setting the right hand side of equations (4.1.1) equal to zero. Doing this yields the following nonlinear algebraic system which must be solved for x, y, z, and P :

$$W_p(1-x-y) - \frac{x}{\tau_2} - D_1 x(1-x-y) = 0 \qquad (4.1.2)$$

$$\frac{x}{\tau_{21}} - \frac{y}{\tau_1} + 2D_1 x(1-x-y) - D_2 y(1-z) = 0 \qquad (4.1.3)$$

$$-\frac{z}{\tau_1'} + D_4 y(1-z) + \beta_1[\gamma(1-z)-1]P = 0 \qquad (4.1.4)$$

$$\left\{\beta_2[1-\gamma(1-z)] - \frac{1}{\tau_c}\right\} P = 0 \qquad (4.1.5)$$

From equation (4.1.5) we have

$$\left\{\beta_2[1-\gamma(1-z)] - \frac{1}{\tau_c}\right\} \equiv 0 \ \textit{or} \ P \equiv 0 .$$

Case 1($P \equiv 0$) Working through the rather involved algebraic manipulations

yields,

$$z = \frac{D_4 W_p + D_4 \left(D_1 x - W_p - \frac{1}{\tau_2} - D_1 \right) x}{(W_p - D_1 x)\left(\frac{1}{\tau_1'} + D_4(1-x) \right) - \frac{D_4 x}{\tau_2}} \tag{4.1.6}$$

and

$$y = \frac{W_p + \left(D_1 x - W_p - \frac{1}{\tau_2} - D_1 \right) x}{W_p - D_1 x} \tag{4.1.7}$$

where x is a root of the quartic equation

$$a_1 x^4 + a_2 x^3 + a_3 x^2 + a_4 x + a_5 = 0 \, . \tag{4.1.8}$$

The coefficients $a_1, \cdots, a_5$ depend on the physical parameters of the laser system and are given by

$$\begin{aligned}
a_1 &= (D_1 D_4 N_T^2)(\alpha_1 + \delta_1 n_T) \\
a_2 &= N_T^3 \left(\alpha_1 \alpha_4 + \frac{D_1 D_4 \alpha_2}{N_T^2} - \delta_1 \delta_4 + \frac{D_1 D_2 \delta_2}{N_T} \right) \\
a_3 &= N_T^2 \left(\alpha_1 \alpha_5 - \frac{D_1 D_4 \alpha_3}{N_T^2} - \delta_2 \delta_4 + \alpha_2 \alpha_4 + D_2 W_p N_T \delta_1 + \frac{D_1 D_2 \delta_3}{N_T} \right) \\
a_4 &= N_T (\alpha_2 \alpha_5 - \alpha_3 \alpha_4 + D_2 W_p N_T \delta_2 - \delta_3 \delta_4) \\
a_5 &= (D_2 W_p N_T \delta_3 - \alpha_3 \alpha_5)
\end{aligned}$$

where

$$\begin{aligned}
\alpha_1 &= \frac{D_1}{N_T} \left(\frac{2}{\tau_2} - \frac{1}{\tau_1} - D_2 - \frac{1}{\tau_{21}} \right) \\
\alpha_2 &= \frac{D_1}{\tau_1} + \frac{1}{\tau_1 \tau_2} + D_1 D_2 + D_2 W_p + \frac{D_2}{\tau_2} + \frac{W_p}{\tau_1} + \frac{W_p}{\tau_{21}} \\
\alpha_3 &= W_p N_T \left(\frac{1}{\tau_1} + D_2 \right)
\end{aligned}$$

$$\alpha_4 = -\frac{1}{N_T}\left(\frac{D_4}{\tau_2} + \frac{D_1}{\tau_1'} + D_1D_4 + D_4W_p\right)$$

$$\alpha_5 = W_p\left(\frac{1}{\tau_1'} + D_4\right)$$

$$\delta_1 = -\frac{D_1D_4}{N_T^2}$$

$$\delta_2 = \frac{D_4}{N_T}\left(W_p + D_1 + \frac{1}{\tau_2}\right)$$

$$\delta_3 = -D_4W_p$$

$$\delta_4 = D_2\left(W_p + \frac{1}{\tau_2} + D_1\right)$$

Employing a subroutine from [14] the four roots of equation (4.1.8) are obtained. Two of the roots are complex conjugates and therefore are discarded. One of the two remaining roots yields negative equilibrium values for both y and z and hence is likewise discarded. The remaining root is positive and yields positive equilibrium values for y and z ; hence, it is the only physically realistic root of equation (4.1.8). Denote this equilibrium value of x by x^1. Substituting x^1 into equations (4.1.6) and (4.1.7) we obtain z^1 and y^1, respectively. Therefore, equilibrium point 1 is given by $(x^1, y^1, z^1, 0)$ and will be denoted **I**.

Case 2$\left(\beta_2[1-\gamma(1-z)] - \frac{1}{\tau_c} \equiv 0\right)$ Denoting the equilibrium values of x, y, z & P by x^2, y^2, z^2, & P^2 respectively and performing the requisite algebra yields

$$y^2 = \frac{\left(D_1x^2 - W_p - \frac{1}{\tau_2} - D_1\right)x^2 + W_p}{W_p - D_1x^2} \tag{4.1.9}$$

$$z^2 = \frac{1}{\beta_2\gamma\tau_c} + \frac{\gamma - 1}{\gamma} \tag{4.1.10}$$

$$P^2 = \frac{1}{\gamma\tau_1'\phi_{norm}}\left\{\left(1-\frac{1}{\sigma v\tau_c n_T}\right)\left(n_T\tau_c + D_2 N_T\tau_c\tau_1'\right)\right.$$

$$\left. -n_T\tau_c\gamma - D_2 N_T\tau_c\tau_1' x^2\left(1+\frac{1}{\tau_2(W_p - D_1x^2)}\right)\right\} \qquad (4.1.11)$$

where x^2 is a nonnegative root of

$$b_1(x)^2 + b_2x + b_3 = 0. \qquad (4.1.12)$$

The coefficients b_1, b_2, b_3 are given in terms of the parameters as

$$\begin{aligned} b_1 &= D_1(\varsigma_2 - 2W_p - \varsigma_3 + 2\varsigma_4) \\ b_2 &= -(W_p\varsigma_2 + 2D_1W_p - \varsigma_3\varsigma_4) \\ b_3 &= -W_p\varsigma_3 \end{aligned}$$

where

$$\begin{aligned} \varsigma_1 &= \frac{1}{\sigma v\tau_c} + (\gamma - 1)n_T \\ \varsigma_2 &= -\left(2D_1 + \frac{1}{\tau_{21}}\right) \\ \varsigma_3 &= D_2 + \frac{1}{\tau_1} - \frac{D_2\varsigma_1}{\gamma n_T} \\ \varsigma_4 &= D_1 + W_p + \frac{1}{\tau_2} \end{aligned}$$

One of the roots of (4.1.12) is negative and one is positive. Discarding the negative root, equilibrium point 2 is given by (x^2, y^2, z^2, P^2) and will be denoted **II.**

4.2 Local Stability Analysis

Having located the equilibrium points a local stability analysis is now conducted to determine the stability properties of **I** and **II**. For the stability of **I**, introduce the new variables $\hat{x} = x - x^1, \hat{y} = y - y^1, \hat{z} = z - z^1$, and $\hat{P} = P - 0$. Substituting these variables into the system of rate equations (4.1.1) yields

$$\begin{aligned}
\frac{d\hat{x}}{dt} &= -W_p\hat{x} - W_p\hat{y} - \frac{\hat{x}}{\tau_2} - D_1\hat{x} + D_1(\hat{x})^2 + D_1x^1\hat{x} + D_1\hat{x}\hat{y} + D_1y^1\hat{x} \\
&+ D_1x^1\hat{x} + D_1x^1\hat{y} + W_p(1 - x^1 - y^1) - \frac{x^1}{\tau_2} - D_1x^1(1 - x^1 - y^1)
\end{aligned}$$

$$\begin{aligned}
\frac{d\hat{y}}{dt} &= \frac{\hat{x}}{\tau_{21}} - \frac{\hat{y}}{\tau_1} + 2D_1\hat{x} - 2D_1(\hat{x})^2 - 2D_1x^1\hat{x} - 2D_1\hat{x}\hat{y} - 2D_1y^1\hat{x} \\
&- 2D_1x^1\hat{x} - 2D_1x^1\hat{y} - D_2\hat{y} + D_2\hat{y}\hat{z} + D_2z^1\hat{y} + D_2y^1\hat{z} \\
&+ \frac{x^1}{\tau_{21}} - \frac{y^1}{\tau_1} + 2D_1x^1(1 - x^1 - y^1) - D_2y^1(1 - z^1)
\end{aligned}$$

$$\begin{aligned}
\frac{d\hat{z}}{dt} &= -\frac{\hat{z}}{\tau_1'} + D_4\hat{y} - D_4\hat{y}\hat{z} - D_4z^1\hat{y} - D_4y^1\hat{z} \\
&+ \beta_1(\gamma - \gamma\hat{z} - \gamma z^1 - 1)\hat{P} - \frac{z^1}{\tau_1'} + D_4y^1(1 - z^1)
\end{aligned}$$

$$\frac{d\hat{P}}{dt} = \left\{\beta_2(1 - \gamma + \gamma\hat{z} + \gamma z^1) - \frac{1}{\tau_c}\right\}\hat{P}$$

Since $(x^1, y^1, z^1, 0)$ is an equilibrium point, this reduces to

$$\begin{aligned}
\frac{d\hat{x}}{dt} &= \left(D_1x^1 - W_p - \frac{1}{\tau_2} - D_1(1 - x^1 - y^1)\right)\hat{x} \\
&+ (D_1x^1 - W_p)\hat{y} + \underbrace{D_1(\hat{x})^2 + D_1\hat{x}\hat{y}}_{\hat{g}_1}
\end{aligned}$$

$$\begin{aligned}
\frac{d\hat{y}}{dt} &= \left(\frac{1}{\tau_{21}} + 2D_1(1-x^1-y^1) - 2D_1x^1\right)\hat{x} \\
&- \left(\frac{1}{\tau_1} + 2D_1x^1 + D_2(1-z^1)\right)\hat{y} + D_2y^1\hat{z} \\
&+ \underbrace{D_2\hat{y}\hat{z} - 2D_1(\hat{x})^2 - 2D_1\hat{x}\hat{y}}_{\hat{g}_2}
\end{aligned}$$

$$\begin{aligned}
\frac{d\hat{z}}{dt} &= (D_4 - D_4z^1)\hat{y} + \left(-\frac{1}{\tau_1'} - D_4y^1\right)\hat{z} \\
&+ \beta_1(\gamma - \gamma z^1 - 1)\hat{P} \underbrace{-D_4\hat{y}\hat{z} - \gamma\beta_1\hat{z}\hat{P}}_{\hat{g}_3}
\end{aligned}$$

$$\frac{d\hat{P}}{dt} = \left\{\beta_2(1-\gamma+\gamma z^1) - \frac{1}{\tau_c}\right\}\hat{P} + \underbrace{\beta_2\gamma\hat{z}\hat{P}}_{\hat{g}_4}$$

This can be written in a more compact form—using $\hat{a}_{ij}$ notation— as

$$\begin{aligned}
\frac{d\hat{x}}{dt} &= \hat{a}_{11}\hat{x} + \hat{a}_{12}\hat{y} + \hat{g}_1 \\
\frac{d\hat{y}}{dt} &= \hat{a}_{21}\hat{x} + \hat{a}_{22}\hat{y} + \hat{a}_{23}\hat{z} + \hat{g}_2 \\
\frac{d\hat{z}}{dt} &= \hat{a}_{32}\hat{y} + \hat{a}_{33}\hat{z} + \hat{a}_{34}\hat{P} + \hat{g}_3 \\
\frac{d\hat{P}}{dt} &= \hat{a}_{44}\hat{P} + \hat{g}_4 \qquad (4.2.1)
\end{aligned}$$

where the $\hat{a}_{ij}$'s are defined in the obvious way. Now let $\hat{X} = [\hat{x},\ \hat{y},\ \hat{z},\ \hat{P}]^T$; $\hat{g} = [\hat{g}_1,\ \hat{g}_2,\ \hat{g}_3,\ \hat{g}_4]^T$; and $\hat{A} = [\,\hat{a}_{ij}\,]$. The above system may now be written

symbollically as

$$\dot{\hat{X}} = \hat{A}\hat{X} + \hat{g} \tag{4.2.2}$$

This is known as an "almost linear system " since $\hat{g}$ consists entirely of sums of quadratic terms and therefore satisfies

$$\lim_{\rho \to 0} \frac{\hat{g}_i}{\rho} = 0 \quad i = 1,2,3,4 \ \textit{where} \ \rho = \| \hat{X} \|_2 = \sqrt{\hat{x}^2 + \hat{y}^2 + \hat{z}^2 + \hat{P}^2}. \tag{4.2.3}$$

The following theorem, due to Poincare and Perron, will prove useful in discussing the stability of the equilibrium points.

Theorem 1 (Poincare and Perron) *Consider the equation* $\mathbf{y}' = A\mathbf{y} + \mathbf{f}(t,\mathbf{y})$. *Suppose all eigenvalues of A have negative real parts,* $\mathbf{f}(t,\mathbf{y})$, *and* $(\partial \mathbf{f}/\partial y_i)(t,\mathbf{y})$ $(i = 1,\cdots,n)$ *are continuous in* $(t,\mathbf{y})$ *for* $0 \le t < \infty$, $\|\mathbf{y}\| < k$ *where* $k > 0$ *is a constant, and* $\mathbf{f}$ *is small in the sense that its components satisfy* (4.2.3) *uniformly with respect to t on* $[0,+\infty)$. *Then the solution* $\mathbf{y} \equiv 0$ *is asymptotically stable .*

Definition 1 *The equilibrium solution* $\overline{y}$ *is stable if for each* $\epsilon > 0$, *there exists a* $\delta > 0$ *such that if* $\mathbf{y}(t)$ *is any solution of the above system satisfying* $\| \mathbf{y}(t_0) - \overline{y} \| < \delta$, *then the solution* $\mathbf{y}(t)$ *exists for all* $t \ge t_0$ *and* $\|\mathbf{y}(t) - \overline{y}\| < \epsilon$ *for* $t \ge t_0$.

Definition 2 *The equilibrium solution* $\overline{y}$ *is asymptotically stable if it is stable and if there exists a number* $\delta > 0$ *such that if* $\|\mathbf{y}(t_0) - \overline{y}\| < \delta$, *then* $\lim_{t \to \infty} \mathbf{y}(t) = \overline{y}$.

The behaviour of the solution of equation (4.2.2) , near $\hat{X}$=0, is expected to be similar to the behaviour of the solution to the linearized system

$$\dot{\hat{X}} = \hat{A}\hat{X}$$

Hence,to determine the stability of $\hat{X}$=**0** we consider the linearized system and solve $det[\hat{A} - \hat{\lambda}I] = 0$ .This yields the following characteristic equation

$$0 = (\hat{a}_{44} - \hat{\lambda})(\hat{\lambda}^3 + A\hat{\lambda}^2 + B\hat{\lambda} + C)$$

where

$$\begin{aligned} A &= -(\hat{a}_{11} + \hat{a}_{22} + \hat{a}_{33}) \\ B &= \hat{a}_{22}\hat{a}_{33} + \hat{a}_{11}\hat{a}_{33} + \hat{a}_{11}\hat{a}_{22} - \hat{a}_{12}\hat{a}_{21} - \hat{a}_{23}\hat{a}_{32} \\ C &= \hat{a}_{11}\hat{a}_{23}\hat{a}_{32} + \hat{a}_{12}\hat{a}_{21}\hat{a}_{33} - \hat{a}_{11}\hat{a}_{22}\hat{a}_{33} \end{aligned}$$

If all of the roots of this equation have negative real parts, then from the preceding theorem, $\hat{X}$=**0** is asymptotically stable; i.e. **I** is asymptotically stable. The following theorem, due to Routh and Hurwitz, gives necessary and sufficient conditions for the real part of the eigenvalues to be negative.

Theorem 2 (Routh-Hurwitz) *Let*

$f(\lambda) = a_0\lambda^n + b_0\lambda^{n-1} + a_1\lambda^{n-2} + b_1\lambda^{n-3} + \cdots$ $(a_0 \neq 0)$. *All roots of* $f(\lambda)$ *have negative real parts iff the following inequalities hold :*

$a_0\Delta_1 > 0 \quad \Delta_2 > 0 \quad a_0\Delta_3 > 0 \quad \Delta_4 > 0 \quad \cdots$

$$\left\{ \begin{array}{ll} a_0\Delta_n > 0 & n \text{ odd} \\ \Delta_n > 0 & n \text{ even} \end{array} \right\}$$

$$where \quad \Delta_1 = b_0 \quad \Delta_2 = det \begin{bmatrix} b_0 & b_1 \\ a_0 & a_1 \end{bmatrix}$$

and in general

$$\Delta_n = det \begin{bmatrix} b_0 & b_1 & b_2 & \cdots & b_{n-1} \\ a_0 & a_1 & a_2 & \cdots & a_{n-1} \\ 0 & b_0 & b_1 & \cdots & b_{n-2} \\ 0 & a_0 & a_1 & \cdots & a_{n-2} \\ 0 & 0 & b_0 & \cdots & b_{n-3} \\ \vdots & \vdots & \vdots & \cdots & \vdots \end{bmatrix}$$

Applying this to our characteristic polynomial yields the following conditions

$$A > 0\ , C > 0\ , AB > C\ ,\ and\ \hat{a}_{44} < 0$$

After substituting the physical parameters in for $A, B, C, \&\ \hat{a}_{44}$, and working through a prodigious amount of algebra the following conditions are obtained :

$$D_1 x^1 - W_p \ \leq \ 0 \tag{4.2.4}$$

$$\beta_2[1 - \gamma(1 - z^1)] - \frac{1}{\tau_c} \ < \ 0 \tag{4.2.5}$$

To show that condition (4.2.4) is always satisfied, consider

$$\frac{dx}{dt} = (W_p - D_1 x)(1 - x - y) - \frac{x}{\tau_2}.$$

Taking $x(0) = 0$ and $y(0) = 0$, we have at $t = 0$

$$\frac{dx}{dt} = W_p$$

which means $x(t)$ is increasing linearly with t for t near zero. Since D_1 is a positive constant this means $D_1 x(t)$ is also increasing near zero. If $D_1 x(t)$ stays

below W_p for all $t > 0$, were done since this would mean that $D_1x(t) - W_p < 0$. Now suppose there exists a point T^* such that $D_1x(T^*) = W_p$ and $0 \leq D_1x(t) < W_p$ for $0 \leq t < T^*$; then at $t = T^*$

$$\frac{d\,D_1x}{dt} = -\frac{D_1x}{\tau_2}$$

and since both D_1 and τ_2 are positive, this implies $D_1x(t)$ is decreasing. But this contradicts $0 \leq D_1x(t) < W_p$ for $0 \leq t < T^*$ and hence no such point exists. Therefore, $D_1x(t) - W_p < 0$ for all $t > 0$ and so condition (4.2.4) is always satisfied. Consequently, condition (4.2.5) is a necessary and sufficient condition for **I** to be asymptotically stable.

It is interesting, at this juncture, to note that condition (4.2.5)— which was obtained strictly from the mathematics— is simply a restatement of the threshold condition (2.3.4) obtained earlier by considering the laser physics. To see this, first recall that condition (2.3.4) must be satisfied for lasing action to occur. Now if condition (4.2.5) holds, then **I** will be asymptotically stable and since the P coordinate of **I** is zero, this means $P(t) \to 0$ as $t \to \infty$, i.e. no lasing. Hence, a necessary condition for lasing is

$$\beta_2[1 - \gamma(1 - z^1)] - \frac{1}{\tau_c} > 0\,,$$

or switching back to the physical variables

$$\sigma v[n_T - \gamma(n_T - n_1^1)] - \frac{1}{\tau_c} > 0\,.$$

Rearranging and using $\gamma = 1 + \dfrac{g_1}{g_0}$ yields

$$n_1^1 - \frac{g_1}{g_0}n_0^1 > \frac{1}{\sigma v \tau_c} \tag{4.2.6}$$

which is precisely condition (2.3.4) with $n_1(t)$ and $n_0(t)$ replaced by their respective equilibrium values. From this simple observation, we see that the physics and mathematics are in agreement.

For the stability analysis of **II**, introduce the variables $\bar{x} = x - x^2$, $\bar{y} = y - y^2$, $\bar{z} = z - z^2$, and $\bar{P} = P - P^2$. Substituting into (4.1.1) and reducing the equations as before yields

$$\begin{aligned}
\frac{d\bar{x}}{dt} &= \left(D_1x^2 - W_p - D_1(1 - x^2 - y^2) - \frac{1}{\tau_2}\right)\bar{x} \\
&+ (D_1x^2 - W_p)\bar{y} + \underbrace{D_1\bar{x}\bar{y} + D_1(\bar{x})^2}_{\vartheta_1}
\end{aligned}$$

$$\begin{aligned}
\frac{d\bar{y}}{dt} &= \left(2D_1(1 - x^2 - y^2) - 2D_1x^2 + \frac{1}{\tau_{21}}\right)\bar{x} \\
&- \left(\frac{1}{\tau_1} + 2D_1x^2 + D_2(1 - z^2)\right)\bar{y} + D_2y^2\bar{z} \\
&+ \underbrace{D_2\bar{y}\bar{z} - 2D_1\bar{x}\bar{y} - 2D_1(\bar{x})^2}_{\vartheta_2}
\end{aligned}$$

$$\begin{aligned}
\frac{d\bar{z}}{dt} &= D_4(1 - z^2)\bar{y} - \left(\gamma\beta_1P^2 + D_4y^2 + \frac{1}{\tau_1'}\right)\bar{z} \\
&- \beta_1[1 - \gamma(1 - z^2)]\bar{P} \underbrace{- D_4\bar{y}\bar{z} - \gamma\beta_2\bar{z}\bar{P}}_{\vartheta_3}
\end{aligned}$$

$$\begin{aligned}
\frac{d\bar{P}}{dt} &= \gamma\beta_2P^2\bar{z} + \underbrace{\gamma\beta_2\bar{z}\bar{P}}_{\vartheta_4}
\end{aligned}$$

This system can be written symbollically as

$$\dot{\bar{X}} = \bar{A}\bar{X} + \bar{g} \tag{4.2.7}$$

where $\bar{X} = [\bar{x},\ \bar{y},\ \bar{z},\ \bar{P}]^T$; $\bar{g} = [\bar{g}_1,\ \bar{g}_2,\ \bar{g}_3,\ \bar{g}_4]^T$; and $\bar{A} = [\bar{a}_{ij}]$ where the $\bar{a}_{ij}$'s are defined in the obvious way. Now since system (4.2.7) is an "almost linear" system, the stability of **II** can be determined by considering

$$\dot{\bar{X}} = \bar{A}\bar{X}$$

and hence we must solve $det[\bar{A} - \bar{\lambda}I] = 0$. This yields the following characteristic equation

$$\bar{\lambda}^4 + a\bar{\lambda}^3 + b\bar{\lambda}^2 + c\bar{\lambda} + d = 0 \tag{4.2.8}$$

where

$$\begin{aligned}
a &= -\bar{a}_{11} - \bar{a}_{22} - \bar{a}_{33} \\
b &= -\bar{a}_{12}\bar{a}_{21} - \bar{a}_{23}\bar{a}_{32} + \bar{a}_{22}\bar{a}_{33} + \bar{a}_{11}\bar{a}_{22} + \bar{a}_{11}\bar{a}_{33} - \bar{a}_{34}\bar{a}_{43} \\
c &= (\bar{a}_{11} + \bar{a}_{22})\bar{a}_{34}\bar{a}_{43} + \bar{a}_{11}\bar{a}_{23}\bar{a}_{32} + \bar{a}_{12}\bar{a}_{21}\bar{a}_{33} - \bar{a}_{11}\bar{a}_{22}\bar{a}_{33} \\
d &= (\bar{a}_{12}\bar{a}_{21} - \bar{a}_{11}\bar{a}_{22})\bar{a}_{34}\bar{a}_{43}
\end{aligned}$$

Invoking the Routh-Hurwitz Theorem yields the following inequalities which must be satisfied in order for **II** to be asymptotically stable

$$a > 0\ ,\ d > 0\ ,\ ab > c\ ,\ a(bc - ad) > c^2 \tag{4.2.9}$$

After an inordinate amount of algebraic manipulations it turns out that the first three conditions will be satisfied if $D_1x^2 - W_p \leq 0$. It was shown above that $D_1x(t) - W_p < 0$ for all $t > 0$ and hence the first three conditions are met. Therefore, it is the fourth condition in (4.2.9) that determines the stability of

II. The algebra associated with this condition, however, is tremendously complicated and therefore we resort to numerical calculations. The numerics indicate there is an interplay of stability between equilibrium points I and II which will now be discussed in some detail in the following section.

4.3 Bifurcation Points

It is well known that nonlinear dynamical systems can exhibit a wide variety of responses as initial conditions or parameter values change. The transition from one response to another is often quite sudden; sometimes referred to as "catastrophic." Bifurcations are said to occur when there is a sudden change in the behaviour of the system as a parameter passes through a critical value called a bifurcation point. A system may contain more than one parameter, each with its own bifurcation points. In this section we discuss the interchange of stability between equilibrium points I and II and show the existence of bifurcation points.

To start with, consider W_p as a parameter and choose it to be "small". Then using the computer program given in Appendix A, we calculate the equilibrium values of I & II and use the Routh-Hurwitz criteria to determine the stability of each point. By gradually increasing W_p and repeating the process we see there is an interchange of stability which goes like this. For W_p small, the P coordinate of II is negative, II is unstable, and I is asymptotically stable (i.e. no lasing). As W_p is increased, the P coordinate of II eventually reaches zero and thus the two equilibrium points coalesce (this is the threshold of lasing). Finally, as W_p

is increased still further, the P coordinate of **II** becomes positive, **II** becomes asymptotically stable, and **I** becomes unstable (i.e. lasing occurs).

This is illustrated in Figure 4.1 where P^2 is graphed as a function of W_p and the stability of **I** and **II** is noted. The value of W_p at which the interchange of stability occurs is a bifurcation point and is denoted W_p^*. From numerical calculations we find $W_p^* \doteq 0.342 \times 10^{-5}$.

It is also of physical interest to see how the system responds as the cavity lifetime of a photon, τ_c, is varied. Choosing τ_c small and following the same procedure as above yields the same interplay of stability as before. Figure 4.2 gives P^2 as a function of τ_c once again noting the stability of each point. From this we see that τ_c has a bifurcation point which will be denoted τ_c^* and is approximated by $\tau_c^* \doteq 4.81 \times 10^{-5}$. It should be noted at this point that bifurcations are related to catastrophes. Loosely speaking, a system experiences a catastrophe when a smooth change in the values of a parameter result in a sudden change in the response of the system [15]. By comparing Figure 4.3 where $\tau_c = 4.8 \times 10^{-5}$ with Figure 4.4 where $\tau_c = 4.9 \times 10^{-5}$, we see that the change in the behaviour of the photon density is both sudden and striking. Hence, as τ_c varies from $\tau_c = 4.8 \times 10^{-5}$ to $\tau_c = 4.9 \times 10^{-5}$ the laser system experiences a catastrophe.

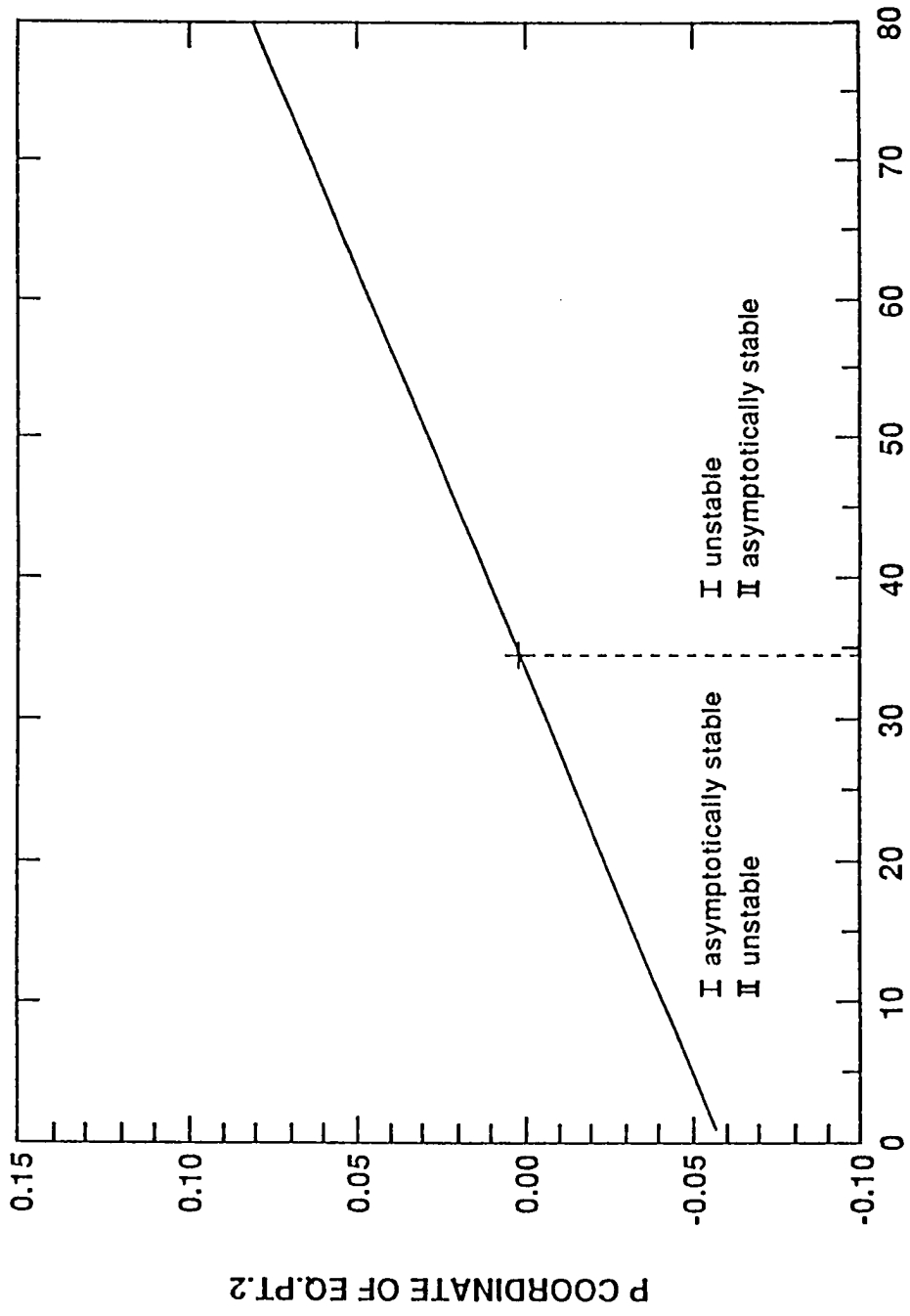

Figure 4.1 P coordinate of equilibrium point two as a function of the pump

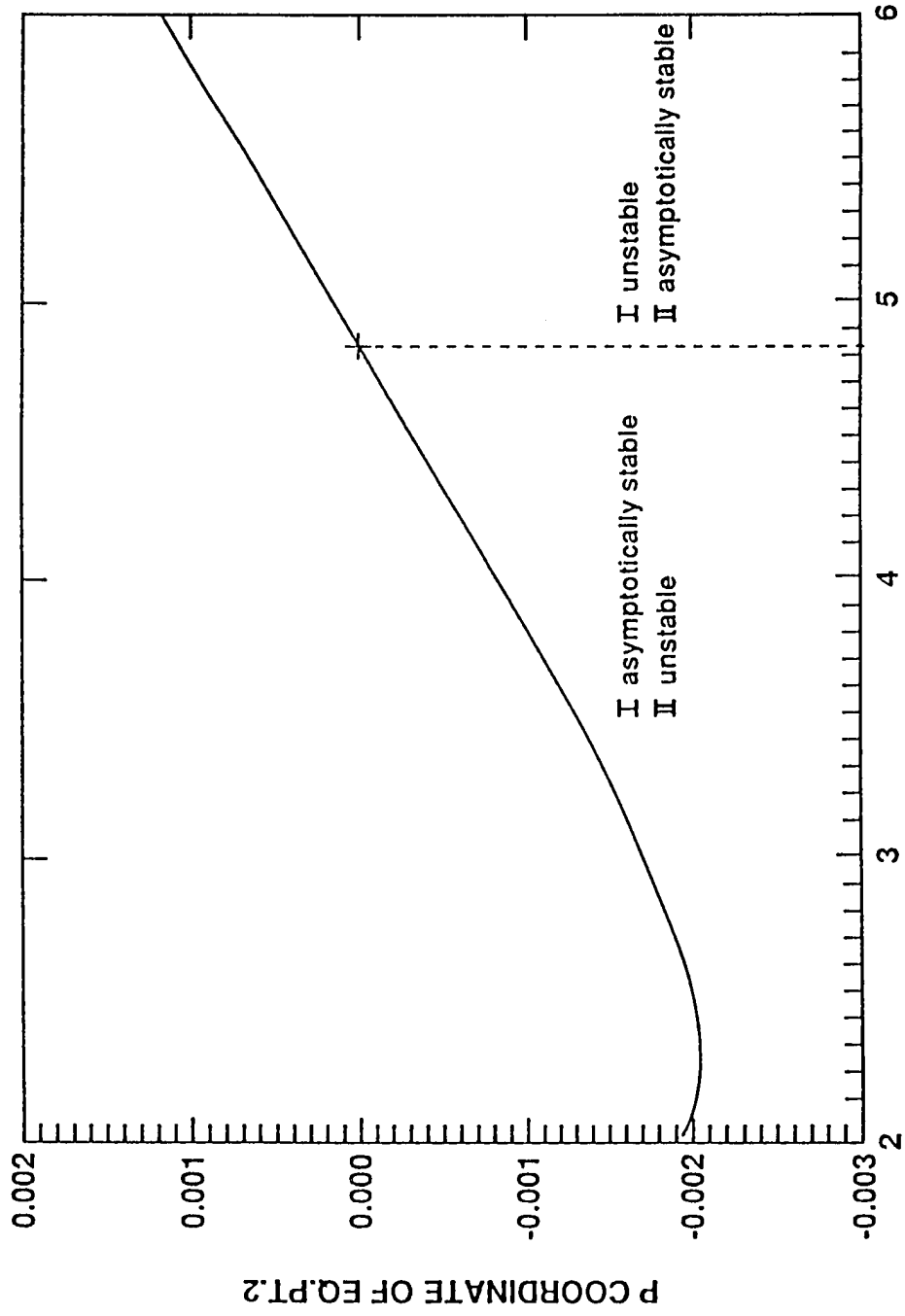

Figure 4.2 P coordinate of equilibrium point two as a function of TAUC

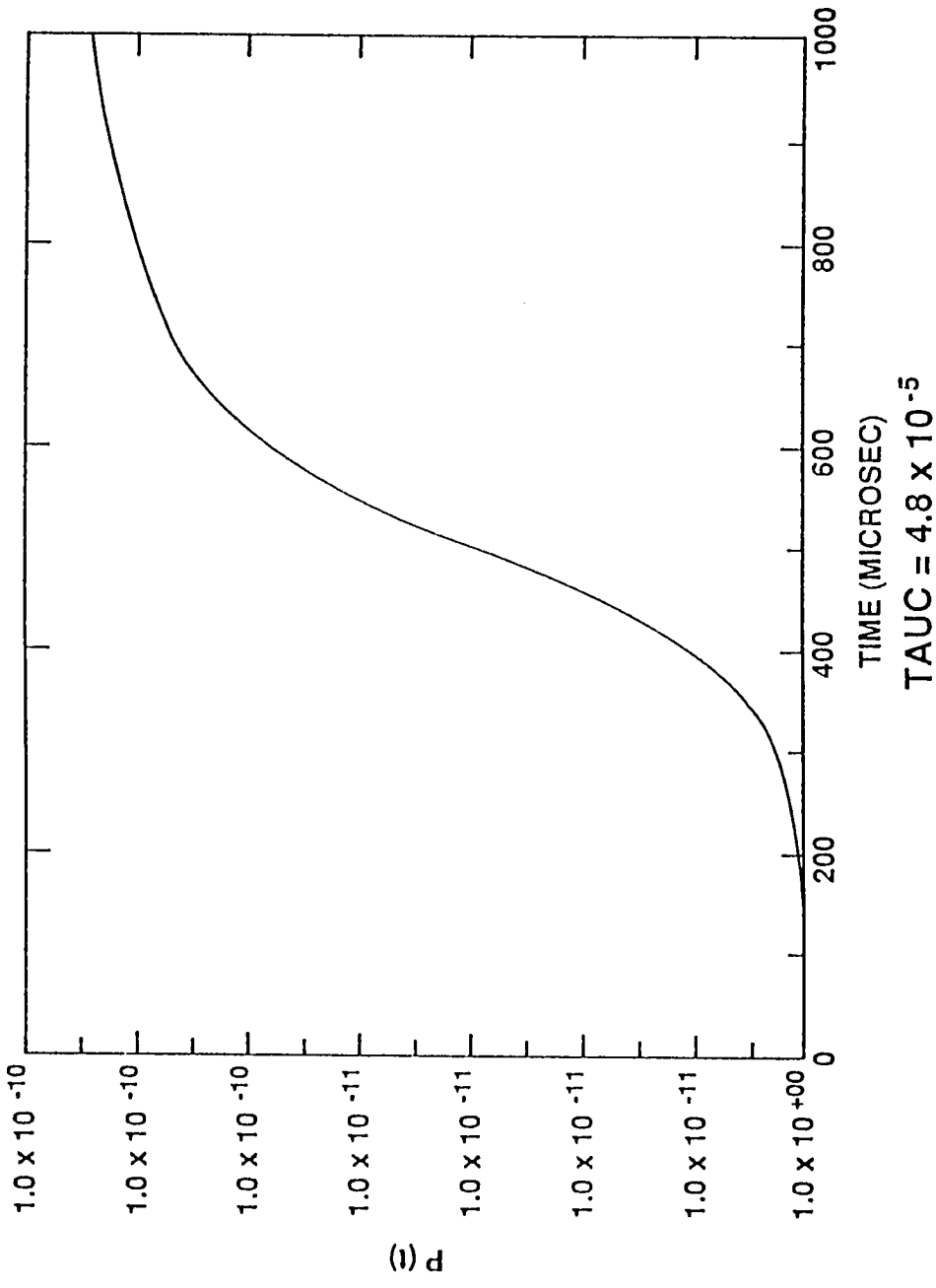

Figure 4.3 The normalized photon density

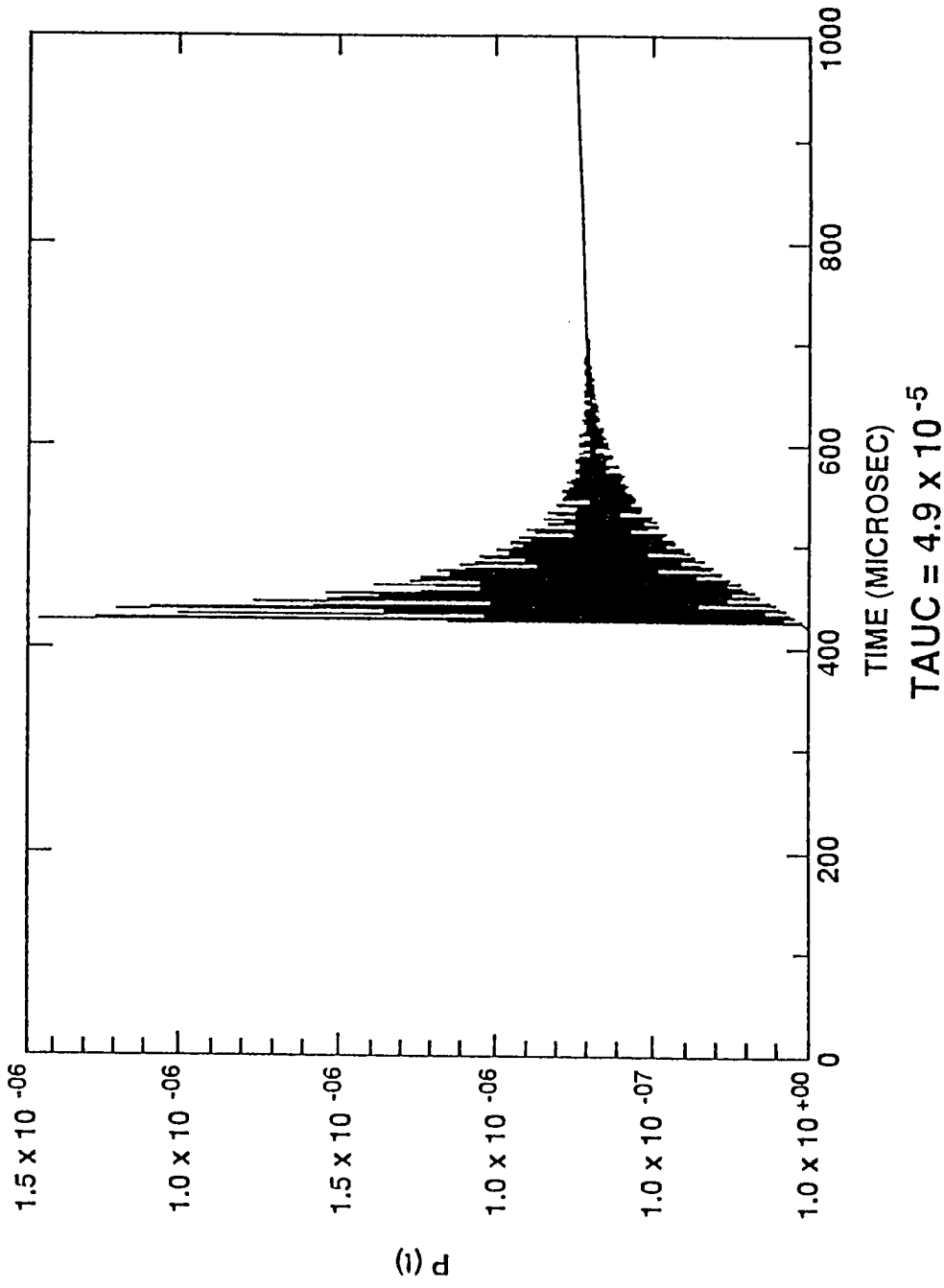

Figure 4.4 The normalized photon density

Chapter 5

Numerical Solutions, Oscillations, and Q-Switching

5.1 Numerical Solutions

In this section the numerical solutions of the system (3.1.1) are obtained. This is done by employing either the subroutine LSODA (when using a VAX 11/750) or the subroutine DDRIV2 (when using an IBM PC). In either case, all computations were performed in double precision arithmetic. LSODA was developed in 1987 at Lawrence Livermore National Laboratory in Livermore, California by L.R. Petzold and A.C. Hindmarsh. DDRIV2 was developed in 1979 and revised in 1987 by D.K. Kahaner, National Bureau of Standards, and C.D. Sutherland of Los Alamos National Laboratory. Both subroutines were created for the numerical integration of stiff and nonstiff systems of first order ordinary differential

equations. When the system is stiff, the subroutines use a backward difference formula (BDF) to perform the numerical integration and when the system is not stiff they use a higher order Adams method. Both LSODA and DDRIV2 have the capability of automatically switching from one method to the other as the system passes from stiff to nonstiff regions. The BDF method was chosen by both d.e. solvers throughout the interval of integration which indicates that system (3.1.1) is stiff. Roughly speaking, a system is stiff when the characteristic equation associated with the system has a root with a "large" negative real part. A more detailed treatment of stiffness can be found in [16]. Tables 5.1-5.4 list the parameter values used in the program.

Table 5.1 Crystal Parameters for Tm-Ho

$N_T = 1 \times 10^{21}/cm^3$

$n_T = 1 \times 10^{20}/cm^3$

$\ell = 0.3\, cm$

$\phi_{norm} = 1 \times 10^{18}/cm^3$

Table 5.2 Cavity Parameters

$\ell_c = 17.5cm$

$R_1 = 1.0$

$R_2 = 0.95$

Table 5.3 Material Parameters for Tm-Ho:YAG

$C = \frac{1}{40 \times 10^{21}}\ cm^3/\mu s$

$C_1 = \frac{1}{475 \times 10^{20}}\ cm^3/\mu s$

$C_1^* = 0.0$

$\tau_2 = 450\mu s$

$\tau_{20} = 900\mu s$

$\tau_{21} = 900\mu s$

$\tau_1 = 11{,}000\mu s$

$\tau_1^{'} = 8{,}500\mu s$

$g_0 = 1$

$g_1 = 1$

$\gamma = 2$

$\sigma = 7 \times 10^{-21}\ cm^2$

$q_1 = 0.0$

$q_1^{'} = 0.0$

Table 5.4 Physical Parameters

$v = 30{,}000\ cm/\mu s$

$\tau_c = 1 \times 10^{-3}\ \mu s$

$W_p = 6 \times 10^{-3}/cm^3 \cdot \mu s$

$sp_o = 1 \times 10^{-6}$

Employing the program given in Appendix B the numerical solutions for $x(t)$, $y(t)$, $z(t)$, & $P(t)$ are obtained and plotted in Figures 5.1-5.4, respectively.

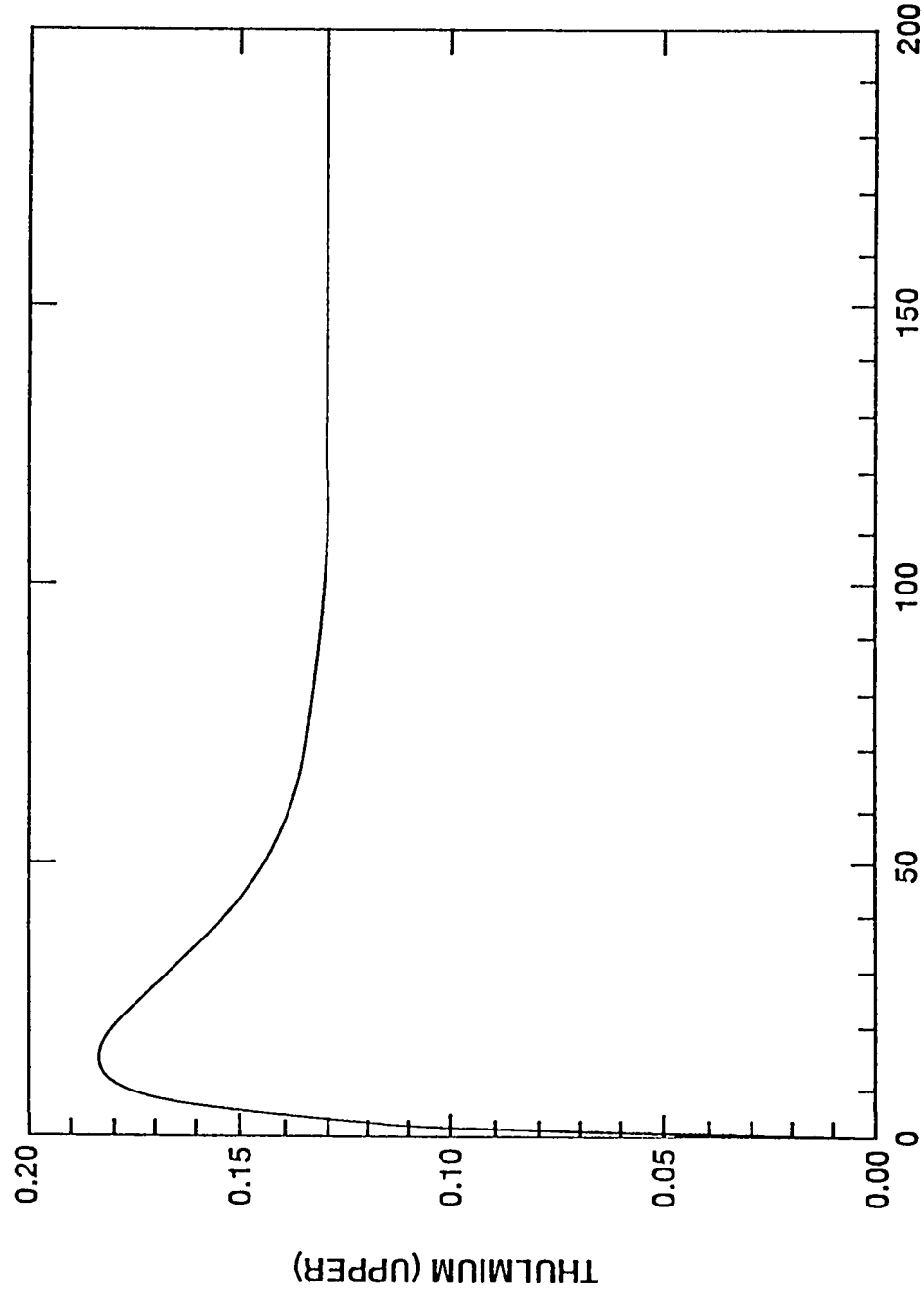

Figure 5.1 The normalized upper thulium energy level, x(t)

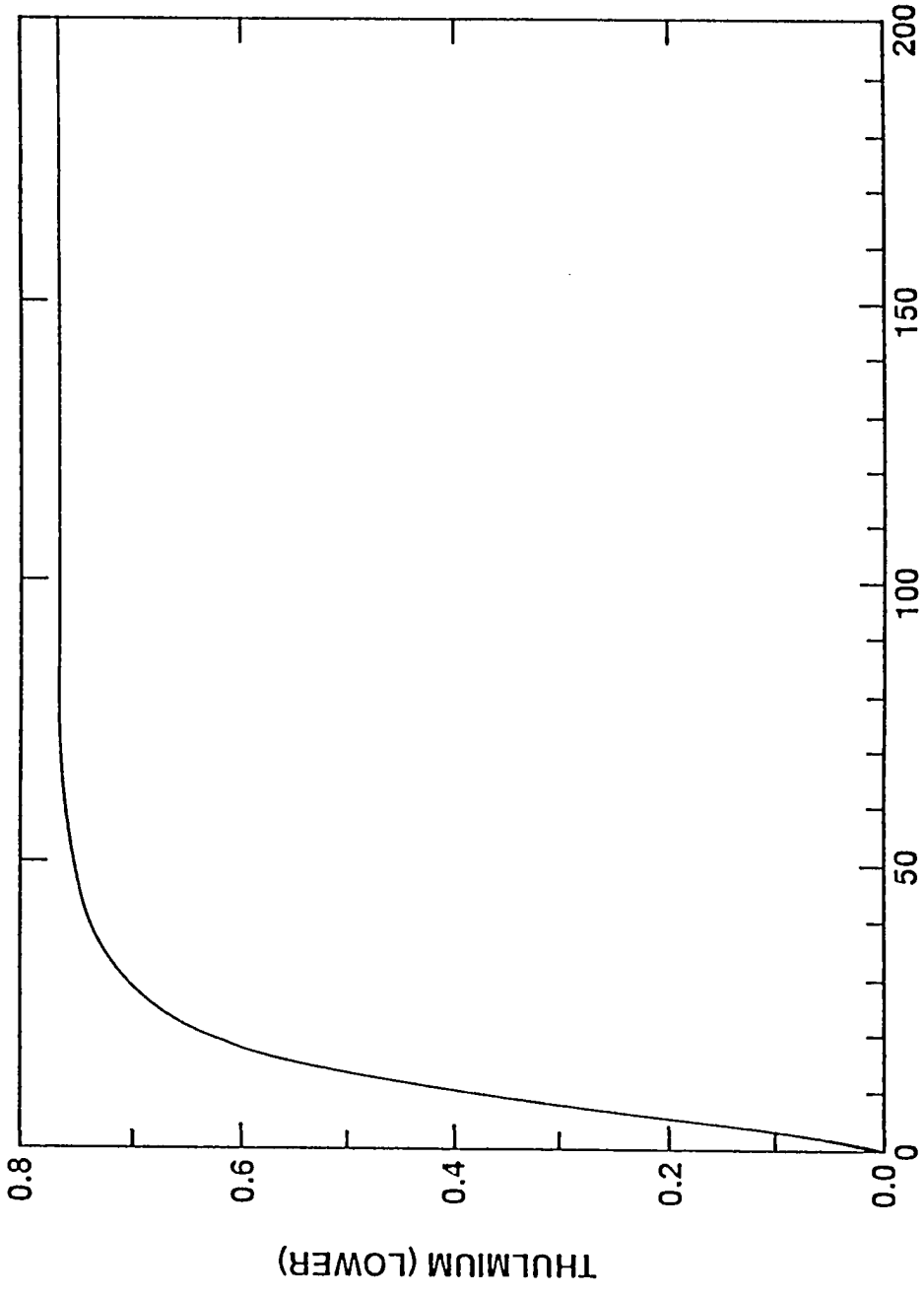

Figure 5.2 The normalized lower thulium energy level, y(t)

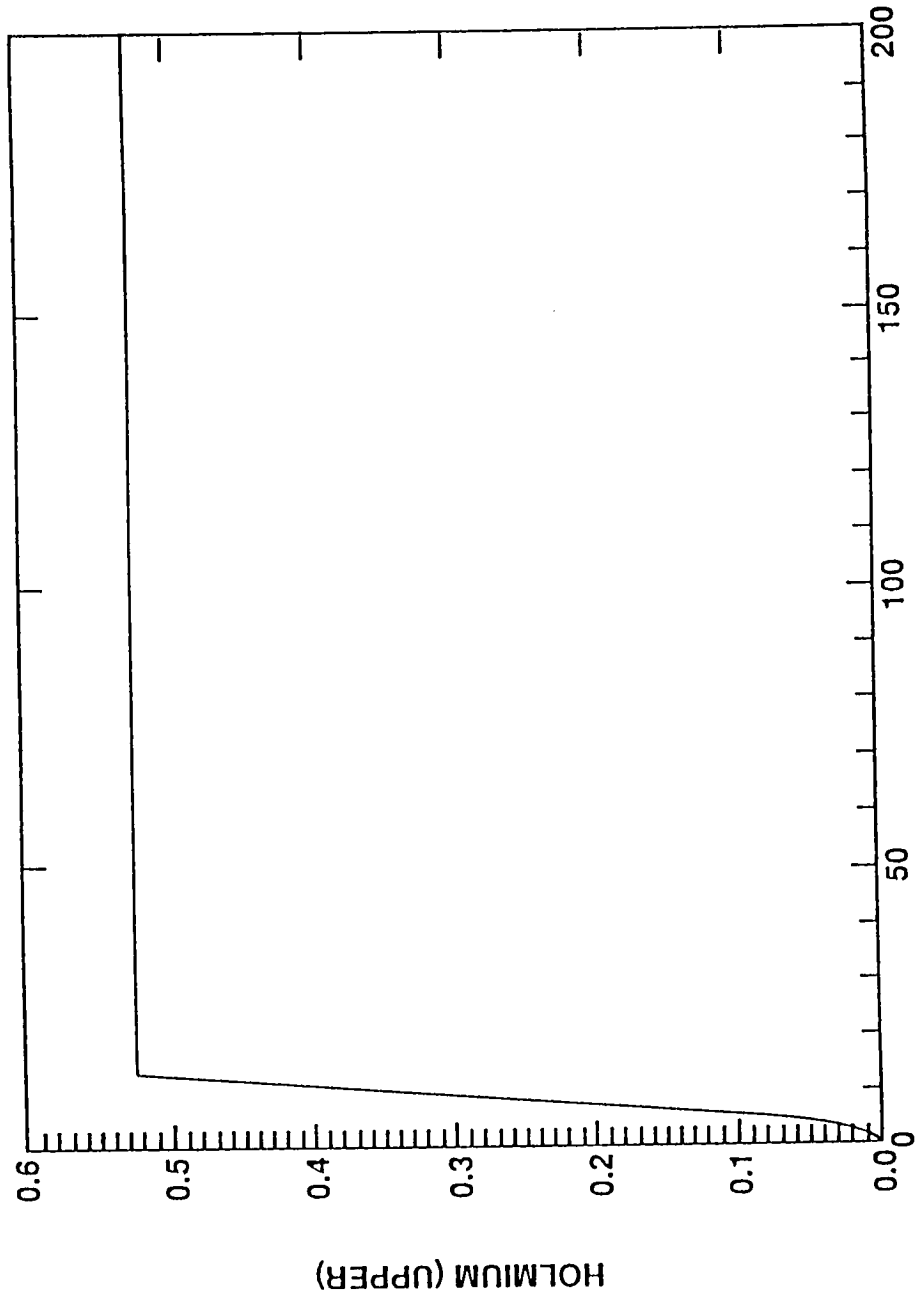

Figure 5.3 The normalized upper lasing level of holmium, z(t)

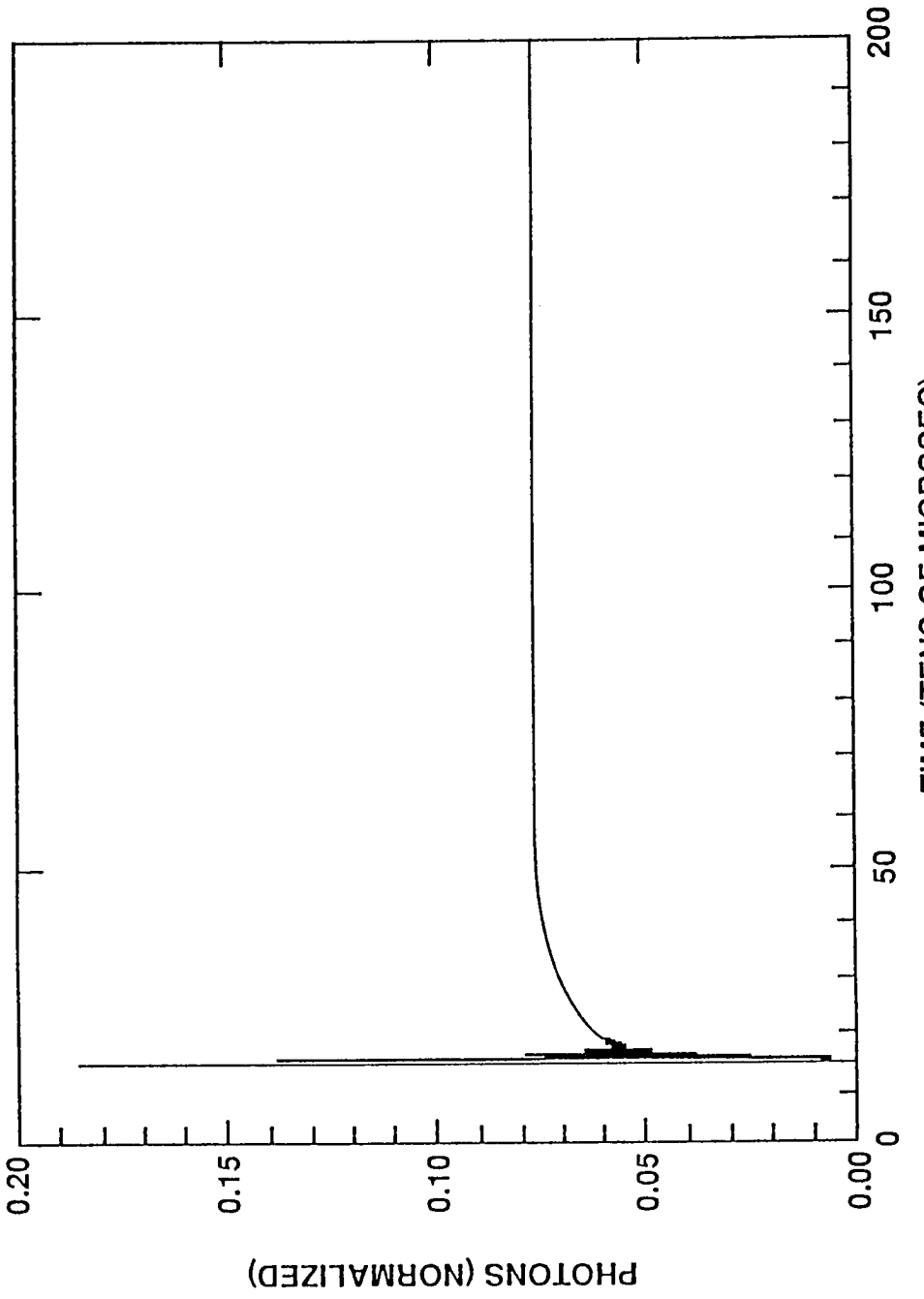

Figure 5.4 The normalized photon density, P(t)

Since W_p is constant a comparison of the "long time" behaviour of the numerical solutions with that of the equilibrium solutions can be performed. Using conditions (4.2.5) and (4.2.9)—which were obtained from the Routh- Hurwitz Theorem—it is found that **II** is asymptotically stable and **I** is unstable. The equilibrium values of **II** are calculated from (4.1.9)–(4.1.12). This yields

$$x^2 = 0.1304363$$

$$y^2 = 0.7637408$$

$$z^2 = 0.5238095$$

$$P^2 = 0.0759492$$

Finally, from Figures 5.1–5.4 it is apparent that the solutions have steadied out by t=2ms and hence are expected to be near their asymptotic values. At t=2ms the following computed values are obtained

$$x = 0.1304372$$

$$y = 0.7637406$$

$$z = 0.5238095$$

$$P = 0.0759491$$

From this it is evident that the stability analysis predicts the "long time" behaviour of the solutions extremely well. Also, since sp_o is nonzero in the computer program, the claim made at the beginning of chapter four—that the spontaneous emission term has a negligible affect on the asymptotic behaviour of the solutions— is substantiated.

Various pumping schemes were considered in the model. Figure 5.5 gives the numerical solution for $P(t)$ when the pumping term is taken to be

$$W_p(t) = \alpha^2 t e^{-\alpha^2 t^2}$$

where $\alpha = .01133$. From this figure we see that the photon density has irregular oscillations and decays rather rapidly, becoming negligible by about $t = 250\mu s$.

5.2 Oscillatory Behaviour of the Solutions

The oscillatory behaviour of the solutions is now examined in greater detail. Figure 5.6 is a plot of the numerical solution of the upper lasing level, $z(t)$, and the normalized photon density, $P(t)$. It is a typical example of the erratic spiking behaviour exhibited by the photon density when lasing occurs.

In Chapter 4 a local stability analysis was conducted by expanding the system (4.1.1) about the equilibrium points. This yielded a system of the form

$$\dot{\mathbf{y}} = A\mathbf{y} + \mathbf{g} \tag{5.2.1}$$

where A was the Jacobian matrix evaluated at an equilibrium point, $\mathbf{y}$ was the vector $\mathbf{x} - \bar{\mathbf{x}}$ (where $\bar{\mathbf{x}}$ was an equilibrium point) and $\mathbf{g}$ was a vector containing all the nonlinear terms of the system. For $\mathbf{g}$ small, in the sense that it satisfied (4.2.3), the behaviour of the solution to (5.2.1) was expected to be similar to the behaviour of the solution to the linearized system

$$\dot{\mathbf{y}} = A\mathbf{y} \tag{5.2.2}$$

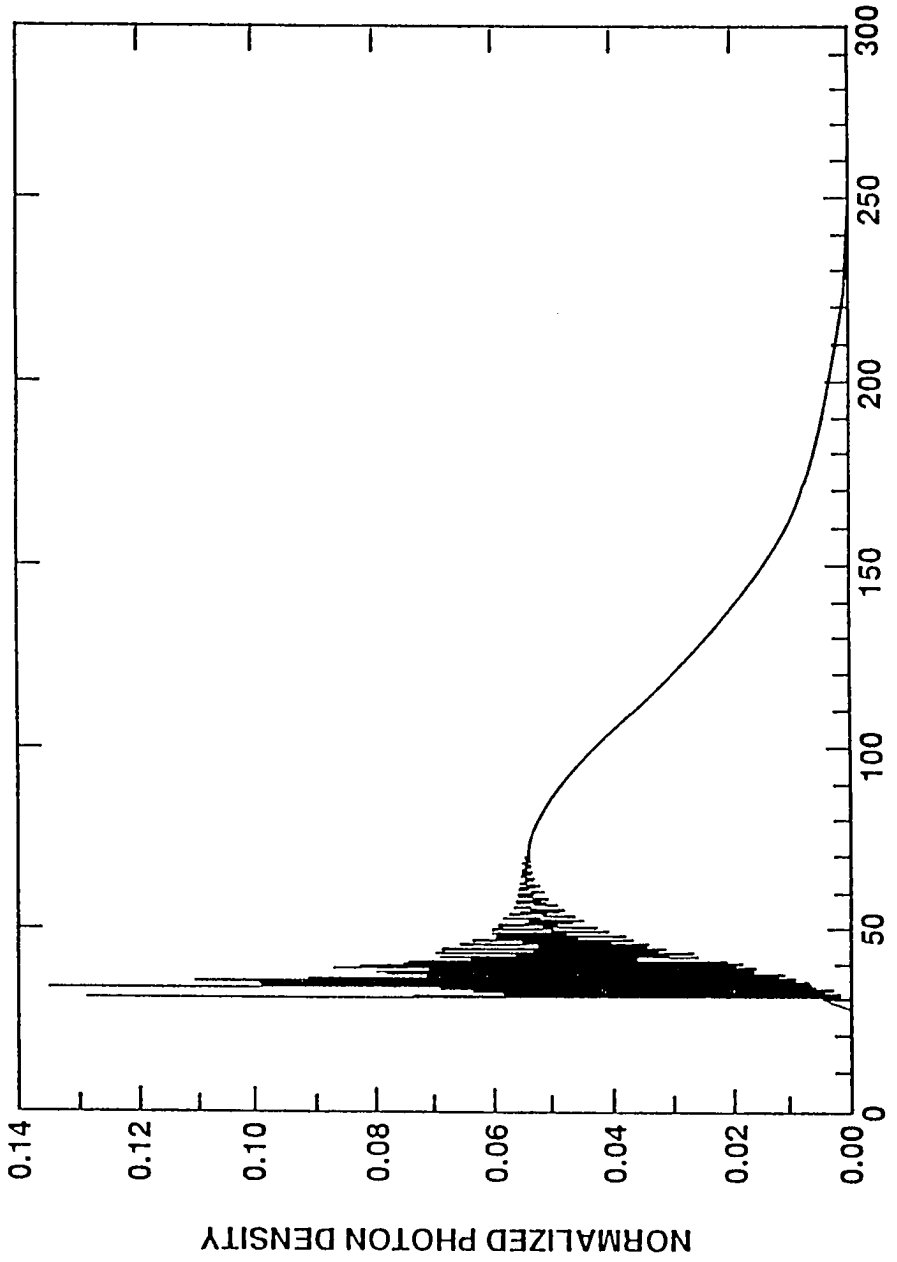

Figure 5.5 Normalized photon density with decaying exponential pump

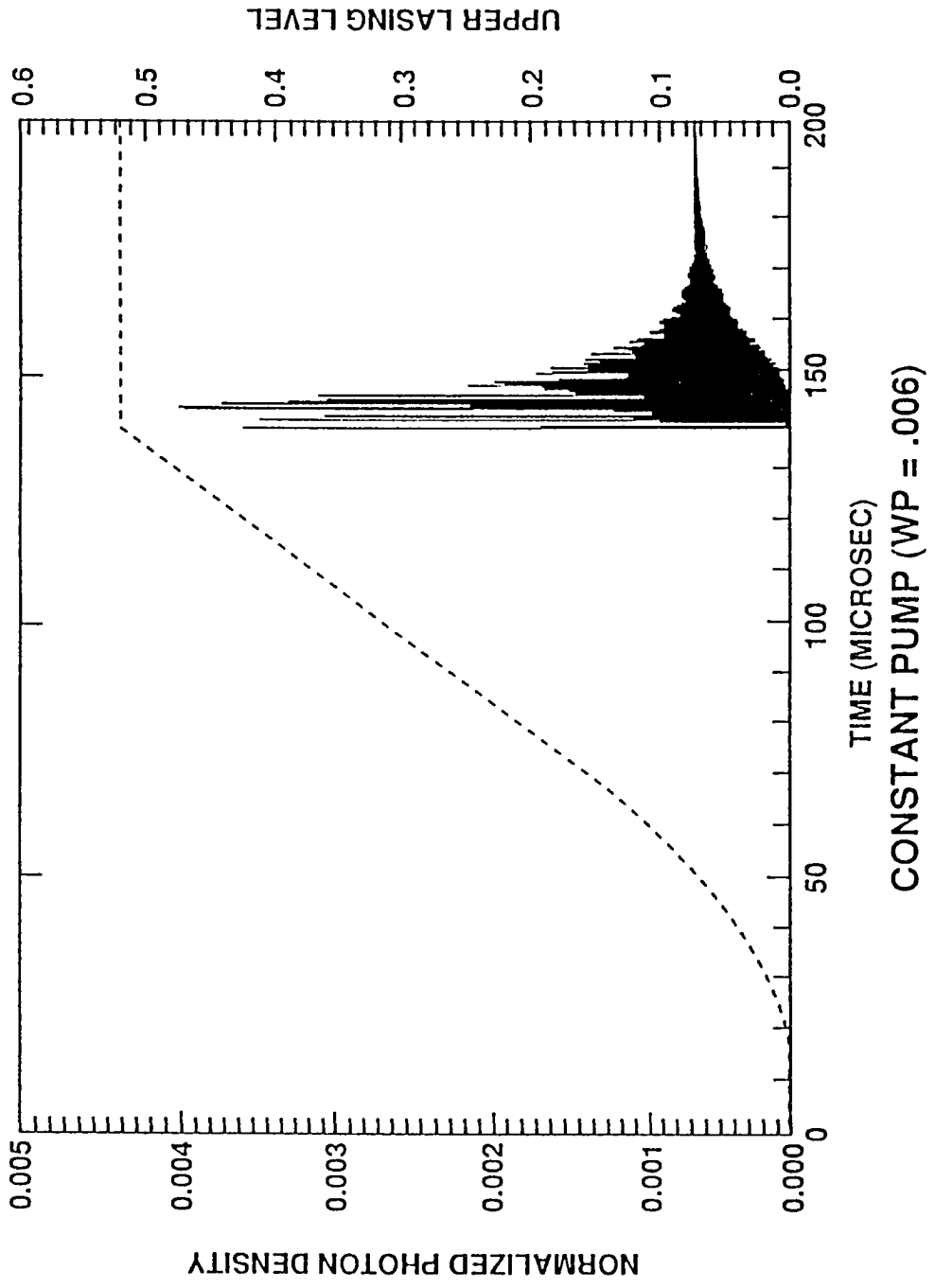

Figure 5.6 Photon density and upper lasing level with a constant pump

Hence, equation (5.2.2) was used to determine the stability of the equilibrium point under consideration. This is the same as saying that if the true solution, $\mathbf{x}$, is "close" enough to the equilibrium solution, $\bar{\mathbf{x}}$, then the nonlinear terms are negligible and consequently the linearized system (5.2.2) can be used to predict the behaviour of the nonlinear system (5.2.1). As seen in the preceding section, this gave good results.

An investigation of the oscillations in the system (3.1.1) will now be conducted by solving the system numerically on the interval [0, 400] and linearizing about the current numerical solution every microsecond. Assuming the current numerical solution, $\mathbf{x}_c$, is "close" to the true solution, $\mathbf{x}$, the nonlinear terms will be negligible and hence the behaviour of the solution to the nonlinear system can be expected to be similar to the behaviour of the solution to the linearized system. In particular, we expect the oscillatory behaviour of the nonlinear system to be predicted by the linearized system. To this end, let the time of linearization be denoted t_c and the numerical solutions at t_c be denoted x_c, y_c, z_c and P_c. Also, let

$$\mathbf{y} = \mathbf{x} - \mathbf{x}_c = \begin{bmatrix} x - x_c \\ y - y_c \\ z - z_c \\ P - P_c \end{bmatrix}$$

Then, linearizing at time t_c about the point (x_c, y_c, z_c, P_c) yields the system

$$\dot{\mathbf{y}} = \mathbf{b} + A\mathbf{y} \,. \tag{5.2.3}$$

Here $A = [a_{ij}]$ where $a_{ij} = \dfrac{\partial f_i}{\partial y_j}(x_c, y_c, z_c, P_c)$, the functions $f_1, \cdots, f_4$ are as defined in section 3.1 and

$$\mathbf{b} = \mathbf{f}(t_c, \mathbf{x}_c)$$

The general solution of equation (5.2.3) will be the sum of the homogeneous solution and the particular solution. Written symbolically

$$\mathbf{y}_g = \mathbf{y}_h + \mathbf{y}_p \, .$$

The homogeneous solution is obtained using the eigenvalue-eigenvector method and the particular solution is given by $\mathbf{y}_p = -A^{-1}\mathbf{b}$. The difference between the general solution and the homogeneous solution is $-A^{-1}\mathbf{b}$, which is a constant real vector. Thus, for the oscillatory behaviour it suffices to consider

$$\dot{\mathbf{y}} = A\mathbf{y} \tag{5.2.4}$$

by forming $det[A - \lambda I] = 0$ which yields the characteristic equation

$$\lambda^4 + a\lambda^3 + b\lambda^2 + c\lambda + d = 0 \tag{5.2.5}$$

where a, b, c and d depend on the parameters and the current values of the numerical solution.

Clearly, the solution to (5.2.4) will have oscillatory behaviour whenever (5.2.5) has at least one root with nonzero imaginary part. Since the coefficients of (5.2.5) are real and the complex roots of a polynomial with real coefficients occur in complex conjugate pairs [5, p.111], another way of stating this is that (5.2.4) will have oscillatory behaviour whenever (5.2.5) has a pair of complex

conjugate roots. This will happen when either discriminant associated with (5.2.5) is negative. Hence, an expression for the discriminants will be obtained by following the procedure explicated in [5, pp.114-115] and only briefly outlined here.

Starting with equation (5.2.5), introduce the new variable $\varsigma = \lambda + \frac{b}{4}$. Substitute ς into (5.2.5), rearrange and simplify to obtain

$$\varsigma^4 + p\varsigma^2 + s\varsigma + r = 0 \tag{5.2.6}$$

where

$$\begin{aligned} p &= b - \frac{3a^2}{8} \\ s &= \frac{a^3}{8} + c - \frac{ab}{2} \\ r &= \frac{ba^2}{16} - \frac{3a^4}{256} - \frac{ac}{4} + d \end{aligned}$$

For any u, equation (5.2.6) is equivalent to

$$\underbrace{\left[\varsigma^2 + \frac{u}{2}\right]^2}_{R^2} - \underbrace{\left[(u-p)\varsigma^2 - s\varsigma + \left(\frac{u^2}{4} - r\right)\right]}_{Q^2} = 0\,. \tag{5.2.7}$$

R^2 is a perfect square with $R = \varsigma^2 + \frac{u}{2}$ and Q^2 is a perfect square for all u such that

$$(-s)^2 - (u-p)(u^2 - 4r) = 0$$

or equivalently

$$s^2 = (u-p)(u^2 - 4r) \tag{5.2.8}$$

Equation (5.2.8) is a cubic equation in u with real coefficients. Hence, [5, p.94] states there exists at least one real number $u_1 \geq p$ satisfying (5.2.8). Since

(5.2.7) holds for all u, we can substitute u_1 in for u so that Q^2 will be a perfect square. This yields

$$R^2 - Q^2 = 0 = (R+Q)(R-Q) \tag{5.2.9}$$

where $Q = \alpha\varsigma - \beta$, $\alpha = \sqrt{u_1 - p}$ and $\beta = \frac{s}{2\alpha}$. Finally, substituting the expressions for R and Q into (5.2.9) yields

$$\left\{\varsigma^2 + \alpha\varsigma + \left(\frac{u_1}{2} - \beta\right)\right\}\left\{\varsigma^2 - \alpha\varsigma + \left(\frac{u_1}{2} + \beta\right)\right\} = 0\,. \tag{5.2.10}$$

Since (5.2.10) is a product of two quadratics we see there will be two discriminants associated with the characteristic equation (5.2.5). Denote the discriminants DISC1 and DISC2 where

$$DISC1 = \alpha^2 - 4\left(\frac{u_1}{2} - \beta\right) \;\;\&\;\; DISC2 = \alpha^2 - 4\left(\frac{u_1}{2} + \beta\right)\,.$$

Oscillations will be present in the linearized system whenever either of the above two discriminants is negative.

Using the program in Appendix B, the values of DISC1 and DISC2 were tracked from t=0 to t=400μs. The roots of (5.2.5) were simultaneously located and tracked using [18] with the following results.

DISC2 starts out negative and remains negative until t=236μs at which time it becomes positive and stays positive for the remainder of the integration interval. The root finder starts out by locating a pair of complex conjugate roots with small imaginary parts ($Im(\lambda) \doteq .005$ so period=$T \doteq 1250\mu s$). The imaginary part decreases monotonically with time and disappears altogether

when $t = 236\mu s$. These observations show the nexus between DISC2 and this complex conjugate pair.

DISC1 starts out positive but goes negative at about t=139μs. While DISC1 is positive, the root finder consistently finds two real roots. When DISC1 becomes negative a pair of complex conjugate roots appear. This new complex conjugate pair—unlike the one associated with DISC2— has a relatively large imaginary part ($Im(\lambda) \doteq 13$) which increases with time. Since oscillations begin—in the nonlinear system—at about 138.8μs and DISC1 predicts oscillations to start—in the linearized system—at about 139μs, we see that the oscillatory nature of the linearized system is indeed similar to that of the nonlinear system. For example, when t=165μs we have, for the linearized system, $Im(\lambda) \doteq 15.4$ and hence

$$period = T = \frac{2\pi}{Im(\lambda)} \doteq 0.477999\ \mu s\ per\ osc.$$

Therefore, the frequency of oscillations in the linearized system is

$$frequency = \frac{1}{T} \doteq 2.45\ osc.\ per\ \mu s$$

Solving the nonlinear system numerically and graphing the photon density on the interval [140, 180] we obtain Figure 5.7 . From this it is seen that on the interval [160, 170] there are 24 oscillations, which gives an average frequency of 2.4 osc. per μs. Thus, the oscillatory behaviour of the linearized system is in excellent agreement with the oscillatory behaviour exhibited by the nonlinear system. Figure 5.8 is a graph of DISC1 and shows that DISC1 goes negative at

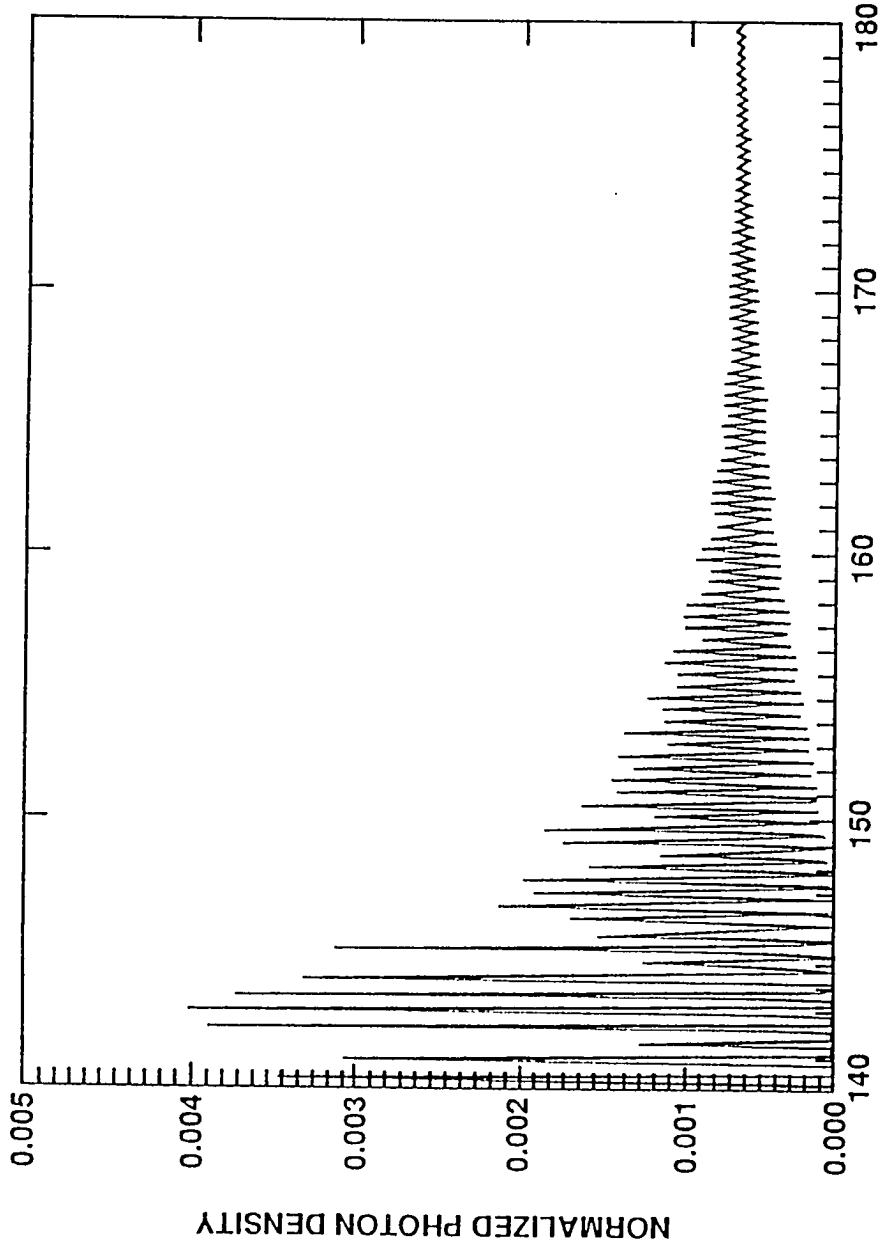

Figure 5.7 The photon density graphed on a stretched out time scale

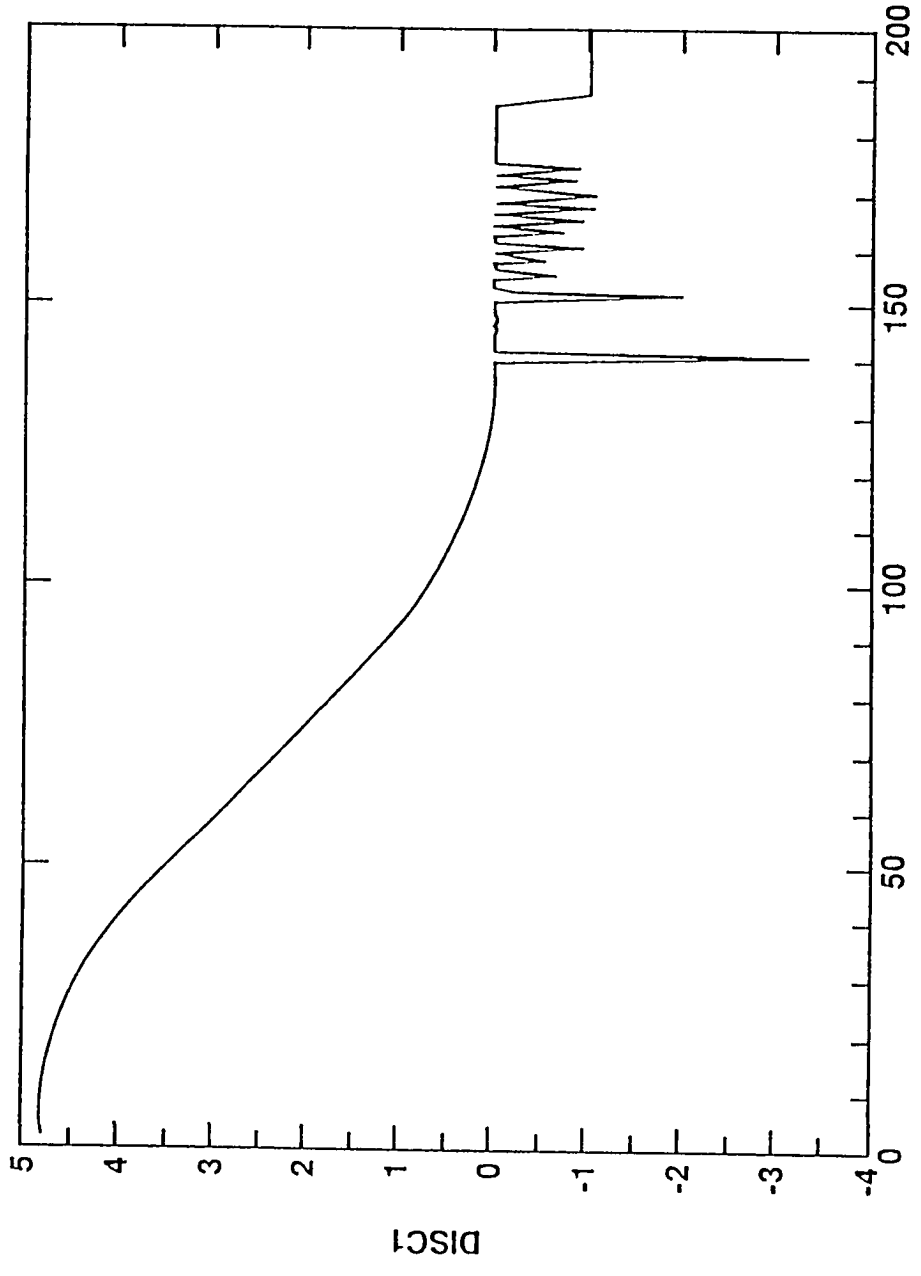

Figure 5.8 One of the discriminants of the time dependent characteristic equation showing oscillations beginning at the onset of lasing

about 139 μs which is the threshold of lasing.

Finally, since equilibrium point two is asymptotically stable we expect the time dependent eigenvalues to approach the eigenvalues associated with **II**. In fact, this is exactly what happens as can be seen by the following information. The eigenvalues associated with **II** are approximated by

$$\begin{aligned}
\bar{\lambda}_1 &= -.1675 + i\,17.86 \\
\bar{\lambda}_2 &= -.1675 - i\,17.86 \\
\bar{\lambda}_3 &= -.0081 \\
\bar{\lambda}_4 &= -.0070
\end{aligned}$$

At $t = 400\mu s$ the time dependent eigenvalues of the linearized system are approximately

$$\begin{aligned}
\lambda_1 &= -.1614 + i\,17.53 \\
\lambda_2 &= -.1614 - i\,17.53 \\
\lambda_3 &= -.0097 \\
\lambda_4 &= -.0061
\end{aligned}$$

A similar approach was taken to investigate the oscillations in the asymptotic behaviour of the solution. The cavity lifetime, τ_c , was taken small and gradually increased until the system lased. For τ_c small, the P coordinate of **II** was negative and DISC1 & DISC2 were both positive. As τ_c was continuously increased, P^2 eventually became positive and DISC1 became negative. These two events

occurred simultaneously when $\tau_c = \tau_c^* \doteq 4.81 \times 10^{-5}$ which is the critical value of τ_c previously reported at the end of section 4.3. Figure 5.9 is a graph of DISC1 as a function of τ_c. This shows that when one of the discriminants (DISC1) associated with **II** becomes negative, the asymptotic behaviour of the system will be oscillatory.

5.3 Q-Switching

Many applications such as drilling, welding, high speed photography and optical radar (i.e. lidar) require high "power" outputs. Q-switching—also known as Q-spoiling or giant-pulse operation—is used to produce short, intense bursts of "energy" from lasers. Distinguishing between power and energy is important. Q-switched lasers produce lower energy outputs but higher power outputs due to the short pulse duration. The relation between energy, power and pulse duration is given in [3] as

$$power\ output\ (watts) = \frac{pulse\ energy\ (joules)}{pulse\ duration\ (seconds)} \qquad (5.3.1)$$

In Q-switching a loss mechanism is introduced into the laser cavity. This enables the population inversion to build up well beyond threshold without laser oscillation beginning. The cavity loss is then reduced abruptly which causes a rapid build-up of the photon density, $P(t)$. This results in all the available energy being emitted in a single, large pulse which quickly depopulates the upper lasing level, $z(t)$, to the extent that it drops below its threshold value and lasing

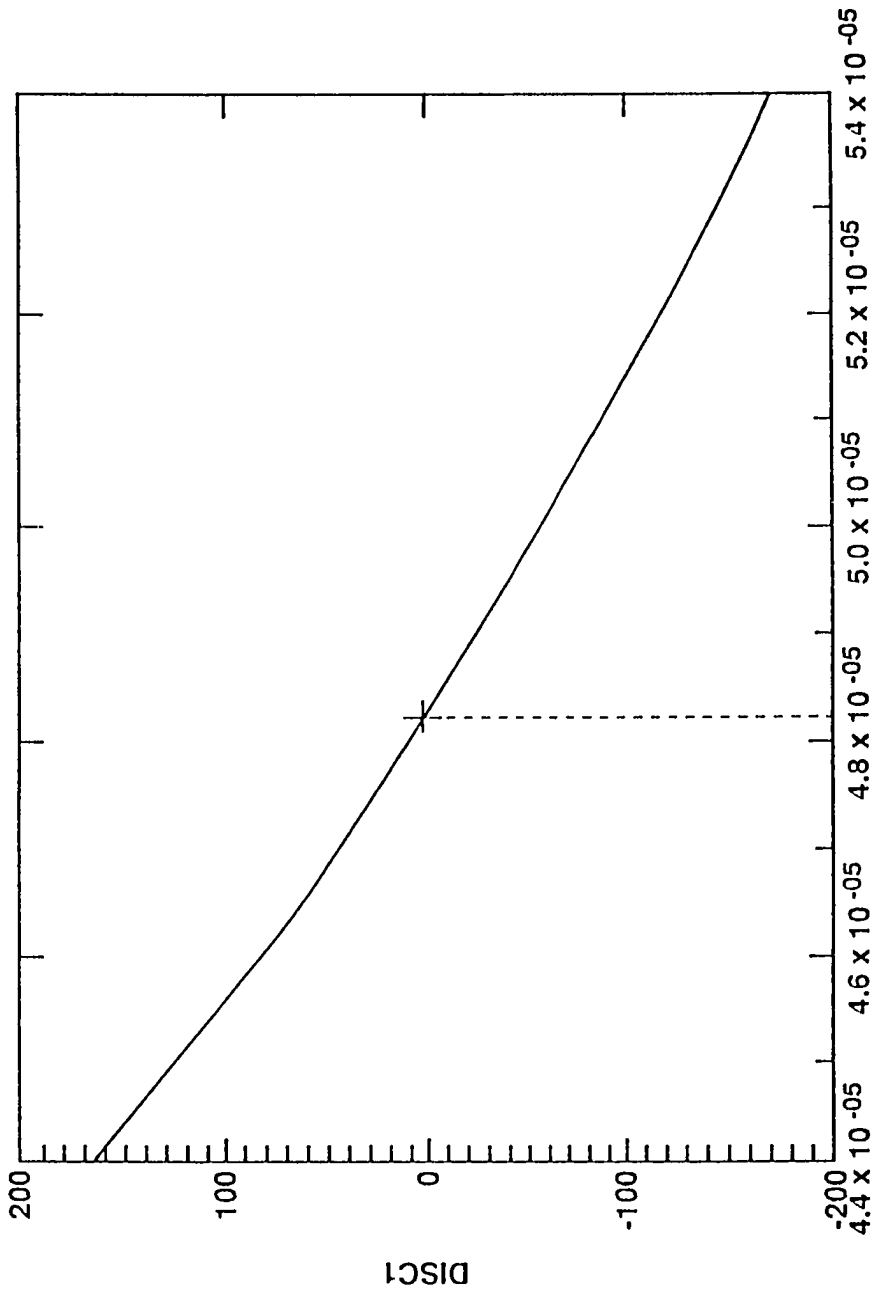

Figure 5.9 DISC1 as a function of TAUC showing when the asymptotic behaviour will be oscillatory

action stops. Thus, Q-switching produces a single pulse of energy with high intensity and short duration.

Q-switching can be implemented, physically, in a variety of ways: rotating mirror, electro-optic, acousto-optic, photochemical (also known as passive Q-switching) and exploding film. To incorporate Q-switching into the mathematical model of the laser dynamics, we replace $\frac{1}{\tau_c}$ in the fourth equation of (3.1.1) by $\frac{1}{Q_c(t)}$ where

$$\frac{1}{Q_c(t)} = \frac{1}{\tau_c}(1 + 999 \cdot QS(t)) \,. \tag{5.3.2}$$

$QS(t)$ is the Q-switch and is given by

$$QS(t) = \left\{ \begin{array}{cc} 1 & if \;\; 0 \leq t \leq TQ \\ 1 - \frac{1}{ST}(t - TQ) & if \;\; TQ < t < TQ + ST \\ 0 & if \;\; t \geq TQ + ST \end{array} \right\}$$

where TQ denotes the time of Q-switching and ST denotes the duration of the Q-switch or the time it takes for the switch to "flip". From (5.3.2) we see that when the Q-switch is on, photons are allowed to leave the laser cavity at a rate 1000 times that of the original rate. This rate is precipitously reduced when the Q-switch is flipped and assumes its original value, $\frac{1}{\tau_c}$, when the Q-switch is completely off.

Taking the time of Q-switching as $TQ = 350\mu s$ and the duration of the switch as $ST = 0.1\,\mu s$, the system (3.1.1) was solved numerically with the rate equation for the normalized photon density replaced by

$$\frac{dP}{dt} = \left\{ \beta_2[1 - \gamma(1 - z)] - \frac{1}{Q_c(t)} \right\} P + \beta_3 z \,. \tag{5.3.3}$$

Figures 5.10 and 5.11 show the behaviour of the upper lasing level and the photon density, respectively. By comparing Figure 5.11 with Figure 5.6 it is seen that the pulse intensity, with Q-switching, is four orders of magnitude greater than it was without Q-switching. In Figure 5.12 the photon density is scaled and plotted with the upper lasing level to show the interplay between the two. The time scale is then stretched, in Figure 5.13, to show the shape of the output pulse. From this figure it is apparent that the peak pulse intensity occurs when the upper lasing level drops to its threshold value. In fact, it can be shown [22] that the peak power output of a Q-switched laser will always occur when the population inversion drops to threshold inversion (which corresponds to $z(t)$ dropping to its threshold or equilibrium value). This shows that the numerical solution agrees well with the laser optics.

Figures 5.14 and 5.15 give the behaviour of all four dependent variables on the intervals $[0, 200]$ and $[170, 170.2]$, respectively. Here the time of Q-switching is $TQ = 170\mu s$ and the duration of the Q-switch is $0.1\mu s$. From Figure 5.15 it is seen that both x and y vary slowly on the interval of Q-switching. Since the d.e. solver spends a considerable amount of time on this interval, due to the rapidly changing photon density, we look for ways of reducing the computational effort involved. One way of doing this is to take x and y as constants on the interval of Q-switching by assigning to them, their respective values at the time Q-switching begins; namely, $x(t) \equiv x(TQ) \equiv \bar{x}$ and $y(t) \equiv y(TQ) \equiv \bar{y}$. In fact, if these assignments are made on [170,200] the difference in the numerical solution

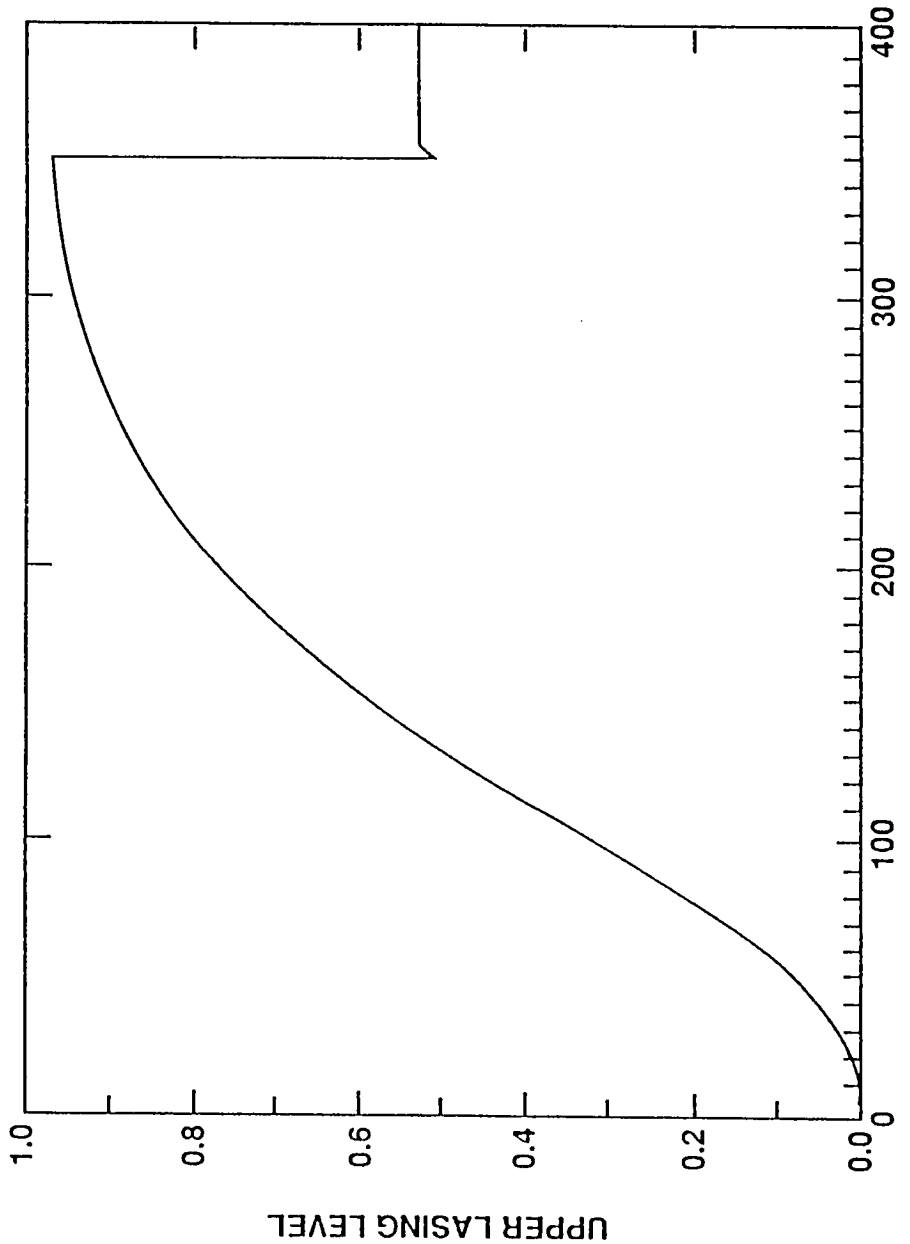

Figure 5.10 Upper lasing level when Q-switching at 350 microseconds

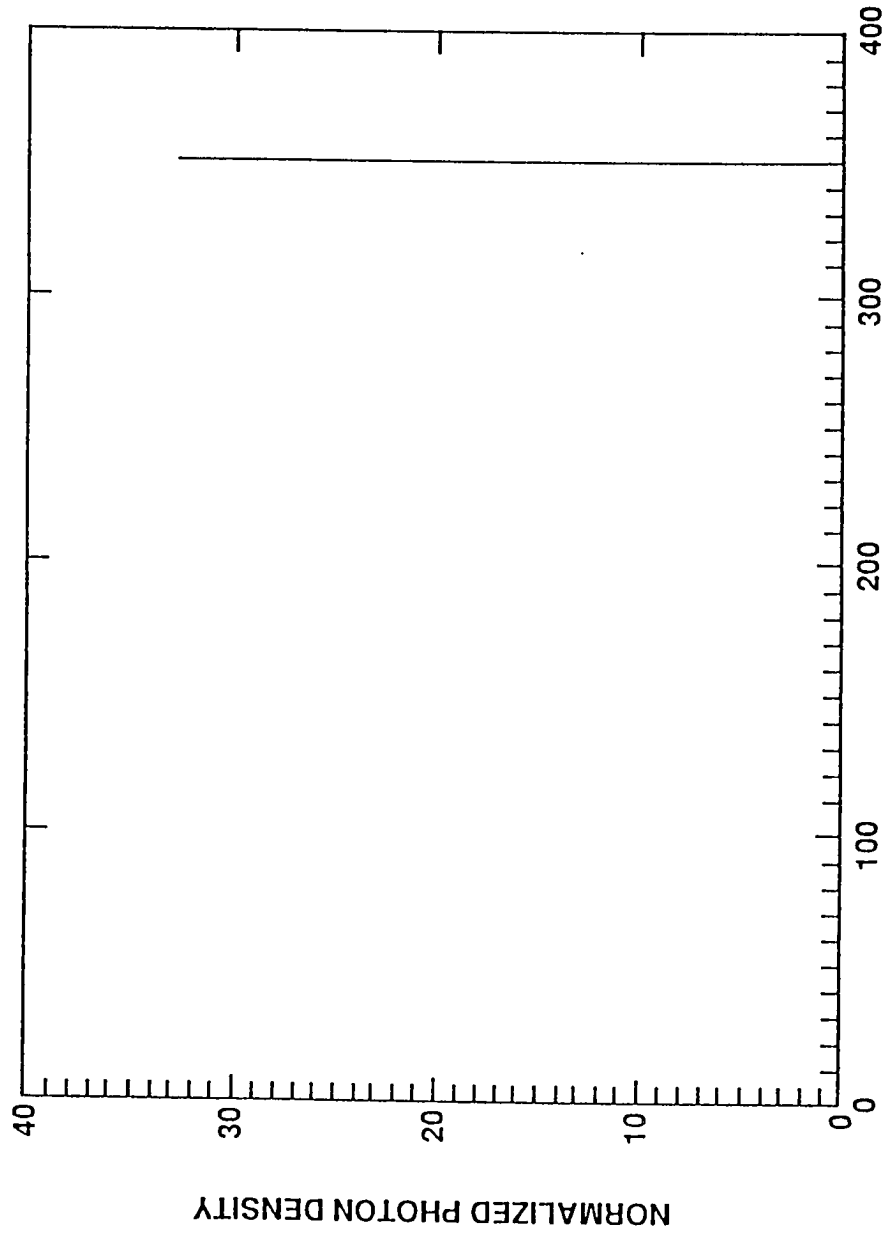

Figure 5.11 Photon density when Q-switching at 350 microseconds

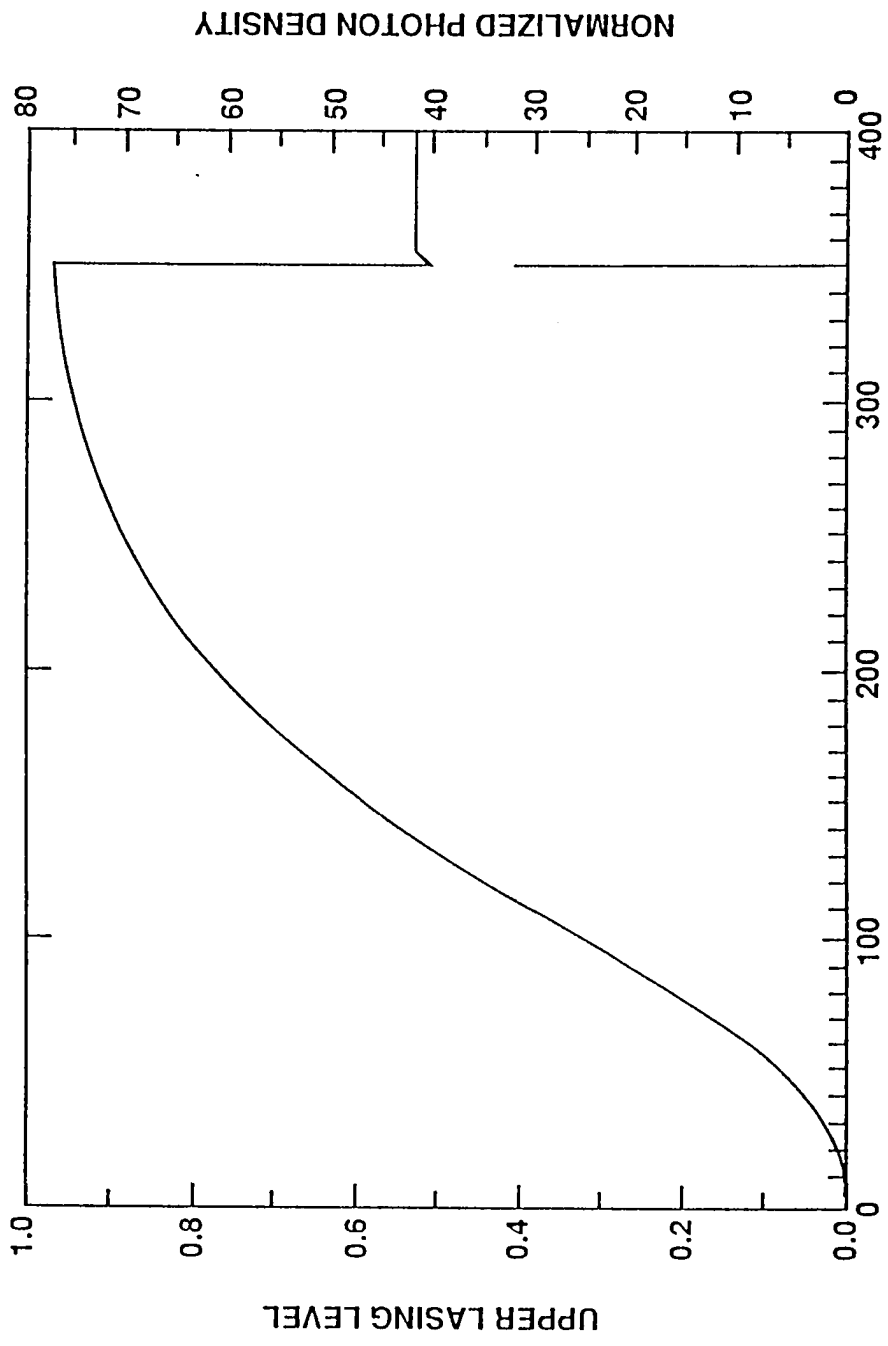

Figure 5.12 Upper lasing level and photon density using separate scales

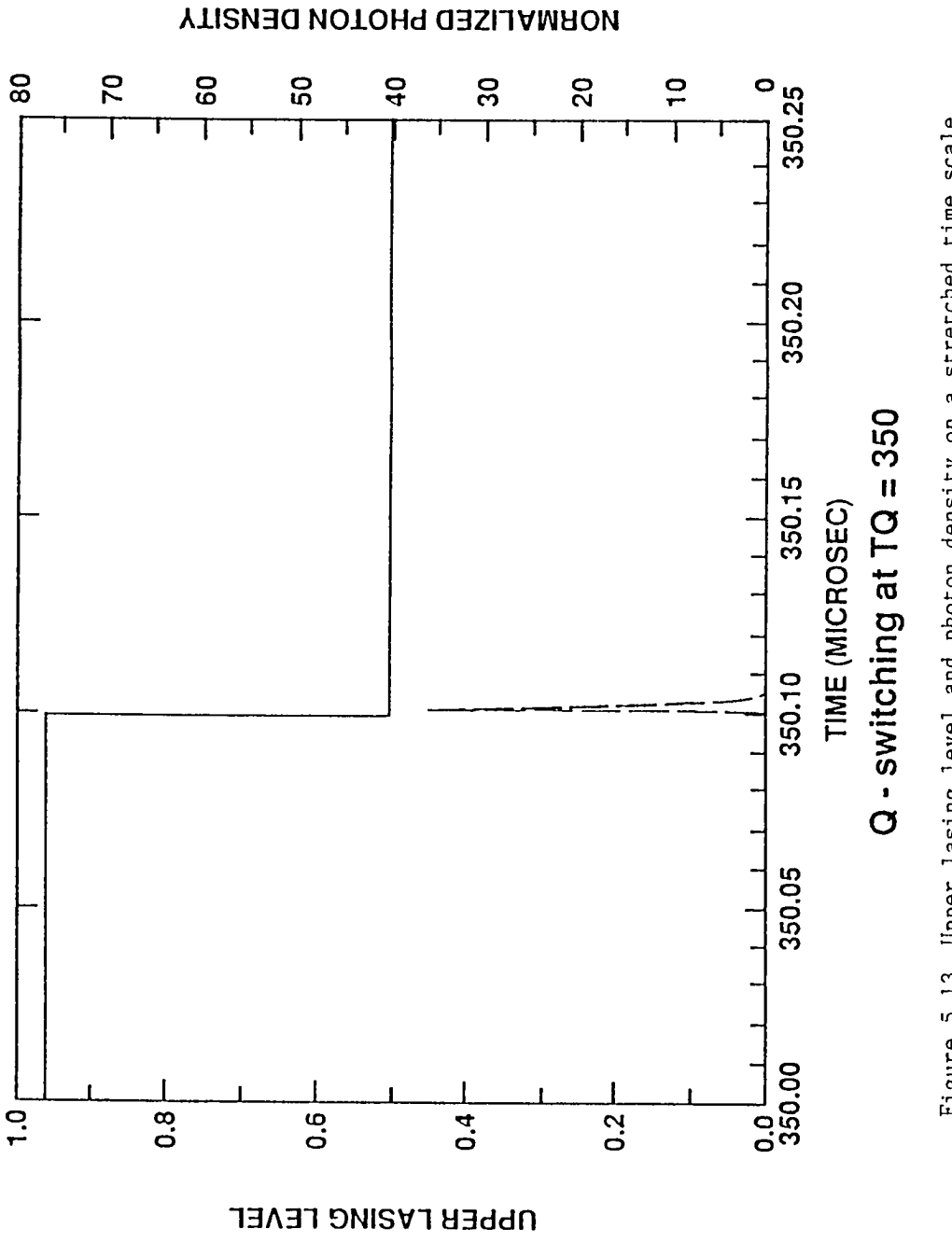

Figure 5.13 Upper lasing level and photon density on a stretched time scale

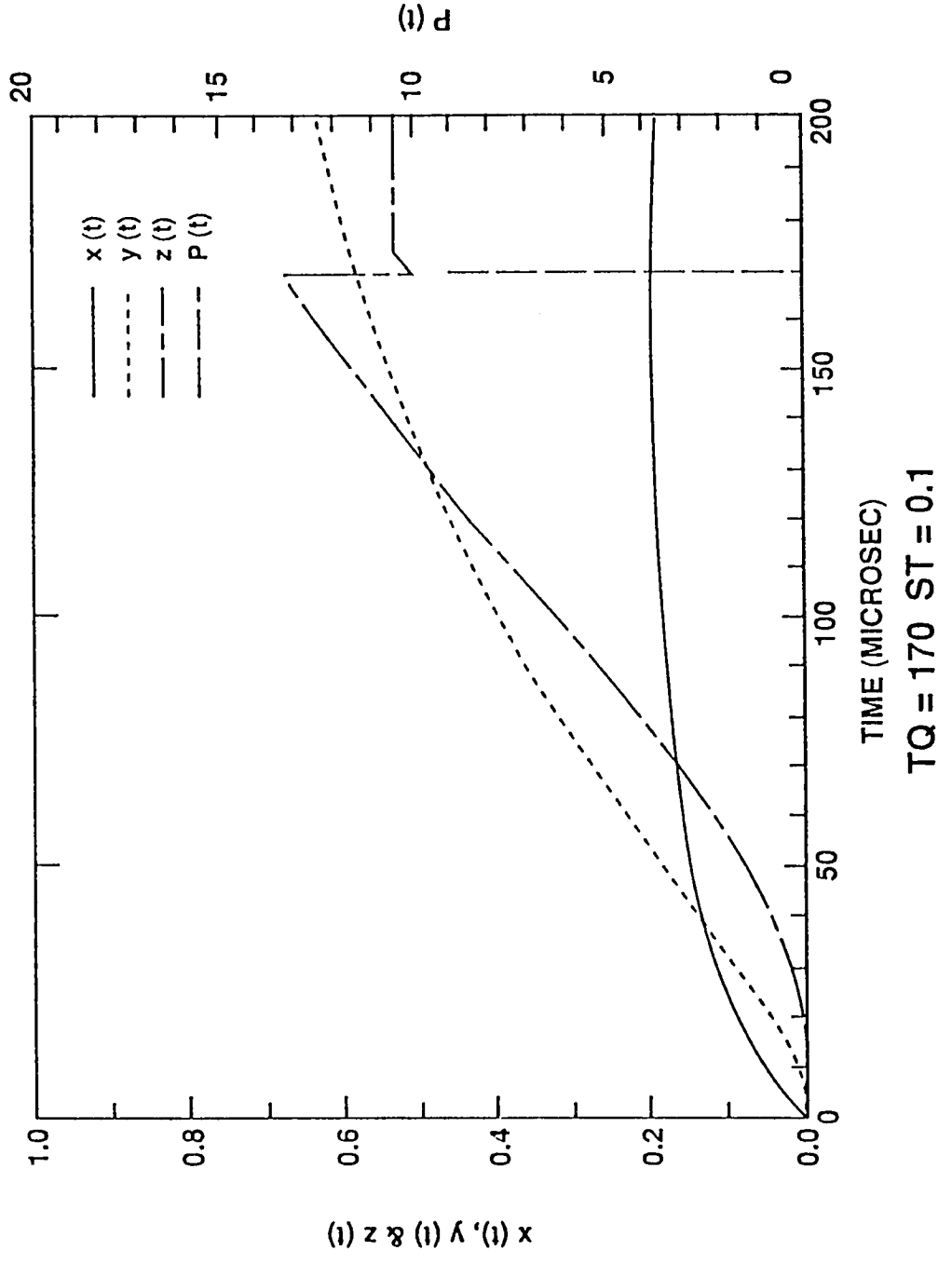

Figure 5.14 All four dependent variables when Q-switching at 170 microseconds

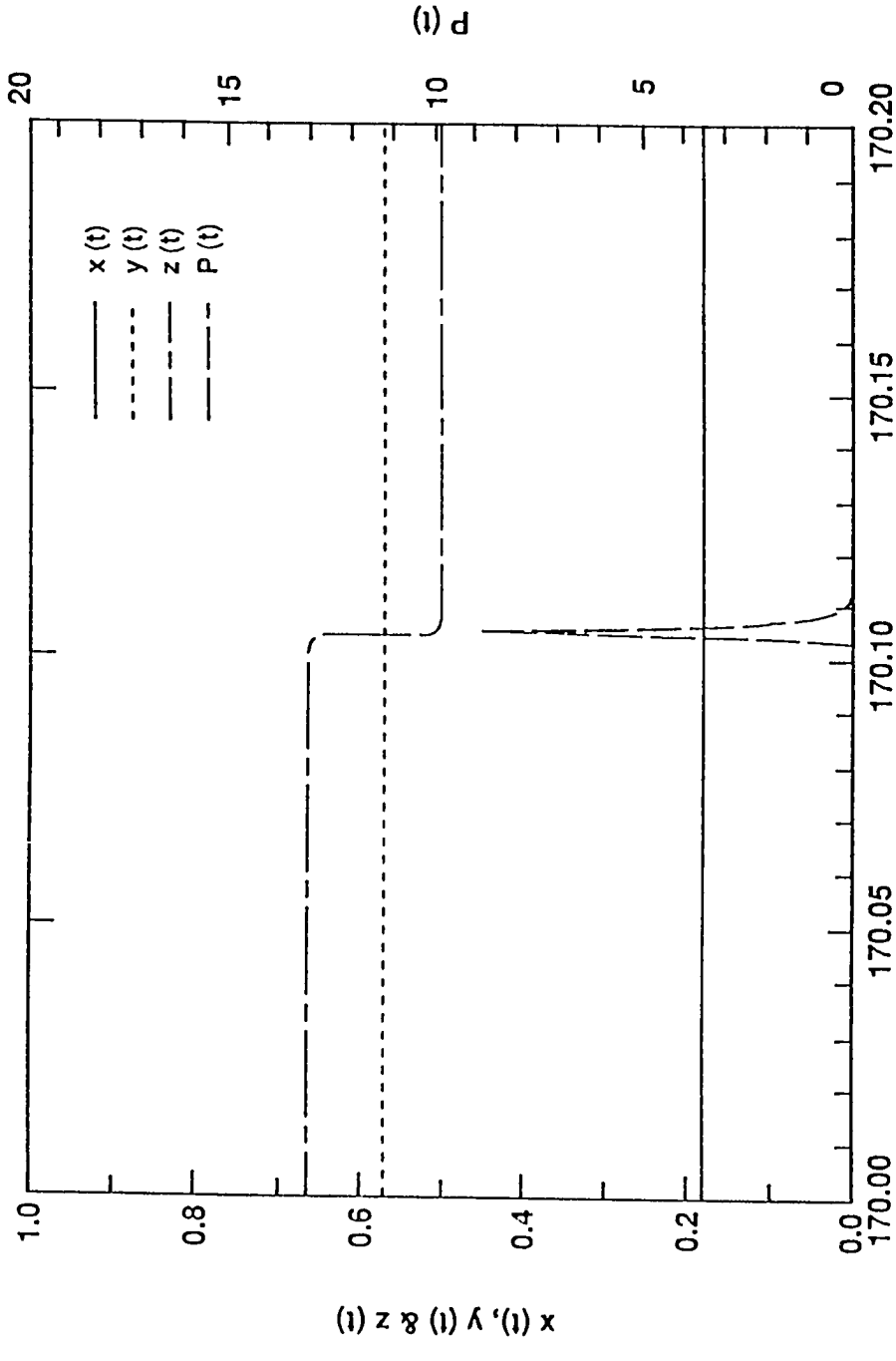

Figure 5.15 All four dependent variables plotted on a stretched time scale

of z and P is virtually unnoticeable as evidenced by Figures 5.16 and 5.17.

Making these assignments is tantamount to reducing the system (3.1.1) to the system

$$\frac{dz}{dt} = -\frac{z}{\tau_1'} + D_4\bar{y}(1-z) + \beta_1[\gamma(1-z)-1]P$$

$$\frac{dP}{dt} = \left\{\beta_2[1-\gamma(1-z)] - \frac{1}{Q_c(t)}\right\}P + \beta_3 z \tag{5.3.4}$$

where equation (5.3.3) has been used for the photon density. System (5.3.4) is a non-autonomous system which will be solved formally by using a method similar to that found in [13]. Let

$$\mathbf{x} = \begin{bmatrix} z \\ P \end{bmatrix} \qquad \mathbf{d} = \begin{bmatrix} D_4\bar{y} \\ 0 \end{bmatrix} \qquad \mathbf{a} = \begin{bmatrix} -\beta_1 \\ \beta_2 \end{bmatrix}$$

and

$$A(t) = \begin{bmatrix} -\left(\frac{1}{\tau_1'} + D_4\bar{y}\right) & \beta_1(\gamma-1) \\ \beta_3 & \beta_2(1-\gamma) - \frac{1}{Q_c(t)} \end{bmatrix} \qquad B = \begin{bmatrix} 0 & 1 \\ 1 & 0 \end{bmatrix}$$

Then, system (5.3.4) can be written symbolically as

$$\dot{\mathbf{x}} = \mathbf{d} + A(t)\mathbf{x} + \frac{\gamma}{2}\mathbf{a}\mathbf{x}^T B\mathbf{x} \tag{5.3.5}$$

The Taylor series expansion for $\mathbf{x}$ about the point $\bar{t} = TQ$ is given by

$$\mathbf{x}(t) = \sum_{k=0}^{\infty} \mathbf{x}_k (t-\bar{t})^k \tag{5.3.6}$$

where

$$\mathbf{x}_k = \frac{\mathbf{x}^{(k)}(\bar{t})}{k!} = \begin{bmatrix} z_k \\ P_k \end{bmatrix} \quad k = 0, 1, 2, \ldots \tag{5.3.7}$$

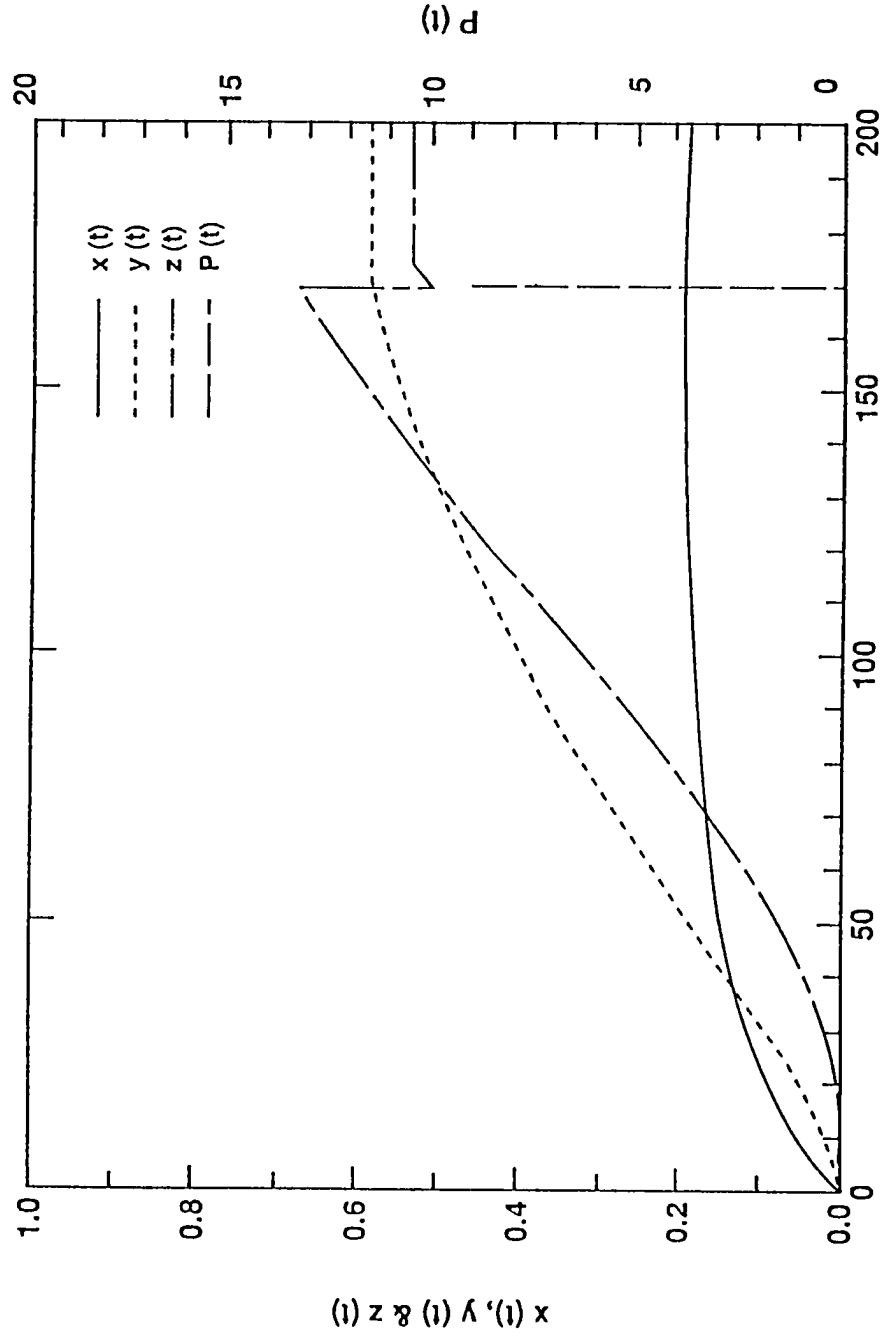

Figure 5.16 All four dependent variables when Q-switching and holding the x & y variable constant subsequent to Q-switching

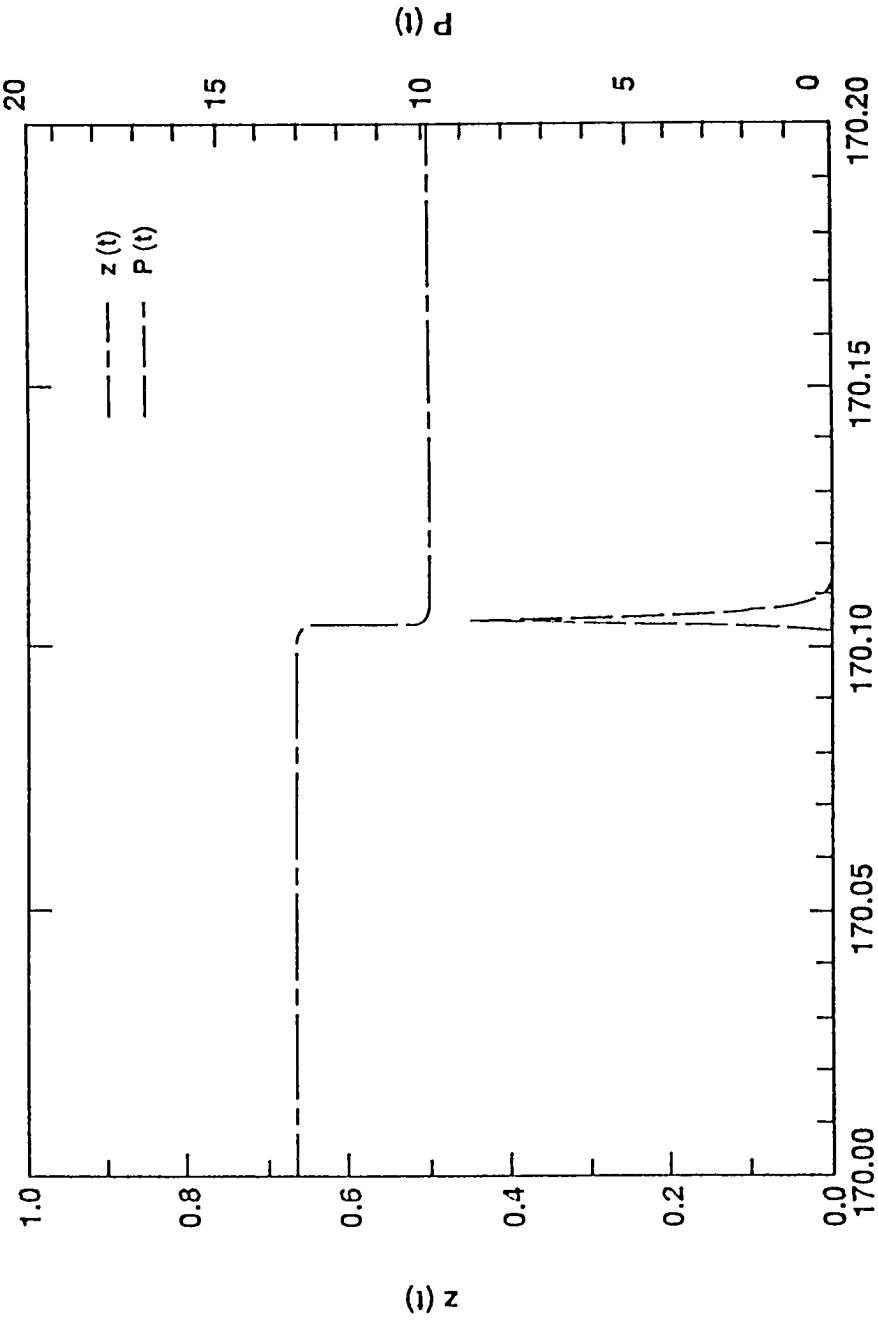

Figure 5.17 Upper lasing level and photon density plotted on a stretched time scale when Q-switching at 170 microseconds

Once a recurrence relationship for the determination of $\mathbf{x}_k$ is obtained, the solution can be computed using (5.3.6). From (5.3.5) and (5.3.7) we get

$$\mathbf{x}_0 = \mathbf{x}(\bar{t}) \tag{5.3.8}$$

$$\mathbf{x}_1 = \mathbf{d} + A(\bar{t})\mathbf{x}_0 + \frac{\gamma}{2}\mathbf{a}\mathbf{x}_0^T B\mathbf{x}_0 \tag{5.3.9}$$

After further differentiation and some rearranging the following relationship is obtained

$$\mathbf{x}_{k+1} = \frac{1}{k+1}\left\{A(\bar{t})\mathbf{x}_k + A'(\bar{t})\mathbf{x}_{k-1} + \frac{\gamma}{2}\mathbf{a}\sum_{j=0}^{k}\mathbf{x}_j^T B\mathbf{x}_{k-j}\right\} \tag{5.3.10}$$

which holds for $k = 1, 2, 3, \ldots$. Hence, a formal solution of the "reduced" system (5.3.4) is given by (5.3.6) where the coefficients, $\mathbf{x}_k$, are obtained from (5.3.8), (5.3.9) and (5.3.10). The recurrence relationship (5.3.10) can also be obtained by assuming solutions of the form

$$z(t) = \sum_{k=0}^{\infty} z_k(t-\bar{t})^k \qquad P(t) = \sum_{k=0}^{\infty} P_k(t-\bar{t})^k \quad ,$$

plugging these expressions for $z(t)$ and $P(t)$ into equations (5.3.4), formally differentiating the left hand side, equating coefficients of like powers of $(t-\bar{t})$ and finally switching back to vector notation.

From numerical calculations it was found that for t close to $\bar{t}$, the series (5.3.6) sums nicely, but eventually the summation breaks down. This is attributed to the ill-conditioning of both matrices $A(\bar{t})$ and $A'(\bar{t})$. Denoting the reciprocal of the condition number of A by $rcond(A)$ we have

$$rcond(A) = \frac{1}{cond(A)} \qquad \& \qquad 0 \leq rcond(A) \leq 1$$

If $rcond(A)$ is close to one then A is well-conditioned, whereas if $rcond(A)$ is near zero then A is ill-conditioned. Using the software package MATLAB, the following was obtained

$$rcond(A(\bar{t})) \doteq 8.74 \times 10^{-9} \quad \& \quad rcond(A'(\bar{t})) = 0.0$$

From this it is evident that both matrices are ill-conditioned.

5.4 Error Analysis

In this section the error incurred by "freezing" the two thulium levels at the time of Q-switching is discussed. To this end, let $\mathbf{X}(\mathbf{x}, t)$ denote the last two equations of the system when Q-switching, so

$$\dot{\mathbf{x}} = \mathbf{X}(\mathbf{x}, t) = \begin{bmatrix} f_1(\mathbf{x}, t) \\ f_2(\mathbf{x}, t) \end{bmatrix} = \begin{bmatrix} -\frac{z}{\tau_1'} + D_4 y(1-z) + \beta_1 P[\gamma(1-z) - 1] \\ \beta_3 z + \left\{\beta_2[1 - \gamma(1-z)] - \frac{1}{Q_c(t)}\right\} P \end{bmatrix} \tag{5.4.1}$$

Also, let $\mathbf{X}^*(\mathbf{x}^*, t)$ denote the last two equations of the Th-Ho system when the two thulium levels are held fixed at their values when Q-switching begins. Then,

$$\dot{\mathbf{x}}^* = \mathbf{X}^*(\mathbf{x}^*, t) = \begin{bmatrix} f_1^*(\mathbf{x}^*, t) \\ f_2^*(\mathbf{x}^*, t) \end{bmatrix} = \begin{bmatrix} -\frac{z^*}{\tau_1'} + D_4 \bar{y}(1-z^*) + \beta_1 P^*[\gamma(1-z^*) - 1] \\ \beta_3 z^* + \left\{\beta_2[1 - \gamma(1-z^*) - \frac{1}{Q_c(t)}\right\} P^* \end{bmatrix} \tag{5.4.2}$$

We will think of $\mathbf{x} = [z \quad P]^T$ as the "true" solution and $\mathbf{x}^* = [z^* \quad P^*]^T$ as the "approximate" solution. The following definitions and theorem from [4] will be useful in obtaining an error bound.

Definition 1 (Approximate Solution) *A vector valued function* $\mathbf{y}$ *is an approximate solution of the vector d.e.* $\mathbf{x}'(t) = \mathbf{X}(\mathbf{x}, t)$ *with error at most* η*, when* $\| \mathbf{x}(t) - \mathbf{y}(t) \|_2 < \eta(t)$ *for all* t *in* $[a, b]$*. Its deviation is at most* ϵ *when* $\mathbf{y}(t)$ *is continuous and satisfies the differential inequality* $\| \mathbf{y}' - \mathbf{X}(\mathbf{y}, t) \|_2 \leq \epsilon$*, for all except a finite number of points* t *in* $[a, b]$*.*

Definition 2 (Lipschitz Condition) *The system* $\mathbf{X}(\mathbf{x}, t)$ *satisfies a Lipschitz condition on* $\mathcal{D}$*, when for some nonnegative constant* L*(Lipschitz constant), it satisfies the inequality* $\| \mathbf{X}(\mathbf{x}, t) - \mathbf{X}(\mathbf{y}, t) \|_2 \leq L \| \mathbf{x} - \mathbf{y} \|_2$ *for all point pairs* $(t, \mathbf{x})$ *and* $(t, \mathbf{y})$ *in* $\mathcal{D}$ *having the same* t*-coordinate.*

Theorem 1 *Let* $\mathbf{x}(t)$ *be an exact solution and* $\mathbf{y}(t)$ *an approximate solution, with deviation* ϵ*, of the d.e.* $\dot{\mathbf{x}} = \mathbf{X}(\mathbf{x}, t)$*. Also, let* $\mathbf{X}$ *satisfy a Lipschitz condition. Then, for* $t \geq a$*, we have*

$$\| \mathbf{x}(t) - \mathbf{y}(t) \|_2 \leq \| \mathbf{x}(a) - \mathbf{y}(a) \|_2 \, e^{L(t-a)} + \frac{\epsilon}{L} \left(e^{L(t-a)} - 1 \right).$$

In order to use this theorem the deviation, call it ϵ^*, must be obtained and a Lipschitz constant must be shown to exist.

For the deviation, consider

$$\begin{aligned} \| \dot{\mathbf{x}}^* - \mathbf{X}(\mathbf{x}^*, t) \|_2 &= \| \mathbf{X}^*(\mathbf{x}^*, t) - \mathbf{X}(\mathbf{x}^*, t) \|_2 \\ &= \left\{ \left(- \left[\frac{1}{\tau_1'} + D_4 \bar{y} \right] z^* + D_4 \bar{y} + \beta_1 P^* [\gamma(1 - z^*) - 1] \right. \right. \\ &\qquad \left. \left. + \left[\frac{1}{\tau_1'} + D_4 y \right] z^* - D_4 y - \beta_1 P^* [\gamma(1 - z^*) - 1] \right)^2 \right. \\ &\qquad + \left(\beta_3 z^* + \left\{ \beta_2 [\gamma(z^* - 1) + 1] - \frac{1}{Q_c(t)} \right\} P^* \right. \end{aligned}$$

$$-\beta_3 z^* - \left\{\beta_2[\gamma(z^*-1)+1] - \frac{1}{Q_c(t)}\right\} P^*\Bigg)^2\Bigg\}^{\frac{1}{2}}$$

$$= D_4 \,|1 - z^*(t)|\;\; |\,\bar{y} - y(t)\,| \qquad (5.4.3)$$

Hence, the deviation is obtained by defining

$$\epsilon^* = \max_{\bar{t}\le t\le b} D_4 \,|1 - z^*(t)|\;\; |\bar{y} - y(t)|\;\; .$$

Since $\mathbf{X}(\mathbf{x}, t)$ is of class C^1 it follows from a Lemma in [4] that $\mathbf{X}(\mathbf{x}, t)$ satisfies a Lipschitz condition on any closed bounded (compact) convex domain. Hence, a Lipschitz constant will exist on any closed interval $[\bar{t}, b]$ where b is finite.

Invoking Theorem 1 and using $\| \mathbf{x}(\bar{t}) - \mathbf{x}^*(\bar{t}) \|_2 = 0$ yields

$$\|\mathbf{x}(t) - \mathbf{x}^*(t)\|_2 \le \frac{\epsilon^*}{L}\left\{e^{L(t-\bar{t})} - 1\right\} \equiv \eta^*(t) \qquad (5.4.4)$$

Hence, $\eta^*(t)$ is an upper bound on the error and from the above definition we see that $\eta^*(t) \to 0$ as $t \to \bar{t}$. Although $\eta^*(t)$ does serve as an error bound on any closed interval $[\bar{t}, b]$, it turns out to be an extremely conservative bound. This is due primarily to the magnitude of the Lipschitz constant. From numerical computations it was found that on the interval of Q-switching the Lipschitz constant is quite large, $L \doteq 869,607$.

Chapter 6

Upgrading the Model

6.1 Back Transfer & An Alternate Averaging Technique

In this section two modifications are made to upgrade the model. The first is to include the terms that account for the back transfer of energy and that were excluded at the beginning of Chapter 3. The second is to replace β_2 & β_3 in the rate equation for the photon density with

$$\beta_2' = \left(\frac{\ell}{\ell_c}\right)\beta_2 \qquad \& \qquad \beta_3' = \left(\frac{\ell}{\ell_c}\right)\beta_3 \,.$$

The rationale for the second change is as follows. A mathematical model that accurately describes the dynamics of a laser system must, of necessity, account for both spatial and temporal variations in the dependent variables. Allowing for both types of variation yields a system of nonlinear partial differential equations

(p.d.e.'). Due to the intractability of the equations and the amount of effort and computer time involved in solving the system numerically, various averaging techniques are used to eliminate the spatial dependence and thus make the system more tractable. L.F. Roberts et.al. [20] gives three such averaging schemes, the simplifying assumptions made for each and the resultant o.d.e. models. She then compares (numerically) the output of the laser as predicted by the p.d.e. model with the laser output predicted by each of the three resultant o.d.e. models. The conclusion of this comparison is that only the temporal model obtained by taking a spatial average over the optical length of the cavity, ℓ_c, yields numerical results that agree qualitatively with those predicted by the spatial and temporal model. This averaging scheme can be incorporated into the model by replacing β_2 and β_3 by the quantities given above. Doing this and including the back transfer terms yields the following system

$$\begin{aligned}
\frac{dx}{dt} &= W_p(t)(1-x-y) - \frac{x}{\tau_2} - D_1 x(1-x-y) \\
\frac{dy}{dt} &= \frac{x}{\tau_{21}} - \frac{y}{\tau_1} + 2D_1 x(1-x-y) - D_2 y(1-z) + D_3 z(1-x-y) \\
\frac{dz}{dt} &= -\frac{z}{\tau_1'} + D_4 y(1-z) - D_5 z(1-x-y) + \beta_1[\gamma(1-z)-1]P \\
\frac{dP}{dt} &= \left\{\beta_2'[1-\gamma(1-z)] - \frac{1}{\tau_c}\right\} P + \beta_3' z
\end{aligned} \tag{6.1.1}$$

The numerical solution to the system (6.1.1) was obtained from the program in Appendix C. Special attention was given to the qualitative behaviour of the photon density for various values of C_1^* and $\frac{\ell}{\ell_c}$. Recall that C_1^* represents the probability of back transfer occurring and both D_3 and D_5 are constant multiples of C_1^*. Also note that $\ell = (\neq)\ell_c$ corresponds to $\beta_2' = (\neq)\beta_2$ and $\beta_3' = (\neq)\beta_3$, respectively. In all four cases which follow, the pumping term was taken to be of the form

$$W_p(t) = \alpha^2 t e^{-\alpha^2 t^2} .$$

In Figure 6.1 back transfer is turned off ($C_1^* = 0$) and the length of the crystal rod (active medium) is equal to the length of the optical cavity ($\ell = \ell_c$). The erratic spiking behaviour is identical to the previously observed behaviour of the photon density. In Figure 6.2, back transfer is turned on and $\ell = \ell_c$. From this we see that the time of lasing is delayed (as expected) and the spiking behaviour persists albeit for a shorter duration. Figure 6.3 corresponds to back transfer once again being turned off and $\ell \neq \ell_c$. From this we see a salient disparity in the qualitative behaviour of the photon density. The previously observed erratic spiking has been replaced by regular and temperate oscillations. Finally, in Figure 6.4 back transfer is turned on and $\ell \neq \ell_c$. The principal difference between the preceding figure and this one is the fewer number of oscillations occuring in the latter. In Figure 6.5 the time scale has been stretched and the photon density plotted on the interval [80, 140]. Figure 6.6 is a picture of the energy output as displayed on the screen of an oscilloscope in the laboratory.

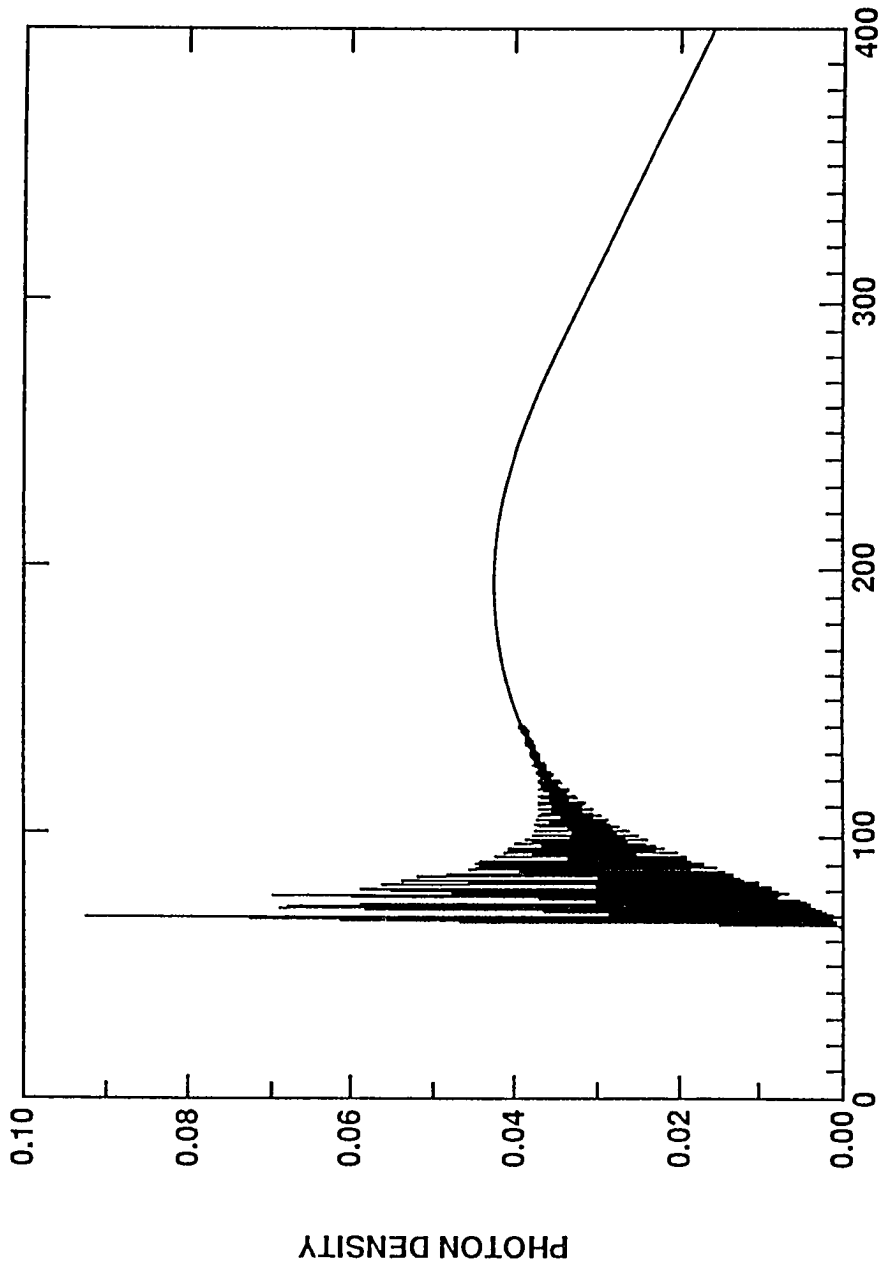

Figure 6.1 The photon density with back transfer turned off and the length of the rod equal to the length of the optical cavity

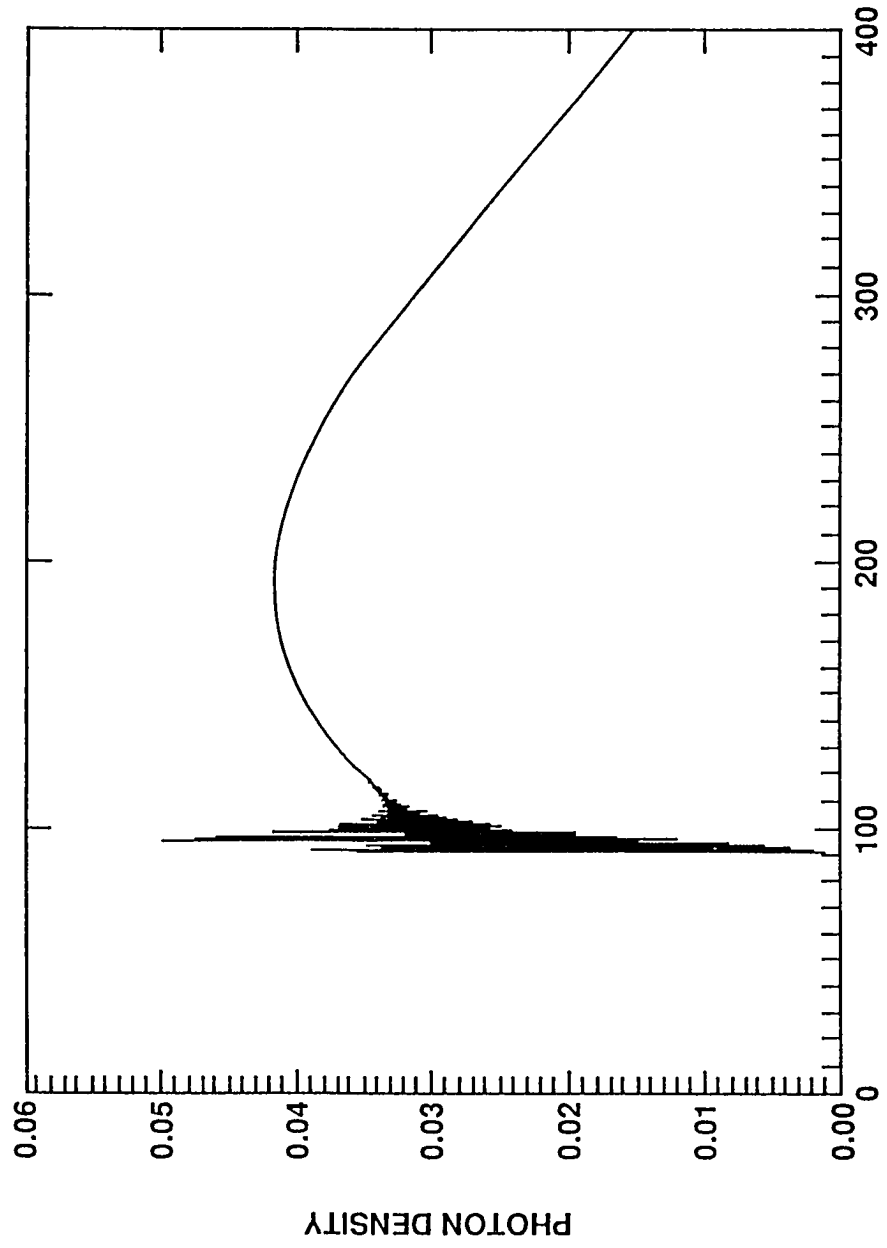

Figure 6.2 The photon density with back transfer turned on and the length of the crystal equal to the length of the optical cavity

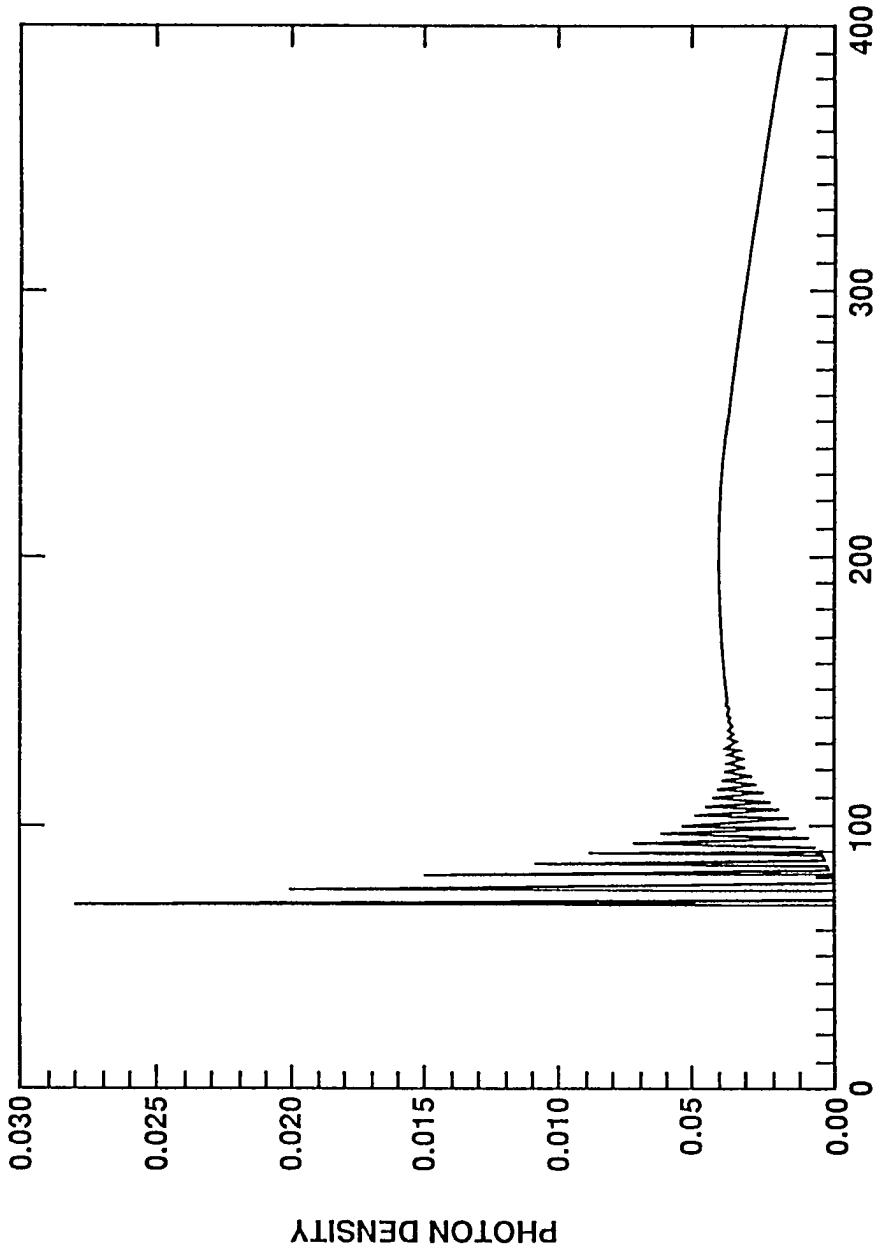

Figure 6.3 The photon density with back transfer turned off and the length of the crystal not equal to the length of the optical cavity

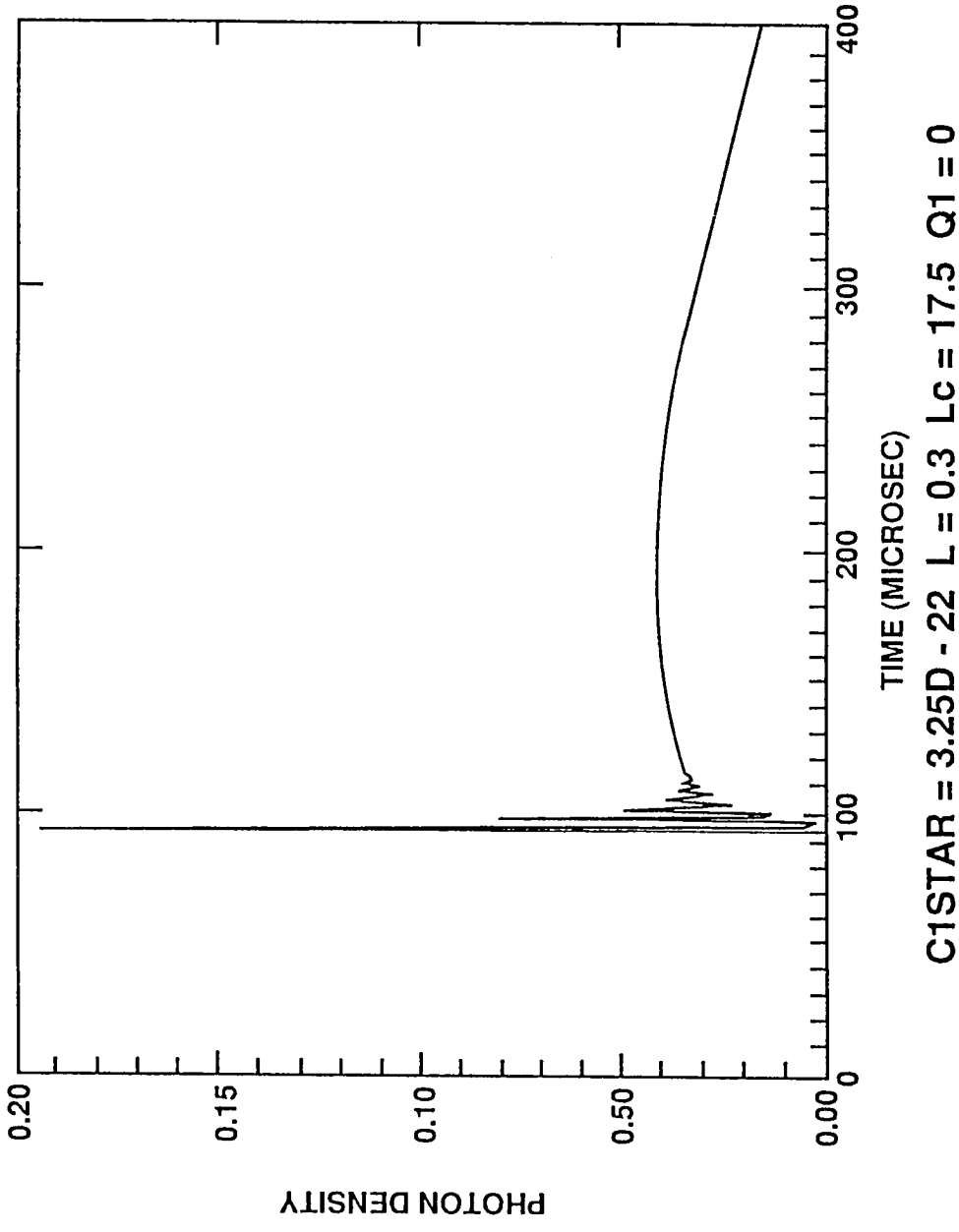

Figure 6.4 The photon density with back transfer turned on and the length of the crystal not equal to the length of the optical cavity

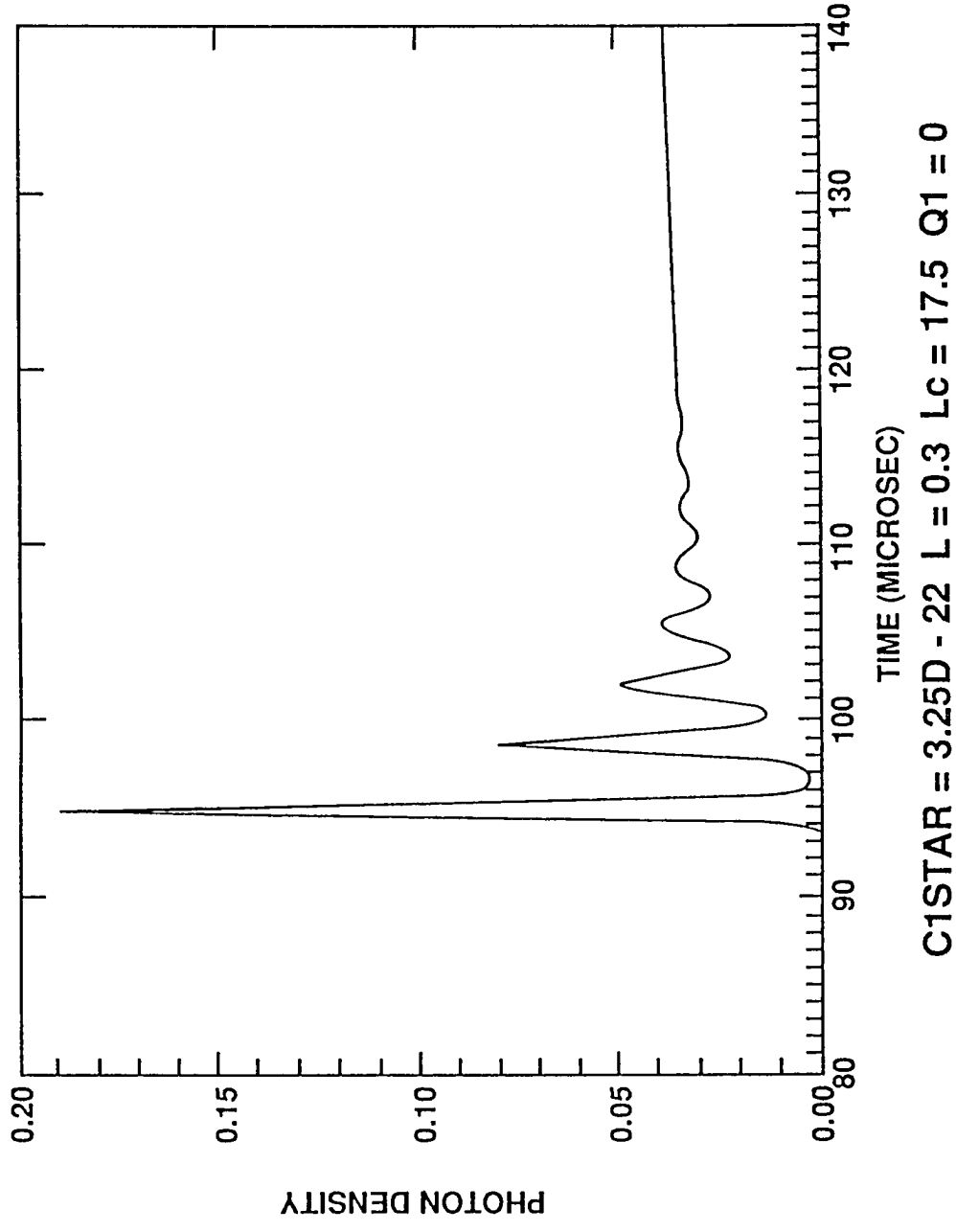

Figure 6.5 The photon density plotted on a stretched time scale

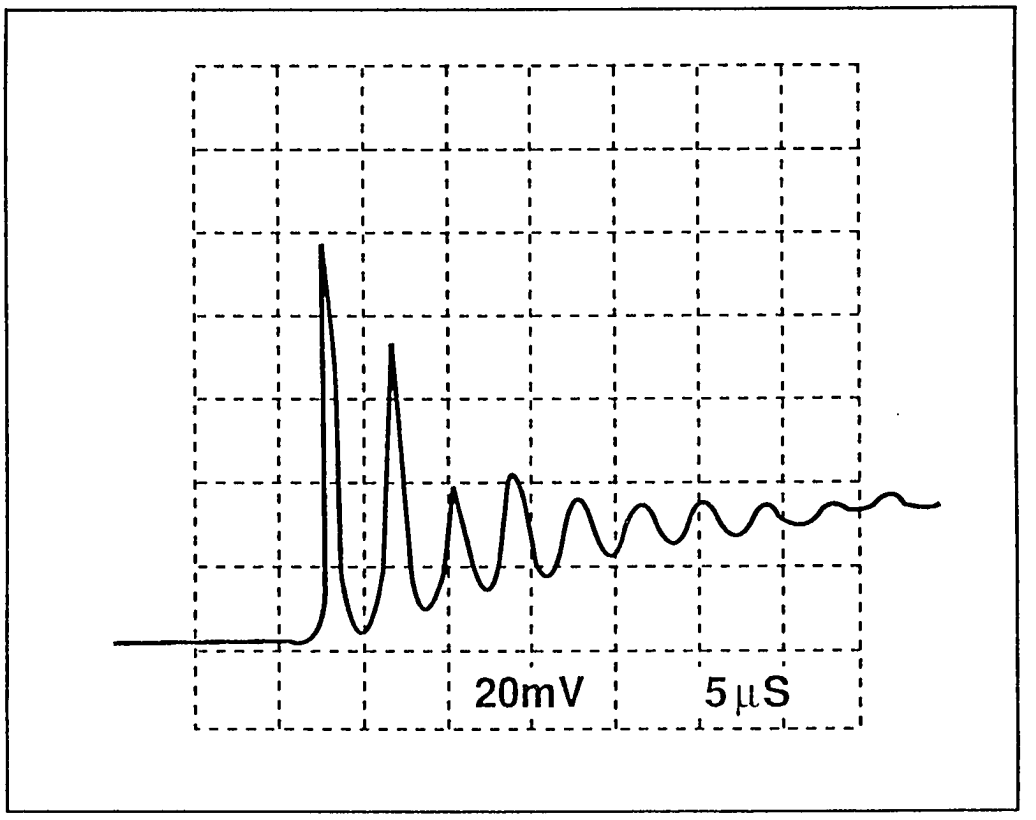

Figure 6.6 The energy output of the Tm-Ho:YAG laser as displayed on the screen of an oscilloscope

By comparing Figure 6.5 with Figure 6.6 we see that the behaviour of the photon density, as predicted by the temporal model, is in remarkable agreement to the behaviour observed in the laboratory (both having about 7 oscillations in 25 μs). From this it is apparent that the inclusion of the back transfer terms affects the time of lasing as well as the magnitude and frequency of the output pulse but it is the $\frac{\ell}{\ell_c}$ term that has the most dramatic affect on the qualitative behaviour of the photon density.

6.2 Up-Conversion

In this section we further upgrade the model by including the terms associated with the up-conversion of energy from the $^5I_7$ energy level to the $^5I_5$ energy level of holmium. An error bound on the solution to the systems with and without up-conversion is obtained and a comparison of the numerical solution of the systems with and without up-conversion is performed.

Let $\mathbf{X}(\mathbf{x}, t)$ denote the system that includes up-conversion, then $\mathbf{X}(\mathbf{x}, t)$ is the right hand side of system (2.5.2) with the exception that β_2 & β_3 are replaced by β_2' & β_3' as defined in the preceding section. Recall that in (2.5.2) the normalized up-conversion level is denoted $w(t)$. Also, let $\tilde{\mathbf{X}}(\tilde{\mathbf{x}}, t)$ denote the system obtained by holding the up-conversion level constant, say $\tilde{w}(t) \equiv \tilde{w} \equiv 0$. Then $\tilde{\mathbf{X}}(\tilde{\mathbf{x}}, t)$ is the right hand side of equations (6.1.1). Denoting the solution to the system with up-conversion (the true solution) by $\mathbf{x}(t)$ and the solution to the system without up-conversion (the approximate solution) by $\tilde{\mathbf{x}}(t)$ we wish to find a

bound, $\tilde{\eta}(t)$, such that

$$\| \mathbf{x}(t) - \tilde{\mathbf{x}}(t) \|_2 \leq \tilde{\eta}(t) .$$

Using Theorem 1 of section 5.4 and proceeding along the same lines as in that section we first find the deviation, which will be denoted $\tilde{\epsilon}$.

Consider,

$$\begin{aligned}
\| \tilde{\mathbf{x}}' - \mathbf{X}(\tilde{\mathbf{x}}, t) \|_2 &= \| \tilde{\mathbf{X}}(\tilde{\mathbf{x}}, t) - \mathbf{X}(\tilde{\mathbf{x}}, t) \|_2 \\
&= \left\{ [D_2 \tilde{y} w + D_6(1 - \tilde{x} - \tilde{y}) w]^2 + [-D_4 \tilde{y} w - \beta_1(\gamma - 1)\tilde{P} w]^2 \right. \\
&\quad \left. + [\beta_2'(\gamma - 1)\tilde{P} w]^2 \right\}^{\frac{1}{2}} \\
&= | w(t) | \left\{ [D_2 \tilde{y} + D_6(1 - \tilde{x} - \tilde{y})]^2 + [D_4 \tilde{y} + \beta_1(\gamma - 1)\tilde{P}]^2 \right. \\
&\quad \left. + [\beta_2'(\gamma - 1)\tilde{P}]^2 \right\}^{\frac{1}{2}} \\
&\equiv \epsilon(t)
\end{aligned}$$

The deviation is now obtained by defining

$$\tilde{\epsilon} = \max_{0 \leq t \leq b} \epsilon(t)$$

Clearly, $\mathbf{X}(\mathbf{x}, t)$ satisfies a Lipschitz constant on the interval $[0, b]$ for b finite. Hence, invoking Theorem 1 of section 5.4 we obtain the bound

$$\| \mathbf{x}(t) - \tilde{\mathbf{x}}(t) \|_2 \leq \frac{\tilde{\epsilon}}{L} \left\{ e^{Lt} - 1 \right\} \equiv \tilde{\eta}(t)$$

which is valid on $[0, b]$ where b is finite.

The program in Appendix C was used to solve the system without up-conversion. This gives the numerical solutions to $\tilde{x}$, $\tilde{y}$, $\tilde{z}$ and $\tilde{P}$. Then, taking

the probability of up-conversion & down-conversion as

$$q_1 = 5.0 \times 10^{-22} \qquad \& \qquad q_1' = 1.2 \times 10^{-23}$$

respectively, the system with up-conversion was solved numerically. This information was used to calculate $\epsilon(t)$ which is graphed in Figure 6.7. Hence, by definition of the deviation we have

$$\tilde{\epsilon} \doteq 0.00497 \, .$$

Figure 6.8 is a plot of the maximal element of the Jacobian from which it is seen that the Lipschitz constant can be taken to be $L = 3150$. This gives the approximate error bound

$$\tilde{\eta}(t) = \frac{.0049}{3150} \left\{ e^{3150t} - 1 \right\} = 1.555 \times 10^{-6} \left\{ e^{3150t} - 1 \right\}$$

Evaluating $\tilde{\eta}(t)$ at $t = 0.25\,\mu s$ yields

$$\tilde{\eta}(.25) \doteq 1.555 \times 10^{-6} \left\{ 10^{342} - 1 \right\}$$

which produces an arithmetic overflow on an IBM PC and indicates that the error bound (although of theoretical import) is of dubious practical use.

Figures 6.9 and 6.10 give plots of the photon density with and without up-conversion, respectively. It is apparent from these figures that the qualitative behaviour of the photon density is unaffected by up-conversion. This suggests that the error bound, $\tilde{\eta}(t)$, is conservative. To get a better understanding of how the two systems compare we denote the numerical solution to the system

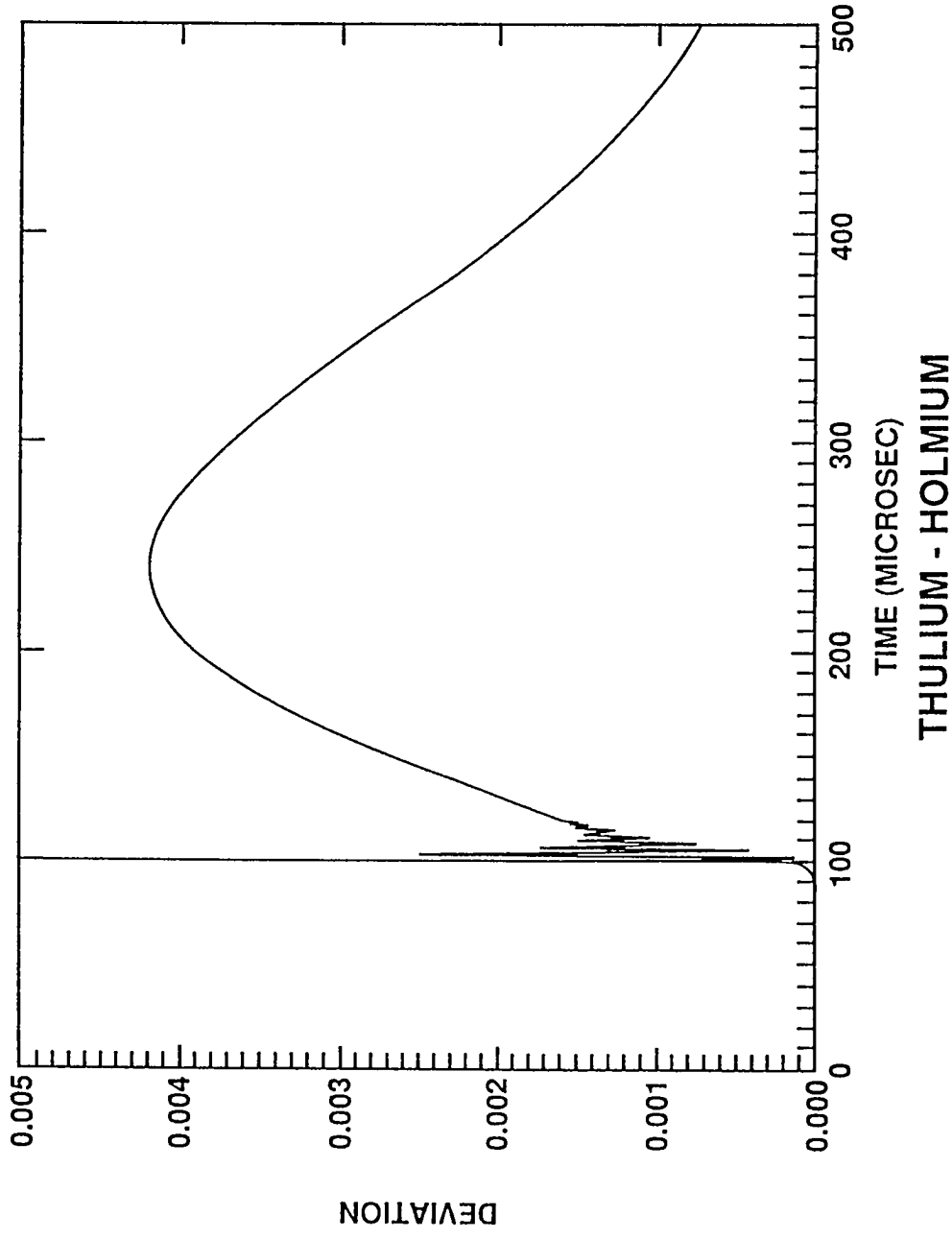

Figure 6.7 Deviation graphed as a function of time

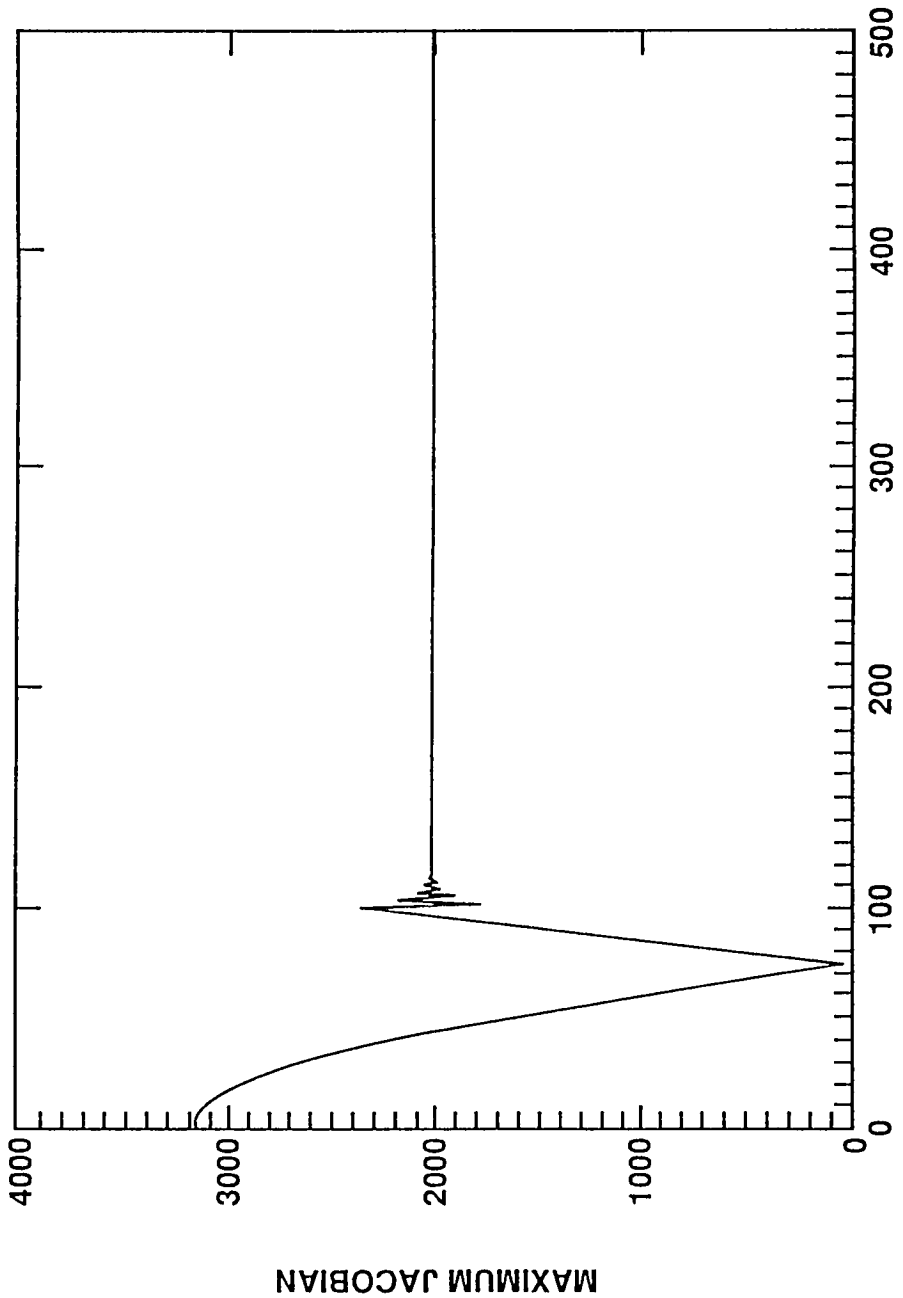

Figure 6.8 A graph of the element of the Jacobian of maximal absolute value

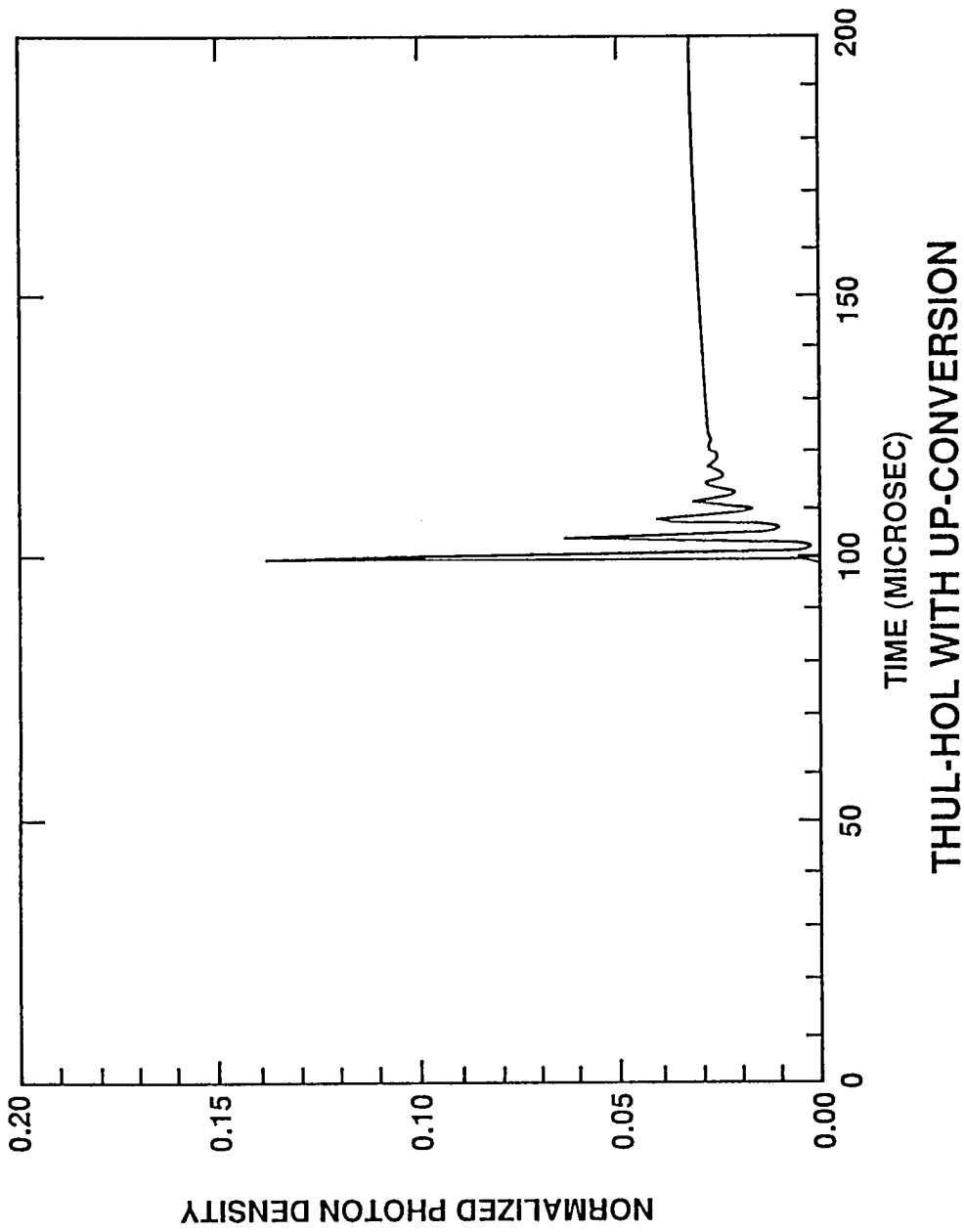

Figure 6.9 Photon density with the up-conversion level included

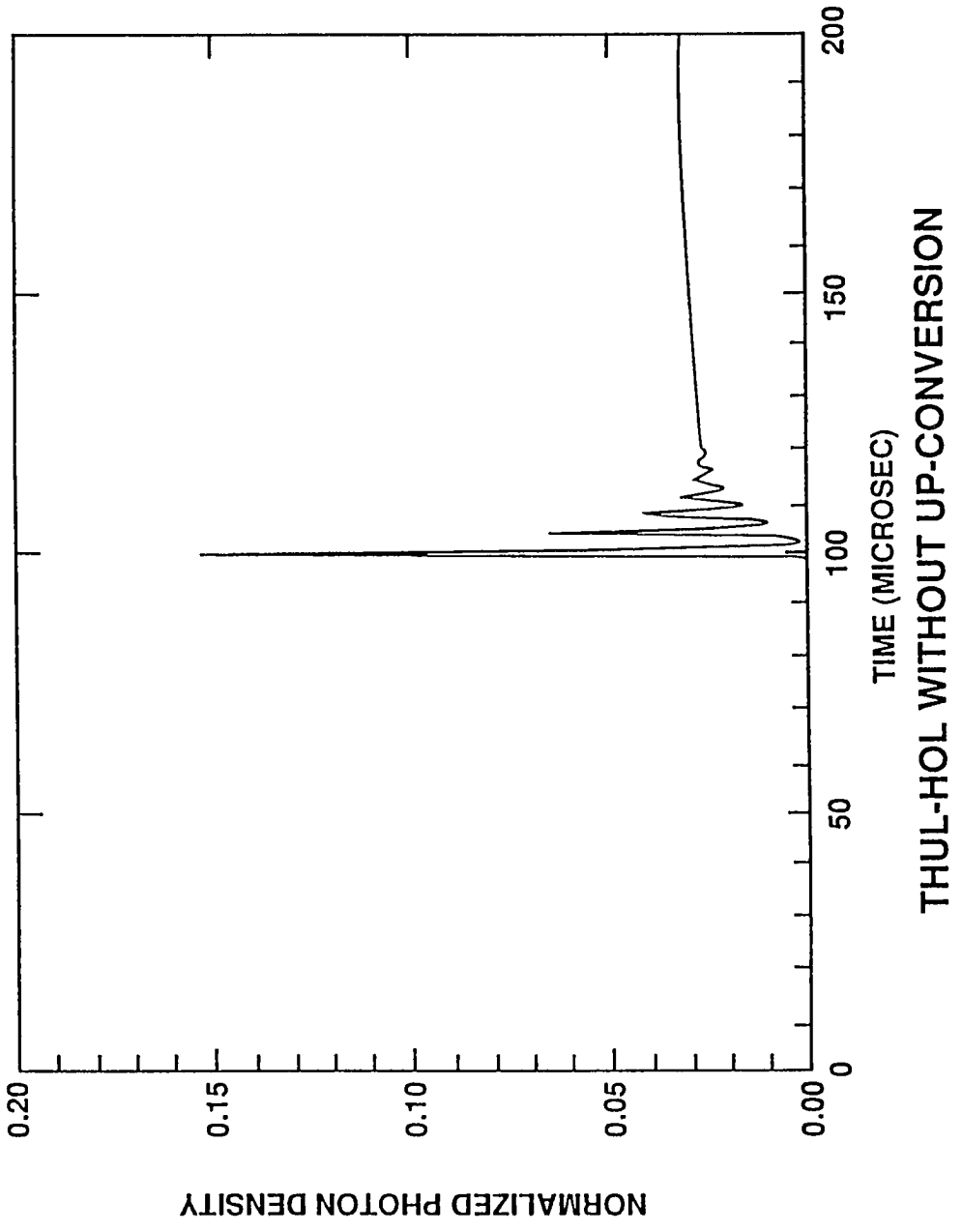

Figure 6.10 Photon density with the up-conversion level excluded

with up-conversion $\mathbf{x}_{num}$ and likewise for the system without up-conversion $\tilde{\mathbf{x}}_{num}$. Now compute the quantity $TOTERR$ on [0, 200] where

$$TOTERR = \| \mathbf{x}_{num} - \tilde{\mathbf{x}}_{num} \|_2 \ .$$

From this it is found that the maximal difference occurs at the onset of lasing and is about 4% as seen in Figure 6.11. Doing the same thing with just the photon density term we define

$$PHOTERR = | P_{num} - \tilde{P}_{num} |$$

In Figure 6.12 $PHOTERR$ is graphed. From this we see that most of the error in $TOTERR$ is contributed by $PHOTERR$. Figure 6.13 shows the interplay between the photon density and the upper lasing level of holmium and Figure 6.14 gives a phase portrait of the same.

From the above observations we conclude that the qualitative behaviour of the photon density is not affected by the up-conversion level, the error bound obtained is extremely conservative (as before) and the major contribution of the error in the numerical solution comes from the fourth component of the solution vector, namely, the photon density. In spite of the qualitative agreement in the photon density it is important to retain the up-conversion level in the model for two reasons: (1) the quantitative difference of 4% may be significant when addressing the efficiency of the laser and (2) the up-conversion level does affect the laser output when Q-switching as will be seen in the next section.

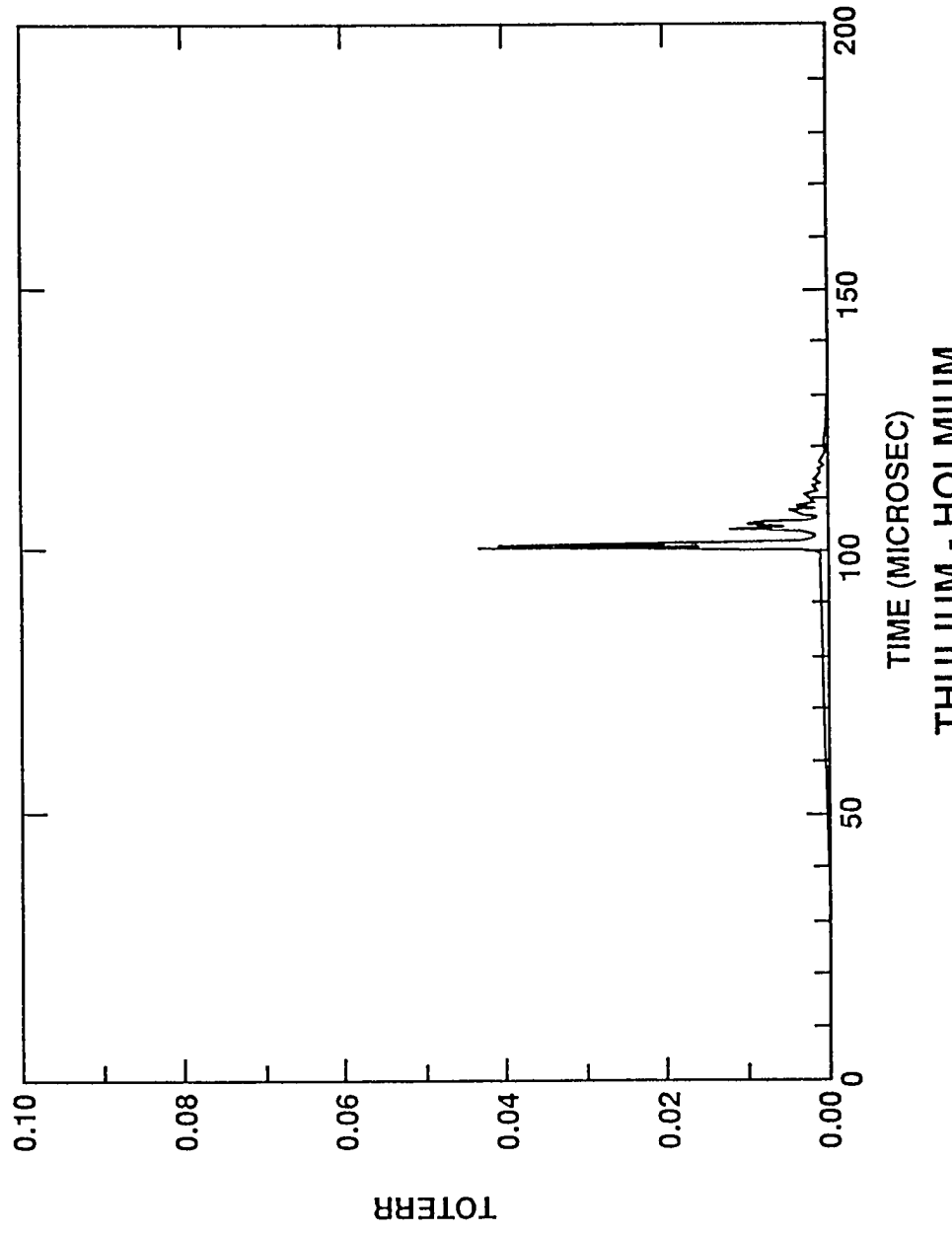

Figure 6.11 The difference between the numerical solution to the system with up-conversion and the solution to the system without up-conversion

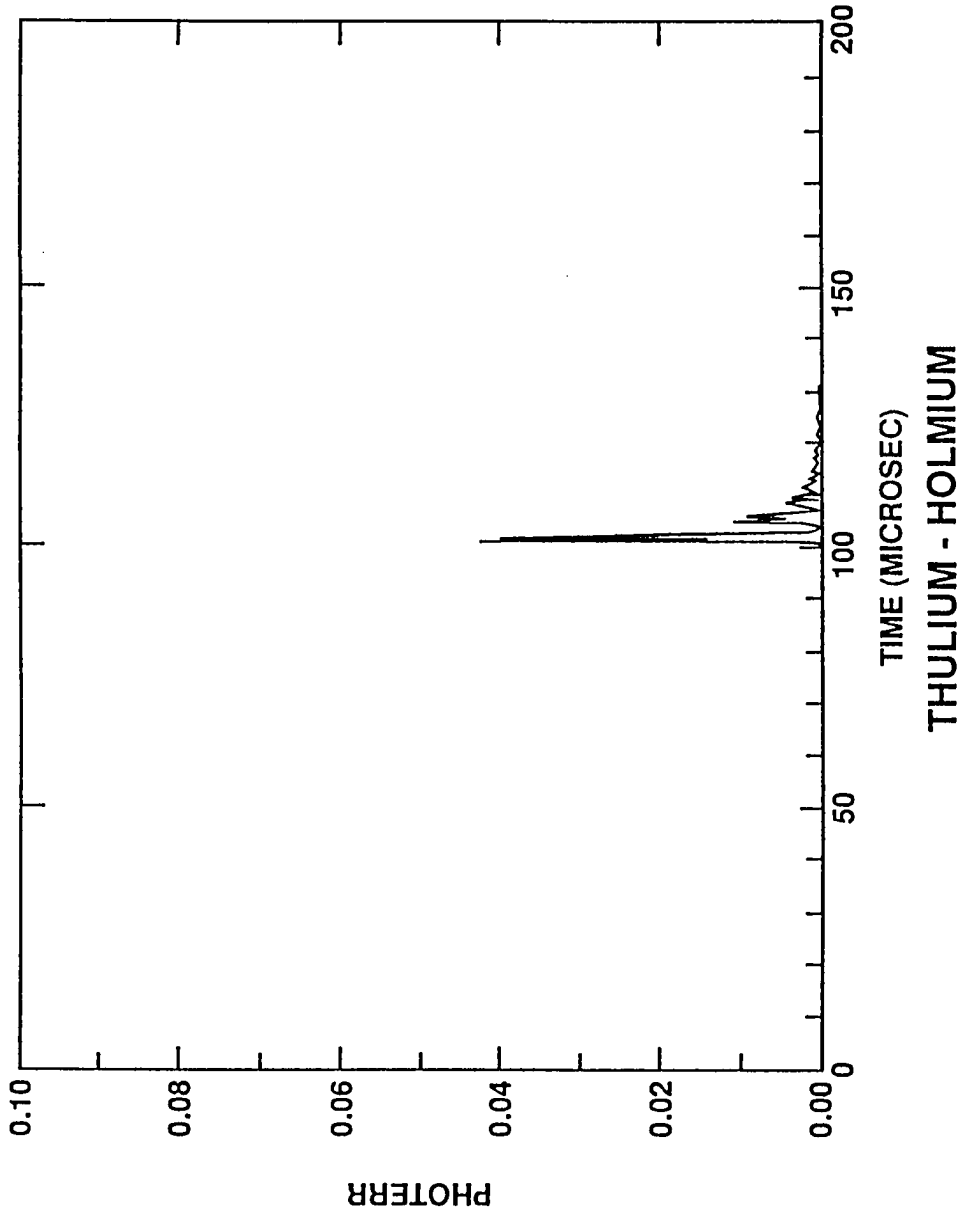

Figure 6.12 The difference between the numerical solution to P(t) with up-conversion and the solution to P(t) without up-conversion

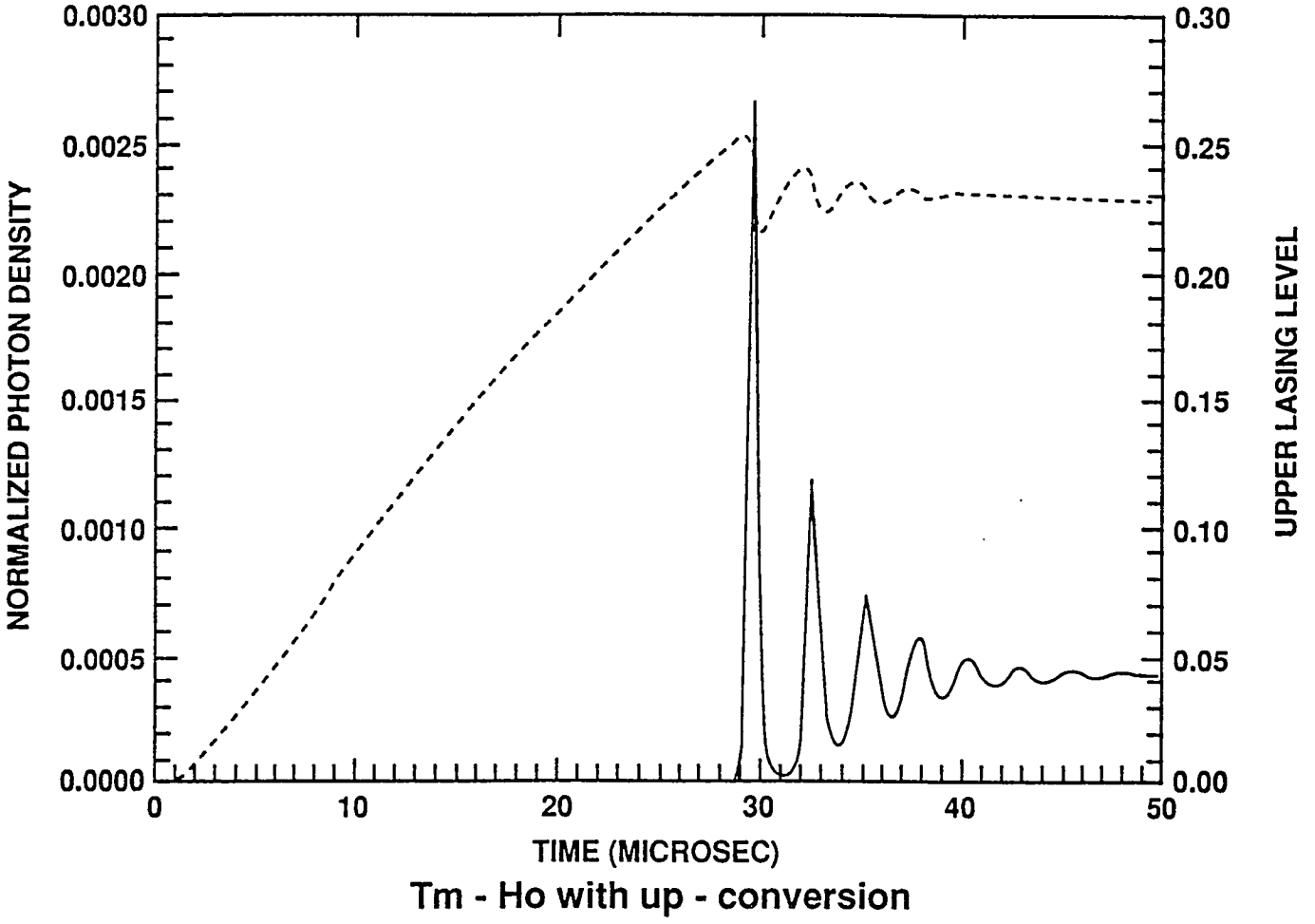

Figure 6.13 Upper lasing level and photon density with up-conversion included in the model

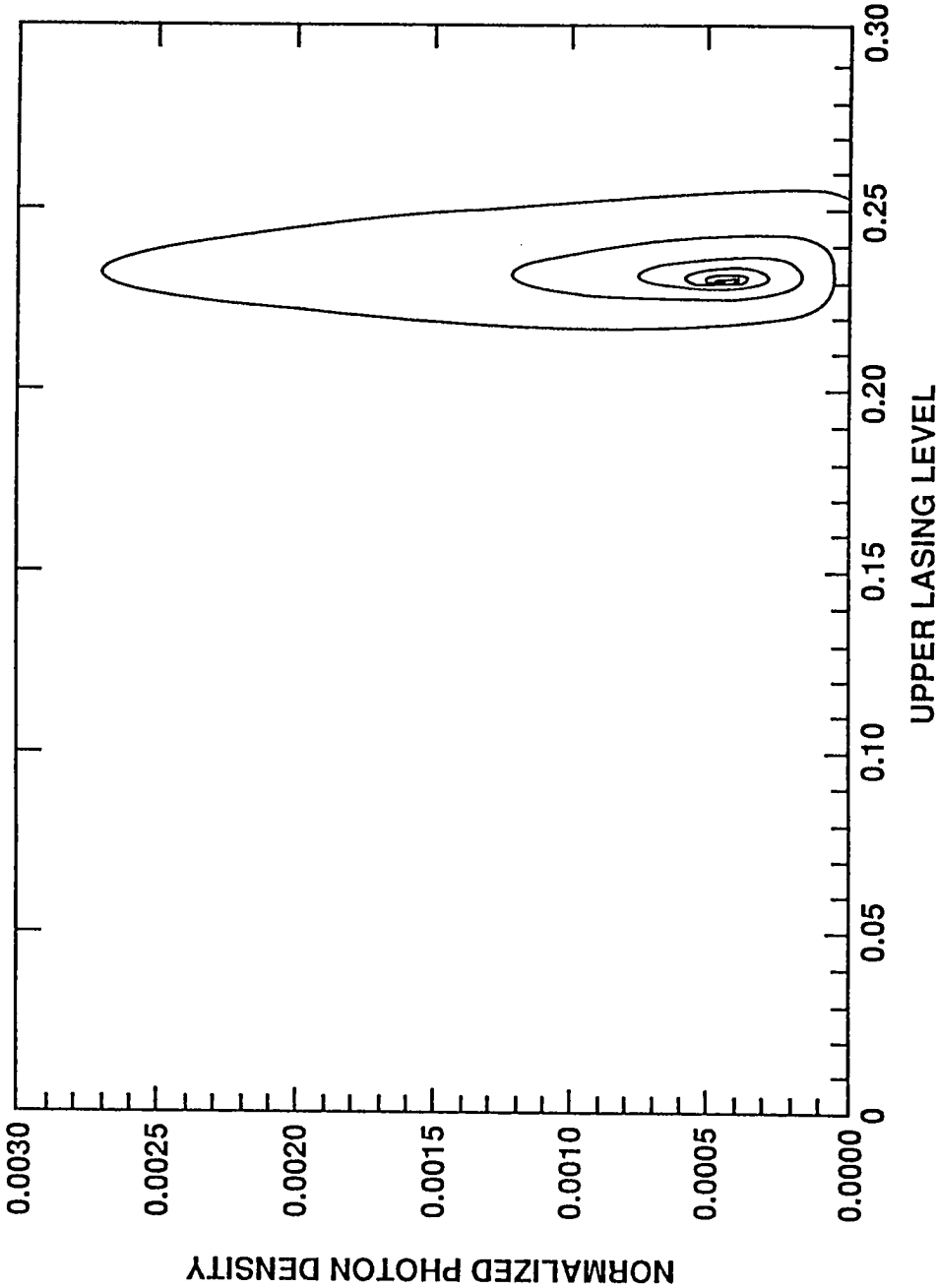

Figure 6.14 Phase portrait of the upper lasing level and the photon density

6.3 Q-Switching Revisited

When the system is Q-switched without the up-conversion level in the model—as in section 5.3—the upper lasing level continues to grow monotonically, asymptoting to one. Hence, the longer Q-switching is delayed, the larger the output pulse. With the up-conversion level included in the model, however, this is not the case. Figure 6.15 and 6.16 graph the upper lasing level and the photon density, respectively, when Q-switching at $180\mu s$. The behaviour of both is similar to that previously observed. In Figures 6.17 and 6.18 the time of Q-switching is delayed to $250\mu s$. From this we see that the electron population of the upper lasing level has started to decline due to energy being transferred to the up-conversion level. Consequently, there are fewer holmium ions available (in the upper lasing level) for stimulated emission and hence when the Q-switch is finally "flipped", the output pulse is less intense than before (as can be seen by comparing figures 6.16 and 6.18).

Now if the probability of up-conversion is reduced to $q_1 = 2 \times 10^{-23}$ and the time of Q-switching kept at $250\mu s$, we obtain Figures 6.19 and 6.20. The latter figure shows that the intensity of the output pulse has increased by an order of magnitude. Thus, the numerics indicate that timing is crucial when Q-switching the system that includes the up-conversion level and the optimal time of Q-switching is closely linked to the up-conversion parameter, q_1.

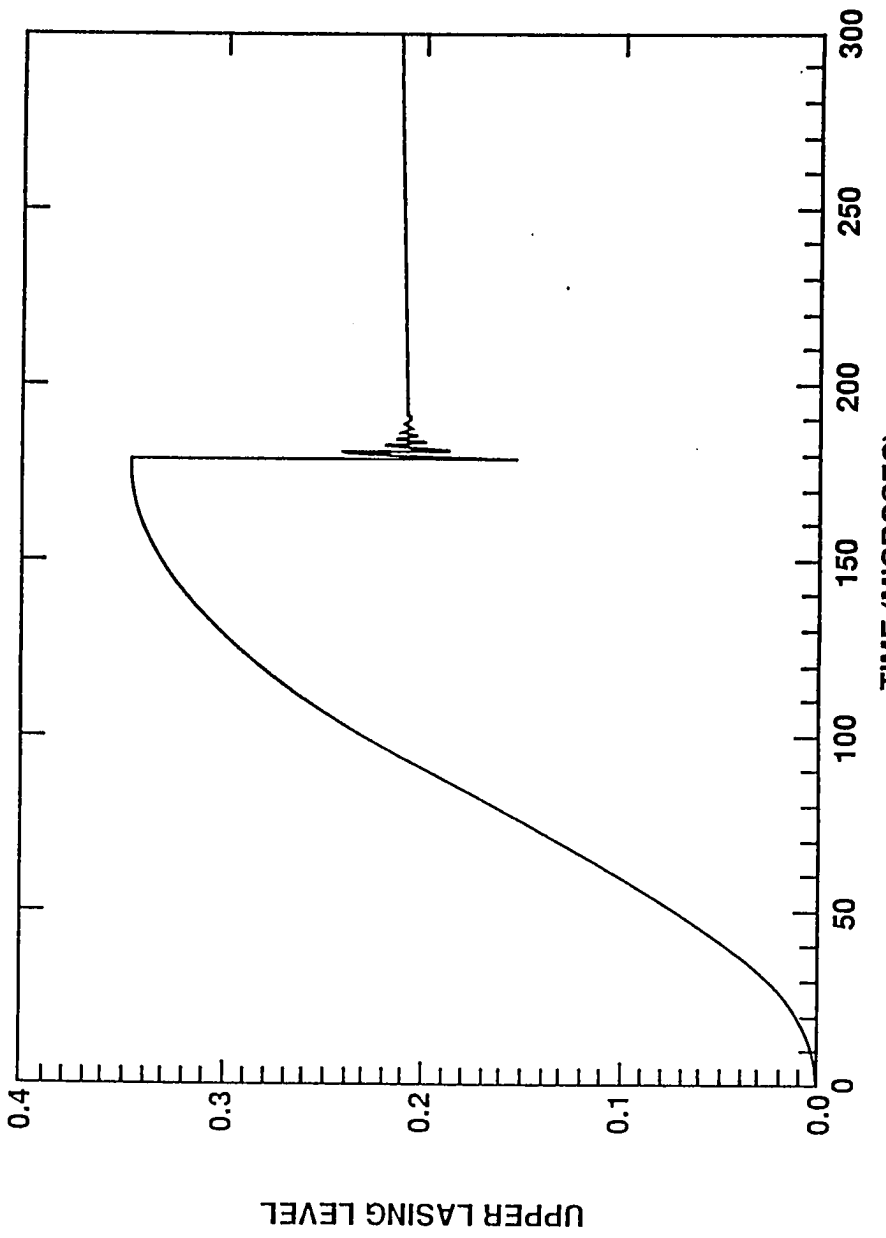

Figure 6.15 Upper lasing level when Q-switching at 180 microseconds with the up-conversion level included in the model

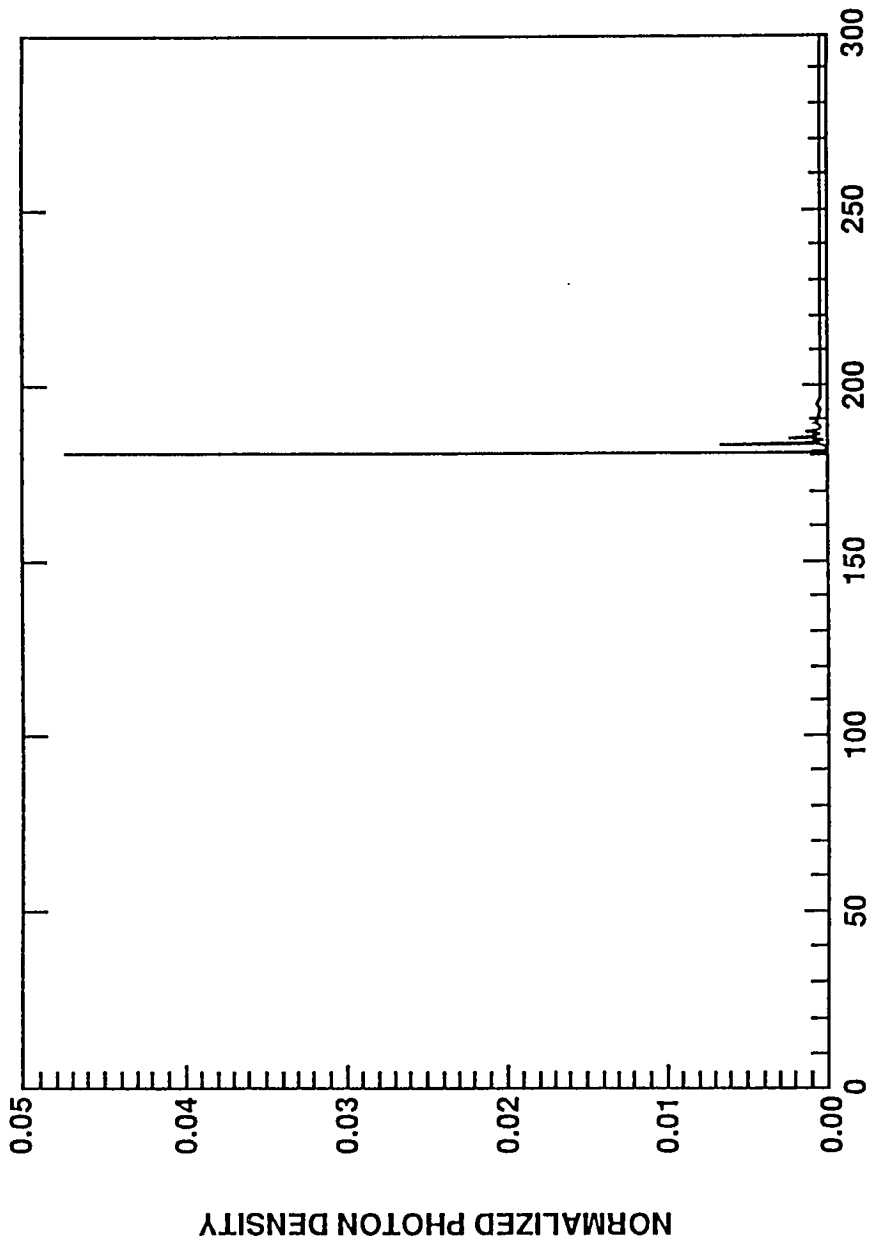

Figure 6.16 Normalized photon density when Q-switching at 180 microseconds with up-conversion level included in the model

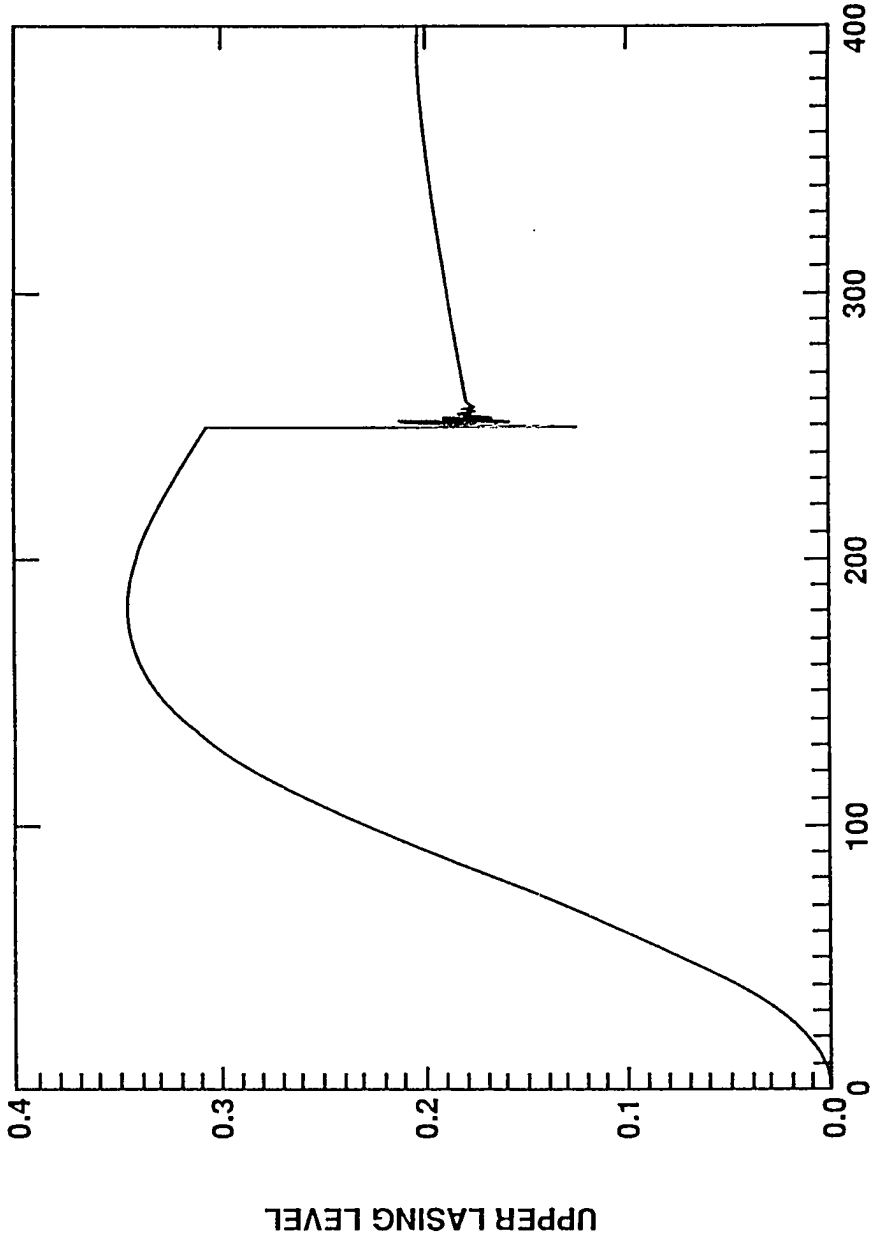

Figure 6.17 Upper lasing level when Q-switching is delayed to 250 micro-seconds and up-conversion level is included in the model

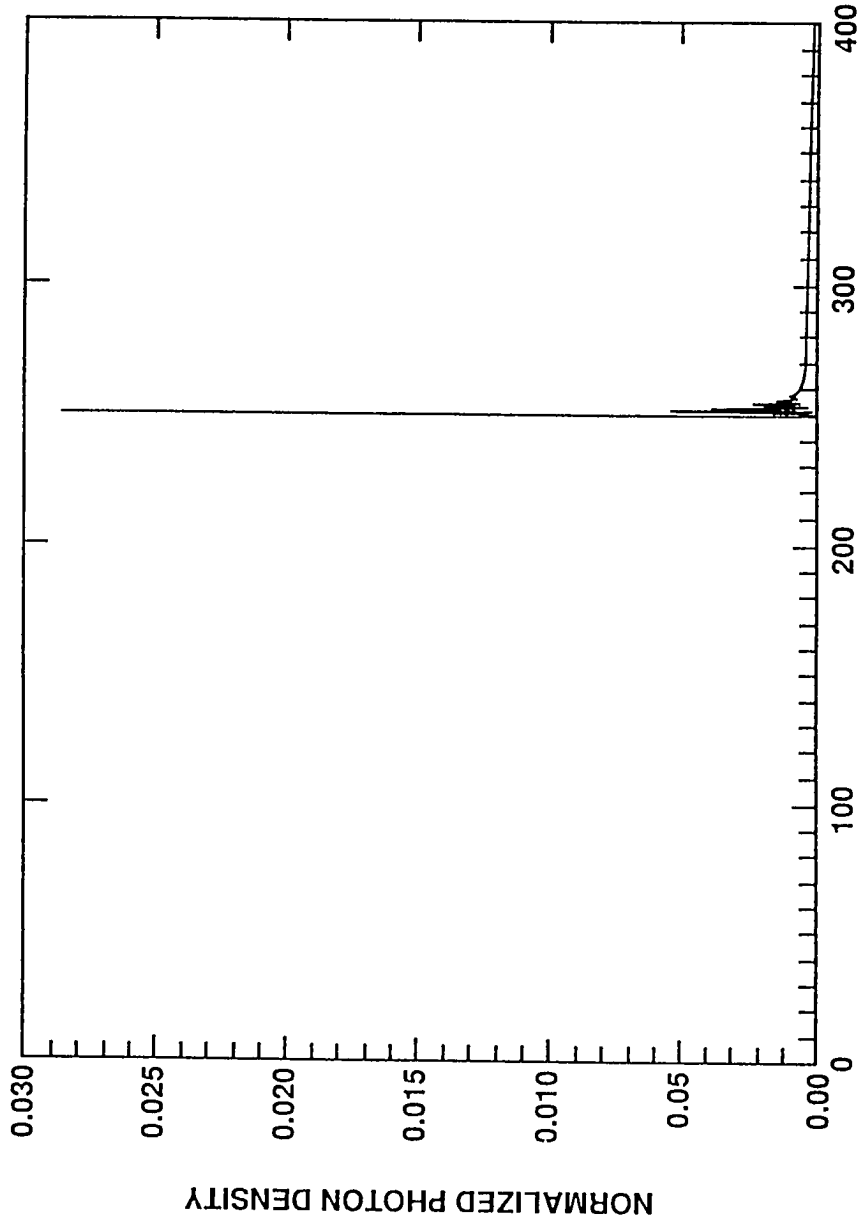

Figure 6.18 Normalized photon density when Q-switching at 250 microseconds and the up-conversion level is included in the model

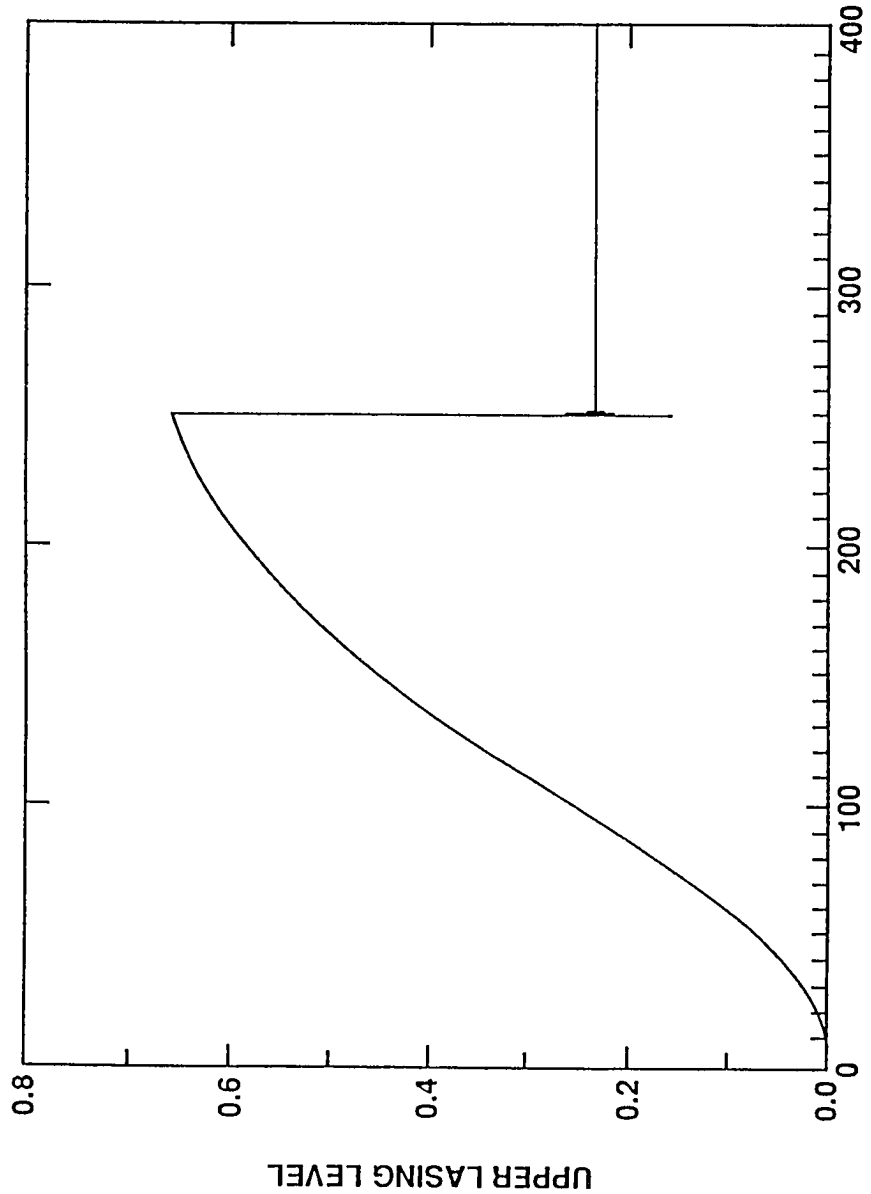

Figure 6.19 Upper lasing level when Q-switching at 250 microseconds and the up-conversion parameter has been reduced

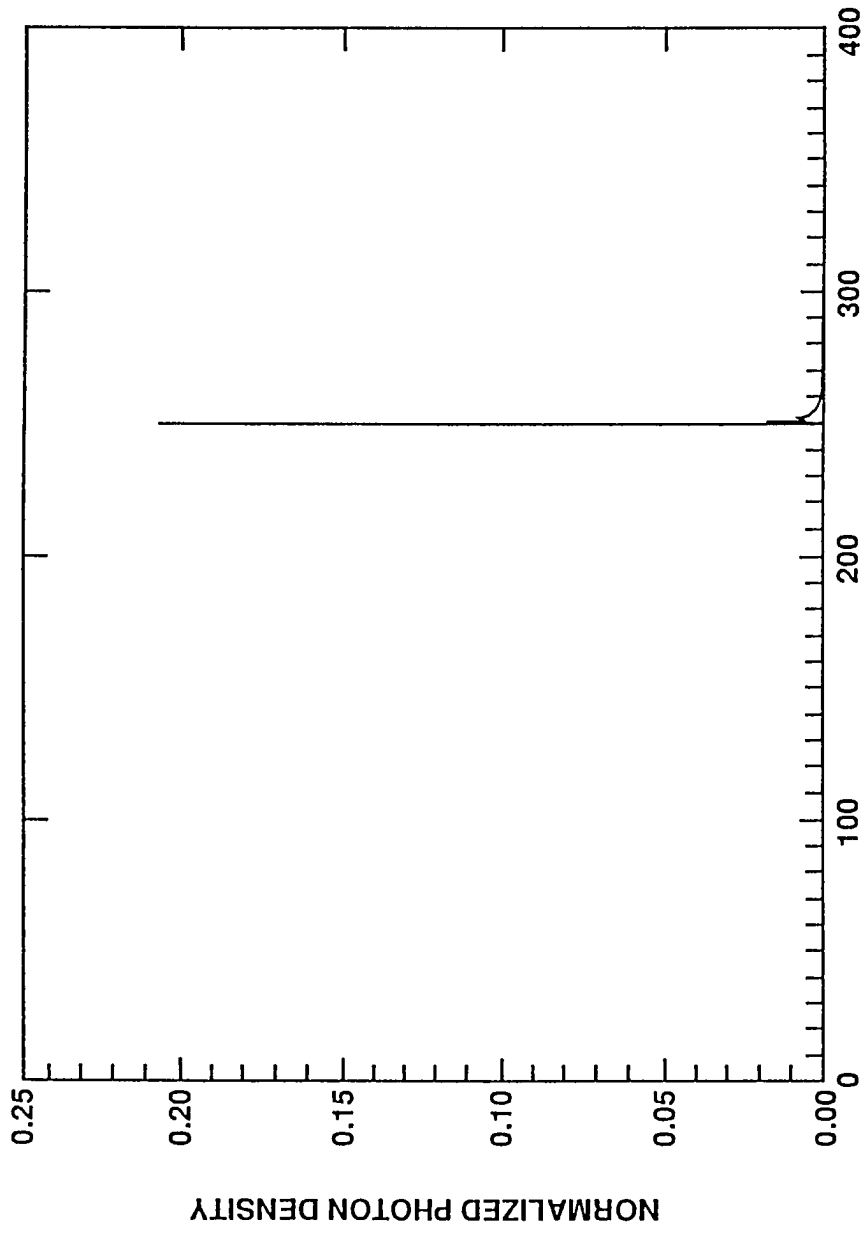

Figure 6.20 Normalized photon density when Q-switching at 250 microseconds and the up-conversion parameter has been reduced

Bibliography

[1] Allario, F.,"NASA Chooses Tunable Solid-State Lasers for Future Remote-Sensing Applications", *Laser Focus*, October 1988, pp.65-74

[2] Armagon, G.,"Recent Progress in the Spectroscopic Studies of $2\mu m$ Laser Materials", LaRC Sensor Review, 1990

[3] Beesley, M.J., *Lasers and Their Applications*, Taylor and Francis LTD, London, Halsted Press, 1976

[4] Birkhoff G. and G. Rota, *Ordinary Differential Equations*, Blaisdell Publishing Company, 1969

[5] Birkhoff G. and S. MacLane, *A Survey of Modern Algebra*, Revised Edition, The Macmillan Company New York, 1953

[6] Brauer F. and J.A. Nohel, *Qualitative Theory of Ordinary Differential Equations*, W.A. Benjamin Inc., 1969, p.26

[7] Brockman P., C.H. Bair, J.C. Barnes, R.V. Hess and E.V. Browell, "Pulsed Injection Control of a Titanium-Doped Sapphire Laser", *Optics Letters*, volume 11, number 11, November 1986

[8] Buoncristiani, A.M., G. Armagon, C.E. Byvik and S. Albin, "Optical Materials for Space Based Laser Systems", *Proceedings SPIE Conference on Aerospace Sensing*, Orlando, Florida, 1989

[9] Buoncristiani, A.M., J.J. Swetits and L.F. Roberts, "Analysis of the Dynamics of Solid State Lasers", Unpublished

[10] Buoncristiani, A.M., L.F. Roberts and J.J. Swetits, "Model of an End-Pumped Injection Seeded Solid-State Laser", *Math. Comput. Modelling*, vol.12, no.3, 1989, pp.303-312

[11] Byvik, C.E. and A.M. Buoncristiani, *IEEE Journal of Quantum Electron.*, QE-21, 1619 (1985)

[12] Dexter, D.L. and J.H. Schulman, *J. of Chem. Phys.*, vol.22, number 6, (1954) pp.1063-1070

[13] Goldberg, J. and A. Schwartz, *Systems of Ordinary Differential Equations: An Introduction*, Harper & Row, 1972, p.201

[14] Hecht, J., *The Laser Guidebook*, McGraw Hill, 1986

[15] Jordan, D.W. and P. Smith, *Nonlinear Ordinary Differential Equations*, Oxford, 1987, p.319

[16] Kahaner, D., C. Moler and S. Nash, *Numerical Methods and Software*, Prentice Hall, 1989

[17] Moulton, P.F., "Spectroscopic and Laser Characteristics of $Ti : Al_2O_3$ ", *Journal of the Optical Society of America B*, vol.3, January 1986, p.125

[18] Press, W.H., B.P. Flannery, S.A. Teukolsky and W. T. Vetterling, Subroutines ZROOTS.FOR & LAGUER.FOR, *Numerical Recipes*, Cambridge University Press, 1986

[19] Roberts, L.F., "Ph.D. Dissertation", Old Dominion University, 1988

[20] Roberts, L.F., A.M. Buoncristiani and J.J. Swetits, "An Investigation of a Mathematical Model of the Dynamics of an End-Pumped $Ti : Al_2O_3$ Laser System", (Pending Publication)

[21] Svelto, O., *Principles of Lasers*, Plenum Press, 1989

[22] Yariv, A., *Introduction to Optical Electronics*, Holt, Rinehart & Winston, New York, 1971, pp.120-125

Appendix A

COMPUTER PROGRAM:

Findroot

```
      PROGRAM FINDROOT
CCCCCCCCCCCCCCCCCCCCCCCCCCCCCCCCCCCCCCCCCCCCCCCCCCCCCCCCCCCCCCCCCCCCCCCC
C                                                                      C
C     THIS IS A PROGRAM THAT CALCULATES THE EQUILIBRIUM POINTS OF THE  C
C     SYSTEM OF NONLINEAR O.D.E.s . IT THEN USES THE ROUTH-HURWITZ     C
C     CRITERIA TO DETERMINE THE STABILITY OF EACH POINT. FINALLY IT    C
C     COMPUTES THE TWO DISCRIMINANTS ASSOCIATED WITH EQ.PT. 2 . TO DO  C
C     ALL THIS IT CALLS THE SUBROUTINE ''DZROOTS'', WHICH CAN BE FOUND C
C     IN THE BOOK ''NUMERICAL RECIPES'' .                              C
C                                                                      C
CCCCCCCCCCCCCCCCCCCCCCCCCCCCCCCCCCCCCCCCCCCCCCCCCCCCCCCCCCCCCCCCCCCCCCCC
      IMPLICIT DOUBLE PRECISION(A-H,N-Z)
      DOUBLE PRECISION IMPART
C      EXTERNAL F
      COMPLEX*16 COEFF,ROOTS,TROOTS,CVEC,RROOTS,COVEC,SROOTS,CO
      INTEGER*4 NN
      LOGICAL PPOLISH,LROOT
      PARAMETER(NN=4,MM=3,PPOLISH=.TRUE.)
      DIMENSION COEFF(5),ROOTS(4),CVEC(4),TROOTS(3),RROOTS(4),
     &COVEC(5),SROOTS(3),CO(4)
      COMMON/POLY/B1,B2,B3,B4,B5
      OPEN(UNIT=1,FILE='EQPT1.DAT')
      OPEN(UNIT=2,FILE='EQPT2.DAT')
      OPEN(UNIT=4,FILE='ROOT.ERR')
      OPEN(UNIT=8,FILE='D1TAUC.DAT')
      OPEN(UNIT=9,FILE='D2TAUC.DAT')
      OPEN(UNIT=10,FILE='PVAL.DAT')
      THNTOT=1.0D21
      HOnTOT=1.0D20
      C=1.0D0/(4.0D1*THNTOT)
      WP=6.0D-3
      TAU2=4.5D2
      TAU1=1.1D4
      C1=1.0D0/(4.75D2*HOnTOT)
      C1STAR=0.0D0
      TAU21=9.0D2
      TAU20=9.0D2
      GAMMA=2.0D0
      SIGMA=7.0D-21
      cc=3.0D4
      TAU1DASH=8.5D3
C      TAUC=1.0D-3
      TAUC=0.44D-4
      ITS=1
  15  CONTINUE
C-----BEGIN TAUC LOOP-------------------------------------------------------
C     THE FOLLOWING CONSTANTS ARE FOR THE CALCULATION OF THE VALUES OF
C     EQ. PT. ONE
      WRITE(1,20)'------------------TAUC=',TAUC,'-------------------'
      WRITE(2,20)'------------------TAUC=',TAUC,'-------------------'
  20  FORMAT(1X,A24,E16.8,A20)
      ALPHA1=2.0D0*C/TAU2 - C/TAU1 - C*C1*HOnTOT - C/TAU21
      ALPHA2=C*THNTOT/TAU1 + 1.0D0/(TAU1*TAU2) + C*C1*HOnTOT*THNTOT +
     1 C1*WP*HOnTOT + C1*HOnTOT/TAU2 + WP/TAU1 + WP/TAU21
      ALPHA3=WP*THNTOT/TAU1 + C1*WP*HOnTOT*THNTOT
      ALPHA4=C1STAR/TAU2 - C1/TAU2 - C/TAU1DASH - C*C1*THNTOT - C1*WP
      ALPHA5=WP/TAU1DASH + C1*WP*THNTOT
      BETA1=2.0D0*C*C1STAR - C*C1
      BETA2=C1*WP+C*C1*THNTOT+C1/TAU2-C1STAR/TAU2-2.0D0*C1STAR*WP -
     1 2.0D0*C*C1STAR*THNTOT
```

```
      BETA3=2.0D0*C1STAR*WP*THNTOT - C1*WP*THNTOT
      BETA4=C1*WP*HOnTOT + C1*HOnTOT/TAU2 + C*C1*HOnTOT*THNTOT

      A1=ALPHA1*C*C1+BETA1*C*C1*HOnTOT
      A2=ALPHA1*ALPHA4+ALPHA2*C*C1-BETA1*BETA4+BETA2*C*C1*HOnTOT
      A3=ALPHA1*ALPHA5+ALPHA2*ALPHA4-ALPHA3*C*C1+
     1 BETA1*C1*WP*HOnTOT*THNTOT-BETA2*BETA4+BETA3*C*C1*HOnTOT
      A4=ALPHA2*ALPHA5-ALPHA3*ALPHA4+BETA2*C1*WP*HOnTOT*THNTOT -
     1 BETA3*BETA4
      A5=BETA3*C1*WP*HOnTOT*THNTOT-ALPHA3*ALPHA5
C      WRITE(1,35)A1,A2,A3,A4,A5
CCCCCCCCCCCCCCCCCCCCCCCCCCCCCCCCCCCCCCCCCCCCCCCCCCCCCCCCCCCCCCCCCCCCCCCCCC
C                                                                       C
C     WE DESIRE TO PLOT THE POLYNOMIAL                                  C
C        P(N2)=A1*N2**4+A2*N2**3+A3*N2**2+A4*N2+A5                      C
C     FIRST I SWITCH TO THE NORMALIZED VARIABLE X=N2/THNTOT AND THEN    C
C     SCALE THE EQUATION TO KEEP THE COEFFICIENTS REASONABLE.           C
C                                                                       C
CCCCCCCCCCCCCCCCCCCCCCCCCCCCCCCCCCCCCCCCCCCCCCCCCCCCCCCCCCCCCCCCCCCCCCCCCC
      VNORM=1.0D15
      B1=A1*THNTOT**4/VNORM
      B2=A2*THNTOT**3/VNORM
      B3=A3*THNTOT**2/VNORM
      B4=A4*THNTOT/VNORM
      B5=A5/VNORM
CCCCCCCCCCCCCCCCCCCCCCCCCCCCCCCCCCCCCCCCCCCCCCCCCCCCCCCCCCCCCCCCCCCCCCCCCC
C                                                                       C
C     MUST FIND THE ROOTS OF THE FOLLOWING POLYNOMIAL:                  C
C     P(X)=B1*X**4 + B2*X**3 + B3*X**2 + B4*X + B5                      C
C                                                                       C
CCCCCCCCCCCCCCCCCCCCCCCCCCCCCCCCCCCCCCCCCCCCCCCCCCCCCCCCCCCCCCCCCCCCCCCCCC

   35 FORMAT(1X,E14.7,1X,E14.7,1X,E14.7,1X,E14.7,1X,E14.7)

      COVEC(5)=DCMPLX(B1)
      COVEC(4)=DCMPLX(B2)
      COVEC(3)=DCMPLX(B3)
      COVEC(2)=DCMPLX(B4)
      COVEC(1)=DCMPLX(B5)
      CALL DZROOTS(COVEC,NN,RROOTS,PPOLISH)
      J=0
  40  J=J+1
      REPART=DREAL(RROOTS(J))
      IMPART=DIMAG(RROOTS(J))
      IF((REPART.GE.0.0D0).AND.(IMPART.LE.1.0D-8))THEN
       X0=REPART
      ELSE IF(J.LE.3)THEN
       GO TO 40
      ELSE
       WRITE(1,44)'NO REAL POSITIVE ROOT FOUND WHEN TAUC=',TAUC
       GO TO 66
      END IF
  44  FORMAT(1X,A40,E16.7)
      N2=X0*THNTOT
      N1=(WP*THNTOT+(C*(N2-THNTOT)-WP-1.0D0/TAU2)*N2)/(WP-C*N2)
      Y0=N1/THNTOT
      E1=WP-C*N2
      ZNUM=C1*(WP*THNTOT+N2*(C*N2-WP-1.0D0/TAU2-C*THNTOT))
      ZDEN=E1/TAU1DASH+C1*E1*(THNTOT-N2)+N2*(C1STAR-C1)/TAU2
      Z0=ZNUM/ZDEN
```

```
      WRITE(1,63)' X0= ',X0
      WRITE(1,63)' Y0= ',Y0
      WRITE(1,63)' Z0= ',Z0
      WRITE(1,62)'    '

C     NOW THAT I HAVE THE VALUES FOR EQ.PT.1 I CHECK ONE OF THE
C     ROUTH-HURWITZ CONDITIONS.

      EQLHS=1.0D0-GAMMA+GAMMA*Z0
      EQRHS=1.0D0/(SIGMA*CC*HOnTOT*TAUC)
      WRITE(1,61)' LHS= ',EQLHS
      WRITE(1,61)' RHS= ',EQRHS
      IF(EQLHS.GT.EQRHS)THEN
       WRITE(1,49)' P=0 IS UNSTABLE '
      ELSE
       WRITE(1,49)'  P=0 IS STABLE  '
      END IF
   49 FORMAT(1X,A18)
   50 FORMAT(1X,A20,1X,E16.8,1X,E16.8)
   55 FORMAT(1X,A15,1X,E16.8,1X,E16.8)
   60 FORMAT(1X,A13,I2)
   61 FORMAT(1X,A6,1X,E16.8)
   62 FORMAT(1X,A3)
   63 FORMAT(1X,A4,1X,E16.8)
   65 FORMAT(1X,A17,1X,E16.8)
CCCCCCCCCCCCCCCCCCCCCCCCCCCCCCCCCCCCCCCCCCCCCCCCCCCCCCCCCCCCCCCCCCCCC
C                                                                     C
C     WE WILL NOW FIND THE ROOTS OF THE CHARACTERISTIC EQUATION       C
C     ASSOCIATED WITH EQ.PT.1                                         C
C                                                                     C
CCCCCCCCCCCCCCCCCCCCCCCCCCCCCCCCCCCCCCCCCCCCCCCCCCCCCCCCCCCCCCCCCCCCC

      D1=C*THNTOT
      D2=C1*HOnTOT
      D3=C1STAR*HOnTOT
      D4=C1*THNTOT
      D5=C1STAR*THNTOT

C     FIRST WE WRITE THE ENTRIES OF THE MATRIX OF LINEARIZATION
C     FOR EQ.PT.1,CALL IT MATRIX B.

      B11=D1*Y0+2.0D0*D1*X0-WP-1.0D0/TAU2-D1
      B12=D1*X0-WP
      B21=1.0D0/TAU21-4.0D0*D1*X0-2.0D0*D1*Y0+2.0D0*D1-D3*Z0
      B22=-(1.0D0/TAU1+2.0D0*D1*X0+D2-D2*Z0+D3*Z0)
      B23=D4*Y0+D5*(1.0D0-X0-Y0)
      B31=D3*Z0
      B32=D3*Z0+D2*(1.0D0-Z0)
      B33=-(1.0D0/TAU1DASH+D4*Y0+D5*(1.0D0-X0-Y0))
      B44=SIGMA*CC*HOnTOT*(GAMMA*Z0+1.0D0-GAMMA)-1.0D0/TAUC
CCCCCCCCCCCCCCCCCCCCCCCCCCCCCCCCCCCCCCCCCCCCCCCCCCCCCCCCCCCCCCCCCCCCC
C                                                                     C
C     THE CHAR.EQ. IS p**3 + Q*p**2 + R*p + S = 0                     C
C     SO I NOW DEFINE THE COEFFICIENTS AS FOLLOWS:                    C
C                                                                     C
CCCCCCCCCCCCCCCCCCCCCCCCCCCCCCCCCCCCCCCCCCCCCCCCCCCCCCCCCCCCCCCCCCCCC
      Q=-(B11+B22+B33)
      R=B22*B33+B11*B33+B11*B22-B12*B21-B23*B32
      S=B11*B23*B32+B12*B21*B33-B12*B23*B31-B11*B22*B33
      CO(4)=DCMPLX(1.0D0)
```

```
      CO(3)=DCMPLX(Q)
      CO(2)=DCMPLX(R)
      CO(1)=DCMPLX(S)
      CALL DZROOTS(CO,MM,SROOTS,PPOLISH)
      WRITE(1,69)'ROOTS OF EQ.PT.1 WHEN TAUC= ',TAUC
      WRITE(1,71)B44
      WRITE(1,72)SROOTS(1)
      WRITE(1,72)SROOTS(2)
      WRITE(1,72)SROOTS(3)
C      WRITE(1,68)' Q= ',Q
C      WRITE(1,68)' R= ',R
C      WRITE(1,68)' S= ',S

CCCCCCCCCCCCCCCCCCCCCCCCCCCCCCCCCCCCCCCCCCCCCCCCCCCCCCCCCCCCCCCCCC
C     WE NOW FIND THE COORDINATES OF THE SECOND EQ.PT.  C
CCCCCCCCCCCCCCCCCCCCCCCCCCCCCCCCCCCCCCCCCCCCCCCCCCCCCCCCCCCCCCCCCC

  66  CONTINUE
      ETA1=1.0D0/(SIGMA*CC*TAUC)+(GAMMA-1.0D0)*HOnTOT
      ETA2=ETA1*C1STAR/GAMMA-2.0D0*C*THNTOT-1.0D0/TAU21
      ETA3=1.0D0/TAU1+C1*HOnTOT+ETA1*(C1STAR-C1)/GAMMA
      ETA4=C*THNTOT+WP+1.0D0/TAU2
      ETA5=ETA1*C1STAR*THNTOT/GAMMA

      ZETA1=D1*(ETA2-ETA3+2.0D0*ETA4-2.0D0*WP)
      ZETA2=ETA3*ETA4-ETA2*WP-2.0D0*D1*WP-ETA5*C
      ZETA3=ETA5*WP/THNTOT-ETA3*WP

      WRITE(2,70)' ZETA1= ',ZETA1
      WRITE(2,70)' ZETA2= ',ZETA2
      WRITE(2,70)' ZETA3= ',ZETA3
  68  FORMAT(1X,A4,1X E16.8)
  69  FORMAT(1X,A30,1X E16.8)
  70  FORMAT(1X,A8,1X,E16.8)
  71  FORMAT(1X,E16.8)
  72  FORMAT(1X,E16.8,E16.8)
      QUADDISC=ZETA2**2-4.0D0*ZETA1*ZETA3
      IF(QUADDISC.GE.0.0D0)THEN
       X2=(-ZETA2+(ZETA2**2.0D0-4.0D0*ZETA1*ZETA3)**0.5D0)/(2.0D0*ZETA1)
       X3=(-ZETA2-(ZETA2**2.0D0-4.0D0*ZETA1*ZETA3)**0.5D0)/(2.0D0*ZETA1)
       WRITE(2,75)' THE 2 ROOTS FOR EQ. PT. TWO ARE : '
       WRITE(2,76)' X2= ',X2
       WRITE(2,76)' X3= ',X3
      ELSE
       WRITE(2,74)' THE QUADRATIC DISCRIMINANT IS NEGATIVE! '
       GO TO 100
      END IF
  74  FORMAT(1X,A42)
  75  FORMAT(1X,A36)
  76  FORMAT(1X,A6,1X,E16.8)
      PHINORM=1.0D16

      IF(X3.LT.0.0D0)THEN
       X=X2
      ELSE
      GO TO 100
      END IF
      Y=((D1*X-WP-1.0D0/TAU2-D1)*X+WP)/(WP-D1*X)
      DMESS=TAUC*SIGMA*CC*HOnTOT
      Z=(GAMMA-1.0D0)/GAMMA+1.0D0/(DMESS*GAMMA)
```

```
      P11=TAUC*HOnTOT/(PHINORM*GAMMA)
      P1=-P11*(1.0D0/TAU1DASH+D5*(1.0D0-X))*(GAMMA-1.0D0+1.0D0/DMESS)
      P2=Y*P11*GAMMA*(D4+(D5-D4)*(GAMMA-1.0D0+1.0D0/DMESS)/GAMMA)
      P=P1+P2
      WRITE(2,80)' THE FOLLOWING ARE VALUES FOR EQ. PT. TWO : '
      WRITE(2,81)' X= ',X
      WRITE(2,81)' Y= ',Y
      WRITE(2,81)' Z= ',Z
      WRITE(2,81)' P= ',P
      WRITE(10,125)TAUC,P
   80 FORMAT(1X,A45)
   81 FORMAT(1X,A4,1X,E16.8)

C     NOW THAT I HAVE VALUES FOR EQ.PT.2 I WILL USE THEM TO FIND
C     THE ROOTS OF THE CHARACTERISTIC EQN. ASSOCIATED WITH EQ.PT. 2.

C     FIRST THE ENTRIES TO THE MATRIX OF LINEARIZATION AROUND EQ.PT. 2
C     ARE GIVEN BY:

      A11=2.0D0*C*THNTOT*X+C*THNTOT*Y-WP-1.0D0/TAU2-C*THNTOT
      A12=C*THNTOT*X-WP
      A21=1.0D0/TAU21-4.0D0*C*THNTOT*X+2.0D0*C*THNTOT-2.0D0*C*THNTOT*Y
     1-C1STAR*HOnTOT*Z
      A22=-(1.0D0/TAU1+2.0D0*C*THNTOT*X+C1*HOnTOT*(1.0D0-Z)+
     1C1STAR*HOnTOT*Z)
      A23=C1*THNTOT*Y+C1STAR*THNTOT*(1.0D0-X-Y)
      A31=C1STAR*HOnTOT*Z
      A32=C1*HOnTOT*(1.0D0-Z)+C1STAR*HOnTOT*Z
      A33=-(GAMMA*SIGMA*CC*PHINORM*P+1.0D0/TAU1DASH+C1*THNTOT*Y+
     1C1STAR*THNTOT*(1.0D0-X-Y))
      A34=-1.0D0/TAUC
      A43=SIGMA*CC*GAMMA*PHINORM*P

C     NOW FOR THE COEFFICIENTS OF THE CHARACTERISTIC EQN. ITSELF!

      A=-(A11+A22+A33)
      B=-A12*A21-A23*A32+A22*A33+A11*A22+A11*A33-A34*A43
      D=(A11+A22)*A34*A43+A11*A23*A32+A12*A21*A33-A11*A22*A33
     1-A12*A23*A31
      E=(A12*A21-A11*A22)*A34*A43
C      WRITE(2,82)' A= ',A
C      WRITE(2,82)' B= ',B
C      WRITE(2,82)' D= ',D
C      WRITE(2,82)' E= ',E
   82 FORMAT(1X,A4,E16.8)
C     NOW I NEED TO SOLVE THE FOLLOWING EQN.
C
C      S**4 + A*S**3 + B*S**2 + D*S + E = 0
C
C     I WILL USE THE ROUTH-HURWITZ CRITERIA TO SEE IF THE ROOTS
C     HAVE NEGATIVE REAL PARTS.

CCCCCCCCCCCCCCCCCCCCCCCCCCCCCCCCCCCCCCCCCCCCCCCCCCCCCCCCCCCCCCCCCCCC
C                                                                    C
C     DEFINE ARGUMENTS FOR SUBROUTINE ZROOTS                         C
C                                                                    C
CCCCCCCCCCCCCCCCCCCCCCCCCCCCCCCCCCCCCCCCCCCCCCCCCCCCCCCCCCCCCCCCCCCC

      COEFF(5)=DCMPLX(1.0D0)
      COEFF(4)=DCMPLX(A)
```

```
      COEFF(3)=DCMPLX(B)
      COEFF(2)=DCMPLX(D)
      COEFF(1)=DCMPLX(E)
      CALL DZROOTS(COEFF,NN,ROOTS,PPOLISH)
      DO 83 K=1,4
       WRITE(2,85)'ROOT= ',ROOTS(K)
  83  CONTINUE
  85  FORMAT(1X,A6,E16.7,E16.7)

CCCCCCCCCCCCCCCCCCCCCCCCCCCCCCCCCCCCCCCCCCCCCCCCCCCCCCCCCCCCCCCCCCCC
C                                                                     C
C     FIND DISCRIMINANT FOR CURRENT VALUE OF TAUC                     C
C                                                                     C
CCCCCCCCCCCCCCCCCCCCCCCCCCCCCCCCCCCCCCCCCCCCCCCCCCCCCCCCCCCCCCCCCCCC

      PP=B-0.375D0*A**2
      QQ=0.125D0*A**3+D-0.5D0*A*B
      RR=0.0625D0*B*A**2-3.0D0*A**4/256.0D0-0.25D0*A*D+E
      CC4=1.0D0
      CC3=-PP
      CC2=-4.0D0*RR
      CC1=4.0D0*PP*RR-QQ**2
      CVEC(4)=DCMPLX(CC4)
      CVEC(3)=DCMPLX(CC3)
      CVEC(2)=DCMPLX(CC2)
      CVEC(1)=DCMPLX(CC1)
      CALL DZROOTS(CVEC,MM,TROOTS,PPOLISH)
      II=1
  87  CONTINUE
      DRE=DREAL(TROOTS(II))
      DIM=DIMAG(TROOTS(II))
      IF((DABS(DIM).LE.1.0D-8).AND.(DRE.GE.PP))THEN
       U1=DRE
       LROOT=.TRUE.
      ELSE
       LROOT=.FALSE.
       IF(II.LE.2)THEN
        II=II+1
        GO TO 87
       END IF
      END IF
      IF(.NOT.LROOT)THEN
       WRITE(2,110)' UNABLE TO LOCATE U1 WHEN TAUC =',TAUC
      END IF
      IF(LROOT)THEN
       AAA=DSQRT(U1-PP)
       BBB=QQ/(2.0D0*AAA)
       DDISC1=AAA**2-2.0D0*U1+4.0D0*BBB
       DDISC2=AAA**2-2.0D0*U1-4.0D0*BBB
       WRITE(8,125)TAUC,DDISC1
       WRITE(9,125)TAUC,DDISC2
       WRITE(2,120)'TAUC=',TAUC,'DISCRIMINANT1=',DDISC1
       WRITE(2,120)'TAUC=',TAUC,'DISCRIMINANT2=',DDISC2
      END IF
CCCCCCCCCCCCCCCCCCCCCCCCCCCCCCCCCCCCCCCCCCCCCCCCCCCCCCCCCCCCCCCCCCCC
C                                                                     C
C     NOW THE ROUTH-HURWITZ CRITERIA                                  C
C                                                                     C
CCCCCCCCCCCCCCCCCCCCCCCCCCCCCCCCCCCCCCCCCCCCCCCCCCCCCCCCCCCCCCCCCCCC
      CONLHS=A*B
```

```
      THELEFT=A*(B*D-A*E)
      THERITE=D*D
      IF((A.GT.0.0D0).AND.(CONLHS.GT.D).AND.(E.GT.0.0D0).AND.
     &(THELEFT.GT.THERITE))THEN
       WRITE(2,93)' ROUTH-HURWITZ CONDITIONS ARE SATISFIED'
      ELSE
       WRITE(2,93)' ROUTH-HURWITZ CONDITIONS NOT SATISFIED'
      END IF
      WRITE(2,94)' '
      WRITE(2,94)' '
   93 FORMAT(1X,A40)
   94 FORMAT(1X,A2)

      ITS=ITS+1
      IF(ITS.GE.1000)THEN
       WRITE(2,130)'TOO MANY ITERATIONS;ITS=',ITS
       GO TO 100
      END IF
      IF((TAUC.LE.5.4D-5).AND.(TAUC.GE.4.4D-5))THEN
       TAUC=TAUC+1.0D-7
       GO TO 15
      END IF
C-----END TAUC LOOP-------------------------------------------

  100 CONTINUE
  110 FORMAT(1X,A33,E16.7)
  120 FORMAT(1X,A5,E16.7,1X,A15,E16.7)
  125 FORMAT(1X,E16.8,E16.8)
  130 FORMAT(1X,A25,1X,I3)
      STOP
      END

      DOUBLE PRECISION FUNCTION F(X)
      IMPLICIT DOUBLE PRECISION(A-H,N-Z)
      COMMON/POLY/B1,B2,B3,B4,B5
      F=B5+X*(B4+X*(B3+X*(B2+B1*X)))
      RETURN
      END
```

Appendix B

COMPUTER PROGRAM:

Oldthho

```
      PROGRAM OLDTHHO
C     THIS IS A PROGRAM TO SOLVE THE THULIUM HOLMIUM LASER SYSTEM BY EMPLOYING
C     LSODA OR DDRIV2.THE CORRESPONDENCE BETWEEN THE VARIABLES IN THE SYSTEM
C     AND THE VARIABLES IN THE PROGRAM IS AS FOLLOWS:
C     Y(1)=NORMALIZED THULMIUM UPPER LASING LEVEL
C     Y(2)=  "    "     THULMIUM LOWER   "      "
C     Y(3)=  "    "     HOLMIUM UPPER LASING LEVEL
C     Y(4)=  "    "     PHOTON DENSITY
      IMPLICIT DOUBLE PRECISION(A-H,O-Z)
      EXTERNAL FEX
      PARAMETER (N=4,DEL=1.0D-7)
      DIMENSION Y(N),WORK(288),IWORK(50),PD(N,N),FPERT(N),F(N),
     &COL(N),COLMAX(N),YPERT(N)
C      DIMENSION Y(N),ATOL(N),RWORK(84),IWORK(24)
      COMMON W,TAU20,TAU21,CC,TAU2,TAU1,TAUC,SPO,C,THNTOT,C1,C1STAR,
     1GAMMA,SIGMA,TAU1DASH,HOnTOT,D1,D2,D3,D4,D5,PHINORM,PAR4,
     2PAR3,ZSTAR
      OPEN(UNIT=6,FILE='OLDTHHO.ERR')
      OPEN(UNIT=7,FILE='TTY1.DAT')
      OPEN(UNIT=8,FILE='TTY2.DAT')
      OPEN(UNIT=9,FILE='TTY3.DAT')
      OPEN(UNIT=10,FILE='TTY4.DAT')
      OPEN(UNIT=12,FILE='INFO.THHO')
      OPEN(UNIT=13,FILE='MAXJAC.DAT')
      OPEN(UNIT=14,FILE='GLB.DAT')
      NEQ=4
      Y(1)=0.0D0
      Y(2)=0.0D0
      Y(3)=0.0D0
      Y(4)=0.0D0
      TOUT=0.1D0
      DELTAT=0.1D0
      NPOINTS=7000

      ZSTAR=0.0D0
      ITEST=0

CCCCCCCCCCCCCCCCCCCCCCCCCCCCCCCCCCCCCCCCCCCCCCCCCCCCCCCCCCCCCCCCCCCCCC
C                                                                      C
C     LSODA PARAMETERS                                                 C
C                                                                      C
CCCCCCCCCCCCCCCCCCCCCCCCCCCCCCCCCCCCCCCCCCCCCCCCCCCCCCCCCCCCCCCCCCCCCC
C      ITOL=2
C      RTOL=1.0D-08
C      ATOL(1)=5.0D-10
C      ATOL(2)=5.0D-10
C      ATOL(3)=5.0D-10
C      ATOL(4)=5.0D-16
C      ITASK=1
C      ISTATE=1
C      IOPT=1
C      LRW=84
C      LIW=24
C      JT=1
CC      MF=21
C      DO 1 I=5,10
C       RWORK(I)=0.0D0
C       IWORK(I)=0
C  1   CONTINUE
C      H0=.01D0
```

```
C       HMAX=.01D0
C       HMIN=1.0D-08
C       MXSTEP=5000
C       RWORK(5)=H0
C       RWORK(6)=HMAX
C       RWORK(7)=HMIN
C       IWORK(6)=MXSTEP

CCCCCCCCCCCCCCCCCCCCCCCCCCCCCCCCCCCCCCCCCCCCCCCCCCCCCCCCCCCCCCCCCCC
C                                                                    C
C     DDRIV2 PARAMETERS                                              C
C                                                                    C
CCCCCCCCCCCCCCCCCCCCCCCCCCCCCCCCCCCCCCCCCCCCCCCCCCCCCCCCCCCCCCCCCCC

      MSTATE=1
      NROOT=0
      EPS=1.0D-9
      EWT=1.0D-22
      MINT=3
      LENW=288
      LENIW=50

      S=1.0D0
CCCCCCCCCCCCCCCCCCCCCCCCCCCCCCCCCCCCCCCCCCCCCCCCCCCCCCCCCCCCCCCCCCCCCC
C                                                                    C
C     S IS A SCALING FACTOR:                                         C
C     IF S=0.001    THEN [T]=THOUSANDS OF MICROSEC.(i.e.MILLISECONDS) C
C     IF S=0.01     THEN [T]=HUNDREDS OF MICROSEC.                   C
C     IF S=0.1      THEN [T]=TENS OF MICROSEC.                       C
C     IF S=1.0      THEN [T]=MICROSEC.                               C
C     IF S=10.0     THEN [T]=TENTHS OF MICROSEC.                     C
C     IF S=100.0    THEN [T]=HUNDRETHS OF MICROSEC.                  C
C     IF S=1000.0   THEN [T]=THOUSANTHS OF MICROSEC.(i.e.NANOSECONDS) C
CCCCCCCCCCCCCCCCCCCCCCCCCCCCCCCCCCCCCCCCCCCCCCCCCCCCCCCCCCCCCCCCCCCCCC

CCCCCCCCCCCCCCCCCCCCCCCCCCCCCCCCCCCCCCCCCCCCCCCCCCCCCCCCCCCCCCCCCCC
C                                                                    C
C      PHYSICAL PARAMETERS                                           C
C                                                                    C
CCCCCCCCCCCCCCCCCCCCCCCCCCCCCCCCCCCCCCCCCCCCCCCCCCCCCCCCCCCCCCCCCCC

      TAU1=S*1.1D4
      TAU2=S*4.5D2
      TAU1DASH=S*8.5D3
      HOnTOT=1.0D20
      THNTOT=1.0D21
      GAMMA=2.0D0
      C=1.0D0/(S*4.0D1*THNTOT)
      CC=3.0D4/S
      TAU20=S*9.0D2
      TAU21=S*9.0D2
      TAUC=S*1.0D-3
C      TAUC=S*4.7D-5
      C1=1.0D0/(S*4.75D2*HOnTOT)
      W=6.0D-3/S
C      SIGMA=7.0D-21
      SIGMA=1.32D-19
      C1STAR=0.0D0
      PHINORM=1.0D18
      D1=C*THNTOT
      D2=C1*HOnTOT
```

```
      D3=C1STAR*HOnTOT
      D4=C1*THNTOT
      D5=C1STAR*THNTOT
      SPO=1.0D-6/S
      PNUM=SPO*HONTOT
      PDEN=PHINORM*TAU1DASH
      PAR4=PNUM/PDEN
      PAR3=SIGMA*CC*HONTOT
CCCCCCCCCCCCCCCCCCCCCCCCCCCCCCCCCCCCCCCCCCCC
C                                           C
C     END OF PHYSICAL PARAMETERS            C
C                                           C
CCCCCCCCCCCCCCCCCCCCCCCCCCCCCCCCCCCCCCCCCCCC

      IF(ITEST.EQ.1)GO TO 100
      IFLAG=1
      TSTART=0.0D0
      T=0.0D0
      IF(IFLAG.EQ.1)THEN
       CALL SCRIBE(N,T,Y)
      END IF

  15  FORMAT(1X,A7,E14.7)
      DO 40 IOUT=1,NPOINTS
C      CALL LSODA(FEX,NEQ,Y,T,TOUT,ITOL,RTOL,ATOL,ITASK,ISTATE,
C     1 IOPT,RWORK,LRW,IWORK,LIW,JEX,JT)
C      IF(ISTATE.LT.0)GO TO 80
      CALL DDRIV2(N,T,Y,FEX,TOUT,MSTATE,NROOT,EPS,EWT,
     &MINT,WORK,LENW,IWORK,LENIW,FEX)
      IF(MSTATE.GT.2)GO TO 80
      IF(T.GE.TSTART)IFLAG=1
      IF(IFLAG.EQ.1)THEN
C      WRITE(6,70)RWORK(14),IWORK(19),IWORK(20)
       IF(IOUT.LE.1000)THEN
        IF(MOD(IOUT,2).EQ.0)THEN
         CALL SCRIBE(N,T,Y)
        END IF
       ELSE IF((IOUT.GT.1000).AND.(IOUT.LT.1700))THEN
        CALL SCRIBE(N,T,Y)
       ELSE IF((IOUT.GE.1700).AND.(IOUT.LT.6700))THEN
        DELTAT=1.0D-4
        IF(MOD(IOUT,10).EQ.0)THEN
         CALL SCRIBE(N,T,Y)
        END IF
       ELSE
        DELTAT=0.1D0
        CALL SCRIBE(N,T,Y)
       END IF
      END IF
C-----THE FOLLOWING SECTION OF CODE DUMPS THE ENTRY OF THE
C-----JACOBIAN WITH LARGEST MAGNITUDE INTO 'BIG2'.  THIS
C-----GIVES US A LOWER BOUND FOR THE LIPSCHITZ CONSTANT.
      CALL JAC(N,T,Y,PD)
      DO 21 I=1,4
       DO 20 J=1,4
        PD(I,J)=DABS(PD(I,J))
  20   CONTINUE
  21  CONTINUE
C      BIG2=DMAX1(PD(1,1),PD(1,2),PD(2,1),PD(2,2),PD(2,3),
C     &PD(3,1),PD(3,2),PD(3,3),PD(3,4),PD(4,3),PD(4,4))
```

```
      BIG2=DMAX1(PD(3,3),PD(3,4),PD(4,3),PD(4,4))
      WRITE(13,98)T,BIG2
C-----END OF JACOBIAN SECTION
C-------------------------------------------------------------
C-----THE FOLLOWING SECTION OF CODE DUMPS AN UPPER LOWER
C-----BOUND FOR THE LIPSCHITZ CONSTANT INTO 'BIG1',WITHOUT
C-----EMPLOYING THE JACOBIAN.
      DO 35 K=1,4
       DO 22 I=1,4
        YPERT(I)=Y(I)
  22   CONTINUE
       YPERT(K)=YPERT(K)+DEL
       CALL FEX(N,T,YPERT,FPERT)
       CALL FEX(N,T,Y,F)
       DO 25 J=1,4
        COL(J)=(FPERT(J)-F(J))/DEL
        COL(J)=DABS(COL(J))
  25   CONTINUE
       COLMAX(K)=DMAX1(COL(1),COL(2),COL(3),COL(4))
  35  CONTINUE
      BIG1=DMAX1(COLMAX(1),COLMAX(2),COLMAX(3),COLMAX(4))
      WRITE(14,98)T,BIG1
C-----END OF LIPSCHITZ SECTION
CCCCCCCCCCCCCCCCCCCCCCCCCCCCCCCCCCCCCCCCCCCCCCCCCCCCCCCCCCC
C                                                           C
C      THE FOLLOWING STATEMENT LINEARIZES THE SYSTEM        C
C      ABOUT THE SOLUTION VALUES EVERY 2 OR 4               C
C      MICROSECONDS                                         C
C                                                           C
CCCCCCCCCCCCCCCCCCCCCCCCCCCCCCCCCCCCCCCCCCCCCCCCCCCCCCCCCCC
C      IF((T.LT.1.38D2).OR.(T.GT.1.76D2))THEN
C       IF(MOD(IOUT,20).EQ.0)THEN
C        CALL JEX(N,T,Y,ML,MU,AA,N)
C        CALL CHARPOLY(T,N,AA)
C       END IF
C      ELSE
C       IF(MOD(IOUT,10).EQ.0)THEN
C        CALL JEX(N,T,Y,ML,MU,AA,N)
C        CALL CHARPOLY(T,N,AA)
C       END IF
C      END IF
  40  TOUT=TOUT+DELTAT
C      WRITE(6,60)IWORK(11),IWORK(12),IWORK(13)
C      WRITE(6,70)RWORK(14),IWORK(19),IWORK(20)
  60  FORMAT(/12H NO. STEPS =,I6,11H  NO. F-S =,
     1I6,11H  NO. J-S =,I6)
  70  FORMAT(1X,'TOLSF=',E14.7,1X,'MUSED=',I2,1X,'MCUR=',I2)
C     MUSED=1 MEANS ADAMS METHOD WAS USED I.E.NON-STIFF
C     MUSED=2 MEANS BDF USED I.E.STIFF
  80  CONTINUE
  95  FORMAT(1X,'ISTATE= ',I3)
  96  FORMAT(1X,A16,I5,A7)
  97  FORMAT(1X,A9,1X,I2)
  98  FORMAT(1X,E16.8,1X,E16.8)
C      WRITE(6,95)ISTATE
      WRITE(6,97)' MSTATE= ',MSTATE
 100  CONTINUE
      STOP
      END
```

```
      SUBROUTINE FEX(NEQ,T,Y,YDOT)
      IMPLICIT DOUBLE PRECISION(A-H,O-Z)
      DIMENSION Y(NEQ),YDOT(NEQ)
      COMMON W,TAU20,TAU21,CC,TAU2,TAU1,TAUC,SPO,C,THNTOT,C1,C1STAR,
     1GAMMA,SIGMA,TAU1DASH,HOnTOT,D1,D2,D3,D4,D5,PHINORM,PAR4,
     2PAR3,ZSTAR
C       TPUMP=0.5D1
C       WWP=W*PUMP(T,TPUMP)
      WWP=W

      TQ=1.7D2
      QDEN=1.0D0+1.0D3*QSWITCH(T,TQ)
      QTAUC=TAUC/QDEN
C       QTAUC=TAUC
CCCCCCCCCCCCCCCCCCCCCCCCCCCCCCCCCCCCCCCCCCCCCCCCCCCCCCCCCCCCCCCCCCC
C                                                                     C
C     THE FOLLOWING IF-THEN-ELSE STATEMENT IS TANTAMOUNT TO           C
C     STOPPING THE INTEGRATION AT T=TQ,INPUTTING CURRENT              C
C     NUMERICAL VALUES OF SOLUTION AS INITIAL CONDITIONS AND          C
C     RESUMING INTEGRATION ON A REDUCED SYSTEM WHERE THE              C
C     UPPER AND LOWER THULMIUM POPULATIONS STAY CONSTANT.             C
C                                                                     C
CCCCCCCCCCCCCCCCCCCCCCCCCCCCCCCCCCCCCCCCCCCCCCCCCCCCCCCCCCCCCCCCCCC
      IF(T.LE.TQ)THEN
       YDOT(1)=(D1*Y(1)-WWP)*Y(2)+(D1*Y(1)-WWP-1.0D0/TAU2-D1)*Y(1)+WWP
       YDOT(2)=-(1.0D0/TAU1+2.0D0*D1*Y(1)+D2*(1.0D0-Y(3))+D3*Y(3))*Y(2)
     1 +(1.0D0/TAU21-2.0D0*D1*(Y(1)-1.0D0)-D3*Y(3))*Y(1)+
     2 D3*Y(3)
      ELSE
       YDOT(1)=0.0D0
       YDOT(2)=0.0D0
      END IF
      YDOT(3)=-(1.0D0/TAU1DASH+D4*Y(2)+D5*(1.0D0-Y(1)-Y(2)))*Y(3)+
     1 D4*Y(2)+ SIGMA*CC*PHINORM*Y(4)*(GAMMA*(1.0D0-Y(3))-1.0D0)
      ZSTAR=PAR3*(GAMMA*(Y(3)-1.0D0)+1.0D0)-1.0D0/QTAUC
      YDOT(4)=PAR4*Y(3)+ZSTAR*Y(4)
      RETURN
      END

      SUBROUTINE SCRIBE(N,T,Y)
      DOUBLE PRECISION T,Y
      DIMENSION Y(N)
C     THIS SUBROUTINE WRITES THE NUMERICAL APPROXIMATION TO THE
C     SOLUTION TO THE DATA FILES.
      WRITE(7,125)T,Y(1)
      WRITE(8,125)T,Y(2)
      WRITE(9,125)T,Y(3)
      WRITE(10,125)T,Y(4)
 125  FORMAT(1X,E16.8,1X,E24.16)
      RETURN
      END


C       SUBROUTINE JEX(NEQ,T,Y,ML,MU,PD,NRPD)
      SUBROUTINE JAC(NEQ,T,Y,PD)
      IMPLICIT DOUBLE PRECISION(A-H,O-Z)
      DIMENSION Y(NEQ),PD(NEQ,NEQ)
      COMMON W,TAU20,TAU21,CC,TAU2,TAU1,TAUC,SPO,C,THNTOT,C1,C1STAR,
     1GAMMA,SIGMA,TAU1DASH,HOnTOT,D1,D2,D3,D4,D5,PHINORM,PAR4,
     2PAR3,ZSTAR
```

```
C       TPUMP=0.5D1
C       WWP=W*PUMP(T,TPUMP)
        WWP=W
        TT=T
        TQ=1.7D2
        QDEN=1.0D0+1.0D3*QSWITCH(T,TQ)
        QTAUC=TAUC/QDEN
C       QTAUC=TAUC
        PD(1,1)=D1*Y(2)+2.0D0*D1*Y(1)-WWP-1.0D0/TAU2-D1
        PD(1,2)=D1*Y(1)-WWP
        PD(1,3)=0.0D0
        PD(1,4)=0.0D0
        PD(2,1)=-2.0D0*D1*Y(2)+1.0D0/TAU21-4.0D0*D1*Y(1)+2.0D0*D1-
       1 D3*Y(3)
        PD(2,2)=-(1.0D0/TAU1+2.0D0*D1*Y(1)+D2*(1.0D0-Y(3))+D3*Y(3))
        PD(2,3)=D2*Y(2)+D3*(1.0D0-Y(1)-Y(2))
        PD(2,4)=0.0D0
        PD(3,1)=D5*Y(3)
        PD(3,2)=PD(3,1)+D4*(1.0D0-Y(3))
        PD(3,3)=-(GAMMA*SIGMA*CC*PHINORM*Y(4)+1.0D0/TAU1DASH+D4*Y(2)+
       1 D5*(1.0D0-Y(1)-Y(2)))
        PD(3,4)=SIGMA*CC*GAMMA*PHINORM*(1.0D0-Y(3))-SIGMA*CC*PHINORM
        PD(4,1)=0.0D0
        PD(4,2)=0.0D0
        PD(4,3)=GAMMA*PAR3*Y(4)+SPO*HOnTOT/(PHINORM*TAU1DASH)
        PD(4,4)=GAMMA*PAR3*(Y(3)-1.0D0)+PAR3-1.0D0/QTAUC
        RETURN
        END

        FUNCTION PUMP(T,TPUMP)
        IMPLICIT DOUBLE PRECISION(A-H,O-Z)
        TEST=T-TPUMP
        IF(TEST.LT.0.0D0)PUMP=1.0D0
        IF(TEST.GE.0.0D0)PUMP=0.0D0
        RETURN
        END

        FUNCTION QSWITCH(T,QT)
        IMPLICIT DOUBLE PRECISION(A-H,O-Z)
C       THIS Q-SWITCH TAKES 0.1 MICROSECONDS TO SWITCH!
        QTEST=T-QT
        ST=1.0D-1
        IF(QTEST.LE.0.0D0)QSWITCH=1.0D0
        IF((QTEST.GT.0.0D0).AND.(QTEST.LT.ST))QSWITCH=1.0D0-QTEST/ST
        IF(QTEST.GE.ST)QSWITCH=0.0D0
        RETURN
        END

        SUBROUTINE CHARPOLY(T,N,A)
CCCCCCCCCCCCCCCCCCCCCCCCCCCCCCCCCCCCCCCCCCCCCCCCCCCCCCCCCCCCCCCCCC
C                                                                  C
C       THIS SUBROUTINE FINDS THE ROOTS OF THE CHARACTERISTIC      C
C       POLYNOMIAL OF THE LINEARIZED SYSTEM USING A ROUTINE        C
C       FROM "NUMERICAL RECIPES" CALLED ZROOTS.                    C
C                                                                  C
CCCCCCCCCCCCCCCCCCCCCCCCCCCCCCCCCCCCCCCCCCCCCCCCCCCCCCCCCCCCCCCCCC
        IMPLICIT DOUBLE PRECISION(A-H,O-Z)
C       EXTERNAL CPOLY
        PARAMETER(M=3)
        COMPLEX*16 COEFF,RROOTS,VAL,CVEC,TROOTS,POINT
```

```
      LOGICAL PPOLISH,LROOT
      DIMENSION A(4,4),CD(5),COEFF(5),RROOTS(4),TROOTS(3),CVEC(4)
      COMMON/AREA1/CD
      OPEN(UNIT=1,FILE='LINEAR.DAT')
      OPEN(UNIT=2,FILE='DISC1.DAT')
      OPEN(UNIT=3,FILE='DISC2.DAT')
      A11=A(1,1)
      A12=A(1,2)
      A13=A(1,3)
      A14=A(1,4)
      A21=A(2,1)
      A22=A(2,2)
      A23=A(2,3)
      A24=A(2,4)
      A31=A(3,1)
      A32=A(3,2)
      A33=A(3,3)
      A34=A(3,4)
      A41=A(4,1)
      A42=A(4,2)
      A43=A(4,3)
      A44=A(4,4)

CC----NOW DEFINE THE COEFFICIENTS OF THE CHAR.POLY.---
      CD(5)=1.0D0
      CD(4)=-(A11+A22+A33+A44)
      CD(3)=A11*(A22+A33+A44)+A22*(A33+A44)+A33*A44-
     1(A34*A43+A23*A32+A12*A21)
      CD(2)=A11*(A23*A32-A22*A44-A33*A44-A22*A33+A34*A43)+
     1A22*(A34*A43-A33*A44)+A23*A32*A44+A12*(A21*A33+A21*A44-A23*A31)
      CD(1)=A11*(A22*A33*A44-A22*A34*A43-A23*A32*A44)+
     1A12*(A23*A31*A44+A21*A34*A43-A21*A33*A44)
CC----END DEFINITION-----------------------------------

      DO 50 K=1,5
       COEFF(K)=DCMPLX(CD(K))
  50  CONTINUE

      B=CD(4)
      C=CD(3)
      D=CD(2)
      E=CD(1)
      P=C-0.375D0*B**2
      Q=0.125D0*B**3+D-0.5D0*B*C
      R=0.0625D0*C*B**2-3.0D0*B**4/256.0D0-0.25D0*B*D+E
      C4=1.0D0
      C3=-P
      C2=-4.0D0*R
      C1=4.0D0*P*R-Q**2
      CVEC(4)=DCMPLX(C4)
      CVEC(3)=DCMPLX(C3)
      CVEC(2)=DCMPLX(C2)
      CVEC(1)=DCMPLX(C1)
      PPOLISH=.TRUE.

C      CALL DZROOTS(COEFF,N,RROOTS,PPOLISH)
C      CALL DZROOTS(CVEC,M,TROOTS,PPOLISH)

      WRITE(1,150)' AT TIME T= ',T,' WE HAVE THE FOLLOWING: '
      DO 100 I=1,4
```

```
      VAL=DCMPLX(CD(5))
      DO 60 K=4,1,-1
       VAL=VAL*RROOTS(I)+DCMPLX(CD(K))
 60    CONTINUE
       VVAL=DREAL(VAL)
        WRITE(1,180)'ZROOT= ',RROOTS(I),' VAL= ',VVAL
100   CONTINUE

150   FORMAT(1X,A12,E16.8,A24)
170   FORMAT(1X,A1)
180   FORMAT(1X,A7,E20.12,E20.12,A6,E20.12)

      I=1
250   CONTINUE
      DDRE=DREAL(TROOTS(I))
      DDIM=DIMAG(TROOTS(I))
      IF((DABS(DDIM).LE.1.0D-6).AND.(DDRE.GE.P))THEN
       U1=DDRE
       LROOT=.TRUE.
      ELSE
       LROOT=.FALSE.
       IF(I.LE.2)THEN
        I=I+1
        GO TO 250
       END IF
      END IF
      IF(.NOT.LROOT)THEN
       WRITE(1,400)' UNABLE TO LOCATE U1 '
      END IF
      IF(LROOT)THEN
       UMINP=U1-P
       WRITE(1,298)' U1-P= ',UMINP
       AA=DSQRT(U1-P)
       BB=Q/(2.0D0*AA)
       DISC1=AA**2-2.0D0*U1+4.0D0*BB
       DISC2=AA**2-2.0D0*U1-4.0D0*BB
CCCCCCCCCCCCCCCCCCCCCCCCCCCCCCCCCCCCCCCCCCCCCCCCCCCCCCCCCCCCCCCCCC
C                                                                  C
C      THE FOLLOWING SCALING IS FOR GRAPHING PURPOSES              C
C                                                                  C
CCCCCCCCCCCCCCCCCCCCCCCCCCCCCCCCCCCCCCCCCCCCCCCCCCCCCCCCCCCCCCCCCC
       IF(DISC1.GT.0.0D0)THEN
        DISC1=DISC1/1.0D8
        WRITE(1,299)' DISC1 > 0 '
       ELSE
        DISC1=DISC1/1.0D3
        WRITE(1,299)' DISC1 < 0 '
       END IF
       IF(DISC2.GT.0.0D0)THEN
        WRITE(1,299)' DISC2 > 0 '
       ELSE
        WRITE(1,299)' DISC2 < 0 '
       END IF
       WRITE(2,300)T,DISC1
       WRITE(3,300)T,DISC2
 298   FORMAT(1X,A8,E16.8)
 299   FORMAT(1X,A12)
 300   FORMAT(1X,E14.7,E14.7)
      END IF
      WRITE(1,450)' TROOTS(1)=',TROOTS(1)
```

```
      WRITE(1,450)' TROOTS(2)=',TROOTS(2)
      WRITE(1,450)' TROOTS(3)=',TROOTS(3)
      WRITE(1,170)' '
      WRITE(1,170)' '
 400  FORMAT(1X,A22)
 430  FORMAT(1X,A24)
 450  FORMAT(1X,A11,E16.8,E16.8)
      RETURN
      END

C      FUNCTION CPOLY(X)
C      IMPLICIT DOUBLE PRECISION(A-H,O-Z)
C      DIMENSION CD(5)
C      COMMON/AREA1/CD
C      VALUE=CD(5)
C      DO 10 K=4,1,-1
C      VALUE=VALUE*X+CD(K)
C  10  CONTINUE
C      CPOLY=VALUE
C      RETURN
C      END
```

Appendix C

COMPUTER PROGRAM:

Newthho

```
      PROGRAM NEWTHHO
CCCCCCCCCCCCCCCCCCCCCCCCCCCCCCCCCCCCCCCCCCCCCCCCCCCCCCCCCCCCCCCCCCCCCCCC
C     THIS IS A PROGRAM TO SOLVE THE THULIUM HOLMIUM LASER SYSTEM BY  EMPLOYINGC
C     LSODA.THE CORRESPONDENCE BETWEEN THE VARIABLES IN THE SYSTEM AND THE     C
C     VARIABLES IN THE PROGRAM IS AS FOLLOWS:                                  C
C     Y(1)=THULIUM PUMP LEVEL(3H4)                                             C
C     Y(2)=THULIUM ENERGY TRANSFER LEVEL(3F4)                                  C
C     Y(3)=HOLMIUM LASING LEVEL(5I7)                                           C
C     Y(4)=PHOTON DENSITY                                                      C
C     Y(5)=HOLMIUM LEVEL(5I5)                                                  C
C     Y(6)=HOLMIUM LEVEL(5S2)                                                  C
CCCCCCCCCCCCCCCCCCCCCCCCCCCCCCCCCCCCCCCCCCCCCCCCCCCCCCCCCCCCCCCCCCCCCCCC
      IMPLICIT DOUBLE PRECISION(A-H,O-Z)
      EXTERNAL FEX
      PARAMETER (N=6,NEQ=5)
      REAL*8 LIPSCHITZ,JMAX,LIP,NEWABSP,NEWPHIOUT
      DIMENSION Y(N),WORK(342),IWORK(27),YNORM(N),YY(NEQ),PD(NEQ,NEQ)
C      DIMENSION Y(N),ATOL(N),RWORK(116),IWORK(26),YPRIME(N),YNORM(N)
      COMMON W,TAU20,TAU21,CC,TAU2,TAU1,TAUC,SPO,C,THNTOT,C1,C1STAR,
     1SIGMA,TAU1DASH,HOnTOT,PHINORM,PAR4,f0,f1,PUMPSIG,RODDIA,
     2S,TQ,IQSWITCH,IPUMP,W1,FWHM1,FWHM2,FWHM3,PI,RODL,OPTLNG,
     3SPOLIFE,SIGMAPP,Q2,Q1,Q1DASH,TAU5,TAU6

      OPEN(UNIT=6,FILE='NEWTHHO.ERR')
      OPEN(UNIT=7,FILE='NEWTY1.DAT')
      OPEN(UNIT=8,FILE='NEWTY2.DAT')
      OPEN(UNIT=9,FILE='NEWTY3.DAT')
      OPEN(UNIT=10,FILE='NEWTY4.DAT')
      OPEN(UNIT=11,FILE='NEWTY5.DAT')
      OPEN(UNIT=13,FILE='NEWTY6.DAT')
      OPEN(UNIT=12,FILE='INFO.NEW')
      OPEN(UNIT=14,FILE='TTDEV.DAT')
      OPEN(UNIT=15,FILE='MAXJAC.DAT')
      OPEN(UNIT=16,FILE='ETA.DAT')
      OPEN(UNIT=17,FILE='PHOTDEV.DAT')
      OPEN(UNIT=18,FILE='BIGONE.DAT')
CCCCCCCCCCCCCCCCCCCCCCCCCCCCCCCCCCCCCCCCCCCCCCC
C                                             C
C          INITIAL CONDITIONS                 C
C                                             C
CCCCCCCCCCCCCCCCCCCCCCCCCCCCCCCCCCCCCCCCCCCCCCC
      Y(1)=0.0D0
      Y(2)=0.0D0
      Y(3)=0.0D0
      Y(4)=0.0D0
      Y(5)=0.0D0
      Y(6)=0.0D0
      PHIOUT=0.0D0
      ABSPUMP=0.0D0
      TOUT=0.25D0
      DELTAT=0.25D0
      NPOINTS=2000
      LIPSCHITZ=0.0D0
      LIP=3149.8496D0
      DEVMAX=.49677547D-2
CCCCCCCCCCCCCCCCCCCCCCCCCCCCCCCCCCCCCCCCCCCCCCCCCCCCCCCCCCCC
C                                                          C
C                   LSODA PARAMETERS                       C
C                                                          C
CCCCCCCCCCCCCCCCCCCCCCCCCCCCCCCCCCCCCCCCCCCCCCCCCCCCCCCCCCCC
```

```
C       ITOL=2
C       RTOL=1.0D-8
C       ATOL(1)=1.0D6
C       ATOL(2)=1.0D6
C       ATOL(3)=1.0D6
C       ATOL(4)=1.0D-1
C       ATOL(5)=1.0D6
C       ATOL(6)=1.0D6
C       ITASK=1
C       ISTATE=1
C       IOPT=1
C       LRW=116
C       LIW=26
C       JT=2
CC       MF=21
C       DO 1 I=5,10
C        RWORK(I)=0.0D0
C        IWORK(I)=0
C  1    CONTINUE
C       H0=.01D0
C       HMAX=.01D0
C       HMIN=1.0D-9
C       MXSTEP=1500
C       RWORK(5)=H0
C       RWORK(6)=HMAX
C       RWORK(7)=HMIN
C       IWORK(6)=MXSTEP

      S=1.0D0
CCCCCCCCCCCCCCCCCCCCCCCCCCCCCCCCCCCCCCCCCCCCCCCCCCCCCCCCCCCCCCCCCCCCCCC
C     S IS A SCALING FACTOR:                                            C
C     IF S=0.001   THEN [T]=THOUSANDS OF MICROSEC.(i.e.MILLISECONDS)    C
C     IF S=0.01    THEN [T]=HUNDREDS OF MICROSEC.                       C
C     IF S=0.1     THEN [T]=TENS OF MICROSEC.                           C
C     IF S=1.0     THEN [T]=MICROSEC.                                   C
C     IF S=10.0    THEN [T]=TENTHS OF MICROSEC.                         C
C     IF S=100.0   THEN [T]=HUNDRETHS OF MICROSEC.                      C
C     IF S=1000.0  THEN [T]=THOUSANTHS OF MICROSEC.(i.e.NANOSECONDS)    C
CCCCCCCCCCCCCCCCCCCCCCCCCCCCCCCCCCCCCCCCCCCCCCCCCCCCCCCCCCCCCCCCCCCCCCC

CCCCCCCCCCCCCCCCCCCCCCCCCCCCCCCCCCCCCCCCCCCCCCCCCCCCCCCCCCCCCCCCCCCCCCC
C                                                                       C
C                      PHYSICAL PARAMETERS                              C
C                                                                       C
CCCCCCCCCCCCCCCCCCCCCCCCCCCCCCCCCCCCCCCCCCCCCCCCCCCCCCCCCCCCCCCCCCCCCCC
      TAU1=1.18D4
      TAU1DASH=9.25D3
      HOnTOT=5.0D19
      THNTOT=8.0D20
C      WRITE(*,*)'PLEASE ENTER HOnTOT'
C      READ(*,*)HOnTOT
C      WRITE(*,*)'PLEASE ENTER THNTOT'
C      READ(*,*)THNTOT
      PHINORM=1.0D16
      f0=0.0115D0
      f1=0.0685D0
      C=4.6D-21
      CC=3.0D4
      TAU20=6.0D2
      TAU21=6.0D2
```

```
      TAU2=1.0D0/(1.0D0/TAU20+1.0D0/TAU21)
      C1=7.0D-21
      SIGMA=1.826D-19
C      C1STAR=0.0D0
      C1STAR=3.25D-22
C      WRITE(*,*)'PLEASE ENTER C1STAR'
C      READ(*,*)C1STAR
      PI=4.0D0*DATAN(1.0D0)
      CAVRAD=0.0415D0
C      WRITE(*,*)'PLEASE ENTER CAVRAD'
C      READ(*,*)CAVRAD
      CAVAREA=PI*CAVRAD**2
      RODL=0.3D0
C      WRITE(*,*)'PLEASE ENTER RODL'
C      READ(*,*)RODL
      CAVL=17.5D0
C      CAVL=RODL
C      WRITE(*,*)'PLEASE ENTER CAVL'
C      READ(*,*)CAVL
      RODDEX=1.78D0
      RODDIA=0.3D0
C      REFLOUT=0.98D0
      WRITE(*,*)'PLEASE ENTER REFLOUT'
      READ(*,*)REFLOUT
      REFLBCK=0.98D0
      RODLOSS=0.0D0
      SURFACET=1.0D0
      OPTLNG=RODL*RODDEX+CAVL-RODL
      ROUNDTT=2.0D0*OPTLNG/CC
C      PUMPE=0.08D0
      WRITE(*,*)'PLEASE ENTER PUMPE'
      READ(*,*)PUMPE
      PUMPLAM=0.785D0
      HC=1.9875D-19
      HNUPUMP=HC/PUMPLAM
      PUMPETA=1.0D0
      PUMPSIG=2.935D-21
      EMISLAM=2.0D0
      B=CAVAREA*4.0D0/(PI*OPTLNG**2)
      SPO=B*RODL/OPTLNG
      SPOLIFE=2.92D3
      TAUC=ROUNDTT/(4.0D0-2.0D0*SURFACET-REFLBCK-REFLOUT+
     12.0D0*RODL*RODLOSS)
      SIGMAPP=0.0D0
      Q2=0.0D0
C      Q1=0.0D0
C      Q1=1.0D-23
      WRITE(*,*)'PLEASE ENTER Q1'
      READ(*,*)Q1
      Q1DASH=1.2D-23
      TAU5=2.0D5
      TAU6=2.0D5
CCCCCCCCCCCCCCCCCCCCCCCCCCCCCCCCCCCCCCCCCCCCCCCCCCCCCCC
C                                                      C
C            PUMP PARAMETERS                           C
C                                                      C
CCCCCCCCCCCCCCCCCCCCCCCCCCCCCCCCCCCCCCCCCCCCCCCCCCCCCCC
      IPUMP=3
      FWHM1=S*2.5D2
      FWHM2=S*3.0D2
```

```
      FWHM3=S*3.0D2
      W1=PUMPETA*PUMPE*PUMPLAM/(HC*CAVAREA*RODL)
      W=1.0D18
CCCCCCCCCCCCCCCCCCCCCCCCCCCCCCCCCCCCCCCCCCCCCCCCCCCCCCCC
C                                                       C
C            IPUMP=0 <----> CONSTANT PUMP               C
C            IPUMP=1 <----> PUMP1                       C
C            IPUMP=2 <----> PUMP2                       C
C            IPUMP=3 <----> PUMP3                       C
C                                                       C
CCCCCCCCCCCCCCCCCCCCCCCCCCCCCCCCCCCCCCCCCCCCCCCCCCCCCCCC

CCCCCCCCCCCCCCCCCCCCCCCCCCCCCCCCCCCCCCCCCCCCCCCCCCCCCCCC
C                                                       C
C             Q-SWITCHING PARAMETERS                    C
C                                                       C
CCCCCCCCCCCCCCCCCCCCCCCCCCCCCCCCCCCCCCCCCCCCCCCCCCCCCCCC
      TQ=2.0D2
      IQSWITCH=0
CCCCCCCCCCCCCCCCCCCCCCCCCCCCCCCCCCCCCCCCCCCCCCCCCCCCCCCC
C                                                       C
C             IQSWITCH=1 <----> Q-SWITCHING             C
C             IQSWITCH=0 <----> NO Q-SWITCHING          C
C                                                       C
CCCCCCCCCCCCCCCCCCCCCCCCCCCCCCCCCCCCCCCCCCCCCCCCCCCCCCCC

CCCCCCCCCCCCCCCCCCCCCCCCCCCCCCCCCCCCCCCCCCCCCCCCCCCCCCCC
C                                                       C
C     DDRIV2 PARAMETERS                                 C
C                                                       C
CCCCCCCCCCCCCCCCCCCCCCCCCCCCCCCCCCCCCCCCCCCCCCCCCCCCCCCC
      MSTATE=1
      NROOT=0
      EPS=1.0D-8
      EWT=1.0D-22
      MINT=3
      LENW=342
      LENIW=27
C-----END DDRIV2 PARAMETERS-------------------------
      IFLAG=1
      TSTART=0.0D0
      T=0.0D0
      IF(IFLAG.EQ.1)THEN
      CALL SCRIBE(N,T,Y)
      END IF
      TT=0.0D0
      DEV=0.0D0
      PHOTDEV=0.0D0
      ETA=0.0D0
      BIGONE=0.0D0
      WRITE(16,42)T,ETA
      WRITE(14,42)TT,DEV
      WRITE(17,42)TT,PHOTDEV
   15 FORMAT(1X,A7,E14.7)
   20 FORMAT(1X,E16.8)
      THN0=THNTOT-Y(1)-Y(2)
      EXARG=-PUMPSIG*RODDIA*THN0
      IF(IPUMP.EQ.0)THEN
      OLDABSP=W*(1.0D0-DEXP(EXARG))
      ELSE IF(IPUMP.EQ.1)THEN
```

```
      OLDABSP=W1*PUMP1(T,FWHM1,PI)*(1.0D0-DEXP(EXARG))
      ELSE IF(IPUMP.EQ.2)THEN
      OLDABSP=W1*PUMP2(T,FWHM2,PI)*(1.0D0-DEXP(EXARG))
      ELSE
      OLDABSP=W1*PUMP3(T,FWHM3)*(1.0D0-DEXP(EXARG))
      END IF
      OLDPHIOUT=Y(4)
      DO 40 IOUT=1,NPOINTS
      CALL DDRIV2(N,T,Y,FEX,TOUT,MSTATE,NROOT,EPS,EWT,
     &MINT,WORK,LENW,IWORK,LENIW,FEX)
      IF(MSTATE.GT.2)GO TO 80
C      CALL LSODA(FEX,N,Y,T,TOUT,ITOL,RTOL,ATOL,ITASK,ISTATE,
C     1 IOPT,RWORK,LRW,IWORK,LIW,JEX,JT)
C      IF(ISTATE.LT.0)GO TO 80
      IF(T.GE.TSTART)IFLAG=1
      IF(IFLAG.EQ.1)THEN
C      WRITE(6,70)RWORK(14),IWORK(19),IWORK(20)
      THNO=THNTOT-Y(1)-Y(2)
      EXARG=-PUMPSIG*RODDIA*THNO
      IF(IPUMP.EQ.0)THEN
       NEWABSP=W*(1.0D0-DEXP(EXARG))
       ABSPUMP=ABSPUMP+(OLDABSP+NEWABSP)*DELTAT/2.0D0
      ELSE IF(IPUMP.EQ.1)THEN
       NEWABSP=W1*PUMP1(T,FWHM1,PI)*(1.0D0-DEXP(EXARG))
       ABSPUMP=ABSPUMP+(OLDABSP+NEWABSP)*DELTAT/2.0D0
      ELSE IF(IPUMP.EQ.2)THEN
       NEWABSP=W1*PUMP2(T,FWHM2,PI)*(1.0D0-DEXP(EXARG))
       ABSPUMP=ABSPUMP+(OLDABSP+NEWABSP)*DELTAT/2.0D0
      ELSE
       NEWABSP=W1*PUMP3(T,FWHM3)*(1.0D0-DEXP(EXARG))
       ABSPUMP=ABSPUMP+(OLDABSP+NEWABSP)*DELTAT/2.0D0
      END IF
      NEWPHIOUT=Y(4)
      PHIOUT=PHIOUT+(OLDPHIOUT+NEWPHIOUT)*DELTAT/2.0D0
      OLDABSP=NEWABSP
      OLDPHIOUT=NEWPHIOUT
      YNORM(1)=Y(1)/THNTOT
      YNORM(2)=Y(2)/THNTOT
      YNORM(3)=Y(3)/HOnTOT
      YNORM(4)=Y(4)/PHINORM
      YNORM(5)=Y(5)/HOnTOT
      YNORM(6)=Y(6)/HOnTOT
      IF(IQSWITCH.EQ.1)THEN
       IF(IOUT.LT.1400)THEN
        IF(MOD(IOUT,2).EQ.0)THEN
         CALL SCRIBE(N,T,YNORM)
        END IF
       ELSE IF((IOUT.GE.1400).AND.(IOUT.LT.6400))THEN
        DELTAT=1.0D-4
        IF(MOD(IOUT,10).EQ.0)THEN
         CALL SCRIBE(N,T,YNORM)
        END IF
       ELSE IF(IOUT.GE.6400)THEN
        DELTAT=0.5D0
        CALL SCRIBE(N,T,YNORM)
       END IF
      ELSE
       CALL SCRIBE(N,T,YNORM)
      END IF
      READ(11,42)TT,X5
```

```
      PHOTDEV=DABS(SIGMA*CC*HOnTOT*RODL*f0*YNORM(4)*X5/CAVL)
      DEV=DABS(X5)*DSQRT((C1*HOnTOT*YNORM(2)+Q1DASH*HOnTOT*
     1(1.0D0-YNORM(1)-YNORM(2)))**2+(C1*THNTOT*YNORM(2)+
     2SIGMA*CC*PHINORM*f0*YNORM(4))**2+
     3(SIGMA*CC*HOnTOT*RODL*f0*YNORM(4)/CAVL)**2)
      WRITE(14,42)TT,DEV
      WRITE(17,42)TT,PHOTDEV
C-----THE FOLLOWING SECTION OF CODE DUMPS THE ENTRY OF THE
C-----JACOBIAN MATRIX WITH LARGEST MAGNITUDE INTO 'BIG'
      DO 29 LL=1,NEQ
       YY(LL)=Y(LL)
  29  CONTINUE
      CALL JAC(NEQ,T,YY,PD)
      JMAX=0.0D0
      DO 31 J=1,NEQ
       DO 30 K=1,NEQ
        PD(J,K)=DABS(PD(J,K))
        IF(PD(J,K).GT.JMAX)THEN
         JMAX=PD(J,K)
         JSAVE=J
         KSAVE=K
        END IF
  30   CONTINUE
  31  CONTINUE
      BIG=JMAX
      BIGONE=DMAX1(PD(4,3),PD(4,4))
      WRITE(18,42)T,BIGONE
      WRITE(15,41)T,BIG,JSAVE,KSAVE
C      WRITE(15,42)YY(3),YY(5)
      IF(BIG.GT.LIPSCHITZ)THEN
       LIPSCHITZ=BIG
      END IF
C      ETA=DEVMAX*(DEXP(LIP*T)-1.0D0)/LIP
C      WRITE(16,42)T,ETA
      END IF
  40  TOUT=TOUT+DELTAT
  41  FORMAT(1X,E16.8,1X,E16.8,'   PD(',I1,',',I1,')')
  42  FORMAT(1X,E16.8,1X,E16.8)
      PHIOUT=PHIOUT*CC*CAVAREA*HC*(1.0D0-REFLOUT)
     &/(EMISLAM*2.0D0)
      ABSPUMP=ABSPUMP*CAVAREA*RODL*HC/PUMPLAM
      WRITE(12,84)' LIPSCHITZ= ',LIPSCHITZ
      WRITE(12,75)' PHIOUT= ',PHIOUT
      WRITE(12,77)' ABSPUMP= ',ABSPUMP
      WRITE(12,78)' IPUMP= ',IPUMP
      IF(IPUMP.EQ.1)THEN
       FFWHM=FWHM1
      ELSE IF(IPUMP.EQ.2)THEN
       FFWHM=FWHM2
      ELSE IF(IPUMP.EQ.3)THEN
       FFWHM=FWHM3
      END IF
      IF(IPUMP.NE.0)THEN
       WRITE(12,73)' FWHM= ',FFWHM
      END IF
      IF(IPUMP.EQ.0)THEN
       WRITE(12,83)' W= ',W
      END IF
      IF(IQSWITCH.EQ.1)THEN
       WRITE(12,79)' QSWITCHING '
```

```
       WRITE(12,75)'    TQ=  ',TQ
      ELSE
       WRITE(12,81)' NO QSWITCHING '
      END IF
      WRITE(12,76)' PUMPE= ',PUMPE
      WRITE(12,77)' REFLOUT= ',REFLOUT
      WRITE(12,76)' SIGMA= ',SIGMA
      WRITE(12,75)' CAVRAD= ',CAVRAD
      WRITE(12,73)' CAVL= ',CAVL
      WRITE(12,73)' RODL= ',RODL
      WRITE(12,75)' RODDEX= ',RODDEX
      WRITE(12,75)' RODDIA= ',RODDIA
      WRITE(12,77)' REFLBCK= ',REFLBCK
      WRITE(12,77)' RODLOSS= ',RODLOSS
      WRITE(12,74)' SURFACET= ',SURFACET
      WRITE(12,75)' OPTLNG= ',OPTLNG
      WRITE(12,77)' PUMPLAM= ',PUMPLAM
      WRITE(12,77)' PUMPETA= ',PUMPETA
      WRITE(12,77)' PUMPSIG= ',PUMPSIG
      WRITE(12,77)' EMISLAM= ',EMISLAM
      WRITE(12,72)' SPO= ',SPO
      WRITE(12,77)' SPOLIFE= ',SPOLIFE
      WRITE(12,82)' Q1= ',Q1
      WRITE(12,75)' Q1DASH= ',Q1DASH
      WRITE(12,73)' TAUC= ',TAUC
      WRITE(12,75)' C1STAR= ',C1STAR
      WRITE(12,82)' C1= ',C1
      WRITE(12,83)' C= ',C
      WRITE(12,82)' CC= ',CC
      WRITE(12,82)' F0= ',F0
      WRITE(12,82)' F1= ',F1
      WRITE(12,77)' PHINORM= ',PHINORM
      WRITE(12,82)' HC= ',HC
      WRITE(12,77)' SIGMAPP= ',SIGMAPP
      WRITE(12,82)' Q2= ',Q2
      WRITE(12,73)' TAU1= ',TAU1
      WRITE(12,73)' TAU2= ',TAU2
      WRITE(12,73)' TAU5= ',TAU5
      WRITE(12,73)' TAU6= ',TAU6
      WRITE(12,76)' TAU20= ',TAU20
      WRITE(12,76)' TAU21= ',TAU21
      WRITE(12,74)' TAU1DASH= ',TAU1DASH
      WRITE(12,75)' HOnTOT= ',HOnTOT
      WRITE(12,75)' THNTOT= ',THNTOT
C      WRITE(6,60)IWORK(11),IWORK(12),IWORK(13)
C      WRITE(6,70)RWORK(14),IWORK(19),IWORK(20)
C  60  FORMAT(/12H NO. STEPS =,I6,11H  NO. F-S =,I6,11H  NO. J-
C     1S =,I6)
   70 FORMAT(1X,'TOLSF=',E14.7,1X,'MUSED=',I2,1X,'MCUR=',I2)
   72 FORMAT(1X,A6,E16.8)
   73 FORMAT(1X,A7,E16.8)
   74 FORMAT(1X,A11,E16.8)
   75 FORMAT(1X,A9,E16.8)
   76 FORMAT(1X,A8,E16.8)
   77 FORMAT(1X,A10,E16.8)
   78 FORMAT(1X,A8,I1)
   79 FORMAT(1X,A12)
   81 FORMAT(1X,A15)
   82 FORMAT(1X,A5,E16.8)
   83 FORMAT(1X,A4,E16.8)
```

```
  84  FORMAT(1X,A12,E16.8)
C     MUSED=1 MEANS ADAMS METHOD WAS USED I.E.NON-STIFF
C     MUSED=2 MEANS BDF USED I.E.STIFF
  80  CONTINUE
  95  FORMAT(1X,'ISTATE= ',I3)
  96  FORMAT(1X,A16,I5,A7)
      WRITE(6,95)ISTATE
 100  CONTINUE
      STOP
      END

      SUBROUTINE FEX(N,T,Y,YDOT)
      IMPLICIT DOUBLE PRECISION(A-H,O-Z)
      DIMENSION Y(N),YDOT(N)
      COMMON W,TAU20,TAU21,CC,TAU2,TAU1,TAUC,SPO,C,THNTOT,C1,C1STAR,
     1SIGMA,TAU1DASH,HOnTOT,PHINORM,PAR4,f0,f1,PUMPSIG,RODDIA,
     2S,TQ,IQSWITCH,IPUMP,W1,FWHM1,FWHM2,FWHM3,PI,RODL,OPTLNG,
     3SPOLIFE,SIGMAPP,Q2,Q1,Q1DASH,TAU5,TAU6
      IF(IPUMP.EQ.0)WWP=W
      IF(IPUMP.EQ.1)WWP=W1*PUMP1(T,FWHM1,PI)
      IF(IPUMP.EQ.2)WWP=W1*PUMP2(T,FWHM2,PI)
      IF(IPUMP.EQ.3)WWP=W1*PUMP3(T,FWHM3)
      IF(IQSWITCH.EQ.1)THEN
       QDEN=1.0D0+1.0D3*QSWITCH(T,TQ,S)
       QTAUC=TAUC/QDEN
      ELSE
       QTAUC=TAUC
      END IF
      THN0=THNTOT-Y(1)-Y(2)
      HOn0=HOnTOT-Y(3)-Y(5)-Y(6)
      ARG1=-PUMPSIG*RODDIA*THN0
      ARG2=-SIGMAPP*RODDIA*Y(3)
      YDOT(1)=WWP*(1.0D0-DEXP(ARG1))-Y(1)/TAU2-C*Y(1)*THN0-
     &Q2*Y(3)*Y(1)
      YDOT(2)=Y(1)/TAU21-Y(2)/TAU1+2.0D0*C*Y(1)*THN0-
     1C1*Y(2)*HOn0+C1STAR*THN0*Y(3)-Q1*Y(2)*Y(3)+Q1DASH*Y(5)*THN0
      YDOT(3)=-Y(3)/TAU1DASH+C1*Y(2)*HOn0-C1STAR*THN0*Y(3)-
     1SIGMA*CC*Y(4)*(f1*Y(3)-f0*HOn0)-Q2*Y(3)*Y(1)-Q1*Y(2)*Y(3)-
     2WWP*(1.0D0-DEXP(ARG2))
      YDOT(4)=SIGMA*CC*Y(4)*(f1*Y(3)-f0*HOn0)*RODL/OPTLNG-
     1Y(4)/QTAUC+SPO*f1*Y(3)/SPOLIFE
      YDOT(5)=Q1*Y(2)*Y(3)-Q1DASH*Y(5)*THN0-Y(5)/TAU5
      YDOT(6)=WWP*(1.0D0-DEXP(ARG2))-Y(6)/TAU6+Q2*Y(3)*Y(1)
      RETURN
      END

C      SUBROUTINE JEX(NEQ,T,Y,ML,MU,PD,NRPD)
      SUBROUTINE JAC(NEQ,T,Y,PD)
      IMPLICIT DOUBLE PRECISION(A-H,O-Z)
      DIMENSION Y(NEQ),PD(NEQ,NEQ)
      COMMON W,TAU20,TAU21,CC,TAU2,TAU1,TAUC,SPO,C,THNTOT,C1,C1STAR,
     1SIGMA,TAU1DASH,HOnTOT,PHINORM,PAR4,f0,f1,PUMPSIG,RODDIA,
     2S,TQ,IQSWITCH,IPUMP,W1,FWHM1,FWHM2,FWHM3,PI,RODL,OPTLNG,
     3SPOLIFE,SIGMAPP,Q2,Q1,Q1DASH,TAU5,TAU6
      IF(IPUMP.EQ.0)WWP=W
      IF(IPUMP.EQ.1)WWP=W1*PUMP1(T,FWHM1,PI)
      IF(IPUMP.EQ.2)WWP=W1*PUMP2(T,FWHM2,PI)
      IF(IPUMP.EQ.3)WWP=W1*PUMP3(T,FWHM3)
      IF(IQSWITCH.EQ.1)THEN
       QDEN=1.0D0+1.0D3*QSWITCH(T,TQ,S)
```

```
 QTAUC=TAUC/QDEN
ELSE
 QTAUC=TAUC
END IF
THN0=THNTOT-Y(1)-Y(2)
HON0=HOnTOT-Y(3)-Y(5)
EXARG=-PUMPSIG*RODDIA*THN0
PD(1,1)=-(1.0D0/TAU2+C*THN0-C*Y(1)+
1WWP*PUMPSIG*RODDIA*DEXP(EXARG))
PD(1,2)=C*Y(1)-WWP*PUMPSIG*RODDIA*DEXP(EXARG)
PD(1,3)=0.0D0
PD(1,4)=0.0D0
PD(1,5)=0.0D0
PD(2,1)=2.0D0*C*THNTOT-4.0D0*C*Y(1)+1.0D0/TAU21-
1C1STAR*Y(3)-2.0D0*C*Y(2)-Q1DASH*Y(5)
PD(2,2)=-(1.0D0/TAU1+2.0D0*C*Y(1)+C1*HON0+
1C1STAR*Y(3)+Q1*Y(3)+Q1DASH*Y(5))
PD(2,3)=C1*Y(2)+C1STAR*THN0-Q1*Y(2)
PD(2,4)=0.0D0
PD(2,5)=C1*Y(2)+Q1DASH*THN0
PD(3,1)=C1STAR*Y(3)
PD(3,2)=PD(3,1)+C1*HON0-Q1*Y(3)
PD(3,3)=-(C1*Y(2)+1.0D0/TAU1DASH+
1C1STAR*THN0+SIGMA*CC*Y(4)*(f0+f1)+Q1*Y(2))
PD(3,4)=-SIGMA*CC*(f1*Y(3)-f0*HON0)
PD(3,5)=-C1*Y(2)-SIGMA*CC*f0*Y(4)
PD(4,1)=0.0D0
PD(4,2)=0.0D0
PD(4,3)=SIGMA*CC*(f0+f1)*Y(4)*RODL/OPTLNG+SPO*f1/SPOLIFE
PD(4,4)=-(PD(3,4)*RODL/OPTLNG+1.0D0/QTAUC)
PD(4,5)=SIGMA*CC*f0*Y(4)
PD(5,1)=0.0D0
PD(5,2)=Q1*Y(3)+Q1DASH*Y(5)
PD(5,3)=Q1*Y(2)
PD(5,4)=0.0D0
PD(5,5)=-Q1DASH*THN0-1.0D0/TAU5
RETURN
END

FUNCTION PUMP1(T,FWHM,PI)
IMPLICIT DOUBLE PRECISION(A-H,O-Z)
ALPHA=PI/FWHM
IF((T.GE.0.0D0).AND.(T.LE.FWHM))PUMP1=ALPHA/PI
IF(T.GT.FWHM)PUMP1=0.0D0
RETURN
END

FUNCTION PUMP2(T,FWHM,PI)
IMPLICIT DOUBLE PRECISION(A-H,O-Z)
ALPHA=PI/(2.0D0*FWHM)
AARG=ALPHA*T
WIDTH=2.0D0*FWHM
IF((T.GE.0.0D0).AND.(T.LE.WIDTH))THEN
 PUMP2=(2.0D0*ALPHA*(DSIN(AARG))**2)/PI
END IF
IF(T.GT.WIDTH)PUMP2=0.0D0
RETURN
END

FUNCTION PUMP3(T,FWHM)
```

```
      IMPLICIT DOUBLE PRECISION(A-H,O-Z)
      ALPHA=1.1331512D0/FWHM
      EARG=-(ALPHA*ALPHA*T*T)
      IF(T.GE.0.0D0)THEN
       PUMP3=2.0D0*ALPHA*ALPHA*T*DEXP(EARG)
      END IF
      RETURN
      END

      FUNCTION QSWITCH(T,QT,S)
      IMPLICIT DOUBLE PRECISION(A-H,O-Z)
      QTEST=T-QT
      SS=S/1.0D2
CCCCCCCCCCCCCCCCCCCCCCCCCCCCCCCCCCCCCCCCCCCCCCCCCCCCCCCCCCCCCCCCCCCCCC
C     THE VALUE OF S DETERMINES THE UNITS OF TIME AND SS IS A  C
C     SCALING PARAMETER WHICH ENSURES THE Q-SWITCHING IS DONE  C
C     IN 10 NANOSECONDS REGARDLESS OF WHICH TIME SCALE I'M     C
C     PRESENTLY USING.                                         C
CCCCCCCCCCCCCCCCCCCCCCCCCCCCCCCCCCCCCCCCCCCCCCCCCCCCCCCCCCCCCCCCCCCCCC
      IF(QTEST.LE.0.0D0)QSWITCH=1.0D0
      IF((QTEST.GT.0.0D0).AND.(QTEST.LT.SS))QSWITCH=1.0D0-QTEST/SS
      IF(QTEST.GE.SS)QSWITCH=0.0D0
      RETURN
      END

      SUBROUTINE SCRIBE(N,T,Y)
      DOUBLE PRECISION T,Y
      DIMENSION Y(N)
C     THIS SUBROUTINE WRITES THE NUMERICAL APPROXIMATION TO THE
C     SOLUTIONS TO THE DATA FILES.
      WRITE(7,10)T,Y(1)
      WRITE(8,10)T,Y(2)
      WRITE(9,10)T,Y(3)
      WRITE(10,10)T,Y(4)
C      WRITE(11,10)T,Y(5)
      WRITE(13,10)T,Y(6)
   10 FORMAT(1X,E16.8,1X,E16.8)
      RETURN
      END
```

Autobiographical Statement

Thomas Gerard Wangler was born in Bismarck, North Dakota on February 11, 1957. He attended Bismarck Junior College for one year before enlisting in the U.S. Navy. Upon separation from active duty he enrolled at Old Dominion University in Norfolk, Virginia where he attended from 1982 to 1985.

In December of 1985 he received a Bachelor of Science degree (Summa Cum Laude) in Applied Mathematics. In January of 1986 he entered the graduate program at Old Dominion University and worked as a teaching assistant while fulfilling the requirements for a Master of Science degree in Computational and Applied Mathematics. In 1986 he received a certificate of recognition for high scholastic achievement from the Honor Society of Phi Kappa Phi.

Continuing on at Old Dominion University he entered the Ph.D. program in January of 1988 and was a research assistant from 1988–1990. His research was conducted at NASA Langley Research Center in Hampton, Virginia and was supported by a fellowship under the NASA Graduate Student Researchers Program.

Currently Mr. Wangler resides in Norfolk, Virginia with his wife and three children. He will receive his Doctor of Philosophy degree in Computational and Applied Mathematics from Old Dominion University in August of 1990. Relocating to the Chicago, Illinois area he will be employed as an Assistant Professor of Mathematics at Illinois Benedictine College in Lisle, Illinois.